Rotaxanes as peptide carriers

Aurélien Viterisi

Degree of Doctor of Philosophy

School of Chemistry

University of Edinburgh

July, 2009

For my parents

Table of Contents

Abstract

Based on the concept of covalent capture of supramolecular assemblies, the idea of mechanical encapsulation is exploited for the protection and delivery of peptide-based molecules. This thesis aims to establish a general method for the encapsulation of peptides within a rotaxane structure, as well as studying their mode of release under specific stimuli. The synthesis of such structures, relying on the elongation of short peptido[2]rotaxanes, is applied to the design of rotaxane peptide carriers whose function is to protect against biological degradation and release peptides under a biological stimulus. These molecules are composed of a rotaxane-encapsulated peptide bearing a biodegradable stopper, the enzyme-specific cleavage of which triggers peptide release, via 'dethreading'.

The synthesis and *in vitro* assessment of rotaxane carriers as agents for anti-cancer therapy will be described in detail. The future challenges and potential applications of the proposed systems will be addressed.

Declaration

The scientific work described in this Thesis was carried out in the School of Chemistry at the University of Edinburgh between November 2005 and November 2008. Unless otherwise stated, it is the work of the Author and has not been submitted in whole or in part in support of an application for another degree or qualification at this or any other University or institute of learning.

Signed…….

Date…….

Meetings and Lectures Attended and Presentations Given

1. **Organic Research Seminars**, School of Chemistry, University of Edinburgh, UK, 2005-2008.
   Oral Presentations:
   a) *Rotaxane-based peptide prodrugs designed to 'seek-and-destroy' solid tumours*, March 2006.
   b) *Rotaxanes from an active-metal template: investigation of the mechanism*, January 2007.
   c) *Rotaxanes from an active-metal template: investigation of the mechanism*, March 2008.

2. **School of Chemistry Visiting Speaker Colloquia**, School of Chemistry, University of Edinburgh, UK, 2005-2008.

3. **RSC Perkin Division 34th Scottish Regional Meeting**, University of Strathclyde, UK, December, 2005.

4. **The Young(-ish!) Giants of Chemistry: A Symposium Marking the Sixty-Fifth Birthday of Sir J. Fraser Stoddart**, University of Edinburgh, June, 2007
   Poster presentation: *'Click' rotaxanes assembled around Cu(I): The first active-metal template strategy.*

5. **Mass spectrometry: Principle and Practise in the 21st century**, School of Chemistry, University of Edinburgh, UK, April, 2007.

6. **RSC Perkin Division 35th Scottish Regional Meeting**, University of Glasgow, UK, December, 2007

7. **Special Symposium in Honour of David Reinhoudt**, School of Chemistry, University of Edinburgh, UK, November, 2008
   Oral presentation: *Rotaxane based nanodevices to seek and destroy solid tumours.*

8. **Supra-nano 2008, joint RSC meeting,** University of Birmingham, UK, December , 2008
   Poster presentation: *Rotaxane based nanodevices to seek and destroy solid tumours*

Acknowledgements

First, I must thank my supervisor, Professor David Leigh, for having given me the opportunity to spend three fabulous years in his research group. I would like to thank him particularly for the freedom he gave me throughout my PhD and for the abundant resources he put at my disposal, which many scientists can only dream of.

The person that deserves most gratitude is Dr. Vincent Aucagne, "Vince", whose impact on my scientific and personal life was very important. Thanks for teaching me all those little things that make a real scientist.

Aside from this unique character, I thank those with whom it has been my pleasure to work over the last three years (in no particular order): Vicki Ronaldson, Pepe Berná, Ai-Lan Lee, Anthony Fernandes (thanks for his big synthetic effort), Kevin Hänni, Barney Walker, Paul Lusby (especially for having listened to me when the relations with my fumehood neighbour were rather tense), Steven Goldup (I'm happy we put our first disagreement aside, and I'm grateful to him for the various useful discussions we had) and James Crowley. Special thanks also to Diego Gonzalez-Cabrera, Mark "de" Symes, Max von Delius and Paul "phenomenal" McGonigal for being patient the numerous times the NMR machine crashed.

As far as collaborators at other universities are concerned, big thanks should go to Dr. Sébastien Papot at the University of Poitiers (France) whose help has been crucial for the elaboration of rotaxane pro-peptides and for helping me write this thesis. Alex Slawin at the University of St. Andrews is gratefully acknowledged for solving an X-ray crystal structure from a particularly poor quality crystal.

Then there are those guys that I didn't get to work with directly, but that have helped to make the Group such a great place to work, in (roughly) chronological order: Euan, Nick, Barney, Drew, Anne-Marie, Julia, Smilja, Steve Mason, Stewart, Laure, Weiquan, Chin-Fa, Andrea, Roy, Marius, Mark (for teaching me the art of Scottish accent impressions and for keeping some level of anarchy in the bay!), Tao, Mike, Monica, Luciana, Bryan, Amaya, Edzard, Satoshi, Daniel, Romen, Max (for having

kept me company in the HPLC room in those difficult moments struggling with the old stubborn apparatus), Christiane, Michael, David (for the secret foot-volley ball games we had in the office), Nathalie, Takeshi, Dominik, Philip, Adam, Katherine, Barry, Jhenyi and all the others that I have surely forgotten…

Amongst my companions special thanks should go to Dr. Mark Symes and Dr. Vicki Ronaldson for (very high quality) proofreading of this thesis.

Thanks also to all the support staff here at Edinburgh University: Louise for keeping up with our mess, and for being so helpful. Amanda and Annette upstairs, Kenny, Tim, Derek and Raymond in stores, Alan Taylor, John Dalrymple and Paul Angus in the mass spec. room and Juraj Bella and John Millar in the NMR suite.

A special thanks should go to Vincent Kielwasser whose incredible CNC milling skills allowed our old Gilson HPLC machine to have greater dwelling volumes than any modern "formula 1" HPLC!

And then there's the people that really matter: the people who don't work in the Chemistry Dept. I have had the chance of spending my three "and a bit more" years of PhD in the company of the most easy-going people ever. Huge thanks must go to my adored house-mates, with whom I have had, without any doubt, the best time of my whole studies. Sergio, Jamie, Emily, Susana, Thomas, Daphne and Kim.

Many thanks to you Hélène, for all your patience and love throughout the years. Thanks for your help and support during the long writing-up period.

And finally, the family. Thank you to Lisa, Laetitia and my parents. Their counsel, love and support (financial, emotional, practical) have seen me through almost ten years of University education – this thesis is for you.

List of Abbreviations

δ	Chemical Shift
ACE	Angiotensin converting enzyme
AcOH	Acetic acid
Bipy	2,2'-Bipyridine
BOC	*tert*-Butyloxycarbonyl
BOP	Benzotriazol-1-yloxytris(dimethylamino)-phosphonium hexafluorophosphate
Calc.	Calculated
CPK	Corey-Pauling-Koltun
dec.	Decomposes
DIPEA	Diisopropylethylamine
DMAP	4-Dimethylaminopyridine
DMF	*N,N'*-Dimethylformamide
DMSO	Dimethylsulfoxide
DNA	Deoxyribonucleic acid
EDCI	1-(3-Dimethylaminopropyl)-3-ethylcarbodiimide hydrochloride
EDTA	Ethylenediaminetetraacetic acid
equiv.	Equivalent(s)
ESI	Electrospray ionisation
Et_2O	Diethyl ether
EtOAc	Ethyl acetate
EtOH	Ethanol
FAB	Fast atom bombardment
HATU	O-(7-Azabenzotriazol-1-yl)-N,N,N',N'-tetramethyluronium Hexafluorophosphate
H-bond	Hydrogen bond
HBTU	O-Benzotriazol-1-yl-N,N,N',N'-tetramethyluronium Hexafluorophosphate
HOBt	1-Hydroxybenzotriazole hydrate
HRMS	High resolution mass spectrometry

J	Coupling constant
LRMS	Low resolution mass spectrometry
Me	Methyl
MeOH	Methanol
MHz	Megahertz
min	minutes
m.p.	Melting Point
MS	Mass spectrometry
m/z	Mass-to-charge ratio
NEt_3	Triethylamine
NMP	*N*-Methylpyrrolidone.
NMR	Nuclear magnetic resonance
3-NOBA	3-Nitrobenzyl alcohol
Petrol.	Petroleum ether
Ph	Phenyl
ppm	Part(s) per million
PTSA	4-*para*-Toluenesulfonic acid
quant.	Quantitative
R_F	Retention front
RP	Reverse phase
RT	Room temperature
R_t	Retention time
TBTU	O-Benzotriazol-1-yl-N,N,N',N'-tetramethyluronium Tetrafluoroborate
TFA	Trifluoroacetic acid
THF	Tetrahydrofuran
THIOG	Thioglycerol
TLC	Thin layer chromatography

Note: conventional abbreviations for units and physical quantities are not included.

General Remarks on Experimental Data

Unless stated otherwise, all reagents were purchased from commercial sources and used without further purification. Dry CH_2Cl_2, $CHCl_3$, THF, MeCN, toluene, and DMF were obtained by passing them through an activated alumina column on a PureSolv^{TM} solvent purification system (Innovative Technologies, Inc., MA). Petrol refers to the fraction of petroleum ether boiling in the range 40-60 °C.

Flash column chromatography was carried out using Kiesegel C60 (Fisher) as the stationary phase, size exclusion chromatography was carried out on a Bio-Rad econo-column (1.5 × 120 cm) packed with Tosoh Toyopearl HW-40 (S-grade, 30 μm) resin at a flow rate of 1 ml/ min, preparative TLC was carried out using precoated silica gel plates (2000 microns thick, Silica gel GF, Uniplate, Germany) or precoated Neutral alumina plates (0.25 mm thick, 60F254, Merck, Germany). Analytical TLC was performed on precoated silica gel plates (0.25 mm thick, 60F254, Merck, Germany) and observed under UV light.

All ^{1}H and ^{13}C NMR spectra were recorded on a Brüker AV 400 instrument, at a constant temperature of 300 K, unless stated otherwise. Chemical shifts are reported in parts per million and referenced to residual solvent. Coupling constants (*J*) are reported in hertz (Hz). Carbon NMR spectra were recorded as "pendant" experiments (^{1}H decoupled). Standard abbreviations indicating multiplicity were used as follows: m = multiplet, quint. = quintet, q = quartet, t = triplet, d = doublet, s = singlet, br = broad. All melting points were determined using a Sanyo Gallenkamp apparatus and are uncorrected. Optical rotations were recorded at room temperature (20 °C) on a Jasco DIP-370 polarimeter (using the sodium D-line; 589 nm) and $[\alpha]_D$ are given in units of 10^{-1} deg cm^2 g^{-1}.

Analytical RP-HPLC was carried out on a Gilson instrument composed of 306 pumps, 811C dynamic mixer (100 μL), 806 manometric module and an Applied Biosciences 759A UV detector with a Phenomenex C18 (2) Luna column (2 × 250 mm, 5 μm, 100A) or a Varian Chromspher C8 column (2 × 250 mm, 5 μm, 100A). Preparative RP-HPLC was carried out on a Gilson instrument composed of 306 pumps, 811C dynamic mixer (1.5 ml), 806 manometric module and a 118 UV detector with a Spherisorb ODS2 column (21.2 × 250 mm, 5 μm, 100A). LCMS was

carried out on a Finnigan Mat system composed of an LCQ mass spectrometer, P4000 pumps, and a UV2000 UV detector with a Phenomenex C18 (2) Luna column (2 × 250 mm, 5μ, 100A). H_2O and MeCN were used as mobile phase, buffered with TFA (0.1% v/v, pH ≈ 2).

Preparative RP-HPLC was carried out on a Gilson instrument composed of 306 pumps, 811C dynamic mixer (1.5 ml), 806 manometric module and a 118 UV detector with a Spherisorb ODS2 column (21.2 × 250 mm, 5 μm, 100A), using H_2O and MeCN as mobile phase, buffered with HCOOH (6.6 mmol/L, pH ≈ 3).

Chromatograms were recorded at 220 nm unless stated otherwise. HPLC purity refers to the relative purity of the main product to other detectable impurities. Purity is calculated as the area percentage of UV-positive (220 nm) material eluting under the main peak of the HPLC chromatogram.

Low resolution ESI spectra were recorded either on a Micromass ZMD or on a Finnigan Mat LCQ spectrometer. MALDI and high resolution ESI spectrometry were carried out by the EPSRC national mass spectrometry service centre (Swansea, UK). FAB mass spectrometry was carried out by the mass spectrometry service at the University of Edinburgh.

The Layout of this Thesis

This thesis is divided into two distinct and non-related parts.

Part 1 expounds the results from a side project developed besides the main project. Chapter one introduces the synthesis of interlocked architectures chronologically. Chapter two is presented in the form of an article that has already been published in a peer-reviewed journal. No attempt has been made to re-write this work out of context, other than to insert references where appropriate and to ensure consistency of presentation throughout this Thesis. This Chapter is reproduced in the Appendix, in its published format.

Part 2 represents the main core of this thesis, composed of three closely related chapters. The first chapter of this second part, Chapter three, outlines some pertinent examples of natural interlocked molecules and the synthesis of synthetic analogues with emphasis on peptide containing structures. Some examples where mechanical interlocking is used to encapsulate substrates are expounded, along with a detailed discussion of the design of future synthetic rotaxane-encapsulated peptide carriers. Chapter four focuses on the optimisation of a methodology developed in the group for the synthesis of peptido-rotaxanes of long peptides. This methodology is then used to synthesize an anticancer therapy-compatible anticancer peptide rotaxane carrier in Chapter five. Chapter six is dedicated to the study of self-immolative stoppers and the functionalization of the macrocycle constituent of peptide carrier models for ligand-targeted anticancer therapy.

CHAPTER ONE

From statistical to active template synthesis of interlocked architectures

"Whoever undertakes to set himself up as a judge of Truth and Knowledge is shipwrecked by the laughter of the gods."

Albert Einstein

1 Synopsis

During the latter half of the 20th century a more comprehensive understanding of the weak forces that govern intermolecular interactions evolved into the interdisciplinary field now known as supramolecular chemistry. One particular application of supramolecular chemistry has been the exploitation of non-covalent forces for the synthesis of mechanically interlocked molecules. The study of such compounds, which was once the domain of a handful of pioneering chemists, has rapidly evolved into an important field in its own right.

A wealth of different supramolecular interactions has been exploited to direct the formation of interlocked architectures. Although Template-directed syntheses are the only methods that produce interlocked molecules in respectable yields, new methodologies for the assembly of such molecules are still being developed. Indeed, the main challenges are to improve the efficiency of the assembly step and to widen the selection of substrates that these reactions can be applied to. This work is of capital importance for the development of (currently highly synthetically demanding) interlocked-architecture-based molecular machines.

This chapter will cover briefly the history of catenane, rotaxane and knot synthesis through the last four decades and summarize the most common templating methods that have been used to date. Finally, a recently developed 'Active Template' technique by Leigh and co-workers for the synthesis of rotaxanes and catenanes will be presented.

1.1 Definition and nomenclature

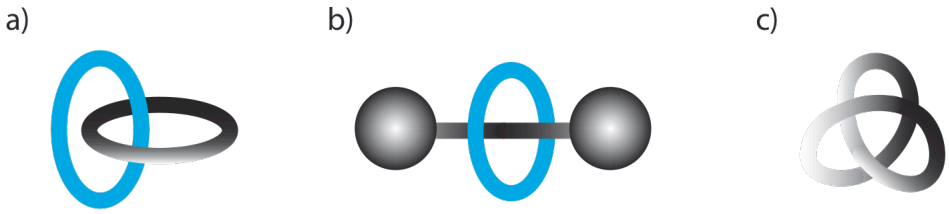

Figure 1.1. Cartoon representations of a) a [2]catenane, b) a [2]rotaxane, c) a trefoil knot

Unambiguous scientific definitions have been assigned to the different classes of mechanically interlocked molecular architectures. A catenane (Figure 1.1.a) consists of two or more interlocked macrocycles connected like links in a chain. In a rotaxane (Figure 1.1.b) one or more macrocycle circumscribe a 'thread' comprised of a linear component terminated by two bulky end groups. Normally, a numerical prefix is added to the descriptor to denote the number of species that are associated, e.g. a [3]catenane is made up of three linked macrocycles. A trefoil knot (Figure 1.1.c) is the simplest non-trivial entangled molecule and, as its name suggests, contains three crossing points within its structure. Critically, all three species depicted in Figure 1.1 are molecules *not supramolecular complexes*, as covalent bonds must be broken in order to separate the mechanically bound fragments.[1]

Three distinct strategies have historically been employed for the synthesis of mechanically interlocked architectures: the 'statistical' method, the covalent bond directed synthesis and the template directed synthesis.

1.2 Early synthetic methodologies to interlocked architectures

1.2.1 Statistical method

The first mechanically interlocked architectures to be realized synthetically were assembled in the absence of any favourable intercomponent interactions using a technique commonly referred to as the 'statistical' method. This concept relies on the statistical threading of one ring by a linear molecule, which is to be formed into the second ring. Although the existence of interlocked molecular rings was discussed, according to Schill,[2] as early as 1912 by Willstätter, it was only at the beginning of the 1960s that Frisch and Wasserman synthesized the first interlocked rings (Figure 1.2).[3]

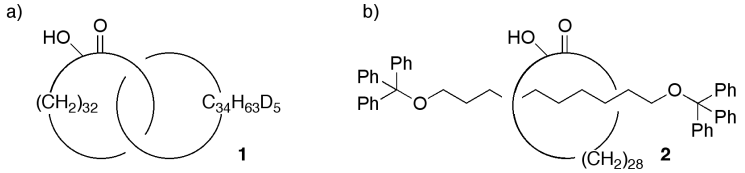

Figure 1.2. Early examples of interlocked molecules reported by a) Wasserman, b) Harrison.

They demonstrated that acycloin condensation of a diester in the presence of a partly deuteriated cyclic hydrocarbon yielded a small amount of catenane. The latter could not be isolated but they provided strong evidence of its formation. Even if this example has no synthetic value, historically it is of great importance because it proved that scientists' early thoughts on interlocked architectures were not only speculation.

From a preparative point of view, statistical threading became significant by the work of Zilkha.[4] Statistical threading of a crown polyether by poly(ethylene glycol)400 led to catenane in 14% yield after cyclization in high-dilution conditions.

Randomness, which is a highly limiting factor in the statistical syntheses of the catenanes discussed above, may become less determining if the threading process is favoured by an even weaker interaction between the linear thread and the ring. As early as 1958, Lüttringhaus *et al.* discussed the formation of a rotaxane-like inclusion between α or β-cyclodextrin and an aromatic long chain dithiol. Unfortunately they could not achieve the expected ring closure that would have led to a catenane

1.2.2 Covalent bond directed synthesis

Four years after Wasserman reported the first [2]catenane synthesis, Schill and Lüttringhaus described the use of covalent bonds as templates in the first 'directed' synthesis of a mechanically interlocked molecule.[2,5] Their elegant synthetic pathway is shown in scheme 1.1. In this multistep synthesis, the carefully planned geometry of intermediate 3 (bond angles, bond lenghts, tetrahedral structure of the ketal carbon atom, size of the polymethylene macrocycle, lengths of the alkyl chloride chains) directs intramolecular macrocyclization in a unique and predetermined way (Schme 1.1).

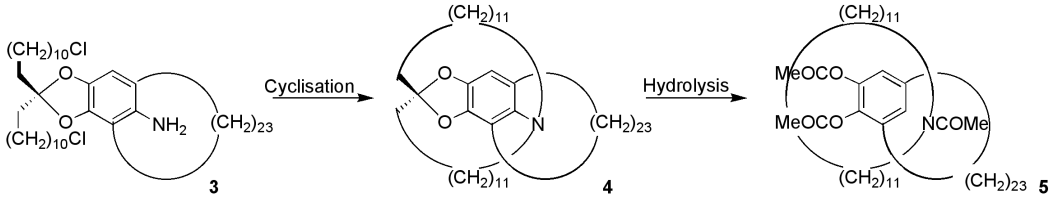

Scheme 1.1. Schill's covalent bond-directed synthesis of a [2]catenane.

Alkylation of the amino group occurs only with the two alkyl chloride chains located one above and one below the plane of the central benzene ring to give **4**. Selective cleavage of the aryl-nitrogen bond and hydrolysis of the ketal group leads to [2]catenane **5**.

The feasibility of constructing mechanically interlocked architectures using a covalent bond template is well illustrated by Schill's ingenious synthetic routes. However, such routes require many synthetic steps and a high level of technical expertise, thus limiting the study of these novel compounds.

1.1. Template directed synthesis of interlocked architectures

1.2.3 Transition metal directed synthesis of catenanes and rotaxanes

Schill's directed synthesis of catenanes may be considered as relying on a central core, the benzo-ketal group, around which the different rings are built up. Another central core around which interlocked architectures could be build, in the way Frisch and Wasserman defined it,[6] could be a transition metal. Interestingly such an

approach was evoked (the term template effect was not used in 1961 or 1972), twice in the past. In 1961 by Frisch and Wasserman[6] and in 1972 by Sokolov.[7]

It was later, in 1983,[8] that Sauvage and co-workers achieved the first metal templated synthesis of a [2]catenane and turned interlocked architectures from chemical curiosities into accessible molecules.

The Strasbourg group took advantage of the ability of transition metals to organize ligands in a predictable spatial orientation creating a crossover point that directs subsequent macrocyclization reactions in an intertwined manner. The preferred tetrahedral geometry of Cu(I) was employed to organize the two bidentate phenentroline ligands **6** in an mutually orthogonal manner (Scheme 1.2, Route A). Alkylation of **7** with a bisalkyl-iodide led to the metallocatenane **8** or *catenate* in 27% yield.

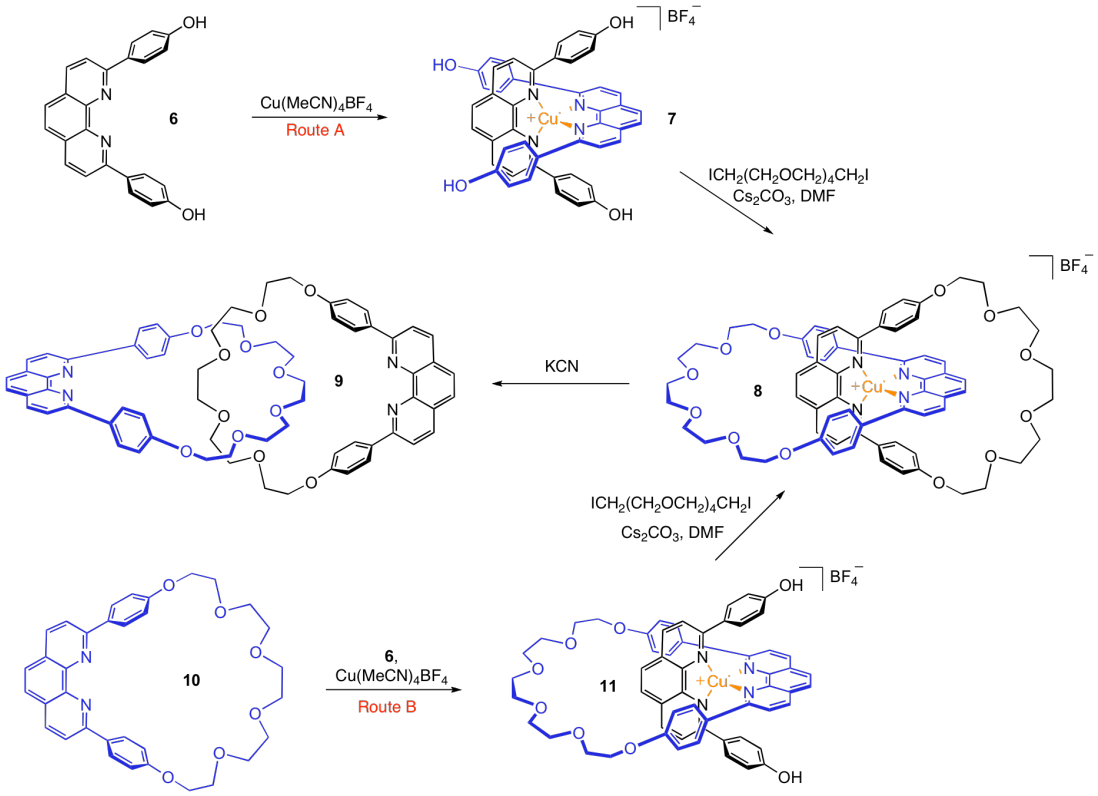

Scheme 1.2. Sauvage's original Cu(I) directed [2]catenate synthesis.

This catenate was de-metallated to give the *catenand* **9** using KCN. The yield was subsequently improved by synthesizing macrocycle **10** and complexing it with an appropriately derivatized phenanthroline unit to give pre-catenane **11**, followed by macrocyclization to furnish the corresponding [2]catenane in 40% yield (Scheme 1.2., Route B).

The first synthesis of a rotaxane based on a metal template was reported by Gibson and co-workers, elaborating on the Sauvage phenanthroline/Cu(I) core (Scheme 1.3).[9] The pseudo-rotaxane **12** was treated with a trityl-terminated alkyl halide and subsequently de-metallated to give rotaxane **13** in 42% yield.

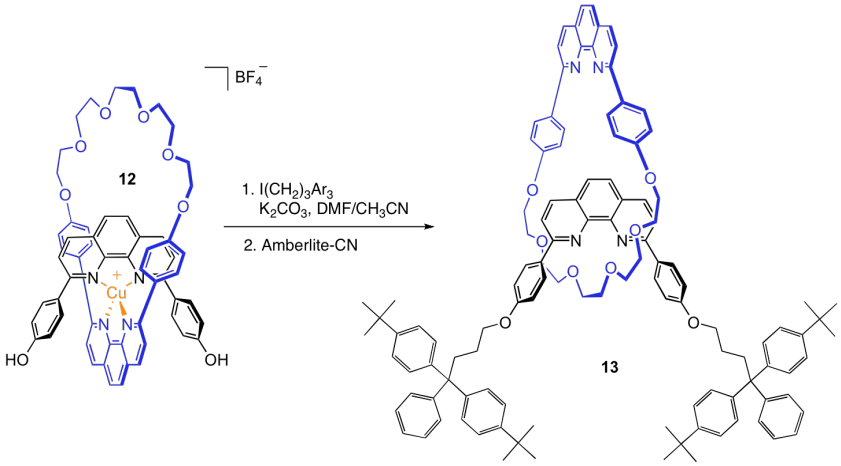

Scheme 1.3. Gibson's Cu(I)-phen based rotaxane synthesis.

1.2.4 Copper mediated synthesis of molecular knots

Schill and co-workers conceived and attempted direct synthesis of a trefoil knot before the 1980s.[10] This strategy, which relied on a benzoacetal central core, is closely related to the one used to prepare catenanes. Unfortunately no desired product could be identified in their case. Following these attempts and building on the copper (I) core, Sauvage reported the first molecular trefoil knot in 1989 (Scheme 1.4),[11] with its intertwined topology confirmed by X-ray crystallography a year later.[12]

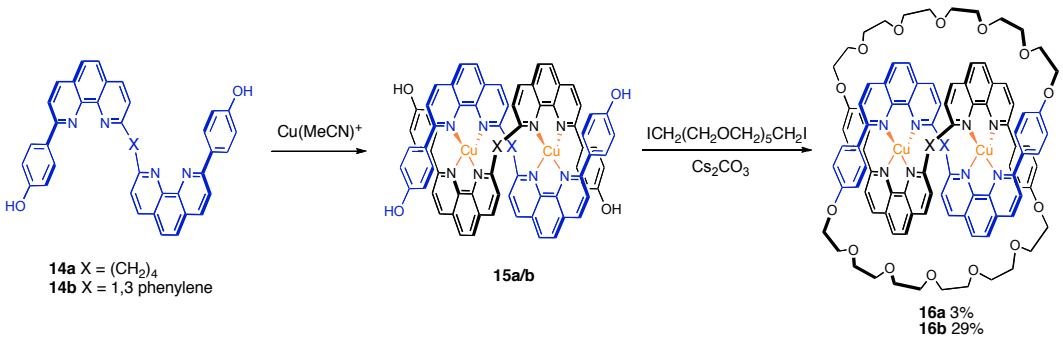

Scheme 1.4. Synthesis of a trefoil knot.

In this strategy, the disposition of two bisphenantroline ligands in a helical arrangement is exploited for the formation of the knot. Two molecules of bis-chelating threads **14** are bound in a tetrahedral manner on two copper (I) centres, leading to double helix **15**. After double macrocyclization to form **16** followed by de-metallation, a knotted system was obtained.

The initial ligand, **14a**, was composed of a $(CH_2)_4$ linker between the two phenantroline units to prevent the complexation of one ligand around a single Cu(I) ion. However it was observed that the desired helical complex, **15a**, was relatively labile and thus able to interconvert with its co-planar analogue. This facile exchange led to a modest 3% yield of **16a** following Williamson reaction. Replacing the $(CH_2)_4$ linker with the more rigid 1,3-phenylene group (**14a→14b**) increased the yield to an excellent 29% of **16b**.[13]

1.3 The assembly of mechanically interlocked molecules using non-transition metal template-based methodologies

Following Sauvage's success, template-directed synthesis has become the only way of synthesizing interlocked architectures. To date, most of these routes depend on the use of neutral or cationic species to achieve the desired template effect, utilizing a variety of noncovalent forces such as metal-ligand coordination, hydrogen bonding, π-π stacking, or hydrophobic interactions.

The template-directed synthesis of rotaxanes and catenanes can be classified in two[14] main strategies: the 'clipping' strategy proceeds *via* a preformed thread (or macrocycle) coordinated to a 'u-shape' which is closed, or 'clipped' around the thread (or macrocycle). The macrocycle may also be assembled around the thread from multiple fragments in this strategy. In the 'stoppering' approach, the axle is threaded through the macrocycle, followed by attachment of the stoppers (Figure 1.3).

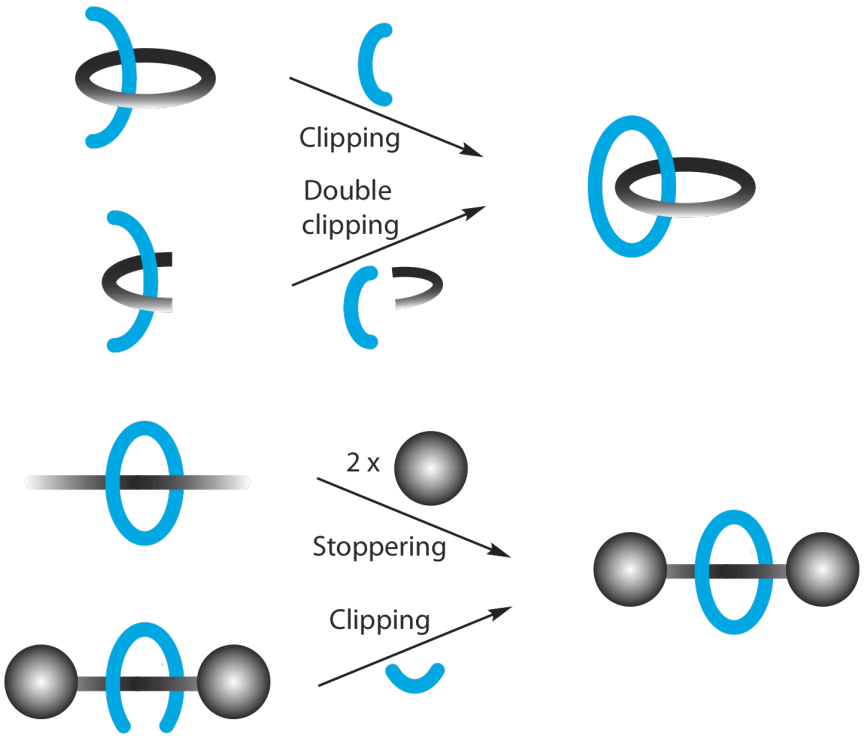

Figure 1.3. Schematic representations of clipping approaches to catenanes and stoppering and clipping approach to rotaxanes.

1.3.1 Hydrophobic effect

The most extensively studied type of rotaxanes formed by the use of the hydrophobic effect is those with a cyclodextrin (CD)-based structure. The CDs posses a hydrophilic exterior, due to the hydroxyl groups on the outer surface, and a hydrophobic core due to the carbon-containing carbohydrate backbone. Such structural properties make them both water-soluble and convenient hosts for complexing lipophilic molecular guests in water.

The group of Ogino first exploited these properties for the synthesis of rotaxanes in 1981.[15] Rotaxane, made from a β-CD and a diaminoalkyl thread was synthesized *via* two slightly different routes (scheme 1.5). Both routes rely on a similar threading event carried out in DMSO and afforded rotaxane in 5% (route A) and 7% (route B) yields.

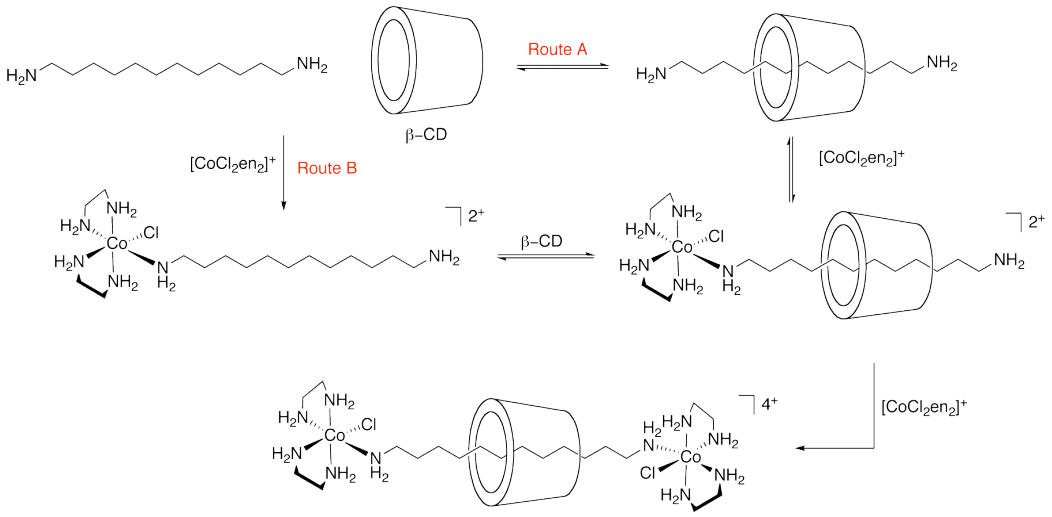

Scheme 1.5. Ogino's cyclodextrin-based [2]rotaxane.

Several other groups have successfully employed the hydrophobic effect to synthesize interlocked molecules based on cyclodextrins. In particular, Harada[16] and Anderson[17] have intensively investigated CD-based rotaxane and polyrotaxane formation. It has proved more difficult to assemble catenanes using cyclodextrins, but such molecules were realized for the first time by Stoddart in 1993. [18]

1.3.2 Aromatic interactions

The discussion of synthetic molecular architectures assembled using aromatic interactions must be centred on the extensive research of Stoddart and co-workers. In the late 1980s they began developing a self-assembly approach to interlocked architectures, based on previous observations of paraquat and a crown forming a host-guest complex.[19] The ability of the π-electron deficient paraquat derivative **17** and π-electron donating macrocycles such as **18** (bis-*p*-phenylene-34-crown-10) to form host-guest complexes was thus used to direct the synthesis of interlocked architectures. The first catenane based on this system was synthesized in 1989 (Scheme 1.6).[20] Treatment of an acetonitrile solution of **17** and **18** with 1,4 dibenzyl bromide resulted in the formation of catenane **19** in an impressive 70% yield.

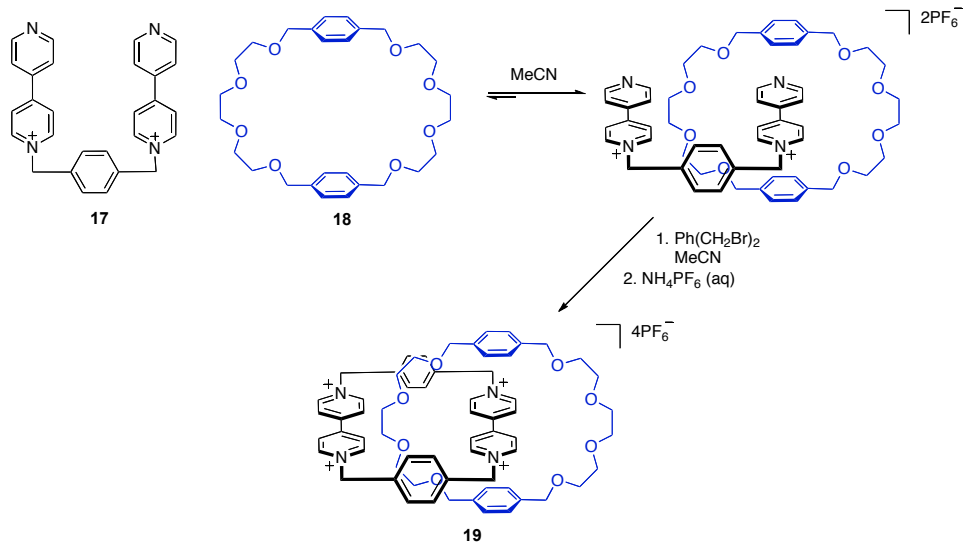

17 18 19

Scheme 1.6. Synthesis of Stoddart's original paraquat-crown ether [2]catenane.

Stoddart and co-workers have mastered the art of building interlocked architectures using the paraquat-crown ether association and have described a wide variety of different structures based on this motif.[21] Almost a decade after the synthesis of their first catenane the group applied the same methodology the synthesis of molecular knots.[22]

1.3.3 Hydrogen bonding interactions

Typically, hydrogen bonds are much weaker than covalent bonds or those in metal complexes. As a consequence, effective H-bonding templates generally contain multiple recognition sites. The most effective H-bonding templates are those with a high level of preorganization.

1.3.3.1 Ammonium-Crown Ether-Based Rotaxanes

Concurrently, Stoddart and Busch demonstrated that dibenzo-24-crown-8 (DB24C8) could form strong inclusion complexes with secondary dialkylammonium cations. [2]Rotaxane **20**, assembled using this system was published by Busch and co-workers in 1995 (Figure 1.4.a).[23]

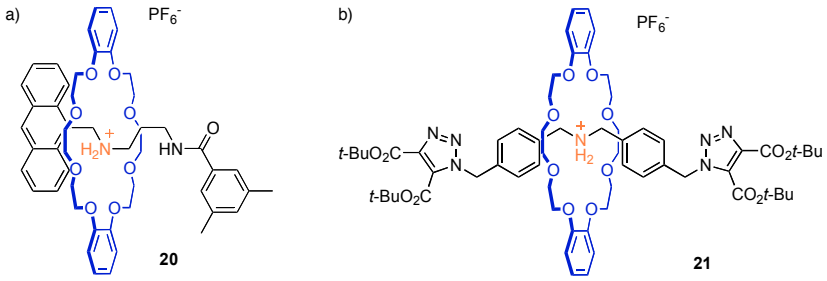

Figure 1.4. Original ammonium-crown ether rotaxanes reported by a) Busch, b) Stoddart.

Stoddart and co-workers showed that the same crown ether and a dibenzyl ammonium ion formed a 1:1 complex. They then went on to describe the synthesis of rotaxanes such as **21**, synthesized by 'capping' the thread component with bulky terminating groups (Figure 1.4.b).[24]

1.3.3.2 Anion-Based Catenanes and Rotaxanes

Vögtle reported the first example of a rotaxane assembled around an anionic phenolate template in 1999.[25] Using a tetra-lactam macrocycle **22**, they took advantage of its hydrogen bonding ability towards anionic species to template the formation of a [2]rotaxane in an impressive yield of 95% (Scheme 1.7). The authors rationalized this yield by the reaction of dibromide **24** with the phenoxide-macrocycle complex **[22+23]** to form mono-stoppered thread **25**. The latter then dissociates from the macrocycle and reacts with another phenoxide-macrocycle complex to form the [2]rotaxane **26** (Scheme 1.7).

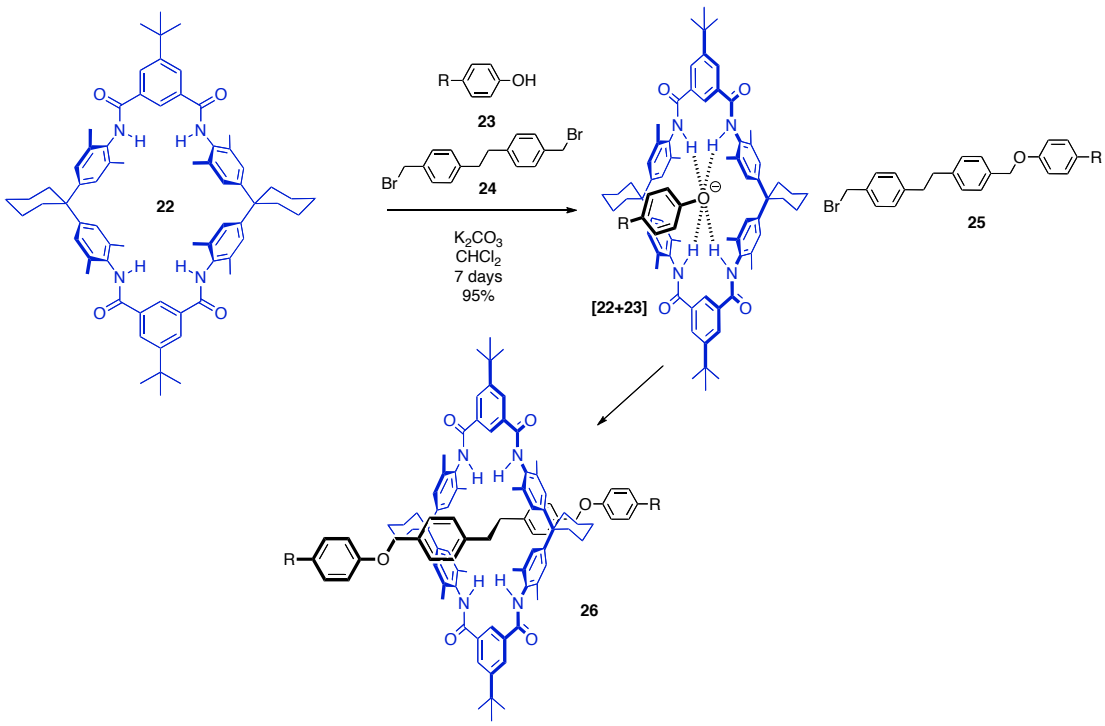

Scheme 1.7. Synthesis of Vögtle [2]rotaxane assembled using a phenoxyde template.

More recently, Beer and co-workers have elegantly shown how chloride ion recognition can be utilized to assemble rotaxanes[26] and catenanes.[27]

1.4 Active template strategies to interlocked architectures

1.4.1 Basic principle of active-metal template

Most template-directed approaches to rotaxanes developed to date require at least stoichiometric quantities of a template, which often involves pre-established strongly binding recognition motifs that 'live on' in the mechanically interlocked molecule that is formed. Besides holding the reactive fragments in an orientation that directs interlocking, the template is generally otherwise passive during the reaction. Building on the principles of transition metal catalysis, the group of Leigh[28] developed a strategy in which template ions could also play an active role in promoting the crucial final covalent bond forming reaction that captures the interlocked structure (i.e. the metal has a dual function; acting as a template for entwining the precursors and catalyzing covalent bond formation between the reactants). This 'active-metal'[29] template process is shown schematically in Figure

1.5 in both stoichiometric (one equivalent of the active template is required) and catalytic (the active template turns over during the reaction) versions.

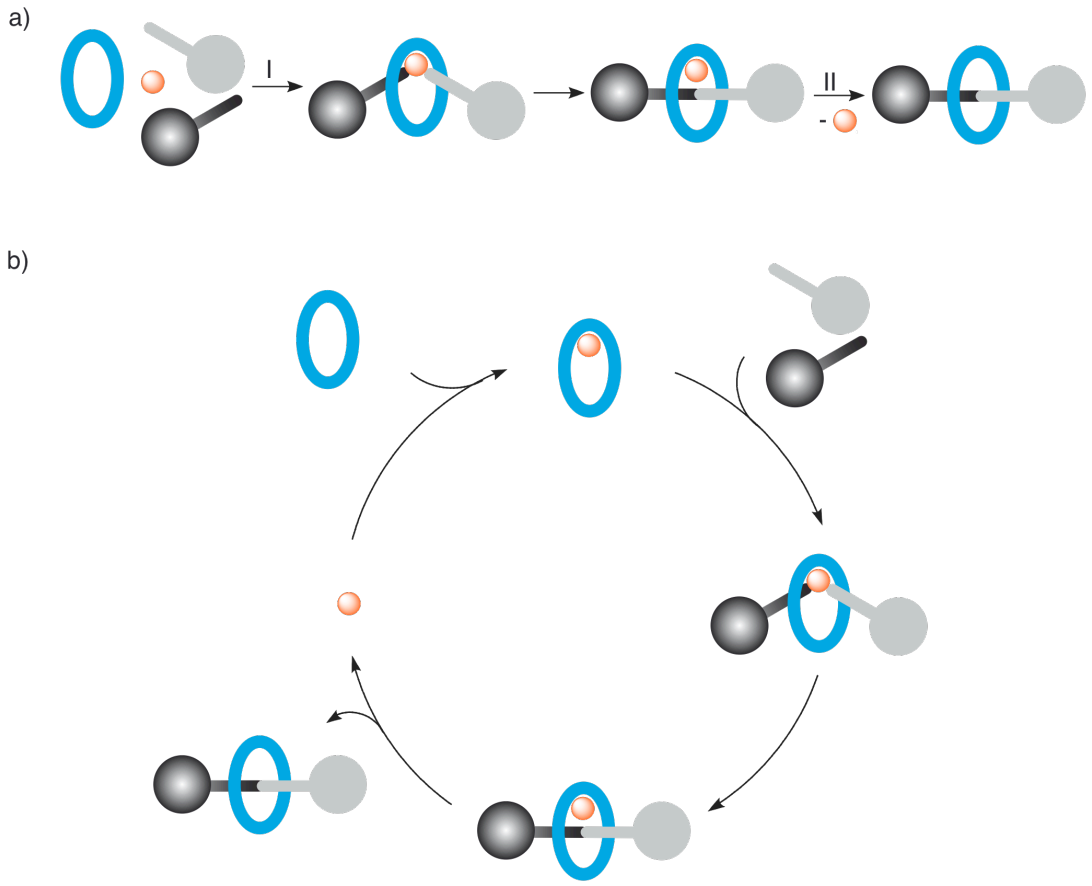

Figure 1.5. The 'active template' strategy to rotaxane architectures. The formation of a covalent bond between the green and orange stoppered units to generate the thread is promoted by the catalyst (shown in grey) and directed through the cavity of the macrocycle (shown in blue) by the catalyst's coordination requirements. (a) (I) Stoichiometric active-metal template synthesis of a [2]rotaxane, (II) subsequent de-metallation; (b) Catalytic active-metal template synthesis of a [2]rotaxane.

There are several potentially attractive features of such a synthetic approach to mechanically interlocked architectures, including:

i) The inherent efficiency of a reaction in which the metal-macrocyclic species performs multiple functions.

ii) The strategy should prove applicable to many different types of well-known transition metal catalyzed (and even organocatalytic) reactions.

iii) The lack of requirement for permanent recognition elements in each component of the interlocked product increases the structural diversity possible in catenanes and rotaxanes and enables their formation to be 'traceless'.

iv) In some cases only substoichiometric quantities of the active template may be required (i.e. the catalytic active-metal template variant, Figure 1.5.b).

v) Reactions that only proceed through a threaded intermediate would allow access to several currently inaccessible mechanically linked macromolecular architectures; and, finally.

vi) The coordination requirements during key stages of the catalytic cycle of active-template reactions could provide insight into the mechanisms of metal-catalyzed reactions.

1.4.2 CuAAC active template formation of rotaxanes

In their first report,[28] they utilized the so called "click" Cu(I)-catalyzed Alkyne-Azide cycloaddition (CuAAC) popularized by Meldal and Fokin a few years before (Scheme 1.8). The macrocycle bearing an endotopic pyridine motif is bound to the copper atom in such a way that the metal-mediated bond formation is directed toward the cavity of the macrocycle.

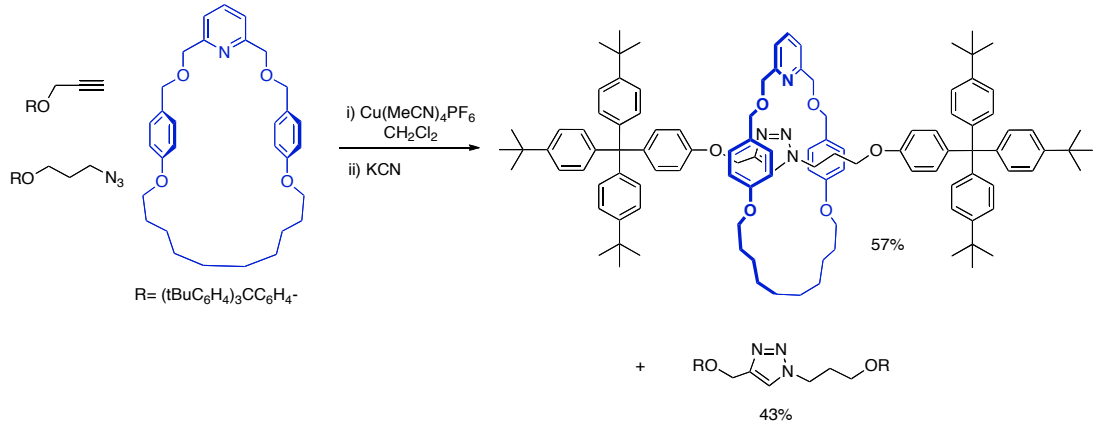

Scheme 1.8. Active-metal template synthesis of triazole containing rotaxanes *via* CuAAC reaction

Simple stirring of a mixture containing the endo-pyridine macrocycle, $Cu(MeCN)_4PF_6$, and azide and alkyne functionalized half-stoppered threads in CH_2Cl_2 overnight, followed by KCN treatment, gave an impressive 57% yield of [2]rotaxane which was increased to 94% using 5 equivalents of half-stoppered in respect to macrocycle (Scheme 1.8). Addition of pyridine to the reaction mixture avoided Cu(I) to be sequestered in the reaction product and thus allowed the metal to

be reused in a further transformation step. Yields were as high as 82 % with only 20 mol% mol of copper catalyst and 3 equivalent of pyridine.

1.4.3 Active-metal templated sythesis of rotaxanes and catenanes *via* Glaser alkyne homo-coupling and C-S bond formation reaction

This methodology proved to be attractive and was adopted soon afterwards by the group of Saito. The Japanese group made use of a Sauvage-type phenantroline-based macrocycle to synthesize [2]rotaxanes[30] and [2]catenanes (Scheme 1.9).[31]

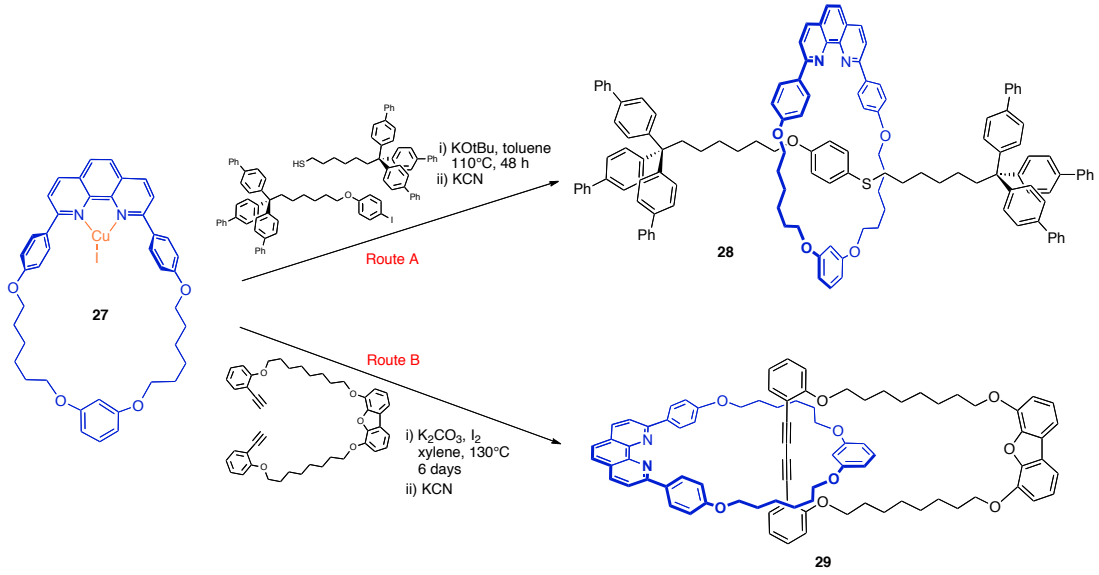

Scheme 1.9. Saito's synthesis of rotaxanes and catenanes *via* active-metal template copper (I) catalyzed reactions

Their procedure was slightly different to the CuAAC example: a Cu(I) iodide macrocycle complex, **27**, was reacted with suitably functionalized half-stoppered threads (Route A) and bis-functionalized U-shaped molecule (Route B) to form [2] rotaxanes and [2]catenanes, respectively. Glaser alkyne homo-couplings and C-S bond formation proved efficient and gave, under optimized conditions, rotaxane in 72% and 27% (**28**) respectively and 64% of [2]catenane **29** (Scheme 1.9). Both these yields were obtained under large excess of substrates and of the majority of the side products were non-interlocked components.

1.4.4 Active-metal templated synthesis of molecular machines

Several other examples of active-metal templated synthesis of rotaxanes have been described over the past three years,[32] and the active-metal template has also been applied to the synthesis of more complex architectures.[33,34] The Cadiot-Chodkiewicz reaction could be well adapted to the method using a bipyridine-based macrocycle. Homo and hetero-coupled adducts were obtained in very good yields and with very good selectivity. A switchable molecular shuttle, which would be difficult or impossible to access *via* traditional methods, was synthesized *via* this Cadiot-Chodkiewicz active template method, demonstrating the usefulness of the reaction (Scheme 1.10).[34]

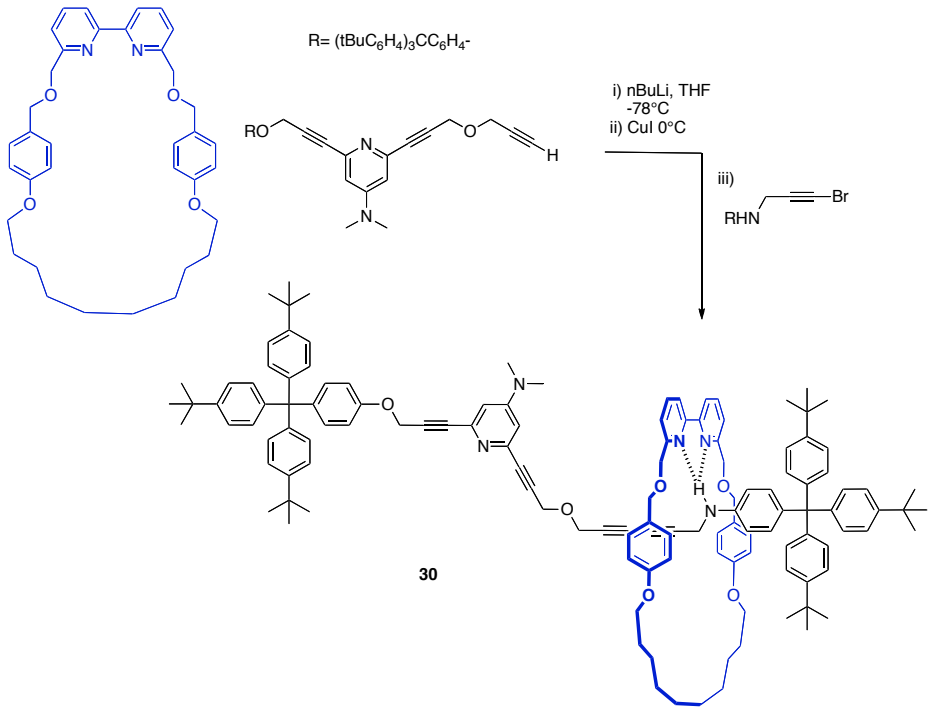

Scheme 1.10. Cadiot-Chodkiewicz active template synthesis of molecular shuttles.

The single H-bond contact that exists between the aniline group of the thread and the bipyridine of the macrocycle is too weak to template rotaxane formation through 'stoppering' or 'clipping' strategies and the bipyridine-pyridine combination would not easily accommodate a metal for passive templated synthesis. Molecular shuttle **30** was obtained in 61% yield, with no homo-coupled rotaxane products being detected.

1.5 References and notes

[1] J. S. Hannam, S. M. Lacy, D. A. Leigh, C. G. Saiz, A. M. Z. Slawin, S. G. Stitchell, *Angew. Chem., Int. Ed.,* **2004**, *43*, 3260-3264.

[2] G. Schill, *Catenanes, Rotaxanes and Knots*; Academic Press: New York, 1971.

[3] E. Wasserman, *J. Am. Chem. Soc.,* **1960**, *82*, 4433-4.

[4] G. Agam, D. Graiver, A. Zilkha, *J. Am. Chem. Soc.,* **1976**, *98*, 5206-5214.

[5] G. Schill, A. Luttringhaus, *Angew. Chem. Int. Ed.,* **1964**, *3*, 546-547.

[6] H. L. Frisch, E. Wasserman, *J. Am. Chem. Soc,* **1961**, *83*, 3789.

[7] V. I. Sokolov, *Russ. chem. rev.,* **1973**, *42*, 452-463.

[8] C. O. Dietrichbuchecker, J. P. Sauvage, J. P. Kintzinger, *Tetrahedron Lett.,* **1983**, *24*, 5095-5098.

[9] C. Wu, P. R. Lecavalier, Y. X. Shen, H. W. Gibson, *Chem. Mater.,* **1991**, *3*, 569-72.

[10] G. Schill, G. Doerjer, E. Logemann, H. Fritz, *Chem. Ber.,* **1979**, *112*, 3603-3615; Boeckman.J, G. Schill, *Tetrahedron,* **1974**, *30*, 1945-1957.

[11] C. O. Dietrichbuchecker, J. P. Sauvage, *Angew. Chem. Int. Ed.,* **1989**, *28*, 189-192.

[12] C. O. Dietrichbuchecker, J. Guilhem, C. Pascard, J. P. Sauvage, *Angew. Chem. Int. Ed.,* **1990**, *29*, 1154-1156.

[13] C. O. Dietrich-Buchecker, J. F. Nierengarten, J. P. Sauvage, N. Armaroli, V. Balzani, L. De Cola, *J. Am. Chem. Soc.,* **1993**, *115*, 11237-44.

[14] It should be noted that a third approach to pseudorotaxane assembly, 'slippage', also exists, whereby a system is heated so that the ring may slip over the stoppers, where it is kinetically trapped upon cooling. However this is not template-directed and the molecules produced are not, according to the IUPAC definition, rotaxanes, see: IUPAC Compendium of Chemical Terminology - the Gold Book (http://goldbook.iupac.org/index.html). Date of access 26/01/09.

[15] H. Ogino, *J. Am. Chem. Soc.,* **1981**, *103*, 1303-1304.

[16] A. Harada, *Acc. Chem. Res.,* **2001**, *34*, 456-464.

[17] M. R. Craig, T. D. W. Claridge, M. G. Hutchings, H. L. Anderson, *Chem. Commun.,* **1999**, 1537-1538; S. Anderson, T. D. W. Claridge, H. L. Anderson, *Angew. Chem., Int. Ed.,* **1997**, *36*, 1310-1313; C. A. Stanier, M. J. O'Connell, W. Clegg, H. L. Anderson, *Chem. Commun.,* **2001**, 493-494; M. R. Craig, M. G.

Hutchings, T. D. W. Claridge, H. L. Anderson, *Angew. Chem., Int. Ed.,* **2001**, *40*, 1071-1074; C. A. Stanier, M. J. O'Connell, W. Clegg, H. L. Anderson, *Chem. Commun.,* **2001**, 787-787; E. J. F. Klotz, T. D. W. Claridge, H. L. Anderson, *J. Am. Chem. Soc.,* **2006**, *128*, 15374-15375.

[18] D. Armspach, P. Ashton, C. P. Moore, N. Spencer, J. F. Stoddart, T. J. Wear, D. J. Williams, *Angew. Chem. Int. Ed.,* **1993**, *32*, 854-858.

[19] B. L. Allwood, N. Spencer, H. Shahriarizavareh, J. F. Stoddart, D. J. Williams, *J. Chem. Soc. Chem. Commun.,* **1987**, 1064-1066; B. Odell, M. V. Reddington, A. M. Z. Slawin, N. Spencer, J. F. Stoddart, D. J. Williams, *Angew. Chem. Int. Ed.,* **1988**, *27*, 1547-1550; J. Y. Ortholand, A. M. Z. Slawin, N. Spencer, J. F. Stoddart, D. J. Williams, *Angew. Chem. Int. Ed.,* **1989**, *28*, 1394-1395.

[20] P. R. Ashton, T. T. Goodnow, A. E. Kaifer, M. V. Reddington, A. M. Z. Slawin, N. Spencer, J. F. Stoddart, C. Vicent, D. J. Williams, *Angew. Chem. Int. Ed.,* **1989**, *28*, 1396-1399.

[21] D. B. Amabilino, J. F. Stoddart, *Chem. Rev.,* **1995**, *95*, 2725-2828; D. Philp, J. F. Stoddart, *Angew. Chem., Int. Ed.,* **1996**, *35*, 1154-1196; D. B. Amabilino, F. M. Raymo, J. F. Stoddart, *Comprehensive Supramolecular Chemistry*, (M. W. Hosseini, J.-P. Sauvage Eds.), Pergamon Press: Cambridge, **1996**, Vol. 9, p 85-130; F. M. Raymo, J. F. Stoddart, *Chem. Rev.,* **1999**, *99*, 1643-1663.

[22] P. R. Ashton, O. A. Matthews, S. Menzer, F. M. Raymo, N. Spencer, J. F. Stoddart, D. J. Williams, *Liebigs Ann.,* **1997**, *1997*, 2485-2494.

[23] A. G. Kolchinski, D. H. Busch, N. W. Alcock, *J. Chem. Soc. Chem. Commun,* **1995**, 1289-91.

[24] P. R. Ashton, P. T. Glink, J. F. Stoddart, P. A. Tasker, A. J. P. White, D. J. Williams, *Chem. Eur. J.,* **1996**, *2*, 729-736.

[25] G. M. Hubner, J. Glaser, C. Seel, F. Vogtle, *Angew. Chem. Int. Ed. Engl.,* **1999**, *38*, 383-386.

[26] J. A. Wisner, P. D. Beer, M. G. B. Drew, M. R. Sambrook, *J. Am. Chem. Soc.,* **2002**, *124*, 12469-12476.

[27] M. R. Sambrook, P. D. Beer, J. A. Wisner, R. L. Paul, A. R. Cowley, *J. Am. Chem. Soc.,* **2004**, *126*, 15364-15365.

[28] V. Aucagne, K. D. Hanni, D. A. Leigh, P. J. Lusby, D. B. Walker, **2006**, *128*, 2186-2187.

[29] 'Active template' is used as a general term to describe a reaction in which a moiety both catalyzes covalent bond formation and acts as a template for the assembly of a particular architecture. The term 'active-metal template' describes a subset of active template reactions in which the 'active' moiety is a metal. A 'catalytic active-metal template' reaction is one in which the metal catalyst turns over; a 'stoichiometric active-metal template' reaction is one in which it does not.

[30] S. Saito, E. Takahashi, K. Nakazono, *Org. Lett.,* **2006**, *8*, 5133-5136.

[31] Y. Sato, R. Yamasaki, S. Saito, *Angew. Chem., Int. Ed.,* **2009**, *48*, 504-507.

[32] J. Berna, J. D. Crowley, S. M. Goldup, K. D. Haenni, A.-L. Lee, D. A. Leigh, *Angew. Chem., Int. Ed.,* **2007**, *46*, 5709-5713; J. D. Crowley, K. D. Hanni, A.-L. Lee, D. A. Leigh, *J. Am. Chem. Soc.,* **2007**, *129*, 12092-12093.

[33] V. Aucagne, J. Berna, J. D. Crowley, S. M. Goldup, K. D. Haenni, D. A. Leigh, P. J. Lusby, V. E. Ronaldson, A. M. Z. Slawin, A. Viterisi, D. B. Walker, *J. Am. Chem. Soc.,* **2007**, *129*, 11950-11963; S. M. Goldup, D. A. Leigh, P. J. Lusby, R. T. McBurney, A. M. Z. Slawin, *Angew. Chem., Int. Ed.,* **2008**, *47*, 3381-3384.

[34] J. Bernà, S. M. Goldup, A.-L. Lee, D. A. Leigh, M. D. Symes, G. Teobaldi, F. Zerbetto, *Angew. Chem., Int. Ed.,* **2008**, *47*, 4392-4396.

CHAPTER TWO

A catalytic 'active-metal' template strategy to [2]rotaxanes, [3]rotaxanes and some observations on the mechanism of the Cu(I)-catalyzed azide-alkyne 1,3-cycloaddition

Published as "*A Catalytic 'Active-Metal' Template Strategy to [2]Rotaxanes, [3]Rotaxanes and Molecular Shuttles and Some Observations on the Mechanism of the Cu(I)-Catalyzed Azide-Alkyne 1,3-Cycloaddition*", V. Aucagne, J. Berná, J. D. Crowley, S. M. Goldup, K. D. Hänni, D. A. Leigh, P. J. Lusby, V. E. Ronaldson, A. M. Z. Slawin, A. Viterisi and D. B. Walker, *J. Am. Chem. Soc.*, **2007**, 129, 11950

Acknowledgments

The following persons are greatfully acknowledged for their contribution to the work in this chapter. Dr. Vincent Aucagne synthesized macrocycles **1b**, **1c**, **1d**, **1e**, **1f**, **1h**, **1i**, **1l** and Rotaxane **4a** for the first time. Dr. Stephen Goldup synthesized macrocycles **1g** and **1j**. Dr. D. Barney Walker carried out the synthesis of macrocycle **1n** for the first time. Dr. Vicki Ronaldson optimized the synthetic route to macrocycles **1a** and **1n**. Paul Lusby synthesized macrocycle **1m**. Dr. James Crowley carried out the synthesis of rotaxane **1k** and performed molecular modeling of macrocycles **1a** to **1o**. Dr. José Bernà synthesized Rotaxanes **S24** and **S26**. Kevin Hänni first carried out the 'Click' rotaxane-forming reactions with macrocycles **1b**, **1c**, **1d**, **1e**, **1f**, **1h**, **1i**, **1n** and carried out copper salt screenings.

Isolation and characterization of rotaxanes **4b**, **4i**, **4j**, **4l**, **4m**, **4n** was done by the author. Rotaxanes **7a** and **7l** were synthesized by the author. Single crystals of **7l** were grown by the author and X-Ray-diffraction was carried out by Dr. Alexandra Slawin (University of St. Andrews). All kinetic studies were carried out by the author.

Patrice Staub and Dr. J.-P. Sauvage (Strasbourg) are greatly acknowledged for generously providing us with a sample of macrocycle **1o**.

2 Synopsis

A synthetic approach to rotaxane architectures is described in which metal atoms catalyze covalent bond formation whilst simultaneously acting as the template for the assembly of a mechanically interlocked structure. This 'active-metal' template strategy is exemplified using the Huisgen-Meldal-Sharpless Cu(I)-catalyzed 1,3-cycloaddition of azides with terminal alkynes (CuAAC), a so-called 'click' reaction. Coordination of Cu(I) to an endotopic pyridine-containing macrocycle allows the alkyne and azide to bind to metal atoms in such a way that the metal-mediated bond-forming reaction occurs through the cavity of the macrocycle or macrocycles forming a rotaxane. A variety of mono- and bidentate macrocyclic ligands are demonstrated to form [2]rotaxanes in this way and, by adding pyridine, the metal can turn over during the reaction giving a catalytic active-metal template assembly process. Under conditions that feature a high macrocycle:copper ratio, [3]rotaxanes (two macrocycles on a thread containing a single triazole ring) are also produced in the active-metal template reaction. The latter observation suggests that under these conditions the mechanism of the Cu(I)-catalyzed terminal alkyne-azide cycloaddition involves a reactive intermediate that features at least two metal ions.

2.1 Introduction

2.1.1 The Cu(I)-Catalyzed terminal alkyne azide cycloaddition (CuAAC reaction)

Recently, there has been a tremendous surge of interest in so-called "click"[1,2] methodologies for functional molecule synthesis, the most popular of which is the Huisgen-Meldal-Sharpless Cu(I)-catalyzed 1,3-cycloaddition of organic azides with terminal alkynes (the CuAAC reaction).[3,4,5] The most common catalyst systems for this reaction employ water or alcohol solvents and use a Cu(II) salt in the presence of a reducing agent (often sodium ascorbate) to generate the required Cu(I) catalyst in situ.[3,6] Metallic copper[3,6] copper clusters[7] or Cu zeolites[8,9] have also been employed as pre-catalysts and, in some cases, Cu(I) salts can be used directly. However, in apolar solvents Cu(I) salts usually require the presence of nitrogen[3,6,10] or phosphorus[11] ligands, or acetonitrile as a co-solvent, to stabilize the Cu(I) oxidation state and undesired alkyne-alkyne homocoupling products are often observed under such reaction conditions.[3,6] The basic mechanism of the CuAAC reaction is believed to be that shown in Scheme 2.1. A [2+3]cycloaddition—the mechanism of the thermal (i.e. uncatalyzed) Huisgen reaction[12]—is ruled out[13] for the Cu(I)-catalyzed reaction on the basis of DFT calculations which show that reaction via a Cu(III)-metallacycle (as shown in Scheme 2.1) is a more favorable pathway by up to 11.7 kcal/mol.[3,14,15,16,17] The same calculations suggest that the rate determining step is the formation of the Cu(III)-metallacycle from a reactive intermediate involving copper-coordinated alkyne and, presumably, azide (organoazido-metal complexes are likely intermediates in many transition metal-mediated reactions of azides and Cu(I)-N_3R complexes have been characterized by X-ray crystallography[18]). However, the exact nature of this reactive intermediate is unclear (Scheme 2.1, A-C).

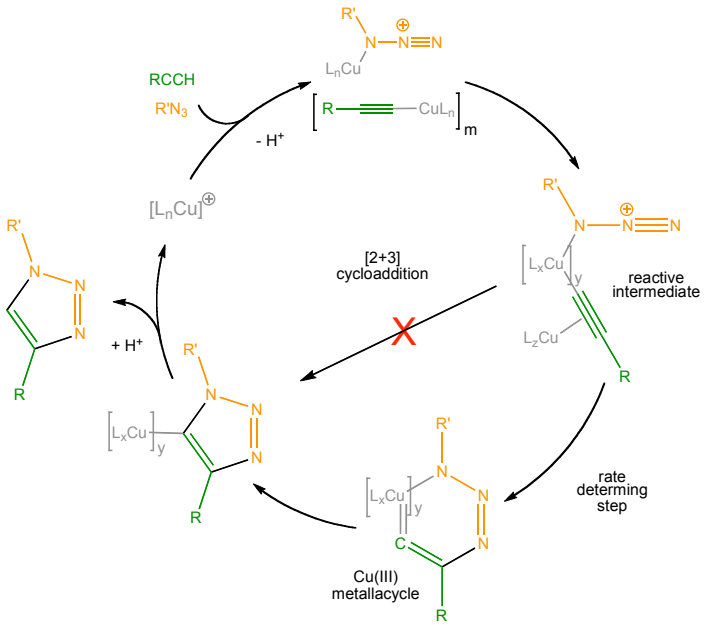

Possible types of reactive intermediate

Type A
(i) one copper atom or (ii) one copper atom + π-activation of Cu-acetylide by a second copper atom

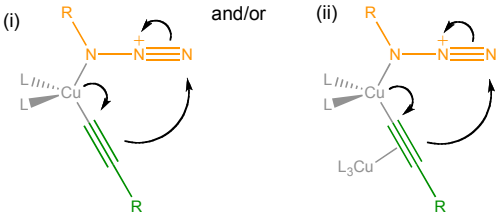

Type B
Glaser-like[x] *bis*-alkyne bridged intermediate - only differs from A (ii) by the two copper atoms being doubly bridged. Doubly-bridged intermediates are not possible with bidentate ligands for copper (assuming RN_3 coordinates to Cu).

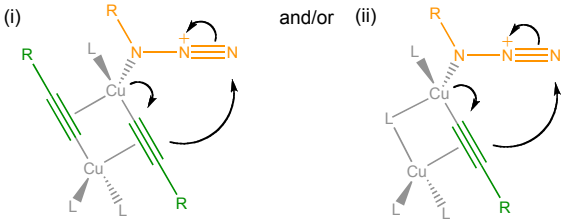

Type C
The azide and alkyne groups that react are on different copper atoms - (i) non-π-activated alkyne, (ii) π-activated alkyne. If the bridging ligands are alkynes, this differs from B only in the location of the alkyne which reacts with the azide. Doubly-bridged intermediates are not possible with bidentate ligands for copper (assuming RN_3 coordinates to Cu).

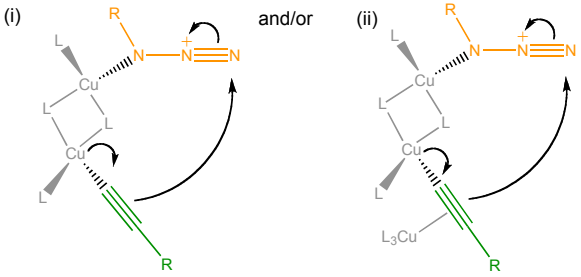

Scheme 2.1. The Proposed Mechanism of the Huisgen-Meldal-Sharpless Cu(I)-Catalyzed Alkyne-Azide Cycloaddition (CuAAC) Reaction.

In the absence of competing ligands,[19] copper(I) acetylides exist as complex multi-metal atom aggregates[20] and kinetic studies[3,21] by Fokin and Finn on the generic ligand-free[19] Cu(I)-catalyzed alkyne-azide reaction show that in DMSO-water mixtures the reaction mechanism is second order with respect to copper. However, relatively little is known about the ligand-promoted Cu(I)-catalyzed cycloaddition in organic solvents. Recent experimental results from Straub,[22] in which mononuclear Cu(I) acetylides ligated by a sterically shielding N-heterocyclic carbene react efficiently with bulky organoazides at room temperature, support the notion that a single copper atom mechanism (A(i), Scheme 2.1) is viable for the reaction, at least when the copper is bound to bulky ligands. Recent DFT calculations[15] suggest that π-activation of the copper-acetylide unit by coordination of a second copper atom (e.g. A(ii) or, more likely under ligand-free conditions or with small monodentate ligands, the bis-alkyne bridged 'Glaser-like'[23] intermediate B, Scheme 2.1) greatly enhances the reactivity of the Cu-σ-acetylide, accelerating formation of the metallacycle. Alternatively, a pathway[21] in which the reacting azide and alkyne are coordinated to different copper(I) atoms (intermediate C(i) or (ii)) would be consistent with the second order kinetics observed in DMSO/water). It may well be that several or all of these types of intermediate[24] can provide viable pathways for the CuAAC reaction, with the different characteristics of the intermediates being relatively favoured or inhibited by factors such as the solvent, bulk and coordination number of an added ligand, the strength of ligand-copper binding and the amount of ligand-free Cu(I) present in solution. Given the tendency of Cu(I)-acetylides to aggregate, it seems likely that the Glaser-like intermediates B or C(ii) feature in the dominant pathways in most reported CuAAC reactions.

2.2 Results and discussion

2.2.1 Preliminary studies

Despite the uncertainty over the precise nature of the reactive intermediate in the CuAAC reaction, since tertiary amines and pyridines facilitate[3,10] the reaction in organic solvents we reasoned that a macrocycle, **1**, bearing an endotopic ligating

nitrogen atom might be able to direct the CuAAC reaction of a stoppered alkyne, **2**, and a stoppered azide, **3**, through the macrocycle cavity to give a [2]rotaxane, **4**, in an active-metal template synthesis (Scheme 2.2).

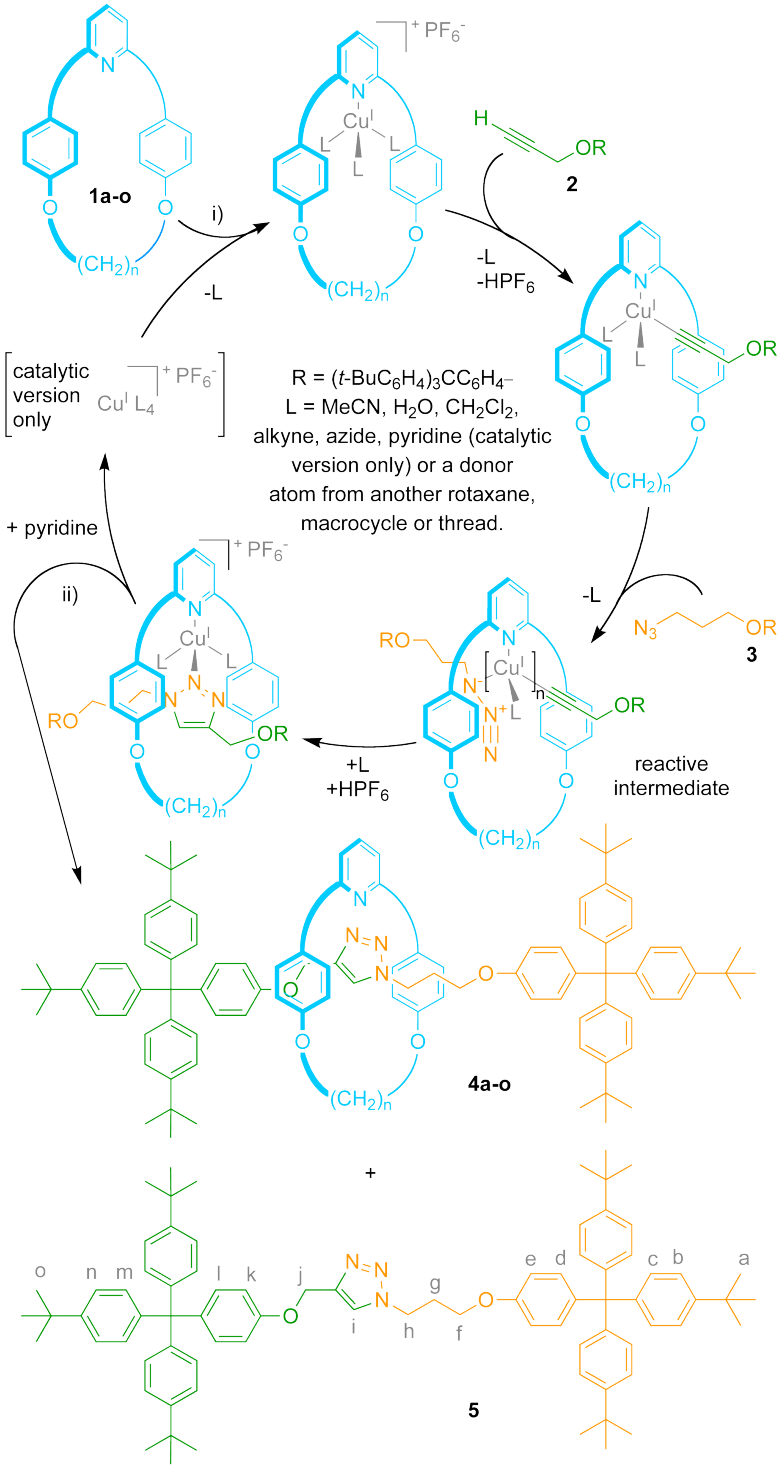

Scheme 2.2. The Active-Metal Template CuAAC Synthesis of [2]Rotaxanes **4a-o** from Alkyne **2**, Azide **3** and Macrocycles **1a-o**. Reaction conditions: (i) **1a-o** (0.01 M), Cu(I) salt (generally $[Cu(CH_3CN)_4](PF_6)$, see text), poorly coordinating solvent (generally CH_2Cl_2, see text) and, in the catalytic version of the active-metal template reaction, 3 equiv. pyridine. (ii) KCN, CH_2Cl_2/CH_3OH.[25] For the effect of reaction conditions and reagent stoichiometry on the yields of **4a** and **5**, see Table 2.1. For relative yields of **4a-o** using a standardized set of reaction conditions see Figure 2.3.

A 2,6-di(alkyloxymethyl)pyridine macrocycle (**1a**), previously used[26,27] as both a mono- and bidentate ligand for various transition metals in classical 'passive' template rotaxane and catenane syntheses, seemed a suitable candidate for initial investigations. Pleasingly, stirring of an equimolar mixture of the pyridine macrocycle **1a**, alkyne **2**, azide **3** and $[Cu(CH_3CN)_4](PF_6)$ in CH_2Cl_2 for 24 hours afforded—after demetallation with KCN—a mixture of [2]rotaxane **4a** (57%) and the non-interlocked triazole thread **5** (41%), together with some of the unconsumed starting macrocycle (Scheme 2.2 and Table 2.1, entry 1).[25]

Table 2.1. The Effect of Reaction Conditions and Reagent Stoichiometry on the Active-Metal Template CuAAC Synthesis of [2]Rotaxane **4a** (Scheme 2.2).[25] [a] All reactions were carried out at 0.01 M concentration with respect to **1a** using the procedure shown in Scheme 2.2; [b] 3 equiv. pyridine; [c] Control experiment with no $[Cu(CH_3CN)_4](PF_6)$ present to demonstrate that the thermal reaction does not occur at these temperatures; [d] 24 h; [e]12 h then 24 h; [f]12 h then 72 h.

Entry	Equiv. of 2 and 3	Equiv. of $[Cu(CH_3CN)_4]PF_6$)	solvent	T (˚C)	conversion to triazole **2+3→4a+5**	yield of rotaxane **1a→4a**
1[a]	1	1	CH_2Cl_2	25d	>95%	57%
2[a]	5	1	CH_2Cl_2	25d	92%	94%
3[b]	5	0.2	CH_2Cl_2	25d	44%	59%
4[b]	5	0.2	$(ClCH_2)_2$	25→70[e]	94%	82%
5[c]	1	0	$(ClCH_2)_2$	25→70[f]	<5%	0%

By varying the reaction conditions and reactant stoichiometry (Table 2.1), yields of up to 94% of [2]rotaxane with respect to the amount of macrocycle used were achieved (5 equiv. **2** and **3**; Table 2.1, entry 2) for this stoichiometric active-metal template reaction (Figure 2.1a). The use of sub-stoichiometric amounts of copper was investigated to determine whether the metal would turn over as both a template and a cycloaddition catalyst (i.e. a catalytic active-metal template synthesis, Figure 2.1b). When using 20 mol% (with respect to 1a) of $[Cu(CH_3CN)_4](PF_6)$ at room temperature, the reaction appeared to stop after [2]rotaxane equivalent to the amount of copper present had been formed, suggesting that the multidentate rotaxane sequesters the transition metal during the reaction inhibiting further catalytic activity. Addition of pyridine as a competing ligand enabled the catalyst to turn over

producing a sub-stoichiometric reaction, but the reaction was extremely slow at 25 °C (Table 2.1, entry 3). Elevating the temperature (70 °C, $ClCH_2CH_2Cl$) gave an improved yield (82%) of rotaxane **4a** in a reasonable time period (36 h) using only 4 mol% Cu(I) with respect to both **2** and **3** (Table 2.1, entry 4).

2.2.2 Effect of the nature of the Cu-(I) source

A number of different Cu(I) salts were screened for the reaction shown in Scheme 2.2 using the conditions shown in Table 2.1, entry 1 but replacing the $[Cu(CH_3CN)_4](PF_6)$ salt with other Cu(I) complexes. The use of CuOTf·benzene gave a 78% conversion of **2** and **3** into triazole products after 24 h but only a 46% yield of [2]rotaxane **4a**. By letting the reaction continue for a further two days (72 h in total) complete conversion of the starting azide and alkyne to triazole products (48% rotaxane) was achieved. Substituting CuI for $[Cu(CH_3CN)_4](PF_6)$ led to very little reaction during the first 24 hours (8% conversion to triazole) presumably due to the low solubility of CuI in CH_2Cl_2, but interestingly, what little alkyne and azide had reacted formed rotaxane with high selectivity (7:1 rotaxane:thread). The reaction proceeded slowly to completion (>98% conversion) over three weeks. However, at the end point of the reaction the product ratio (56:44 rotaxane:thread) was identical to that of the analogous $[Cu(CH_3CN)_4](PF_6)$-mediated experiment.

We also synthesized and isolated various discrete Cu(I)-**1a** complexes and tested their efficacy in the active-metal template reaction. The macrocycle, **1a**, and the different Cu(I) salts were mixed in CH_3CN solution and the resulting Cu(I)-**1a** complexes obtained as solids by vapour diffusion with diethyl ether. The preformed Cu(I)-**1a** complexes were then submitted to the standard rotaxane-forming reaction conditions (Table 2.1, entry 1). The preformed $[Cu(CH_3CN)_4](PF_6)$-**1a** complex gave 76% conversion to triazole and a 53% yield of [2]rotaxane; the preformed CuOTf-**1a** complex gave 53% conversion triazole but only a 5% yield of [2]rotaxane; the preformed CuI-**1a** complex gave identical results to the Cu(I)-**1a** complex formed in situ (i.e. >98% triazole conversion over 3 weeks; 56% rotaxane).

Although there is some variation in the efficacy of the various Cu(I) salts on the rotaxane-forming reaction, and some unexplained variation in the rotaxane:thread

ratio during the course of the reaction with some sources of Cu(I), simple addition of $[Cu(CH_3CN)_4](PF_6)$ is the most convenient way of maximizing the CuAAC yield of rotaxane.[28]

2.2.3 Kinetic studies

Some simple kinetic measurements were made to determine whether, under these reaction conditions, the Cu(I)-catalyzed alkyne-azide cycloaddition is actually accelerated by pyridine-based ligands. The rate of formation of triazole products (i.e. thread, plus rotaxane where relevant) was compared for the ligand-free reaction and reactions containing pyridine, 2,6-dimethylpyridine (lutidine), 2,6-di(alkyloxymethyl)pyridine macrocycle **1a**, and **6**, a close but acyclic analogue of **1a**. The results (Figure 2.1) show that both lutidine and **6**, the acyclic analogue of **1a**, significantly accelerate the CuAAC reaction rate (essentially complete conversion to triazole after 3 h) compared to the Cu(I)-catalyzed reaction when no pyridine-based ligand is added (complete conversion after 6 h).

The presence of pyridine also initially accelerates the reaction, but the conversion tails off after 2 h suggesting that using unsubstituted pyridine as a ligand facilitates the oxidation of Cu(I) to non-catalytic Cu(II) under the reaction conditions. The role of the pyridine ligands in this rate acceleration is probably to break up extended Cu(I)-acetylide aggregates to form smaller reactive intermediates of the type shown in Scheme 2.1, although we cannot rule out an electronic effect of the ligand on the metal as well.

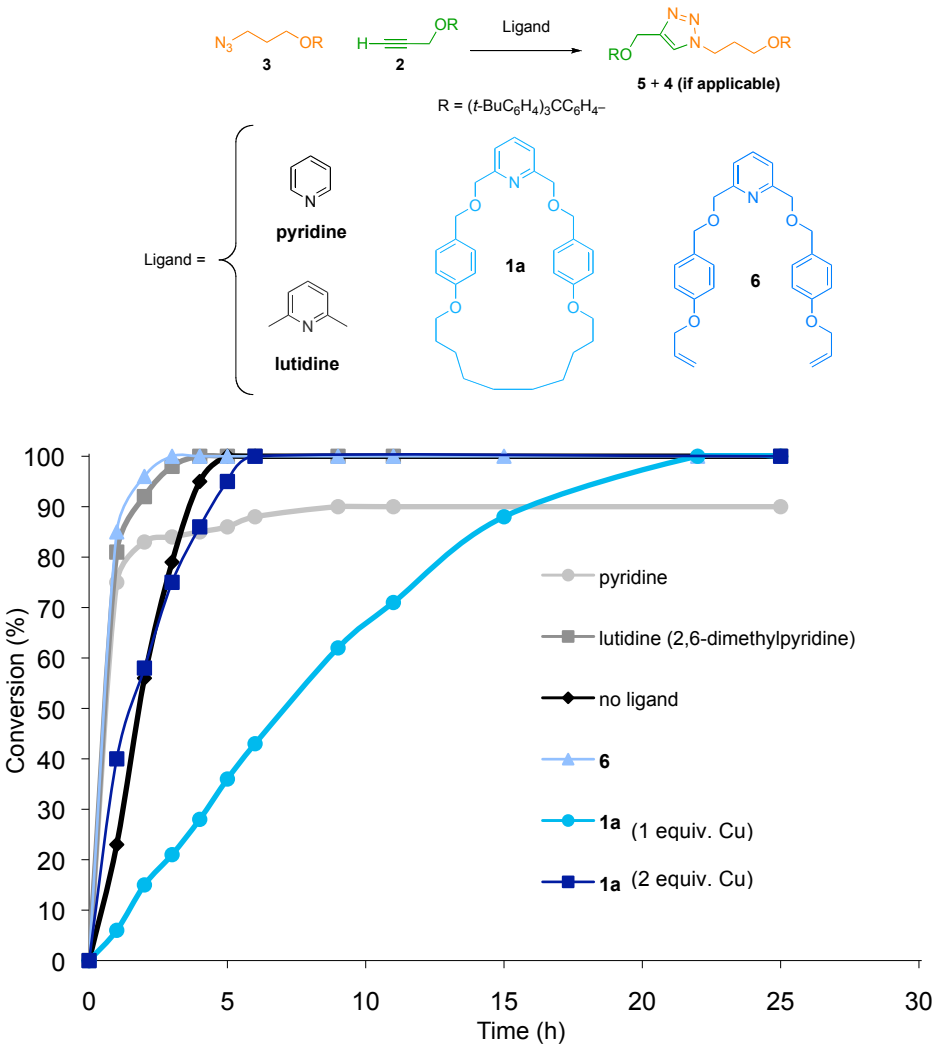

Figure 2.1. Conversion to triazole (i.e. thread + rotaxane if applicable) vs. time for different pyridine-based ligands for the CuAAC reaction. Conditions: i) ligand (1 equiv.), alkyne **2** (1 equiv.), azide **3** (1 equiv.), $[Cu(CH_3CN)_4](PF_6)$ (1 equiv.; 1 or 2 equiv. with **1a**), CD_2Cl_2, RT, 0.01 M. The conversion of **2** and **3** into the triazole products (thread **5**, + rotaxane **4a** where relevant) was monitored by ^{1}H NMR.

Interestingly, the Cu(I)-catalyzed formation of triazole products (both rotaxane and thread) in the presence of macrocycle **1a** (with 1 equiv. of Cu)—which also presumably breaks up the Cu-acetylide aggregates—is actually slower (24 h cf 6 h) than the ligand-free Cu(I)-catalyzed reaction. Whilst it might seem surprising that the active-metal template reaction is slower than the ligand-free reaction given that excellent yields of rotaxane are obtained under both stoichiometric and catalytic active-metal template conditions (Table 2.1), the rationale for this is quite straightforward. First, the reaction might be expected to be slower with the macrocyclic ligand since the alkyne-azide cycloaddition must take place through the macrocycle cavity, a sterically restricted environment compared to the ligandless Cu(I)-catalyzed reaction, effecting the solvation of the reactive species as well as

hindering any motion required to achieve bond formation or changes of geometry at the copper centre. Second, the macrocyclic ligand might disfavour certain types of reactive intermediate (e.g. B) on steric grounds and so the reaction may proceed through another, type of slower reacting, but still viable, intermediate (e.g. A or C rather than B). The reason that the ligandless formation of triazole thread does not dominate given the slow rate of rotaxane formation is that the macrocycle is an excellent ligand for the Cu(I) and sequesters it, preventing the inherently faster ligand-free reaction (probably via B or A(ii)) from occurring. Accordingly, addition of a second equivalent of Cu(I) to the reaction containing **1a** should increase the rate of triazole formation to close to that of the ligand-free rate. Indeed, this was found to be the case (Figure 2.1 and 2.2). However, whilst one might expect this increase to be totally due to thread formation, analysis shows that the rate of rotaxane formation is also slightly increased by adding an extra equivalent of Cu(I) to this reaction (Figure 2.2). In fact, the final yield of [2]rotaxane only falls from 57% to 22% even though the triazole-forming reaction is complete in 6 h instead of 24 h. The acceleration of the rotaxane-forming reaction by excess Cu(I) strongly suggests that π-activation of the copper-acetylide unit (i.e. reactive intermediate A(ii), B or C(ii)) is the dominant process in the CuAAC reaction mechanism of **1a**.

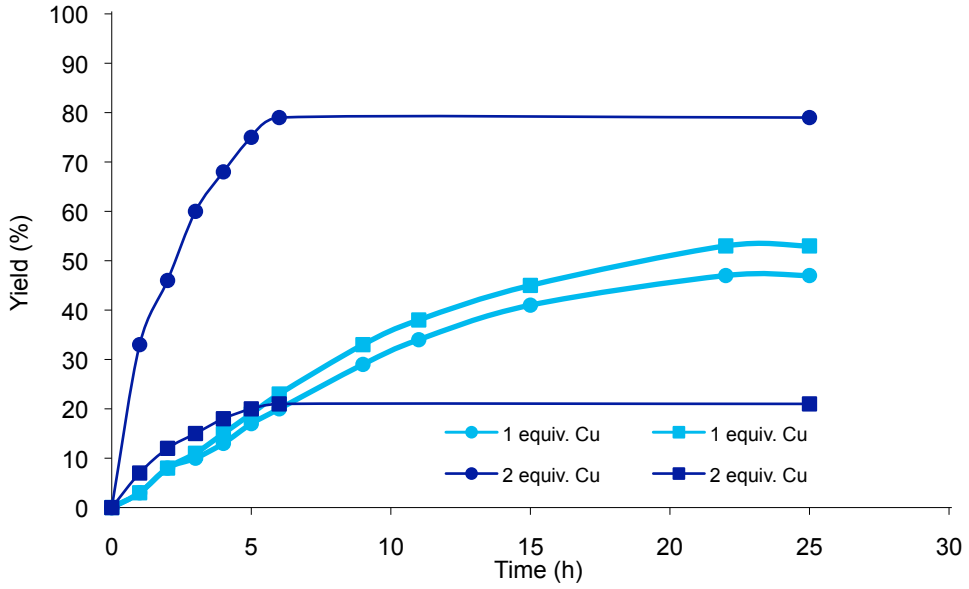

Figure 2.2. Formation of triazole products (rotaxane **4a** ■, thread **5** ●) *vs* time for the CuAAC reaction in the presence of macrocycle **1a**. Conditions: i) **1a** (1 equiv.), **2** (1 equiv.), **3** (1 equiv.), $[Cu(CH_3CN)_4](PF_6)$ (1 or 2 equiv.), CD_2Cl_2, RT, 0.01 M. The conversion of **2** and **3** into thread **5** and rotaxane **4a** was monitored by ^1H NMR.

2.2.4 Effect of the macrocycle structure on [2]rotaxane formation

To further investigate both the scope and the mechanism of the active template rotaxane-forming reaction shown in Scheme 2.1 the structure of the pyridine-based macrocycle was varied. The macrocycles used in the study are shown in Figure 2.3 and their syntheses are detailed in the experimental part. In order to compare the relative yields of rotaxane and thread within the ligand series, the macrocyclic ligands were screened using a standard, rather than optimized,[29] set of stoichiometric active-metal template reaction conditions in which the original macrocycle (**1a**) generates appreciable quantities of both rotaxane and thread. The conditions used were 1 equiv. macrocycle (**1a-o**), 1 equiv. alkyne **2**, 1 equiv. azide **3** and 1 equiv. $[Cu(CH_3CN)_4](PF_6)$, at a concentration of 0.01 M in CH_2Cl_2 at room temperature for 24 h. In most cases the starting alkyne (**2**) and azide (**3**) were completely consumed during the course of the reaction. After 24 h (72 h for **1n** and **1o**) each reaction was treated with KCN to remove the Cu(I), analyzed by ^{1}H NMR to determine the yield (shown in Figure 2.4) under the standard set of conditions, and then purified to give authenticate samples of each [2]rotaxane. Molecular ions corresponding to $[M+H]^+$, $[M+Na]^+$, $[M+K]^+$ for the intact rotaxanes were detected by ESI-MS mass spectroscopy of the KCN-treated reaction mixtures as the major or sole peaks in the 1.2-2 kDa range. The yield (the percentage shown in red in Figure 2.3) of each rotaxane is the conversion of the macrocycle (**1a-o**) to the corresponding [2]rotaxane (**4a-o**). The conversion to triazole (the percentage shown in parentheses in Figure 2.3) is the overall conversion of the alkyne (**2**) and azide (**3**) into both thread (**5**) and rotaxane (**4a-o**).

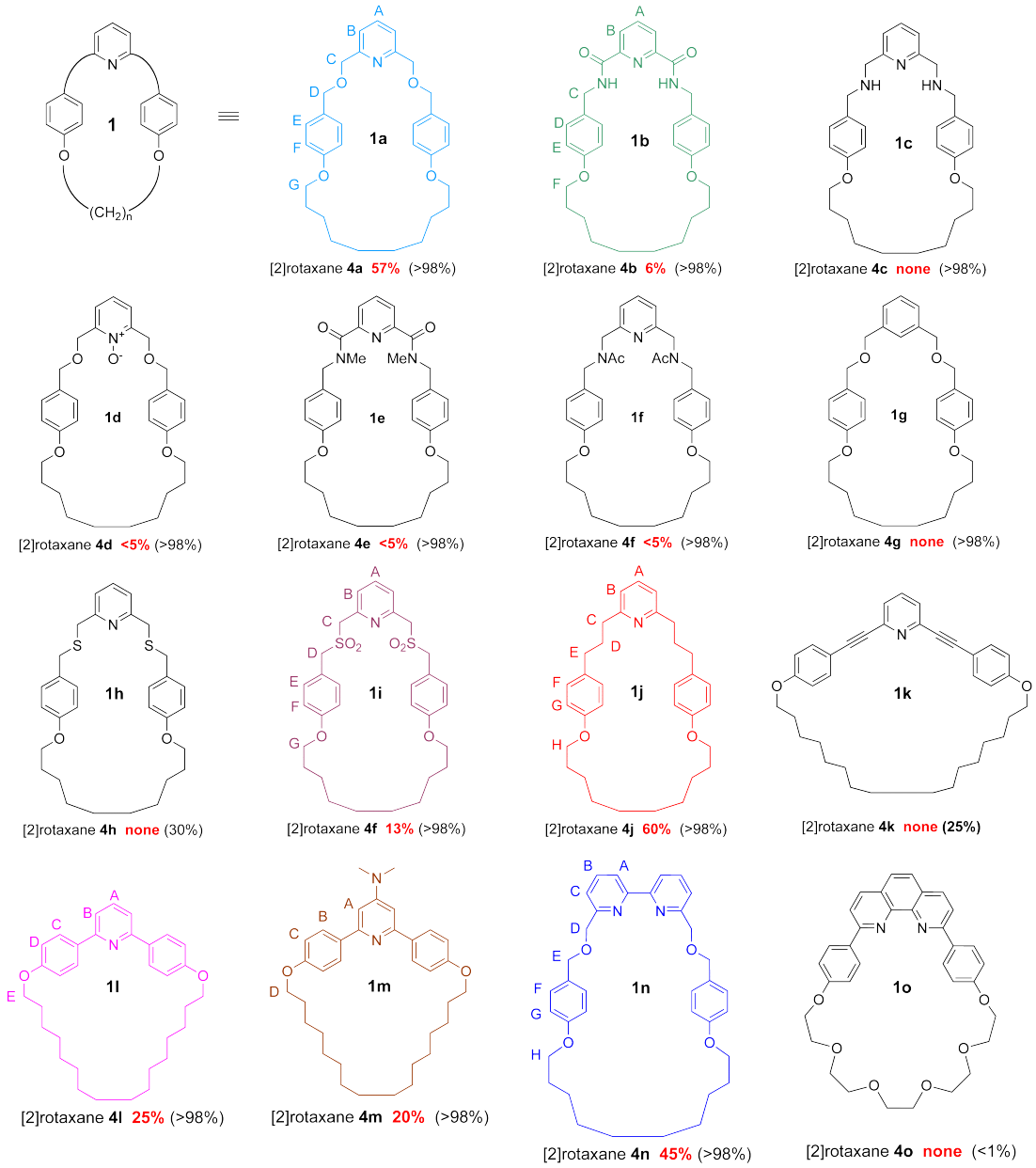

Figure 2.3. Influence of macrocycle structure on the active-metal template CuAAC rotaxane-forming reaction in Scheme 2.2 using a standardized set of reaction conditions. Conditions for Scheme 2.2: (i) **1a-o**, **2**, **3**, $[Cu(CH_3CN)_4](PF_6)$, CH_2Cl_2, RT, 24 h (72 h for **4n** and **4o**); 0.01 M concentration with respect to each of **1a-o**, alkyne **2**, azide **3** and $[Cu(CH_3CN)_4](PF_6)$. The reactions were not run under an inert atmosphere, nor using distilled or dried solvents. (ii) KCN, CH_2Cl_2/CH_3OH. The conversion of each macrocycle to [2]rotaxane is given as a percentage yield in red and the overall conversion of **2** and **3** into triazole products (rotaxane **4a-o** and thread **5**) is shown for each macrocycle in parentheses. 'Trace' means that the rotaxane was observed by ESI-MS but could not be detected by ^{1}H NMR. 72 h reaction time. The colours and lettering correspond to the signals and assignments of the ^{1}H NMR spectra shown in Figure 2.4 and Figure 2.5.

2.2.4.1 Mono- and tridentate macrocycles

In addition to the strongly coordinating pyridine nitrogen, macrocycle **1a** has two ether oxygen atoms that could potentially be involved in (albeit presumably weak) coordination to the metal atom during the active template reaction, making **1a** a monodentate or possibly weakly bidentate or very weakly tridentate ligand.[30,27] Macrocycle **1b** is not only missing the ether oxygen atoms, but the pyridine nitrogen atom lone pair is tied up in strong intramolecular bifurcated hydrogen bonds to the adjacent amide groups[31] and so it was rather surprising to find that [2]rotaxane **4b** was successfully produced in the active-metal template reaction, albeit in only 6% yield. Presumably coordination of **1b** to the copper is able to occur at the expense of the intramolecular hydrogen bonds[32,33] and **1b** is then able to act as a monodentate ligand. In contrast the use of **1c**, a tridentate macrocyclic ligand with three hard donor atoms, gave a similar overall conversion to triazole but with no rotaxane formed. Upon addition of **1c** to the copper catalyst and other reagents the solution changed colour immediately from colourless to blue-green. This suggests that some of the Cu(I) is rapidly oxidized to Cu(II) upon coordination to **1c**.[34] The resulting Cu(II)-**1c** complex is not catalytically active for the alkyne-azide cycloaddition and any tridentate Cu(I)-**1c** complex lacks the free coordination sites necessary to bind azide and alkyne in the same aggregate.[35,36] However, enough of the copper in the reaction is not tied up as the **1c** complex for the ligandless thread-forming triazole reaction to proceed to completion within 24 h.

Macrocycle **1d** has a similar structure to **1a** except that the pyridine nitrogen is oxidized. The result, >98% conversion to triazole but only a trace of rotaxane when using **1d** as the macrocycle in the active template reaction, show that the N-oxygen atom greatly affects the ligands ability to coordinate to Cu(I). Macrocycle **1e** also has a similar constitution to **1b**, but the secondary amides are methylated, eliminating their ability to form hydrogen bonds. AM1 calculations[37,38]using Spartan (see Experimental Section) show that the methyl groups distort and partially fill the macrocycle cavity. The result is that, like **1d**, little of the CuAAC reaction is directed through the macrocycle cavity to form rotaxane. The same effect is seen for macrocycle **1f**, the bis-N-acetylated analogue of **1c**.

Removing the pyridine nitrogen atom, macrocycle **1g**, completely switches off rotaxane formation, confirming the need for a ligating donor atom. Replacing the benzylic oxygens of **1a** by more strongly coordinating sulfur atoms produces another tridentate macrocycle, **1h**. As with **1c**, no rotaxane is formed—consistent with the premise that tridentate ligand complexes of Cu(I) lack the vacant coordination sites necessary to bind both azide and alkyne[35]—and the yield of triazole is also only 30%, indicating that **1h** is particularly effective in sequestering the copper. Oxidation of the sulfide groups to sulfones, macrocycle **1i**, restores the ability of the macrocycle to bind to the Cu(I) as a monodentate ligand and, despite the increased bulk around the coordinated metal ion, a significant amount (13%) of [2]rotaxane **4i** is formed by the stoichiometric active-metal template reaction. In fact, substitution of the benzylic ether oxygen atoms by methylene groups confirms that only a monodentate macrocycle with a single strongly coordinating donor atom is required for an efficient active template rotaxane-forming reaction; macrocycle **1j** generates just as much [2]rotaxane as the parent macrocycle **1a**. It should be noted that the cavity of macrocycle **1j** is probably rather more flexible than **1a**, yet this is not detrimental for rotaxane formation.

To test whether other macrocycle geometries would be tolerated by the active template reaction, we prepared **1k** and **1l**, in which the substituted benzylic units were replaced by arylalkyne and aryl groups, respectively. The 2,6-bisalkyne pyridine unit proved to be unstable[39,40] under the reaction conditions, suppressing the overall yield of the CuAAC reaction with no rotaxane being produced. However, the active-metal template CuAAC reaction with **1l** proceeded smoothly, albeit generating rather less rotaxane (25%) than the most effective examples of other macrocycle geometries (**1a** and **1j**). AM1 calculations[37] using Spartan (see Experimental Section) indicate that **1l** has a well-defined persistent cavity suitable for the threading of a molecular chain. However, the phenyl groups flanking the pyridine sterically encumber the nitrogen donor atom of the macrocycle, and a combination of steric and electronic factors probably reduces the binding strength of this macrocycle for Cu(I) ions. The weaker binding leads to more ligandless Cu(I) in solution, resulting in higher conversion of the substrates into the non-interlocked thread, **5** and the relatively modest yield of [2]rotaxane **4l**. Increasing the steric bulk at the 4-position of the pyridine group, whilst simultaneously increasing the electron-donating ability

of the heterocyclic nitrogen atom, (macrocycle **1m**) had little effect on the rotaxane yield.

2.2.4.2 Bidentate macrocycles

Having established that monodentate ligands of several different macrocycle geometries and donor atom orientations (**1a**, **1j**, **1l**, **1m**) efficiently promote active template rotaxane formation, whereas tridentate macrocycles (**1c** and **1h**) do not, the efficacy of bidentate macrocycles **1n** and **1o** was then investigated.[10,41]The bipyridyl macrocycle, **1n**, directs the CuAAC reaction through its cavity to form rotaxane almost as efficiently as the best monodentate macrocycles (45% **1n→4n** cf 57% **1a→4a** and 60% **1j→4j**). However, it severely inhibits the rate of the Cu(I)-catalyzed reaction and it took 3 days for the active-metal template reaction **1n→4n** to go to completion, compared to 24 h for **1a→4a** and 6 h for the ligand-free Cu(I)-catalyzed control reaction (Figure 2.2). The inhibition of the Cu(I)-catalyzed cycloaddition is even more dramatic with the other bidentate ligand investigated, the 2,9-diphenylphenanthroline macrocycle (**1o**) used extensively to assemble rotaxanes and catenanes by the Sauvage group.[42] Macrocycle **1o** completely inhibits the CuAAC reaction. Even after 3 days under the standard stoichiometric active-metal reaction conditions in the presence of 1o, no triazole products were observed. This latter result is particularly interesting given that phenanthroline ligands have previously been reported.[10] to promote the CuAAC reaction. The lack of reactivity is presumably a result of the steric bulk about the Cu(I) centre in the complex preventing the complex from adopting various orientations required for reaction to take place (e.g. tolerating the change in geometry from Cu(I) to Cu(III), Scheme 2.1), together with the macrocycle being very effective in sequestering the Cu(I) in this unreactive form. A related Cu(I)-macrocycle complex has recently been reported to act as a stoichiometric active-metal template for the formation of [2]rotaxanes via a Glaser alkyne homocoupling.[43] However, in that case, intermediates of type B (Scheme 2.1) are possible with a bidentate ligand for copper because no azide need be coordinated to the metal atom.

2.2.5 ^{1}H NMR spectra of the metal-free [2]rotaxanes

The ^{1}H NMR spectra (400 MHz, 298 K, $CDCl_3$) for each of the rotaxanes formed in >5% yield is shown in Figure 2.4. The ^{1}H NMR spectra of the rotaxanes (Figure 2.4b-g) all show upfield shifts of several signals with respect to the non-interlocked components (thread **5**, Figure 2.4a, and the macrocycles **1a**, **1b**, **1i**, **1j**, **1m** and **1n**, see experimental section). Such shielding is typical of interlocked structures in which the aromatic rings of one component are positioned face-on to another component and is observed for all the non-stopper resonances of the axle ($H_{f\text{-}j}$) indicating that the macrocycle is able to access the full length of the thread in the rotaxanes. This is as expected; there should be no strong intercomponent non-covalent interactions between the thread and the macrocycle in the metal-free rotaxanes. The one exception is the amide containing rotaxane **4b** (Figure 2.4c), which exhibits a significant downfield shift of the amide resonance with respect to free macrocycle (see Experimental Section). This is presumably due to the formation of hydrogen bonds between the amides of the macrocycle and the triazole unit of the thread in an interaction similar to that previously observed between interlocked amide and pyridine components in rotaxanes and catenanes.[26,27,44]

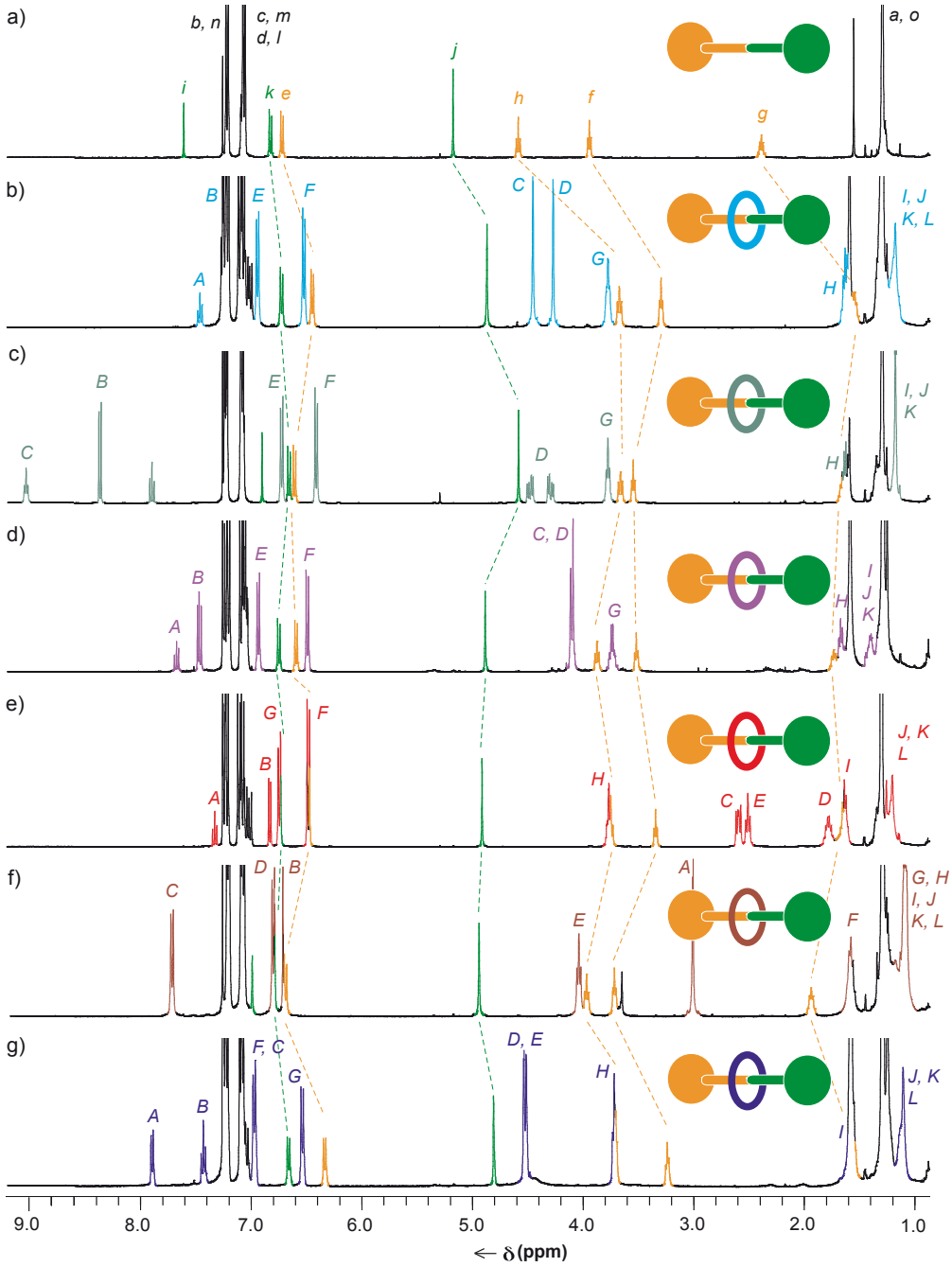

Figure 2.4. ^{1}H NMR spectra (400 MHz, $CDCl_3$, 300 K) of a) triazole thread **5**, b) [2]rotaxane **4a**, c) [2]rotaxane **4b**, d) [2]rotaxane, **4i**, e) [2]rotaxane, **4j**, f) [2]rotaxane, **4m**, g) [2]rotaxane, **4n**. The assignments correspond to the lettering shown in Scheme 2.2 and Figure 2.3.

2.2.6 The active-metal template CuAAC reaction at high macrocycle:Cu(I) ratios: the unexpected formation of [3]rotaxanes

The picture of the active-metal template CuAAC reaction that we can build up that is consistent with the experimental observations so far is that the ligand-free $[Cu(CH_3CN)_4](PF_6)$ salt and macrocycles **1a-o** are in equilibrium with the corresponding copper(I)-macrocycle complex in which, in most cases, the metal atom directs the cycloaddition of the azide and alkyne through the macrocycle cavity. Although the ligand-free reaction is inherently faster than the active-metal template one, the coordinating ability of the macrocycle means that the rotaxane-forming reaction can become competitive with, or even dominate, the thread-forming reaction. In general, a stronger binding macrocyclic ligand (e.g. **1a** cf **1b**) should move this equilibrium in favour of rotaxane formation. However, some changes in coordination geometry about the metal are required for the CuAAC mechanism to operate (Scheme 2.1) and so the most strongly binding macrocycle (**1o**), which apparently does not tolerate such changes, actually inhibits the rotaxane-forming reaction. In view of this, we decided to investigate other conditions in which the rotaxane-forming reaction might be increased at the expense of the formation of thread.

In an attempt to minimize the amount of ligandless Cu(I) present in the reaction, we carried out the active metal template CuAAC protocol under the standard conditions (1 equiv. **2**, 1 equiv. **3**, 1 equiv. $[Cu(CH_3CN)_4](PF_6)$, CH_2Cl_2, RT) used previously but in the presence of 10 equivalents of macrocycle (Scheme 2.3). Our initial experiments were carried out with monodentate macrocycle **1l**, because it is a rather poor ligand (we were unable to generate several other metal complexes with it) due to the steric crowding around the pyridine nitrogen and the π-electron density presented to the low oxidation state copper from the adjacent aromatic rings. The rather weak Cu(I) binding affinity—meaning there is more ligandless Cu(I) present in solution than many of the other macrocycles shown in Figure 2.3—would account for the modest yield of rotaxane using 1 equiv. of this macrocycle. This, we reasoned, should be improved by increasing the macrocycle:copper ratio.

We were immediately intrigued to find that the reaction was much slower with 10 equivalents of the macrocycle than it had been with 1 equivalent (Figure 2.2), the higher macrocycle:Cu(I) reaction taking more than one week to go to completion. Upon reaching this endpoint, the mixture of triazole products was found to consist of 30% thread **5**, 37% [2]rotaxane **4l** and, to our surprise, 33% [3]rotaxane, **7l** (yields quoted with respect to the alkyne and azide reactants). A reaction using macrocycle **1a** under the same experimental conditions (1 equiv. **2**, 1 equiv. **3**, 1 equiv. $[Cu(CH_3CN)_4](PF_6)$ and 10 equiv. **1a**, CH_2Cl_2, RT) was again slower than the same reaction with 1 equivalent of macrocycle (3 days to reach completion cf. 24 h) generating a product mixture of 5% thread **5**, 90% [2]rotaxane **4a** and 5% [3]rotaxane **7a** (yields quoted with respect to the alkyne and azide reactants). A similar but less dramatic trend was seen with bidentate macrocycle **1n**; with 10 equivalents of **1n** the reaction took 10 days to complete (cf. 7 days with 1 equivalent) producing 3% thread **5** and 97% [2]rotaxane **4n** (in this case no traces of [3]rotaxane, **4n**, could be detected by ^{1}H NMR spectroscopy or mass spectrometry).

The remarkable features of these high macrocycle:Cu(I) ratio active-metal template reactions are:

i) The exceptional combined rotaxane yields: 95% ([2]rotaxane **4a** + [3]rotaxane **7a**) cf 57% **4a** with 1 equiv. **1a**; 70% ([2]rotaxane **4l** + [3]rotaxane **7l**) cf 25% **4l** with 1 equiv. **1l**; 97% ([2]rotaxane **4n**) cf 45% **4n** with 1 equiv. **1n**.

ii) The significant decrease in the reaction rates compared to the low macrocycle:Cu(I) ratio reactions. The largest effect on rates is with the weakly copper-binding macrocycle **1l**; the smallest effect on rates is with the strongly copper-binding macrocycle **1n**. Again, this is strongly suggestive that the dominant mechanism of the CuAAC reaction under these conditions involves π-activation of the copper-σ-acetylide unit by a second, preferably ligandless for steric reasons, copper atom (i.e. I or II, Scheme 2.3, which correspond to reactive intermediates for the CuAAC reaction of type A(ii), II, or B or C(ii), I, in Scheme 2.1).

iii) The formation of [3]rotaxane (in 33% yield using macrocycle **1l**)—i.e. TWO macrocycles being threaded during the formation of ONE triazole ring. Molecular models show that this can most reasonably occur through

the sort of bridged two copper atom intermediate III shown in Scheme 2.3.

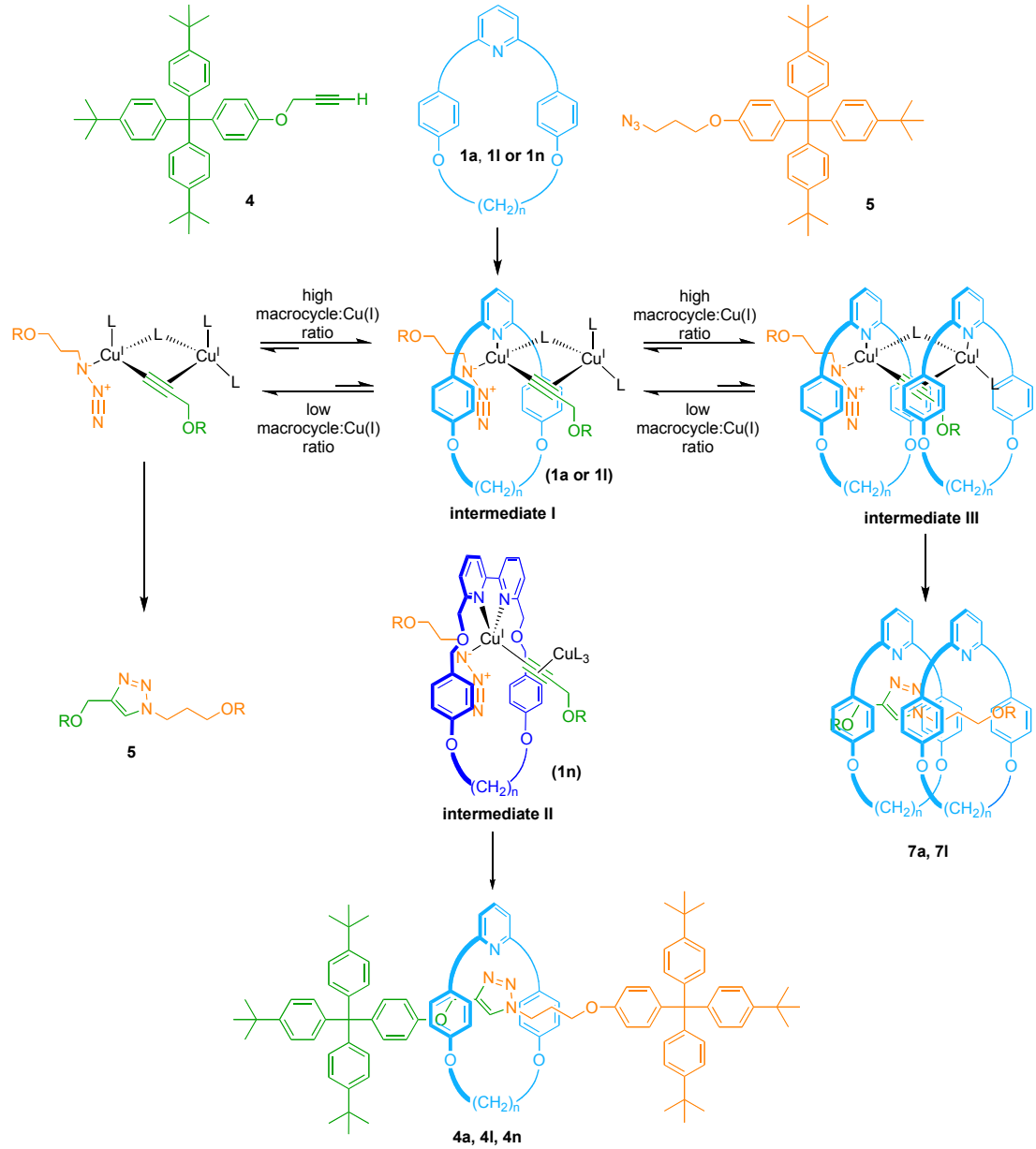

Scheme 2.3. The Effect of the Macrocycle:Cu(I) Ratio on the Active-Metal Template CuAAC Reaction. Reagents and conditions: (i) **1a**, **1l** or **1n** (10 equiv.), **2** (1 equiv.) and **3** (1 equiv.), $[Cu(CH_3CN)_4](PF_6)$ (1 equiv.), CH_2Cl_2, RT, 24 h (**1a**); 7 days (**1l**); 10 days (**1n**). (ii) KCN, CH_2Cl_2/CH_3OH. Product yields starting from macrocycle **1a**: thread **5** (5%), [2]rotaxane **4a** (90%), [3]rotaxane **7a** (5%). Product yields starting from macrocycle **1a**: thread **5** (5%), [2]rotaxane **4i** (33%), [3]rotaxane **7l** (37%). Product yields starting from macrocycle **1n**: thread **5** (3%), [2]rotaxane **4n** (97%), [3]rotaxane **7n** (0%). In the reactive intermediates shown, the Cu-azide (orange) reacts with any of the Cu-alkyne units shown in green. L can be any non-reacting ligand, including other alkyne and azide groups.

The ^{1}H NMR spectra of [2]rotaxane **4l** and [3]rotaxane **7l** are shown in Figure 2.5b and 2.5c, respectively. The resonances for the axle ($H_{f\text{-}j}$) of the rotaxanes are shifted upfield compared to the free non-interlocked thread **5** (Figure 2.5a), and unsurprisingly, this effect is more pronounced in the [3]rotaxane (Figure 2.5c) than in the [2]rotaxane (Figure 2.5b). Also, due to the asymmetry of the thread the ^{1}H NMR spectrum of [3]rotaxane **7l** (Figure 2.5c) displays inequivalent but overlapping peaks for the two macrocycle components, which are double the intensity of the corresponding macrocycle signals in the [2]rotaxane. Single crystals of **7l** suitable for X-ray crystallography were grown by slow cooling of a hot, saturated solution of **7l** in acetonitrile. The solid state structure (Figure 2.6) confirmed the structure of **7l** as a [3]rotaxane. Although it may appear at first glance that face to face π-stacking interactions might help to orient the two macrocycles on the thread, in the solid state structure the aromatic rings of adjacent macrocycles are not co-planar and their interplanar separation is somewhat large (> 3.8 A°) to be considered π-stacking.

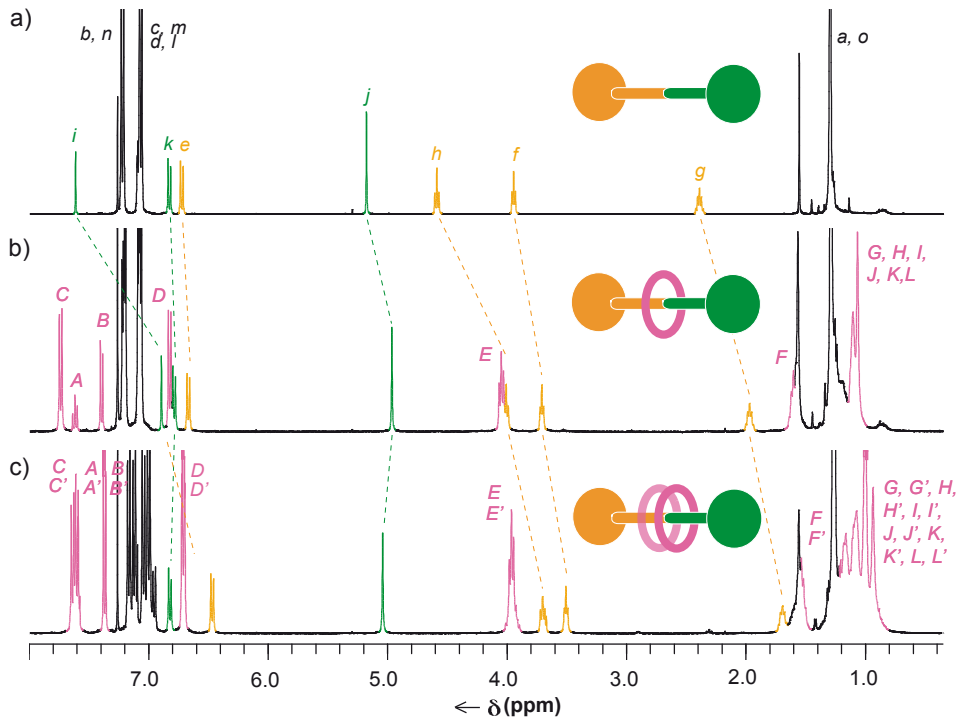

Figure 2.5. ^{1}H NMR spectra (400 MHz, $CDCl_3$, 300 K) of a) triazole thread **5**, b) [2]rotaxane **4l**, c) [3]rotaxane **7l**. The assignments correspond to the lettering shown in Scheme 2.2 and Figure 2.3.

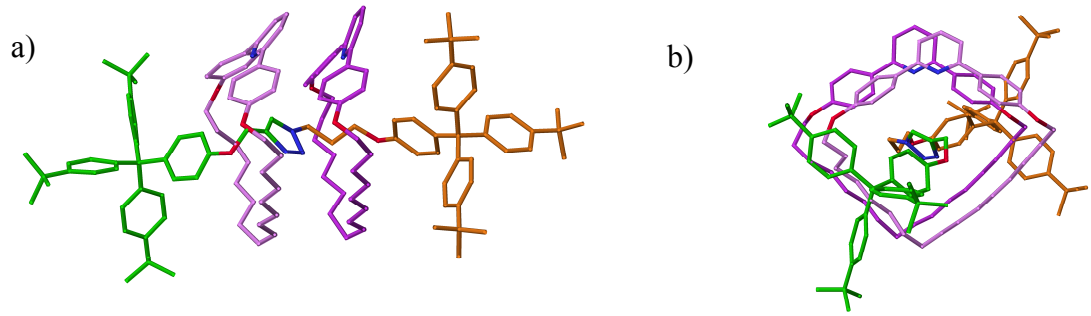

Figure 2.6. X-Ray structure of [3]rotaxane **7l**, from a single crystal obtained from a saturated acetonitrile solution: (a) viewed side-on; (b) viewed along axis of the thread. For clarity, different shades of purple are used for the carbon atoms of the two rings.

2.3 Conclusion

The Cu(I)-catalyzed 1,3-cycloaddition of azides with terminal alkynes is a highly effective reaction for the active-metal template synthesis of rotaxanes, with this new synthetic approach being illustrated through both stoichiometric (up to 97% yield) and catalytic (up to 82% yield) versions of the strategy. The reaction tolerates a wide variety of both monodentate and bidentate macrocyclic ligands which, although inherently slower than the ligand-free Cu(I)-catalyzed reaction, all work by sequestering the majority of the Cu(I) present so that the rotaxane-forming CuAAC reaction becomes competitive with—and, under many conditions, dominates—the ligand-free CuAAC reaction. The addition of pyridine enables the Cu(I) active-metal template to turnover without significantly compromising the yield of rotaxane. Amongst several potentially attractive features of this type of synthetic strategy is that it offers an unusual probe of reaction mechanism. The increase in rates of rotaxane formation by excess ligand-free Cu(I) support the suggestion that in CH_2Cl_2 the copper-σ-acetylide is activated by π-coordination to a second ligand-less[19] copper atom, and the remarkable formation of [3]rotaxanes at high macrocycle:Cu(I) ratios suggest that, under these conditions, the CuAAC reaction proceeds via a multi-copper atom complex in which the reacting azide and alkyne are almost certainly located on different copper atoms.

The template-directed assembly of otherwise difficult-to-access molecules and the catalysis of covalent bond formation are two of the most useful tasks that transition metals can perform in organic chemistry. The present work demonstrates that the combination of these apparently disparate functions can produce high yielding, mild

and effective synthetic routes to complex molecular architectures that require only substoichiometric amounts of metal. The already great amount of work published so far regarding 'active-metal' templated reactions seems to be in accordance with this statement.

2.4 Experimental section

2.4.1 Experimental procedures for the formation of "click" rotaxanes

General method for the formation of "click" rotaxanes

CAUTION: copper acetylides, which are potential by-products of this reaction, are shock-sensitive when dry. Care should be taken if performing these reactions on a large scale that these are not isolated in other than trace amounts by washing with basic ammonium citrate or dilute HCl.

A solution of macrocycle, (1 equiv.), azide, (1 equiv.), alkyne, (1 equiv.) and $[Cu(CH_3CN)_4](PF_6)$ (1.1 eq) in dry CH_2Cl_2 (5 mL) and under N_2 was stirred at room temperature for 24 h. The resulting mixture was diluted with CH_2Cl_2 (5 mL) and methanol (15 mL). Then a solution of KCN (10 equiv.) in methanol (2 mL) was added and the resulting suspension stirred vigorously for 1 h. Solvents were evaporated (80 ºC) and the residue was partitioned between water (15 mL) and CH_2Cl_2 (20 mL). The layers were separated and the aqueous layer was extracted with CH_2Cl_2 (3 × 10 mL). The combined organic fractions were washed with water (10 mL) and brine (10 mL), then dried ($MgSO_4$) and concentrated under reduced pressure. The resulting solid was purified by flash column chromatography and/or preparative TLC to give pure "click" rotaxane.

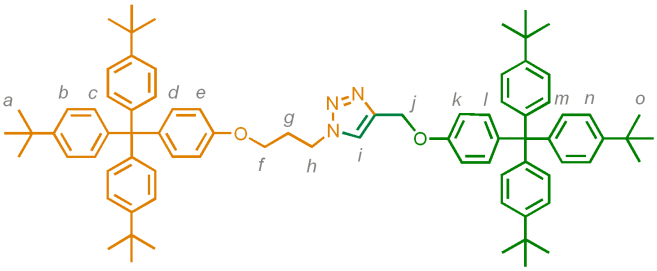

5

Spectroscopic data of the non-interlocked thread **5** generated during click reactions: **^{1}H NMR (400 MHz, $CDCl_3$):** δ = 7.61 (s, 1H, H_i), 7.21 (d, 12H, J = 8.52 Hz, H_b, H_n), 7.03-7.11 (m, 16H, H_c, H_d, H_m, H_l), 6.82 (d, 2H, *J* = 8.92 Hz, H_k), 6.72 (d, 2H, *J* = 8.89 Hz, H_e), 5.17 (s, 2H, H_j), 4.59 (t, 2H, *J* = 6.92 Hz, H_h), 3.94 (t, 2H, *J* = 5.53 Hz, H_f), 1.23-1.43 (m, 2H, *J* = 6.26 Hz, H_g), 1.29 (s, 54H, *t*Bu). **^{13}C NMR (100 MHz, $CDCl_3$):** δ = 156.1, 156.0, 148.3 (×2), 144.3, 144.0 (×2), 140.1 (×2), 132.3 (×2), 130.6 (×2), 124.0 (×2), 123.1, 113.2, 112.9, 63.7, 63.0 (×2), 61.9, 47.2, 34.2 (×2), 31.3 (×2), 29.9; **HRFAB-MS (3-NOBA matrix):** m/z = 1130.75171 (calcd. for $C_{80}H_{95}N_3O_2$, 1130.62920).

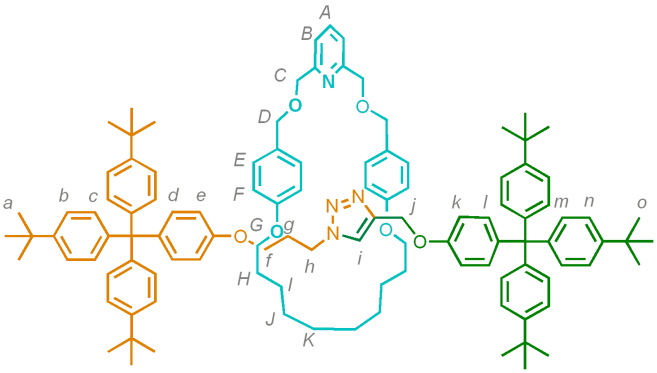

4a

Following the general procedure, macrocycle **1a** (100 mg, 0.2 mmol) was reacted with alkyne **2** and azide **3** to give a crude yellow solid. Purification by column chromatography (CH_2Cl_2 then a gradient from 5 to 20 % CH_3CN in CH_2Cl_2) gave pure rotaxane **4** as a colourless solid (180 mg, 54%). **^{1}H NMR (400 MHz, $CDCl_3$):** δ = 7.50 (t, 1H, *J* = 7.7 Hz, H_A), 7.31 (s, 1H, H_i), 7.22-7.30 (m, 14H, H_B, H_b and H_n), 7.09-7.17 (m, 12H, H_m and H_c), 7.08 (d, 2H, *J* = 8.6 Hz, H_l), 7.04 (d, 2H, *J* = 8.6 Hz, H_d), 6.97 (d, 4H, *J* = 8.3 Hz, H_E), 6.77 (d, 2H, *J* = 8.6 Hz, H_k), 6.56 (d, 4H, *J* = 8.3 Hz, H_F), 6.48 (d, 2H, *J* = 8.6 Hz, H_e), 4.91 (br s, 2H, H_j), 4.49 (br s, 4H, H_D), 4.31 (br s, 4H, H_C), 3.76-3.87 (m, 4H, H_G), 3.71 (t, 2H, *J* = 7.1 Hz, H_h), 3.34 (t, 2H, *J* = 5.4

Hz, H_f), 1.61-1.73 (m, 4H, H_H), 1.54-1.62 (m, 2H, H_g), 1.34 (s, 27H, H_a or H_o), 1.33 (s, 27H, H_a or H_o), 1.17-1.41 (m, 12H, H_I, H_J and H_K); **^{13}C NMR (100 MHz, $CDCl_3$):** δ = 158.8, 157.7, 156.4 (× 2), 146.4 (×2), 144.4, 144.3, 143.5, 139.9, 139.7, 137.3, 132.3, 132.1, 130.1, 130.0, 129.1 (× 2), 124.2, 124.1, 123.6, 120.2, 114.4, 113.3, 113.1, 72.6, 71.4, 67.2, 64.0 (× 2), 63.2, 61.6, 46.7, 34.4, 34.3, 31.5 (× 2), 29.7, 29.5, 28.7 (× 2), 25.8; **LRESI-MS:** *m/z* = 1619 $[M+H]^+$; **HRFAB-MS (3-NOBA matrix):** *m/z* = 1621.04087 (calcd. for $^{13}C^{12}C_{110}H_{135}N_4O_6$, 1621.04152).

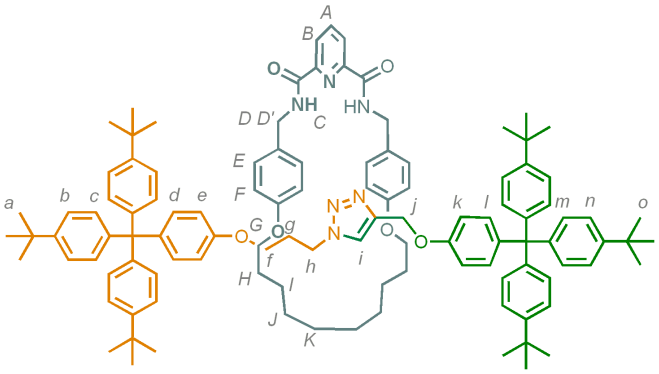

4b

Using general method, macrocycle **1b** (260 mg, 0.50 mmol, 1.0 equiv.), azide **3** (296 mg, 0.50 mmol, 1.0 equiv.), alkyne **2** (300 mg, 0.55 mmol, 1.1 equiv.), $[Cu(CH_3CN)_4](PF_6)$ (206 mg, 0.55 mmol, 1.1 eq) and KCN (327 mg, 5.03 mmol, 10 equiv.) gave the crude product as a mixture of rotaxanes **4b**, thread **5** (5:95, by ^{1}H NMR spectroscopy), macrocycle **4b**. Purification by flash column chromatography (Acetone/CH_2Cl_2; 2:96 to 5:95) followed by preparative TLC on silica gel (2 elutions in Acetone/CH_2Cl_2; 4:96) gave the rotaxane **4b** as a white solid (20 mg, 3%). **M.p.** 165-168 °C; **^{1}H NMR (400 MHz, $CDCl_3$):** δ = 9.02 (t, 2H, *J* = 6.3 Hz, H_C), 8.37 (d, 2H, *J* = 7.8 Hz, H_B), 7.90 (t, 1H, *J* = 7.9 Hz, H_A), 7.24-7.22 (m, 12H, H_b and H_n), 7.13-7.03 (m, 16H, H_c, H_d, H_m, H_l), 6.90 (s, 1H, H_i), 6.72 (d, 4H, *J* = 8.5 Hz, H_E), 6.66 (d, 2H, *J* = 8.9 Hz, H_k), 6.61 (d, 2H, *J* = 8.9 Hz, H_e), 6.41 (d, 4H, *J* = 8.6 Hz, H_F), 4.58 (s, 2H, H_j), 4.48 (dd, 2H, *J* = 6.6 Hz, *J* = 14.6 Hz, H_D), 4.29 (dd, 2H, *J* = 6.5 Hz, *J* = 14.6 Hz, $H_{D'}$), 3.77 (t, 4H, *J* = 6.0 Hz, H_G), 3.66 (t, 2H, *J* = 7.5 Hz, H_h), 3.55 (t, 2H, *J* = 5.8 Hz, H_f), 1.71-1.54(m, 6H, H_g, H_H), 1.47-1.10 (m, 12H, H_I, H_J, H_K), 1.30 (s, 27H, H_a or H_o), 1.29 (s, 27H, H_a or H_o); **^{13}C NMR (100 MHz, $CDCl_3$):** δ = 163.6, 157.7, 155.8, 155.6, 149.1, 148.3, 148.3, 143.9 (×2), 143.8, 140.4, 140.2, 138.6, 132.2 (×2), 130.6 (×2), 130.2, 129.0, 125.2, 124.1 (×2), 122.4, 113.8, 112.8, 112.6, 66.7, 63.8, 63.0 (×2), 60.8, 46.7, 42.5, 34.2 (×2), 31.3 (×2), 29.4, 28.6, 28.4,

28.3 and 25.5; **LRFAB-MS (3-NOBA matrix):** *m/z* = 1647 $[M+H]^+$; **HRFAB-MS (3-NOBA matrix):** *m/z* = 1646.03336 (calcd. for $^{13}C^{12}C_{110}H_{133}N_6O_6$, 1646.02866).

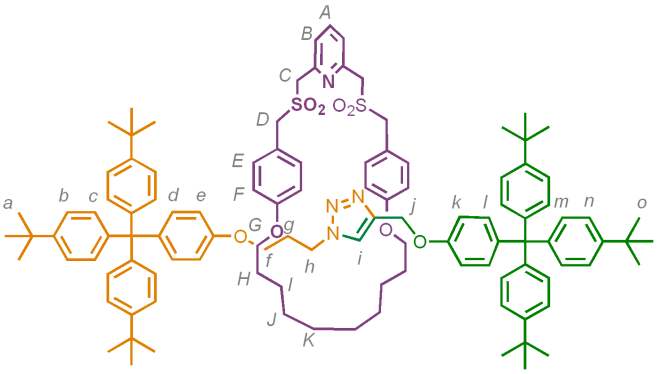

4i

Using general method, macrocycle **1i** (20.0 mg, 34.1 µmol, 1.0 equiv.), azide **3** (20.0 mg, 34.1 µmol, 1.0 equiv.), alkyne **2** (20.3 mg, 37.5 µmol, 1.1 equiv.), $[Cu(CH_3CN)_4](PF_6)$ (14.0 mg, 37.5 µmol, 1.1 eq) and KCN (22.2 mg, 0.34 mmol, 10 equiv.) gave the crude product as a mixture of rotaxane **4i**, thread **5** (13:87, by ^{1}H NMR spectroscopy), macrocycle **1i**. Purification by preparative TLC on silica gel (1 elution in CH_3CN/CH_2Cl_2/Petrol; 11:29:60) gave the rotaxane **4i** as a white solid (5 mg, 8%). **M.p.** 92-95°C; **^{1}H NMR (400 MHz, $CDCl_3$):** δ = 7.67 (t, 1H, *J* = 7.6 Hz, H_A), 7.48 (s, 1H, H_i) 7.46 (d, 2H, *J* = 8 Hz, H_B), 7.26-7.15 (m, 12H, H_b, H_n), 7.15-7.00 (m, 16H, H_c, H_d, H_m, H_l), 6.93 (d, 4H, *J* = 8.6 Hz, H_E), 6.75 (d, 2H, *J* = 8.9 Hz, H_k), 6.59 (d, 2H, *J* = 8.9 Hz, H_e), 6.49 (d, 4H, *J* = 8.6 Hz, H_F), 4.88 (s, 2H, H_j), 4.11 (s, 4H, H_C), 4.09 (s, 4H, H_D), 3.87 (t, 2H, *J* = 7.3 Hz, H_h), 3.78-3.69 (m, 4H, H_G), 3.52 (t, 2H, *J* = 6.0 Hz, H_f), 1.73 (quint., 2H, *J* = 6.5 Hz, H_g), 1.67 (quint., 4H, *J* = 6.6 Hz, H_H), 1.47-1.09 (m, 12H, H_I, H_J, H_K); 1.30 and 1.29 (2s, 54H, H_a, H_o); **^{13}C NMR (100 MHz, $CDCl_3$):** δ = 159.6, 156.2 (×2), 148.2, 147.7 (×2), 144.1, 144.0, 143.3, 139.7, 139.6, 137.5, 132.1, 132.0, 131.6, 130.6 (×2), 126.3, 124.0 (×2), 123.8, 118.4, 114.9, 113.0 (×2), 67.4, 64.2, 63.0 (×2), 60.1, 58.3 (×2), 46.6, 34.2 (×2), 31.3 (×2), 29.6, 29.0, 28.5, 28.3, 25.4; **LRFAB-MS (3-NOBA matrix):** *m/z* = 1716 $[M+H]^+$; **HRFAB-MS (3-NOBA matrix):** *m/z* = 1716.97173 (calcd. for $^{13}C^{12}C_{110}H_{135}N_4O_8S_2$, 1716.97549).

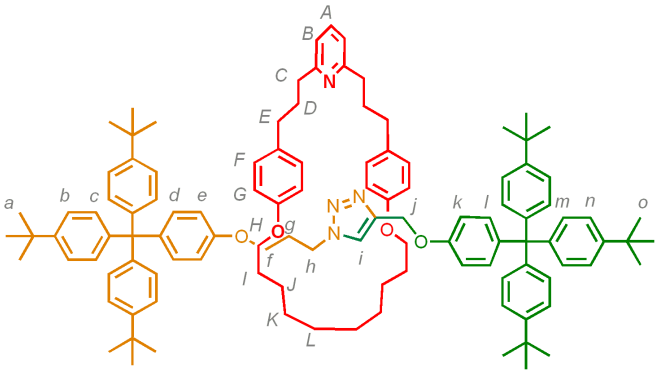

4j

Using general method, macrocycle **1j** (12.1 mg, 25.0 µmol, 1.0 equiv.), azide **3** (14.7 mg, 25.0 µmol, 1.0 equiv.), alkyne **2** (14.9 mg, 27.5 µmol, 1.1 equiv.), $[Cu(CH_3CN)_4](PF_6)$ (10.0 mg, 27.5 µmol, 1.1 eq) and KCN (16.0 mg, 0.25 mmol, 10 equiv.) gave the crude product as a mixture of rotaxane **4j**, thread **5** (60:40, by ^{1}H NMR spectroscopy), macrocycle **1j**. Purification by preparative TLC on silica gel (2 elutions in CH_3CN/CH_2Cl_2/Petrol; 3.5:40:56.5) gave the rotaxane **4j** as a white solid (17 mg, 42%). **M.p.** 128-132 °C; **^{1}H NMR (400 MHz, $CDCl_3$):** δ = 7.33 (t, 1H, *J* = 7.6 Hz, H_A), 7.24 (d, 6H, J = 8.5 Hz, H_n), 7.21-7.01 (m, 23H, H_b, H_c, H_d, H_i, H_l, H_m), 6.83 (d, 2H, *J* = 7.7 Hz, H_B), 7.74 (br d, 6H, *J* = 8.4 Hz, H_F, H_k), 6.48 (d, 6H, *J* = 8.6 Hz, H_G, H_e), 4.91 (s, 2H, H_j), 3.81-3.70 (m, 6H, H_H, H_h), 3.34 (t, 2H, *J* = 5.8 Hz, H_f), 2.60 (2d, 4H, *J* = 6.8 Hz, H_C), 2.51 (t, 4H, *J* = 7.3 Hz, H_E), 1.84-1.72 (m, 4H, H_D), 1.70-1.60 (m, 6H, H_I, H_g), 1.57-1.11 (m, 12H, H_J, H_K H_L), 1.31 and 1.30 (2s, 54H, H_a, H_o); **^{13}C NMR (100 MHz, $CDCl_3$):** δ = 161.4, 156.9, 156.1 (×2), 148.2 (×2), 144.1, 144.0, 143.5, 139.7, 139.5 (×2), 133.5, 132.1, 132.0, 130.6 (×2), 129.1, 124.0 (×2), 123.1, 119.6, 114.2, 113.0, 112.9, 67.0, 63.8, 63.0 (×2), 61.5, 46.7, 37.9, 35.0, 34.2 (×2), 32.4, 31.3 (×2), 29.4, 29.3, 28.6, 28.5, 25.6; **LRFAB-MS (3-NOBA matrix):** *m/z* = 1617 $[M+H]^+$; **HRFAB-MS (3-NOBA matrix):** *m/z* = 1617.08218 (calcd. for $^{13}C^{12}C_{112}H_{139}N_4O_4$, 1617.08299).

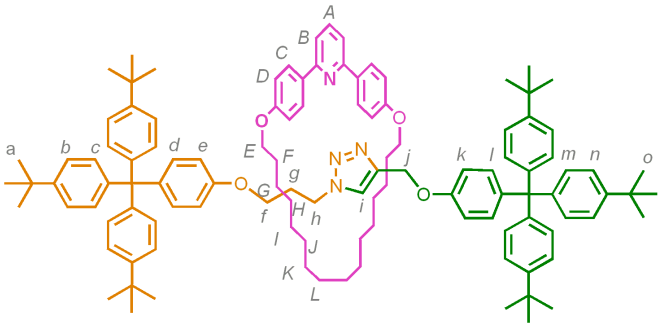

4l

Using general method, macrocycle **1l** (29.0 mg, 60.4 µmol, 1.0 equiv.), azide **3** (35.5 mg, 60.4 µmol, 1.0 equiv.), alkyne **2** (36.0 mg, 66.4 µmol, 1.1 equiv.), $[Cu(CH_3CN)_4](PF_6)$ (24.8 mg, 66.4 µmol, 1.1 eq) and KCN (40 mg, 0.66 mmol, 10 equiv.) gave the crude product as a mixture of rotaxane **4l**, thread **5** (25:75, by ^{1}H NMR spectroscopy), macrocycle **1l**. Purification by flash column chromatography (CH_3CN/CH_2Cl_2/Petrol; 2.5:20:77.5) gave the rotaxane **4l** as a white solid (15 mg, 14%). **M.p.** 130-132°C; **^{1}H NMR (400 MHz, $CDCl_3$):** δ = 7.73 (d, 4H, *J* = 8.8 Hz, H_C), 7.61 (t, 1H, *J* = 7.8 Hz, H_A), 7.39 (d, 2H, *J* = 7.8 Hz, H_B), 7.22-7.18 (m, 12H, H_b, H_n), 7.10-7.03 (m, 16H, H_c, H_d, H_m, H_l), 6.89 (s, 1H, H_i), 6.82 (d, 4H, *J* = 8.8 Hz, H_D), 6.78 (d, 2H, *J* = 8.9 Hz, H_k), 6.66 (d, 2H, *J* = 8.9 Hz, H_e), 4.96 (s, 2H, H_j), 4.04 (t, 4H, *J* = 7.2 Hz, H_E), 4.00 (t, 2H, *J* = 7.1 Hz, H_h), 3.70 (t, 2H, *J* = 5.6 Hz, H_f), 1.97 (quint., 2H, *J* = 6.4 Hz, H_g), 1.60 (quint, 4H, *J* = 7.0 Hz, H_F), 1.33-0.98 (m, 24H, H_G, H_H, H_I, H_J, H_K, H_L), 1.30 and 1.29 (2s, 54H, H_a, H_o); **^{13}C NMR (100 MHz, $CDCl_3$):** δ = 158.9, 156.9, 156.2 (×2), 148.2 (×2), 144.0 (×2), 143.5, 139.8 (×2), 137.3, 132.5 (×2), 132.1, 130.7, 130.6, 128.8, 124.0 (×2), 123.2, 117.2, 115.3, 113.1, 112.8, 68.0, 63.9, 63.0 (×2), 61.7, 46.7, 34.2 (×2), 31.3 (×2), 30.1, 30.0, 29.6 (×2), 29.5 (×2), 28.2, 25.7; **LRFAB-MS (3-NOBA matrix):** *m/z* = 1617 $[M+H]^+$; **HRFAB-MS (3-NOBA matrix):** *m/z* = 1617.08485 (calcd. for $^{13}C^{12}C_{112}H_{139}N_4O_4$, 1617.08299).

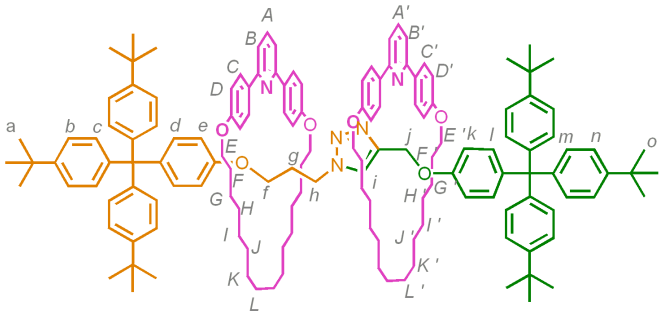

7l

A solution of macrocycle **1l** (170 mg, 0.35 mmol, 10 equiv.), azide **3** (20.6 mg, 35.0 μmol, 1.0 equiv.), alkyne **2** (19.0 mg, 35.0 μmol, 1.1 equiv.), $[Cu(CH_3CN)_4](PF_6)$ (14.3 mg, 38.5 μmol, 1.1 eq) in CH_2Cl_2 (10 mL) and under N_2 was stirred at RT for 8 days. The solution was then refluxed for further 48 h then cooled to RT. The resulting mixture was diluted with CH_2Cl_2 (5 mL) and methanol (15 mL). Then a solution of KCN (25 mg, 0.38 mmol, 10 equiv.) in methanol (2 mL) was added and the resulting suspension stirred vigorously for 1 h. Solvents were evaporated (80 ºC) and the residue was partitioned between water (15 mL) and CH_2Cl_2 (20 mL). The layers were separated and the aqueous layer was extracted with CH_2Cl_2 (3 × 10 mL). The combined organic fractions were washed with water (10 mL) and brine (10 mL), then dried ($MgSO_4$) and concentrated under reduced pressure to give the crude product as a mixture of [2]rotaxane **4l**, [3]rotaxane **7l**, thread **5** (33:37:30, by ^{1}H NMR spectroscopy), macrocycle **1l**, remaining azide **3** and alkyne **2**, (75% overall conversion). Purification by preparative TLC on silica gel (3 elutions in CH_3CN/CH_2Cl_2/Petrol; 3.5:40:56.5) gave the [3]rotaxane **7l** as a white solid (15 mg, 20%). **M.p.** 302-304 °C; **^{1}H NMR (400 MHz, $CDCl_3$):** δ = 7.68 (m, 10H, H_C, $H_{C'}$, H_A, $H_{A'}$), 7.37 (d, 4H, *J* = 7.8 Hz, H_B, $H_{B'}$), 7.20 -7.10 (m, 12H, H_b, H_n), 7.09 (s, 1H, H_i), 7.05-6.91 (m, 16H, H_c, H_m, H_d, H_l), 6.82 (d, 2H, *J* = 8.9 Hz, H_k), 6.74-6,65 (m, 8H, H_D, $H_{D'}$), 6.46 (d, 2H, *J* = 8.9 Hz, H_e), 5.04 (s, 2H, H_j), 4.03-3.89 (m, 8H, *J* = 7.2 Hz, H_E, $H_{E'}$), 3.70 (t, 2H, *J* = 7.5 Hz, H_h), 3.50 (t, 2H, *J* = 5.7 Hz, H_f), 1.69 (br. quint., 2H, *J* = 6.7 Hz, H_g), 1.54 (br. quint, 8H, *J* = 7.35 Hz, H_F), 1.40-0.81 (m, 48H, H_G, $H_{G'}$, H_H, $H_{H'}$, H_I, $H_{I'}$, H_J, $H_{J'}$, H_K, $H_{K'}$, H_L, $H_{L'}$), 1.27 and 1.26 (2s, 54H, H_a, H_o); **^{13}C NMR (100 MHz, $CDCl_3$):** δ = 158.9, 158.8, 156.8, 156.7, 156.2, 156.1, 148.1, 148.0, 144.0 (×2), 143.1, 139.7, 139.5, 137.1, 136.9, 132.5, 132.1, 132.0, 131.8, 130.6 (×2), 128.6 (×2), 123.9 (×2), 123.1, 116.9, 116.7, 115.2, 115.0, 113.3, 113.0, 68.2, 68.1, 64.1, 62.9 (×2), 61.7, 46.7, 34.2 (×2), 31.3 (×2), 30.1, 29.9 (×2), 29.7

(×2), 29.6 (×2) , 29.5 (×2), 29.4 (×2), 28.3, 28.2 and 25.7 (×2); **LRFAB-MS (3-NOBA matrix):** *m/z* = 2101 $[M]^+$; **HRFAB-MS (3-NOBA matrix):** *m/z* = 2102.41114 $[M+H]^+$ (calc. for $^{12}C_{145}{}^{13}CH_{182}N_5O_6$, 2102.41237 $[M+H]^+$).

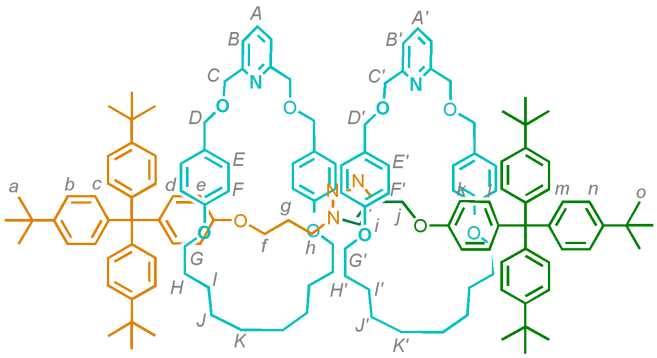

7a

A solution of macrocycle **1a** (400 mg, 0.817 mmol, 10 equiv.), alkyne **2** (48.0 mg, 8.17 μmol, 1.0 equiv.), azide **3** (44.3 mg, 8.17 μmol, 1.0 equiv.), $Cu(CH_3CN)_4PF_6$ (30.0 mg, 38.5 μmol, 1.0 eq) in dry CH_2Cl_2 (10 mL) and under N_2 was stirred at RT for 72 h. The solution was refluxed for further 48 h then cooled to RT. The resulting mixture was diluted with CH_2Cl_2 (15 mL) and methanol (25 mL). Then a solution of KCN (106 mg, 1.63 mmol, 20 equiv.) in methanol (2 mL) was added and the resulting suspension stirred vigorously for 2 h. Solvents were evaporated (80 ºC) and the residue was partitioned between water (15 mL) and CH_2Cl_2 (20 mL). The layers were separated and the aqueous layer was extracted with CH_2Cl_2 (3 × 15 mL). The combined organic fractions were washed with water (10 mL) and brine (10 mL), then dried ($MgSO_4$) and concentrated under reduced pressure to give the crude product as a mixture of [2]-rotaxane **4a**, [3]-rotaxane **7a**, thread **5** (90:5:5, by ^{1}H NMR spectroscopy) and macrocycle **1a**. Purification by column chromatography (CH_3CN-CH_2Cl_2-Petrol; 5:35:60) followed by preparative TLC on silica gel (5 elutions in CH_3CN-CH_2Cl_2-Petrol; 7:33:60) gave pure rotaxane **7a** as a white solid (3.5 mg, 2%); **M.p.** 210-212 °C; **^{1}H NMR (400 MHz, $CDCl_3$):** δ = 7.48 (m, 2H, H_A, $H_{A'}$), 7.27-7.20 (m, 16H, H_B, $H_{B'}$, H_b, H_n), 7.19 (s, 1H, H_i), 7.10 (d, 6H, *J* = 8.5 Hz, H_c or H_m), 7.07 (d, 6H, *J* = 8.5 Hz, H_c or H_m), 6.98 (d, 4H, *J* = 8.4 Hz, H_E or $H_{E'}$), 6.94 (d, 4H, *J* = 8.4 Hz, H_E or $H_{E'}$), 6.76 (t, 4H, *J* = 8.8 Hz, H_d, H_l), 6.52 (d, 4H, *J* = 8.5 Hz, H_F or $H_{F'}$), 6.49 (d, 4H, *J* = 8.5 Hz, H_F or $H_{F'}$), 6.15 (d, 2H, *J* = 8.8 Hz, H_k), 5.99 (d, 2H, *J* = 8.8 Hz, H_e), 4.54-4.45 (m, 8H, H_C, $H_{C'}$), 4.39 (s, 2H, H_j), 4.25(s, 8H, H_D, $H_{D'}$), 3,84-3.66 (m, 8H, H_G, $H_{G'}$), 3.66-3.56 (m, 2H, H_h), 3.00 (t, 2H, *J* = 5.8 Hz, H_f),

1.70-1.52 (m, 10H, H_H, $H_{H'}$, H_g), 1.47-0.93 (m, 24H, H_I, $H_{I'}$, H_J, $H_{J'}$, H_K, $H_{K'}$), 1.31 (2s, 54H, H_a, H_o); **^{13}C NMR (100 MHz, $CDCl_3$):** δ = 158.6 (×2), 157.6 (×2), 155.9 (×2), 148.0 (×2), 144.3(×2), 143.1, 139.1, 139.0, 136.9 (×2), 131.6, 131.5, 130.7 (×2), 129.8 (×2), 129.0, 128.8, 124.0 (×2), 123.2, 119.4 (×2), 114.3 (×2), 112.8, 112.7, 72.4, 72.3, 70.9, 70.8, 67.0 (×2), 63.8, 62.9 (×2), 61.0, 46.7, 34.2 (×2), 31.4 (×2), 29.6 (×2), 29.6, 28.7, 28.6, 28.5 (×2), 25.6, 25.5; **LRFAB-MS (3-NOBA matrix):** *m/z* = 2110 $[M+H]^+$; **HRFAB-MS (3-NOBA matrix):** *m/z* = 2110.33050 $[M+H]^+$ (calc. for $^{12}C_{141}{}^{13}CH_{174}N_5O_{10}$, 2110.32943 $[M+H]^+$).

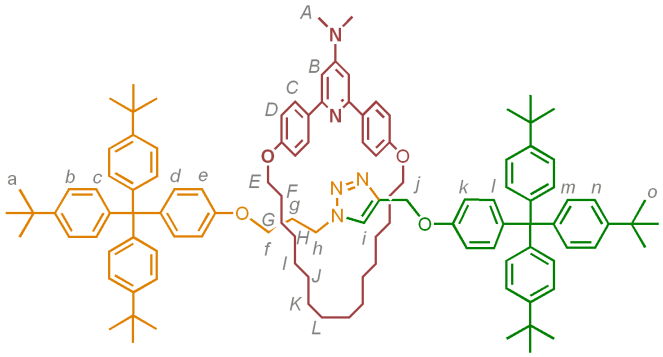

4m

Using general method, macrocycle **1m** (12.1 mg, 25.0 µmol, 1.0 equiv.), azide **2** (14.7 mg, 25.0 µmol, 1.0 equiv.), alkyne **3** (14.9 mg, 27.5 µmol, 1.1 equiv.), $[Cu(CH_3CN)_4](PF_6)$ (10.0 mg, 27.5 µmol, 1.1 eq) and KCN (16.0 mg, 0.25 mmol, 10 equiv.) gave the crude product as a mixture of rotaxane **4m**, thread **5** (20:80, by ^{1}H NMR spectroscopy), macrocycle **1m**. Purification by flash column chromatography (CH_3CN/CH_2Cl_2/Petrol; 3.5:20:76.5) followed by preparative TLC on alumina (3 elutions in CH_3CN/CH_2Cl_2/Petrol; 2.5:15:82.5) gave the rotaxane **4m** as a white solid (10 mg, 16 %). **M.p.** 99-101 °C; **^{1}H NMR (400 MHz, $CDCl_3$):** δ = 7.71 (d, 4H, *J* = 8.6 Hz, H_C), 7.21 (d, 6H, J = 8.5 Hz, H_b), 7.20 (d, 6H, J = 8.5 Hz, H_n) 7.12-7.03 (m, 16H, H_c, H_d, H_m, H_l), 6.99 (s, 1H, H_i). 6.80 (d, 6H, *J* = 8.6 Hz, H_D, H_k), 6.71 (s, 2H, H_B), 6.69 (d, 2H, *J* = 8.8 Hz, H_e), 4.91 (s, 2H, H_j), 4.04 (t, 4H, *J* = 7.1 Hz, H_E), 3.97 (t, 2H, *J* = 7.1 Hz, H_h), 3.72 (t, 2H, *J* = 5.8 Hz, H_f), 3.00 (s, 6H, H_A), 1.94 (br quint., 2H, *J* = 6.5 Hz, H_g), 1.58 (br quint, 4H, *J* = 7.1 Hz, H_F), 1.46-0.97 (m, 24H, H_G, H_H, H_I, H_J, H_K, H_L), 1.29 (s, 54H, H_a, H_o); **^{13}C NMR (100 MHz, $CDCl_3$):** δ = 158.5, 157.5, 156.3 (×2), 155.8, 148.2 (×2), 144.0 (×2), 143.3, 139.7 (×2), 133.8, 132.1 (×2), 130.7 (×2), 128.8, 124.0 (×2), 123.5, 115.1, 113.1, 112.9, 100.8, 68.0, 64.1, 63.0 (×2), 61.6, 46.7, 39.4, 34.2 (×2), 31.3 (×2), 30.1, 30.0, 29.7, 29.6, 29.5

(×2), 28.2, 25.7; **LRFAB-MS (3-NOBA matrix):** *m/z* = 1660 $[M+H]^+$; **HRFAB-MS (3-NOBA):** *m/z* = 1659.13501 $[M]^+$ (calc. for $^{13}C^{12}C_{114}H_{143}N_5O_4$, 1659.11736 $[M+H]^+$).

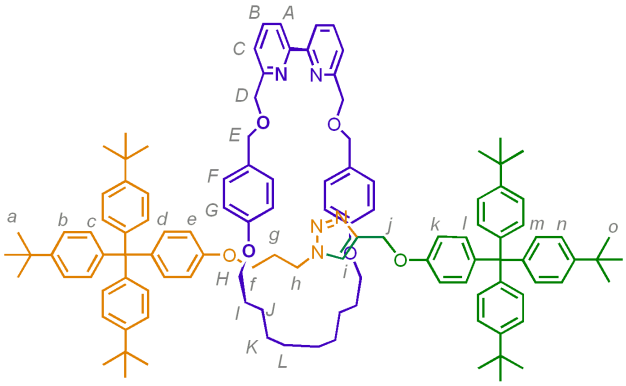

4n

Using general method, macrocycle **1n** (9.9 mg, 17.4 µmol, 1.0 equiv.), azide **2** (10.2 mg, 17.4 µmol, 1.0 equiv.), alkyne **3** (10.4 mg, 19.2 µmol, 1.1 equiv.), $[Cu(CH_3CN)_4](PF_6)$ (7.1 mg, 19.2 µmol, 1.1 eq) and KCN (11.4 mg, 0.17 mmol, 10 equiv.) gave the crude product as a mixture of rotaxanes **4n**, thread **5** (45:65, by ^{1}H NMR spectroscopy), macrocycle **1n**. Purification by flash column chromatography (acetone/CH_2Cl_2; 4:96) followed by preparative TLC on alumina (3 elutions in diethyl ether/Petrol; 1:1) gave the rotaxane **4n** as a white solid (10 mg, 35%). **M.p.** 90-94°C; **^{1}H NMR (400 MHz, $CDCl_3$):** δ = 7.89 (d, 2H, *J* = 7.7 Hz, H_A), 7.43 (t, 2H, *J* = 7.7 Hz, H_B), 7.30-7.17 (m, 14H, H_b, H_n, H_C), 7.17-7.00 (m, 16H, H_c, H_d, H_m, H_l), 7.00-6,92 (m, 5H, H_F, H_i), 6.66 (d, 2H, *J* = 8.8 Hz, H_k), 6.54 (d, 4H, *J* = 8.5 Hz, H_G), 6.33 (d, 2H, *J* = 8.8 Hz, H_e), 4.81 (s, 2H, H_j), 4.54 (s, 4H, H_D), 4.51 (s, 4H, H_E), 3.75-3.66 (m, 6H, H_H, H_h), 3.24 (t, 2H, *J* = 5.6 Hz, H_f), 1.65-1.50 (m., 6H, H_I, H_g), 1.40-1.03 (m, 12H, H_J, H_K, H_L), 1.30 and 1.29 (2s, 54H, H_a, H_o); **^{13}C NMR (100 MHz, $CDCl_3$):** δ = 158.5 (×2), 158.1, 156.1 (×2), 148.2 (×2), 144.1, 144.0, 143.4, 139.8, 139.5, 137.1, 132.1, 131.9, 130.6 (×2), 129.6, 129.5, 124.0 (×2), 123.1, 121.5, 119.9, 114.2, 113.0, 112.7, 72.4, 72.2, 67.5, 63.6, 63.0 (×2), 61.5, 46.7, 34.2 (×2), 31.3 (×2), 29.6, 29.2, 28.7 (×2), 25.7; **LRFAB-MS (3-NOBA matrix):** *m/z* = 1698 $[M+H]^+$; **HRFAB-MS (3-NOBA matrix):** *m/z* = 1698.06527$[M+H]^+$ (calc. for $^{13}C^{12}C_{115}H_{138}N_5O_6$ 1698.06807 $[M+H]^+$).

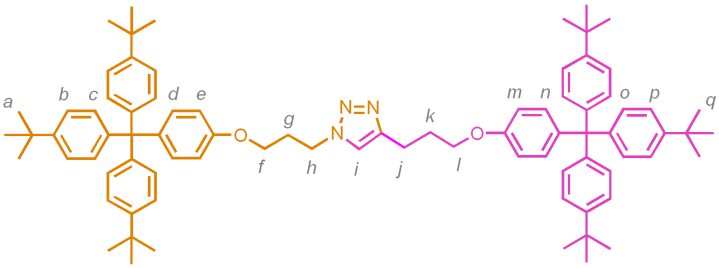

S23

Spectroscopic data of the non-interlocked thread **S23** generated during the synthesis of rotaxane **S24**: **^{1}H NMR (400 MHz, $CDCl_3$):** δ = 7.31 (s, 1H, H_i), 7.22 (m, 12H, H_b, H_p), 7.10-7.05 (m, 16H, H_c, H_d, H_n, H_o), 6.73 (d, 2H, *J* = 9.0 Hz, H_m/H_e), 6.72 (d, 2H, *J* = 8.9 Hz, H_m/H_e), 4.53 (t, 2H, *J* = 6.9 Hz, H_h), 3.96 (t, 2H, *J* = 6.1 Hz, H_l), 3.92 (t, 2H, *J* = 5.5 Hz, H_f), 2.90 (t, 2H, *J* = 7.5 Hz, H_j), 2.35 (quint, 2H, *J* = 6.4 Hz, H_g), 2.14 (quint, 2H, *J* = 6.3 Hz, H_k), 1.29 (s, 54H, H_a, H_q); **^{13}C NMR (100MHz, $CDCl_3$):** δ = 156.6, 156.2, 148.3, 148.2, 147.2, 144.1, 144.0, 139.9, 139.5, 132.3, 132.2, 130.7 (x 2), 124.0, 123.9, 121.4, 112.8, 112.7, 66.6, 63.8, 63.0 (x 2), 46.9, 34.2 (x 2), 31.3, 30.0, 29.6, 28.9, 22.1; **LRESI-MS:** m/z = 1158 $[M+1]^+$; **HRFAB-MS (3-NOBA matrix):** *m/z* = 1155.78059 $[M+H]^+$ (calcd. for $C_{82}H_{100}N_3O_2$, 1158.78155).

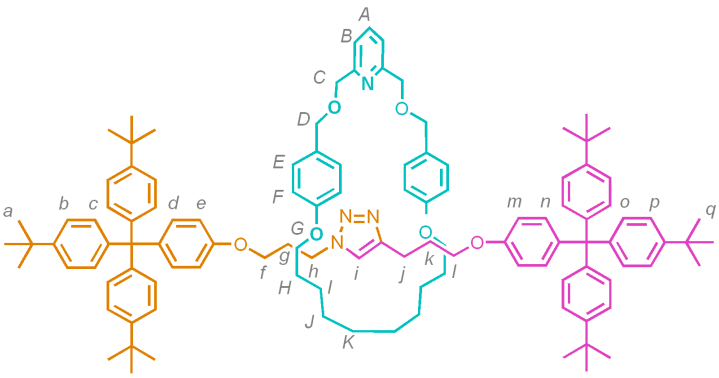

S24

Using general method, macrocycle **1a** (24.0 mg, 50.0 μmol, 1.0 equiv.), azide **3** (29 mg, 25.0 μmol, 1.0 equiv.), alkyne **2a** (29.0 mg, 50.0 μmol, 1.0 equiv.), $[Cu(CH_3CN)_4](PF_6)$ (19.0 mg, 27.5 μmol, 1.1 eq) and KCN (33.0 mg, 0.5 mmol, 10 equiv.) gave the crude product as a mixture of rotaxane **S24**, thread **S23** (60:40, by ^{1}H NMR spectroscopy) and macrocycle **1a**. Purification by preparative TLC on silica gel (3 elutions in CH_3CN/CH_2Cl_2/hexane; 5:40:55) gave the rotaxane **S24** as a white solid (44 mg, 53%); **M.p.** 130-131 °C; **^{1}H NMR (400 MHz, $CDCl_3$):** δ = 7.51 (t, 1H, *J* = 7.7 Hz, H_A), 7.27-7.23 (m, 14H, H_B, H_b, H_p), 7.13-7.09 (m, 12H, H_c, H_o),

7.05 (d, 2H, J = 8.8 Hz, H_n/H_d), 7.04 (d, 2H, J = 8.8 Hz, H_n/H_d), 6.99 (d, 4H, J = 8.5 Hz, H_E), 6.86 (s, 1H, H_i), 6.63 (d, 2H, J = 8.8 Hz, H_e/H_m), 6.60 (d, 4H, J = 8.5 Hz, H_F), 6.49 (d, 2H, J = 8.8 Hz, H_e/H_m), 4.89 (s, 4H, H_C), 4.27 (s, 4H, H_D), 3.84-3.78 (m, 6H, H_G, H_h), 3.71 (t, 2H, J = 6.2 Hz, H_l), 3.34 (t, 2H, J = 5.8 Hz, H_f), 2.60 (t, 2H, J = 7.7 Hz, H_j), 1.87 (quint, 2H, J = 6.4 Hz, H_k), 1.68 (quint, 2H, J = 6.0 Hz, H_g), 1.65 (quint, 4H, J = 6.5 Hz, H_H), 1.32-1.15 (m, 12H, H_I, H_J, H_K); 1.32 and 1.31 (2s, 54H, H_a, H_q); **^{13}C NMR (100 MHz, CDCl$_3$):** δ = 158.6, 157.5, 156.6, 156.2, 148.2, 148.1, 146.6, 144.1 (x 2), 139.5, 139.2, 137.0 (x 2), 132.0 (x 2), 130.6, 129.8, 129.0, 124.0 (x 2), 121.1, 119.8, 114.3, 112.8, 72.4, 71.1, 67.0, 66.5, 63.8, 63.0 (x 2), 46.5, 34.2 (x 2), 31.3 (x 2), 29.6, 29.5 (x 2), 28.7, 28.6 (x 2), 25.6, 22.0; **LRESI-MS:** m/z = 1648 $[M]^+$; **HRFAB-MS (3-NOBA matrix):** m/z = 1649.07254 $[M+H]^+$ (calcd for $^{13}C^{12}C_{112}H_{139}N_4O_6$, 1649.07282).

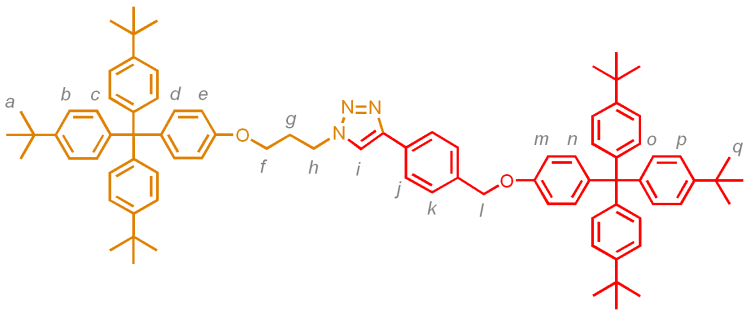

S25

Spectroscopic data of the non-interlocked thread **S25** (derived from **2c** and **3**) generated during the synthesis of rotaxane **S26**: **^{1}H NMR (400 MHz, CDCl$_3$):** δ = 7.82 (d, 2H, J = 8.1 Hz, H_k), 7.77 (s, 1H, H_i), 7.48 (d, 2H, J = 8.1 Hz, H_k), 7.25-7.22 (m, 12H, H_b, H_p), 7.12-7.07 (m, 16H, H_c, H_d, H_n, H_o), 6.85 (d, 2H, J = 8.9 Hz, H_m), 6.77 (d, 2H, J = 8.8 Hz, H_e), 5.05 (s, 2H, H_l), 4.64 (t, 2H, J = 6.8 Hz, H_h), 3.98 (t, 2H, J = 5.5 Hz, H_f), 2.43 (quint, 2H, J = 6.3 Hz, H_g), 1.30 (s, 54H, H_a, H_q); **^{13}C NMR (100 MHz, CDCl$_3$):** δ = 156.5, 156.1, 148.3, 148.2, 147.3, 144.0 (x 2), 140.1, 139.8, 137.0, 132.3, 132.2, 130.7, 130.6, 130.2, 128.0, 125.8, 124.0 (x 2), 120.2, 113.2, 112.9, 69.6, 63.7, 63.0 (x 2), 47.1, 34.2 (x 2), 31.3 (x 2), 30.0; **LRESI-MS:** m/z = 1206 $[M+H]^+$; **HRFAB-MS (3-NOBA matrix):** m/z = 1206.78135 $[M+H]^+$ (calcd. for $C_{86}H_{100}N_3O_2$, 1206.72516).

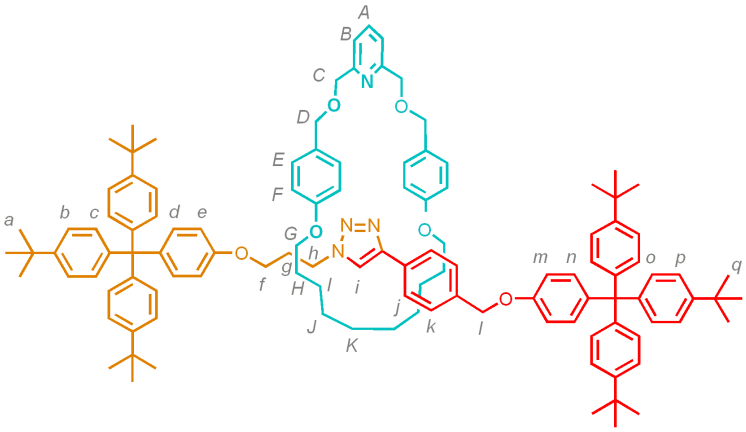

S26

Using general method, macrocycle **1a** (24.0 mg, 50.0 μmol, 1.0 equiv.), azide **3** (29 mg, 25.0 μmol, 1.0 equiv.), alkyne **2c** (31.0 mg, 50.0 μmol, 1.0 equiv.), $[Cu(CH_3CN)_4](PF_6)$ (19.0 mg, 27.5 μmol, 1.1 equiv.) and KCN (33.0 mg, 0.5 mmol, 10 equiv.) gave the crude product as a mixture of rotaxane **S26**, thread **S25** (33:66, by ^{1}H NMR spectroscopy) and macrocycle **1a**. Purification by preparative TLC on silica gel (5 elutions in CH_3CN/CH_2Cl_2/hexane; 5:40:55) gave the rotaxane **S26** as a white solid (33 mg, 39%); **M.p.** 142-143 °C; **^{1}H NMR (400 MHz, $CDCl_3$):** δ = 7.66 (d, 2H, *J* = 7.8 Hz, H_k), 7.59 (s, 1H, H_i), 7.51 (d, 1H, *J* = 7.7 Hz, H_A), 7.29-7.22 (m, 16H, H_B, H_b, H_j, H_p), 7.12-7.05 (m, 14H, H_c, H_n/H_d, H_o), 7.02 (d, 2H, *J* = 8.1 Hz, H_n/H_d), 6.94 (d, 4H, *J* = 7.9 Hz, H_E), 6.75 (d, 2H, *J* = 8.9 Hz, H_e/H_m), 6.54-6.49 (m, 6H, H_F, H_e/H_m), 4.87 (s, 2H, H_l), 4.47 (d, 2H, *J* = 11.8 Hz, H_C), 4.44 (d, 2H, *J* = 11.7 Hz, $H_{C'}$), 4.29 (s, 4H, H_D), 3.84-3.75 (m, 6H, H_G, H_h), 3.41 (br t, 2H, H_f), 1.68-1.58 (m, 6H, H_H, H_g), 1.35-1.14 (m, 12H, H_I, H_J, H_K); 1.30 and 1.29 (2s, 54H, H_a, H_q); **^{13}C NMR (100 MHz, $CDCl_3$):** δ = 158.6, 157.5, 156.5, 156.2, 148.2 (x 2), 146.7, 144.1 (x 2), 139.7, 139.6, 137.1, 136.5, 132.1, 132.0, 130.6 (x 2), 130.5, 129.8 (x 2), 127.7, 125.5, 124.0 (x 2), 120.5, 120.0, 114.2, 113.2, 112.9, 72.5, 71.2, 69.5, 67.1, 63.8, 63.0 (x 2), 46.6 (x 2), 34.2, 31.3 (x 2), 29.6, 29.5, 29.4, 28.5, 25.6; **LRESI-MS:** *m/z* = 1696 $[M+H]^+$; **HRFAB-MS (3-NOBA matrix):** *m/z* = 1697.07342 $[M+H]^+$ (calcd. for $^{13}C^{12}C_{116}H_{139}N_4O_6$, 1697.07282).

2.4.2 Crystal data and structure refinement for 7l .

Single crystals of **7l** suitable for x-ray crystallography were grown by slow cooling of a hot, saturated solution of **7l** in acetonitrile.

Structural data for **7l** were collected at 173 K using a Rigaku Saturn diffractometer (MM007 high-flux RA/MoKa radiation, confocal optic). All data collections employed narrow frames (0.3–1.08) to obtain at least a full hemisphere of data. Intensities were corrected for Lorentz polarization and absorption effects (multiple equivalent reflections). The structure was solved by direct methods, non-hydrogen atoms were refined anisotropically with CH protons being refined in riding geometries (SHELXTL) against F2. The structure determination for **7l** proved particularly problematic; we collected full datasets using a variety of collection routines on more than 10 different crystals from several different crystallization experiments. The data were always poor, principally because of disorder arising from the alkyl chain and solvent molecules and this disorder was not resolved. Atoms C20-C22 and C81 to C88 refined isotropically subject to DFIX constraints.

Identification code	**7l**	
Empirical formula	$C_{146}H_{181}N_5O_6$	
Formula weight	2101.96	
Temperature	173(2) K	
Wavelength	1.54178 Å	
Crystal system	Triclinic	
Space group	P-1	
Unit cell dimensions	a = 14.0813(12) Å	α = 84.390(4)°.
	b = 19.2182(17) Å	β = 73.528(4)°.
	c = 24.208(2) Å	γ = 83.845(4)°.
Volume	6230.5(10) $Å^3$	
Z	2	
Density (calculated)	1.120 Mg/m^3	
Absorption coefficient	0.511 mm^{-1}	
F(000)	2280	

Crystal size	0.200 x 0.200 x 0.100 mm^3
Theta range for data collection	2.32 to 44.72°.
Index ranges	-12<=h<=12, -17<=k<=17, -22<=l<=22
Reflections collected	31202
Independent reflections	9695 [R(int) = 0.1469]
Completeness to theta = 25.00°	99.2 %
Absorption correction	Multiscan
Max. and min. transmission	1.0000 and 0.0040
Refinement method	Full-matrix least-squares on F^2
Data / restraints / parameters	9695 / 16 / 1319
Goodness-of-fit on F^2	1.819
Final R indices [I>2sigma(I)]	R1 = 0.1765, wR2 = 0.4507
R indices (all data)	R1 = 0.2049, wR2 = 0.4713
Extinction coefficient	0.0007(3)
Largest diff. peak and hole	1.211 and -0.559 e.$Å^{-3}$

2.4.3 Computational Details (Molecular Modeling)

The energy minimized equilibrium geometries shown below were computed using the AM1 Semi-Empirical method as implemented in the SPARTAN 06 molecular modelling program.[45]

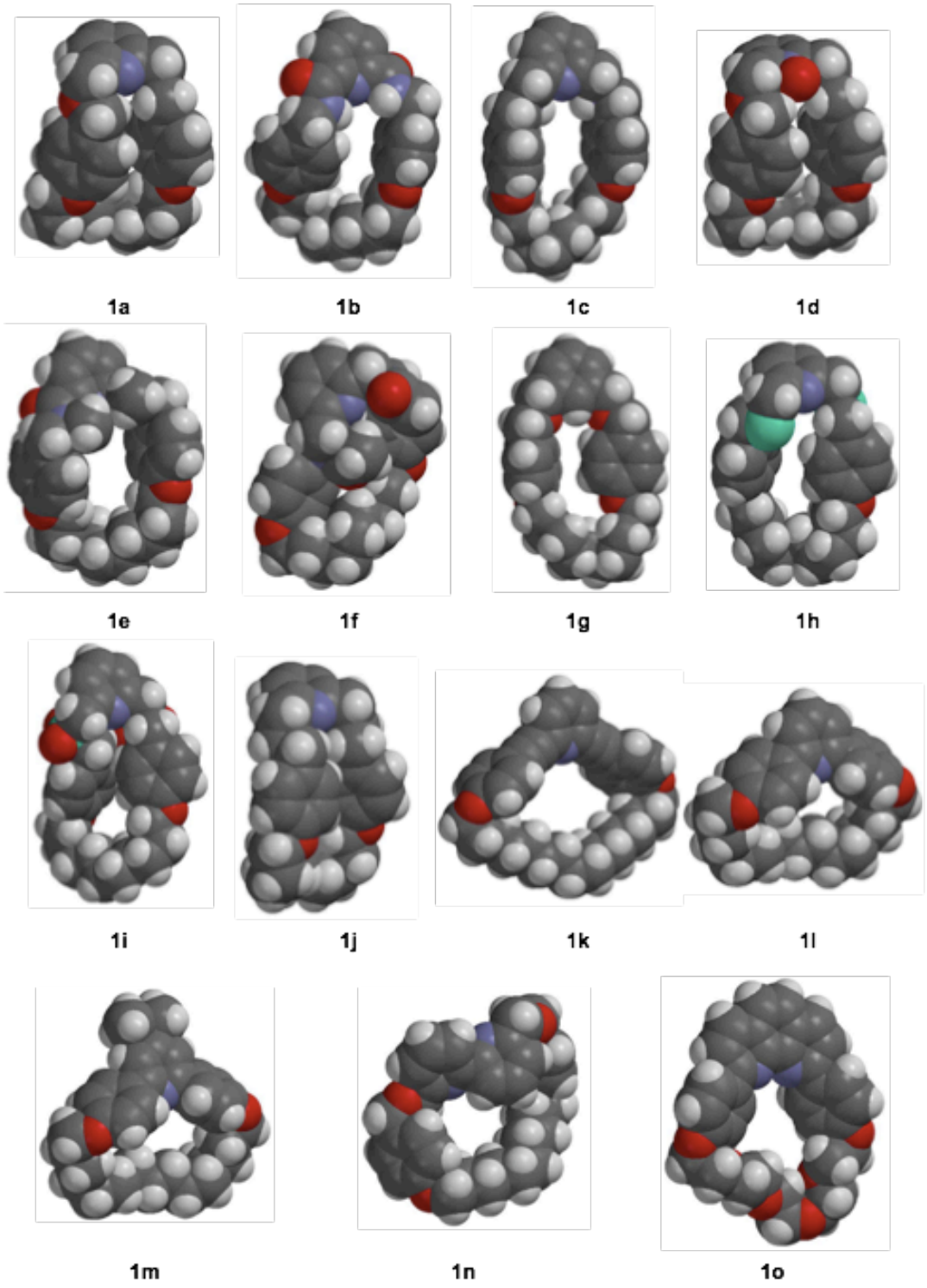

2.5 References and notes

[1] H. C. Kolb, M. G. Finn, K. B. Sharpless, *Angew. Chem. Int. Ed. Engl.,* **2001**, *40*, 2004-2021; H. C. Kolb, K. B. Sharpless, *drug discovery today,* **2003**, *8*, 1128-1137; P. Ball, *Chem. World,* **2007**, *4*, 46-51.

[2] A listing of examples of the use of "click chemistry" is available at http://www.scripps.edu/chem/sharpless/click.html. Date of access 30/11/2009.

[3] C. W. Tornoe, C. Christensen, M. Meldal, *J. Org. Chem,* **2002**, *67*, 3057-3064.

[4] V. V. Rostovtsev, L. G. Green, V. V. Fokin, K. B. Sharpless, *Angew. Chem., Int. Ed. Engl.,* **2002**, *41*, 2596-2599.

[5] V. D. Bock, H. Hiemstra, J. H. van Maarseveen, *Eur. J. Org. Chem,* **2005**, 51-68; W. Peng, V. V. Fokin, *Aldrichimica Acta,* **2007**, *40*, 7-17; N. K. Devaraj, J. P. Collman, *QSAR Comb. Sci.,* **2007**, *26*, 1253-1260; J. E. Moses, A. D. Moorhouse, *Chem. Soc. Rev.,* **2007**, *36*, 1249-1262; Y. L. Angell, K. Burgess, *Chem. Soc. rev.,* **2007**, *36*, 1674-1689; T. P. Gian Cesare Tron, Richard A. Billington, Pier Luigi Canonico, Giovanni Sorba, Armando A. Genazzani,, **2008**, *28*, 278-308; J.-F. Lutz, Z. Zarafshani, *Adv. Drug Delivery Rev.,* **2008**, *60*, 958-970; M. Meldal, C. W. Tornoe, *Chem. Rev.,* **2008**, *108*, 2952-3015.

[6] V. D. Bock, R. Perciaccante, T. P. Jansen, H. Hiemstra, J. H. Van Maarseveen, **2006**, *8*, 919-922.

[7] L. D. Pachon, J. H. van Maarseveen, G. Rothenberg, *Adv. Synth. Catal.,* **2005**, *347*, 811-815.

[8] S. Chassaing, M. Kumarraja, A. S. S. Sido, P. Pale, J. Sommer, *Org. Lett.,* **2007**, *9*, 883-886; A. Alix, S. Chassaing, P. Pale, J. Sommer, *Tetrahedron,* **2008**, *64*, 8922-8929.

[9] S. Chassaing, A. S. S. Sido, A. Alix, M. Kumarraja, P. Pale, J. Sommer, *Chem.--Eur. J.,* **2008**, *14*, 6713-6721.

[10] T. R. Chan, R. Hilgraf, K. B. Sharpless, V. V. Fokin, *Org. Lett.,* **2004**, *6*, 2853-2855; W. G. Lewis, F. G. Magallon, V. V. Fokin, M. G. Finn, *J. Am. Chem. Soc.,* **2004**, *126*, 9152-9153.

[11] F. Perez-Balderas, M. Ortega-Munoz, J. Morales-Sanfrutos, F. Hernandez-Mateo, F. G. Calvo-Flores, J. A. Calvo-Asin, J. Isac-Garcia, F. Santoyo-Gonzalez, *Org. Lett.,* **2003**, *5*, 1951-1954.

[12] *1,3-Dipolar Cycloadditions Chemistry*; R. Huisgen, Ed., Wiley: New York, **1984**; Vol. 1; R. Huisgen, *Pure Appl. Chem.,* **1989**, *61*, 613-28.

[13] If the [2+3]cycloaddition was the preferred mechanism of the Cu-catalyzed reaction, the structures A-C shown in Scheme 2.1 would still be relevant as reactive

intermediates. Interestingly, Sommer and Pale recently demonstrated that the CuAAC reaction can proceed through a different type of mechanism when catalysed by zeolites (see ref. [9]). Based on deuterium labelling studies, they demonstrated that no copper acetylide species is formed during the reaction. Their proposed intermediate, where the alkyne is bound to the copper via a π-bond instead of a σ-bond, and where the azide is bound to the copper via its N-terminal nitrogen atom, is however not believed to go through a classical cyclo-addition process. The π-complex would, instead, undergo syn nucleophilic addition of the azide (e.g. carbocupration) to the terminal end of the coordinated alkyne, leading to a Cu (III) metallacycle.

[14] F. Himo, T. Lovell, R. Hilgraf, V. V. Rostovtsev, L. Noodleman, K. B. Sharpless, V. V. Fokin, *J. Am. Chem. Soc.,* **2005**, *127*, 210-216.

[15] M. Ahlquist, V. V. Fokin, *Organometallics,* **2007**, *26*, 4389-4391.

[16] B. F. Straub, *Chem. Commun.,* **2007**, 3868-3870.

[17] Computational studies by Straub *et. al* (ref. [16]) employing copper(I) μ-acetylide aggregates as the starting intermediate in the reaction cycle suggest that the Cu(III) metallacycle proposed by Fokin is, however, energetically unfavourable. Straub suggests a less energetic species where the strained alkenylidene carbon in Fokin's metallacycle is bound to a second copper atom.

[18] H. V. R. Dias, S. A. Polach, S.-K. Goh, E. F. Archibong, D. S. Marynick, *Inorg. Chem.,* **2000**, *39*, 3894-3901.

[19] In this chapter we use the phrases 'ligandless' and 'ligand-free' to describe copper that is not bound to the pyridine ligands added to the CuAAC reactions to generate the active-template synthesis. As discussed in the text, any Cu(I) that is not coordinated to pyridine units will be complexed by molecules of acetonitrile, azide, alkyne, water or other donor atoms present.

[20] B. M. Mykhalichko, O. N. Temkin, M. G. Mys'kiv, *Russ. chem. rev.,* **2000**, 957.

[21] V. O. Rodionov, V. V. Fokin, M. G. Finn, *Angew. Chem., Int. Ed.,* **2005**, *44*, 2210-2215.

[22] C. Nolte, P. Mayer, B. F. Straub, *Angew. Chem., Int. Ed.,* **2007**, *46*, 2101-2103.

[23] F. Bohlmann, H. Schönowsky, E. Inhoffen, G. Grau, **1964**, *97*, 794-800.

[24] Cu(I)-acetylides are generally complex extended multi-atom aggregates, at least in the solid state and in the absence of good nitrogen ligands (see Ref [20]). The types of reactive intermediates shown in Scheme 2.1 are not meant to be precise or definitive structures—indeed, some of them (e.g. A(ii) and B) are very closely related—but rather are meant to illustrate different (possible) features of the putative reactive intermediate: How many copper atoms are needed to play significant structural or electronic roles during the catalysis? Is the Cu-σ-acetylide π-activated

by an additional Cu atom? If the intermediate has two or more copper atoms is it doubly bridged—as envisaged for a Glaser coupling, which can be ruled out with bidentate ligands for Cu if azide is also coordinated—or singly bridged? Are the reacting azide and alkyne attached to the same or different Cu atoms? etc.

[25] V. Aucagne, K. D. Hanni, D. A. Leigh, P. J. Lusby, D. B. Walker, **2006**, *128*, 2186-2187.

[26] A.-M. Fuller, D. A. Leigh, P. J. Lusby, I. D. H. Oswald, S. Parsons, D. B. Walker, *Angew. Chem., Int. Ed.,* **2004**, *43*, 3914-3918; A.-M. L. Fuller, D. A. Leigh, P. J. Lusby, A. M. Z. Slawin, D. B. Walker, *J. Am. Chem. Soc,* **2005**, *127*, 12612-12619; D. A. Leigh, P. J. Lusby, A. M. Z. Slawin, D. B. Walker, *Chem. Commun.,* **2005**, 4919-4921; A.-M. L. Fuller, D. A. Leigh, P. J. Lusby, *Angew. Chem., Int. Ed.,* **2007**, *46*, 5015-5019.

[27] D. A. Leigh, P. J. Lusby, A. M. Z. Slawin, D. B. Walker, *Angew. Chem., Int. Ed.,* **2005**, *44*, 4557-4564.

[28] We also examined the effect of different alkyne substrates, on the rotaxane formation. The alkynes (see experimental section) were submitted to the standard click reaction conditions (Scheme 2.1) Using a longer, more flexible, alkyl alkyne or an aryl alkyne in the place of **2** led to similar yields of the corresponding [2]rotaxanes (and similar overall conversions of the substrates into triazole products), indicating the rotaxane forming reaction is relatively insensitive to substrate modifications.

[29] The standard reactions conditions use one equivalent of each reagent and low temperatures to minimize the background uncatalyzed thermal cycloaddition. These conditions were chosen to allow the relative efficacy of the different macrocycles in promoting rotaxane formation to be assessed. No attempt was made to optimize the reaction conditions to improve the rotaxane yields reported in Figure 2.1. For macrocycles **1a**, **1i**, **1j**, **1f**, **1l**, **1m**, **1n**—all of which produce significant rotaxane and are not degraded under the reaction conditions—virtually all the macrocyclic ligand can be converted to rotaxane by using extended reaction times and excess of the azide and alkyne building blocks.

[30] For an X-ray structure of **1a** as a monodentate ligand (Pd(II) as metal atom) see ref [26] and c; for X-ray structures of a related pyridine diether ligand acting as a bidentate ligand (Cu(II) or Ni(II) as metal atom) see ref [27].

[31] C. A. Hunter, D. H. Purvis, *Angew. Chem., Int. Ed..*, **1992**, 31, 792-795; A.G. Johnston, D. A. Leigh, L. Nezhat, J. P. Smart, M. D. Deegan, *Angew. Chem., Int. Ed.*, **1995**, 34, 1212-1216; D. A. Leigh, K. Moody, J. P. Smart, K. J. Watson, A. M. Z. Slawin, *Angew. Chem., Int. Ed.*, **1996**, 35, 306-310; D. A. Leigh, A. Murphy, J. P. Smart, A. M. Z. Slawin, *Angew. Chem. Int. Ed.* **1997**, 36, 728-732; D. A. Leigh, A. Murphy, J. P. Smart, M. S. Deleuze, F. Zerbetto, *J. Am. Chem. Soc.*, **1998**, 120, 6458-6467; M. S. Deleuze, D. A. Leigh, F. Zerbetto, *J. Am. Chem. Soc.* **1999**, 121, 2364-2379; W. Clegg, C. Gimenez-Saiz, D. A. Leigh, A. Murphy, A. M. Z. Slawin, S. J. Teat, *J. Am. Chem. Soc.,* **1999**, 121, 4124-4129; F. Biscarini, M. Cavallini, D. A. Leigh, S. Leon, S. J. Teat, J. K. Y. Wong, F. Zerbetto, *J. Am. Chem. Soc.*, **2002**, 124, 225-233; G. Bottari, F. Dehez, D. A. Leigh, P. J. Nash, E. M. Pérez, J. K. Y.

Wong, F. Zerbetto, *Angew. Chem., Int. Ed.*, **2003**, 42, 5886-5889; D. A. Leigh, A. Venturini, A. J. Wilson, J. K. Y. Wong, F. Zerbetto, *Chem. --Eur. J.*, **2004**, 10, 4960-4969.

[32] Hydrogen bond energies are usually in the range of 1-10 kcal/mole whereas coordinate bonds have energies of 20-80 kcal/mole, (ref [33]) thus the stabilization of the copper(I) ion upon coordination should compensate for the loss of the two hydrogen bond interactions. In fact all of the pyridine containing macrocycles studied exhibit complexation induced shifts in the ^{1}H NMR spectra ($CDCl_3$) upon addition of $[Cu(CH_3CN)_4](PF_6)$ indicating that copper(I) ions interact with the macrocycles in every case.

[33] A. J. Goshe, J. D. Crowley, B. Bosnich, *Helv. Chim. Acta,* **2001**, *84*, 2971-2985.

[34] This oxidation of Cu(I) to Cu(II) in the presence of **1c** occurs even when great care is taken to exclude both moisture and oxygen from the reaction mixture. It appears that the macrocycle itself is the oxidant. However there is some remaining $[Cu(CH_3CN)_4](PF_6)$ which catalyzes the formation of the thread, **5**.

[35] The multidentate ligand tris[(1-benzyl-1H-1,2,3-triazol-4-yl)methyl]amine (TBTA) is a highly effective copper ligand for the CuAAC reaction [see refs. [34], [10] and Gupta, S. S.; Kuzelka, J.; Singh, P.; Lewis, W. G.; Manchester, M.; Finn, M. G. *Bioconjugate Chem.* **2005**, 16, 1572-1579. However, the individual triazole-functionalized 'arms' of TBTA are weakly coordinating ligands and so TBTA probably functions by the alkyne and azide displacing two of the triazole groups to form the reactive intermediate.

[36] Q. Wang, T. R. Chan, R. Hilgraf, V. V. Fokin, K. B. Sharpless, M. G. Finn, *J. Am. Chem. Soc.,* **2003**, *125*, 3192-3193.

[37] Minimum energy conformations were calculated for each of the metal-free macrocycles using the Spartan molecular modeling program (Semi-Empirical, AM1). The results are reported in the Experimental Section.

[38] In the case of **1e** no hydrogen bonds are present, thus allowing the Cu(I) ion better access to the macrocycles pyridine nitrogen atom. However, in each of the new macrocycles (**1e** and **1f**) the nitrogen atom of the pyridine is more hindered, which may reduce the binding ability of the ligand.

[39] Internal alkynes have been shown to react under CuAAC click conditions, see Diéz-Gonzàlez, S.; Correa, A.; Cavallo, L.; Nolan, S. P. *Chem.--Eur. J.* **2006**, 12, 7558-7564.

[40] Macrocycle **1k** is also photosensitive and decomposes slowly in ambient light.

[41] Bidentate bipyridine and phenanthroline ligands have been shown to significantly enhance the kinetics of the CuAAC reaction, see ref [10].

[42] *Molecular Catenanes Rotaxanes and Knots*; J.-P. Sauvage, C. O. Dietrich-Buchecker, Eds., Wiley-VCH: Weinheim, **1999**; C. Dietrich-Buchecker, B. X. Colasson, J.-P. Sauvage, *Top. Curr. Chem.,* **2005**, 261-283.

[43] S. Saito, E. Takahashi, K. Nakazono, *Org. Lett.,* **2006**, *8*, 5133-5136.

[44] E. Kay, D. Leigh, *Top. Curr. Chem.,* **2005**, 133-177.

[45] Hehre, W. J. *SPARTAN '06*, 1.1; Wavefunction, Inc.: Irvine, CA 92612, **2006**.

CHAPTER THREE

From naturally occurring interlocked architectures to mechanically encapsulated peptides

3 Synopsis

The interlocking of one ore more chemical entities occur in natural molecules. Most systems discovered so far, in which constituents are covalently bound in an intertwined manner, exhibit very different properties compared to their non-interlocked analogues. Exploring these structures reveals that in most cases, interlocking in biological systems has a defined function. It can be used, for example, to hold two or more parts together in a molecular machine in order to create motion of one element relative to the other, or, in the simplest case to give extra stability to a supramolecular assembly.

Biosynthesis of naturally occurring interlocked molecules arises from the reversible or non-reversible covalent capture of self-assembled elements. The first synthetic approaches to interlocked architectures however, relied on random pairing events until chemists exploited self-assembly in a similar way to nature. These synthetic analogues, although discovered at the very end of the synthetic chemistry era, have already proved to be capable of achieving similar tasks to their natural analogues and have often displayed similar properties. The unique nature of the mechanical bond has allowed synthetic chemists to create devices that could be operated at the nanoscopic scale.

This chapter gives a general overview of some biological and synthetic interlocked architectures and their functions, with particular emphasis on structures containing peptidic backbones and on interlocked architectures whose function is to encapsulate and deliver guest molecules. The basic principles for the design and operation of rotaxane-based devices that encapsulate, deliver and release bioactive peptides under specific stimuli will be defined.

3.1 Naturally occurring interlocked molecules

The synthesis of interlocked architectures and their corresponding synthetic machines has been greatly inspired by their naturally occurring homologues. Nature's chemical building blocks (*e.g.* amino acids, nucleotides, nucleosides) are composed mainly of hydrogen-bond donors and acceptors, which are essential for recognition and self-assembly. It is not surprising that interlocked architectures are widely available in living organisms as self-assembly can potentially occur in an intertwined manner and direct the synthesis of the interlocked architecture. However, in order to form, an extra stabilization factor is required to counteract the entropy loss occasioned by the assembly.

The properties of these interlocked species (*e.g.* strong bioactivity, high chemical stability) are, in most cases, very different to that of their non-interlocked analogues. In section 3, some of the most significant naturally-occurring interlocked architectures, and some ideas on how they may form *in vivo*, are discussed.

3.1.1 DNA-based interlocked architectures

As early as 1967 the group of Vinograd described the first topologically interlocked double stranded circular mitochondrial DNA. Isolated by centrifugation of HeLa cell mitochondria and human leukaemic leucocytes, what appeared to be linked monomeric circular units of DNA exhibited high stability under denaturing conditions. Careful analysis of electron micrographs revealed these species to be [2]catananes and [3]catenanes of a few micrometre size (Figure 3.1).[1]

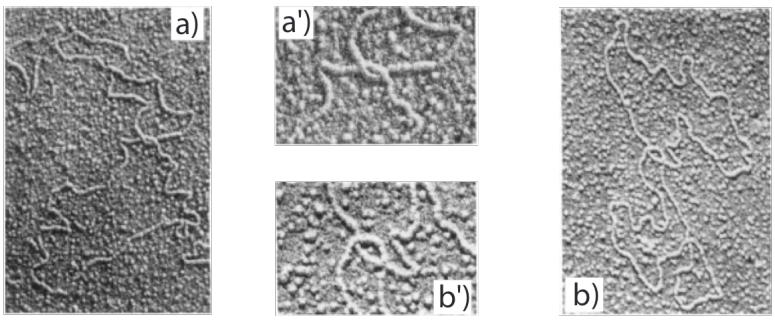

Figure 3.1. Electron micrographs showing the interlocked nature of the mitochondrial DNA dimers. a) and b) × c. 18775, a') and b') × c. 34600. Adapted with permission form Nature publishing group.

The formation of such architectures was postulated to occur in the course of replication or recombination. [2]Catenanes would results from a double recombination between two circular mitochondrial DNA molecules. Higher degree catenanes are formed by the double recombination between a monomer and a catenated dimer (Scheme 3.1). If this simplified theory gives an explanation of the interlocking process, it does not take into account the recognition pattern necessary to form the entangled precursor.

Since then scientists have been able to construct several synthetic topologically linked molecules based on DNA strands.[2]

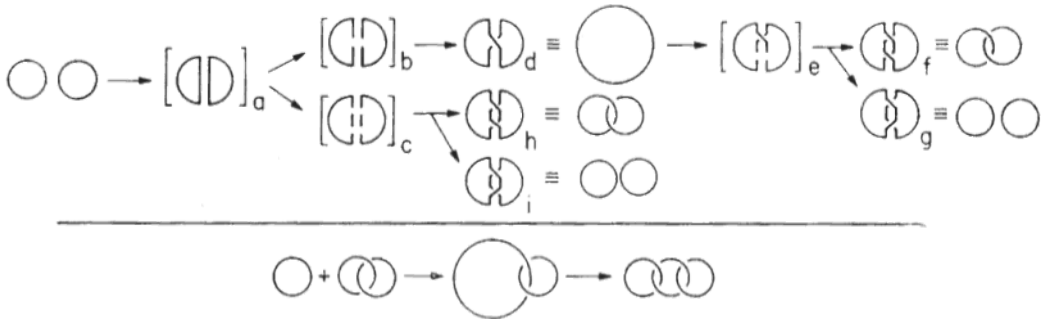

Scheme 3.1. Vinograd's explanation of catenane formation from circular mitochondrial DNA. The circular mitochondrial DNA strands first pair (a) and recombine in different ways (d), (h), (i) according to the breaking pattern of intermediates (b), (c), (e). Higher degree of catenation occurs via the double recombination of a monomeric circular entity and a just formed catenane. Reproduced with permission from Nature Publishing Group.

3.1.2 The viral capsid catenane

Recently, it was found that the capsid of HK 97 bacteriophage consists of a network of deeply catanated hexameric and pentameric proteins units (Figure 3.2). The structure and formation of this unique catenane assembly as been well studied by Duda[3] and was later confirmed by an X-ray diffraction structure of the empty capsid obtained by Johnson et al.[4] The fascinating formation of the capsid goes through several protein assembly and maturation sequences. Three capsid intermediates are subsequently modified before leading to the final covalently linked protein chainmail (Figure 3.2).

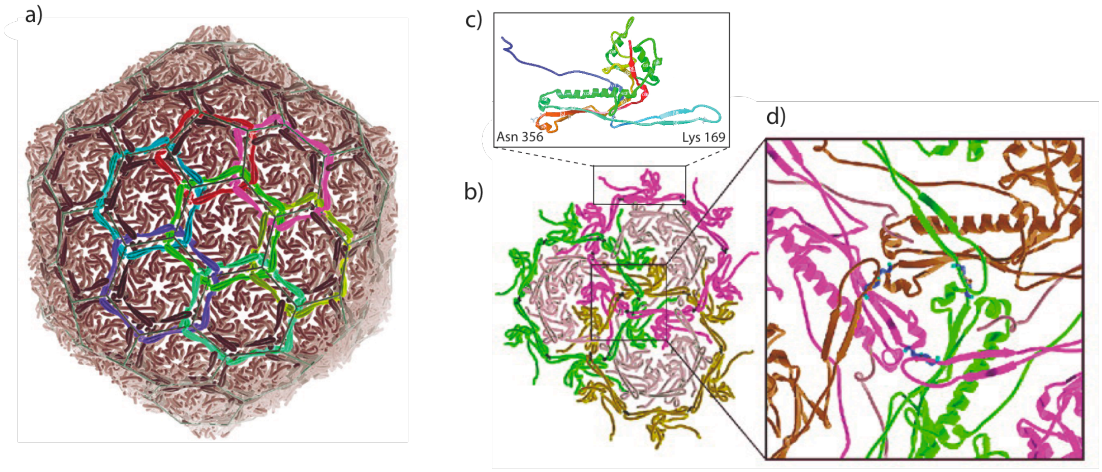

Figure 3.2. a) Three-dimensional view of HK 97 capsid. The subunits cross-linked into pentamers and hexamers are highlighted. The coloured ring shows the catenated nature of the link. b) Three hexamers each with a surrounding metahexamer ring of covalently bonded subunits (magenta, green, and blue). c) Expanded view on one subunit, showing the residues involved in cross-linking d) expanded view on the interlocked cross-linked region, isopeptidic bonds are highlighted in blue. Adapted from ref. [4] with permission from American Association for the Advancement of Science.

The first step is the assembly of head subunits into hexamers and pentamers, assisted by *Escherichia coli* GroEL/ES, and subsequent formation of the shell (prohead I) (Scheme 3.2). The protein subunits are then cleaved at residue 104 and 385 and the resulting prohead II is packed with double stranded DNA (dsDNA, the genetic information of the virus). Final ligation of each subunit forms covalently linked interpenetrated hexamers and pentamers. This links occurs between Lys 169 of one subunit and Asn 356 of the second one, in a process which appears to be auto-catalyzed by a Glu 363 residue of the third subunit (Figure 3.2.c and 3.2d).

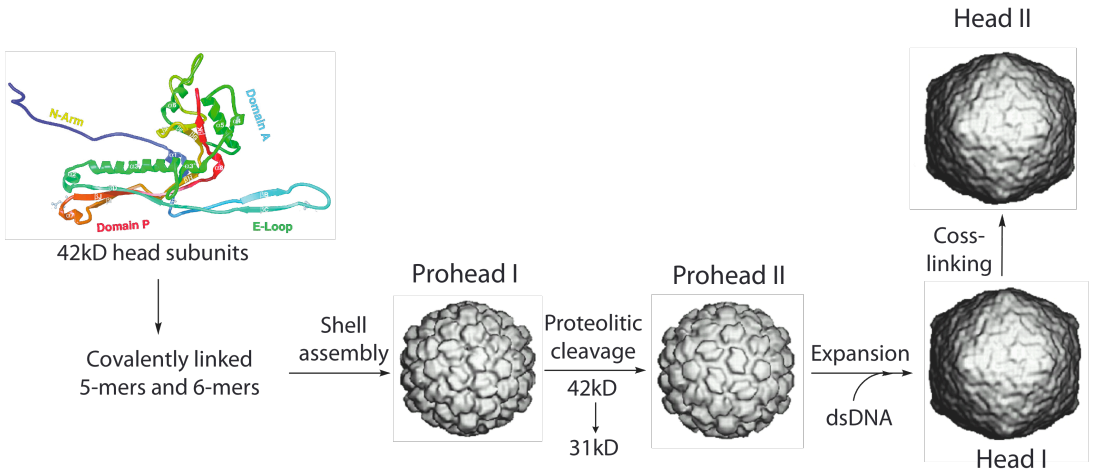

Scheme 3.2. The biosynthesis of HK97 capsid. Adapted from ref. [3] with permission from American Association for the Advancement of Science.

The most likely function of the chainmail is to stabilize the HK 97 capsid, and it has indeed been proven that the capsid is more stable than its non-topologically linked analogue (Head I) towards denaturation. Recent studies have shown that the cross linking is essential for production of a viable HK 97 phage.[5]

3.1.3 Cysteine knots

The so-called cysteine knots are a class of small proteins whose backbone is arranged in a tangled manner. These proteins, originally thought to be rare, have in fact found to be common and are usually referred as covalent knots[6] as they involve disulfide covalent bonds.[7,8] Their high disulfide bond content gives them a compact shape, accounting for their remarkably high stability[9] and specific biological properties. Being the constituent of several toxins, cysteine knots have attracted much interest due to their potential for pharmacological use.[8,10] Their structure consists of a macrocyclic moiety, formed by two disulfide-bonded peptidic segments threaded by a third disulfide bond (Figure 3.3).

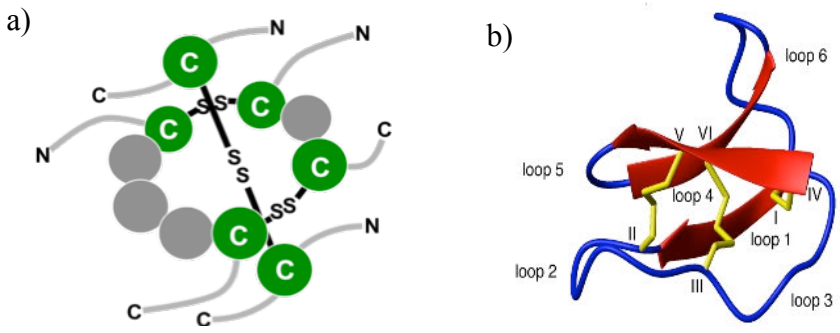

Figure 3.3. a) A Schematic representation of a generic cysteine knot showing the arragement of the six cysteine residues involved in the knot. b) Structure of Kalata B1 the first cyclic cysteine knot to be isolated,[11] showing the interpenetrating β-sheets. Reproduced with permission from the American Society for Biochemistry and Molecular Biology.

Cysteine knots can be divided into three different classes: growth factor cysteine knots (GFCK), inhibitor cysteine knots (ICK) and cyclic cysteine knots (CCK). These three classes differ topologically from the order in which the cysteine residues are interconnected. Figure 3.4 shows the three types of knots and their connectivity. The three structures exhibit a remarkable similarity, featuring a set of three or four anti parallel beta-strands interconnected via disulfide bonds.

Extensive folding studies on toxin cysteine knots has revealed that both ICK and CCK can be folded artificially from mature protein sequences. Interestingly, each disulfide bond appears to stabilize the native protein conformation and directs the formation of the other two.[12]

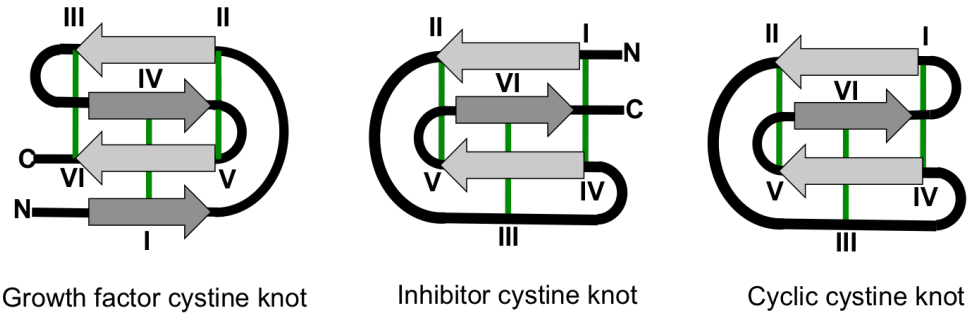

Figure 3.4. The three classes of cysteine knots. The β-strands are represented as arrows, the cysteine residues are labelled I–VI in order from the N- to C-terminus and the disulfide bonds are represented as green lines. The penetrating disulfide bond for the growth factor cysteine knot is Cys(I–IV) whereas it is Cys(III–VI) in the inhibitor cysteine knot and cyclic cysteine knot peptides

3.1.4 Lasso peptides

Lasso peptides (or protoknots) are a class of relatively short peptides that have one linear end threaded through a macrocyclic loop, formed by linkage between the N-terminus and a side chain amino acid residue.[13]

Originally believed to be circular, Microcin J25 (Mcc J25) (Figure 3.5), probably the most studied of the family,[14] was later found to have a lasso structure.[15] Made out of a 21 amino acid sequence, the C-terminus end is threaded through an 8 amino acid-wide macrocycle, resulting from the condensation of the N-terminus -NH_2 and the carboxylic acid of Asp 8 (Figure 3.5).

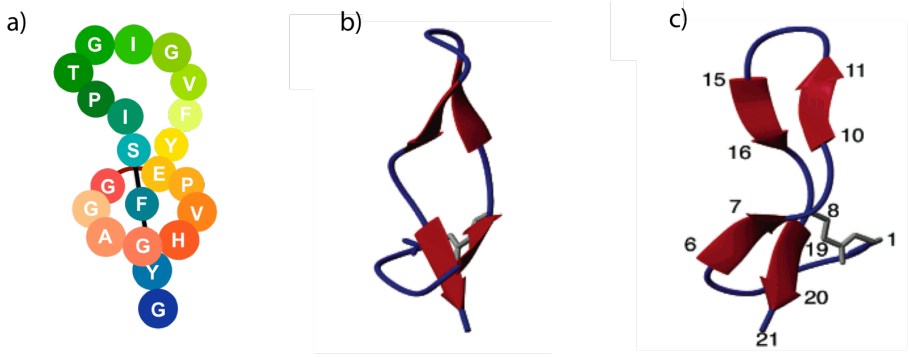

Figure 3.5. Representations of MccJ25 a) simplified structure b and c) ribbon structure of the lowest energy conformation illustrating the two small antiparallel-sheet. Reproduced with permission from the American chemical society

The C-terminus end is maintained threaded in the loop by the consecutive Phe and Tyr residues. Structural analysis suggests the presence of two small anti-parallel beta-sheets, each comprising two strands. The first sheet comprises residues 6-7 and 18-19 and is formed between part of the ring and the penetrating segment. The second sheet involves residues 10-11 and 15-16 (Figure 3.5b and 3.5c).

Secreted by certain strains of *E. Coli* to combat competing microbes, Mcc J25 inhibits bacterial transcription by interfering with the nucleotide uptake channel of bacterial RNA polymerase. As well as high level of biological activity, Mcc J25 also exhibits high resistance to thermal and proteolysis degradation, due to its interlocked nature. Its bio-synthesis has recently been achieved *in vivo* and has demonstrated that two enzymes encoded by genes belonging to the Mcc J25 gene cluster are responsible for converting the 58 amino acid precursor (coded by one of the four genes of the cluster) into the interlocked 21 amino acid lasso structure.[16]

3.2 Synthetic Interlocked architectures based on amides, peptides and proteins

3.2.1 Amide-Based Catenanes and Rotaxanes and knots

Amide bond were first used to direct the assembly of interlocked architectures in 1992. During attempts to increase the yield of a macrocyclization, Hunter serendipitously discovered a two step synthesis of the first amide-based catenane (Figure 3.6).[17]

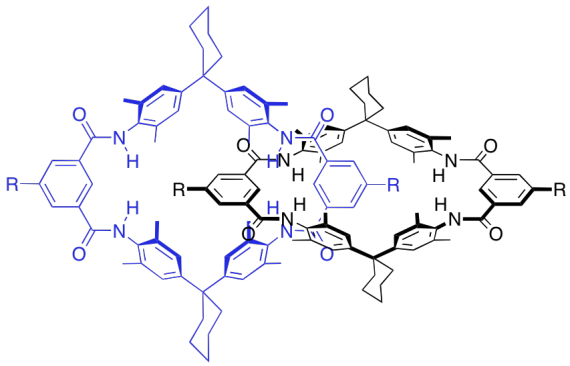

Figure 3.6. The first amide-based [2]catenane reported by Hunter (R = H) and Vögtle (R = OMe).

This supramolecular self-assembly process, wherein multiple H-bonds direct the synthesis of two interlocking rings, resulted in a 34% yield of [2]catenane, the

remainder of the product being a tetrameric species and the free macrocycle. This was closely followed by the publication of a very similar molecule by Vögtle (Figure 3.6).[18]

A rather similar, but structurally simpler, amide-based [2]catenane was discovered a few years later by Leigh and co-workers.[19] The combination of isophthaloyl dichloride **2** and *para*-xylylenediamine **3** at high dilution was expected to form the [2 + 2] macrocyclic adduct, but [2]catenane **6** formed instead, in 20% yield (Scheme 3.3, Route A).

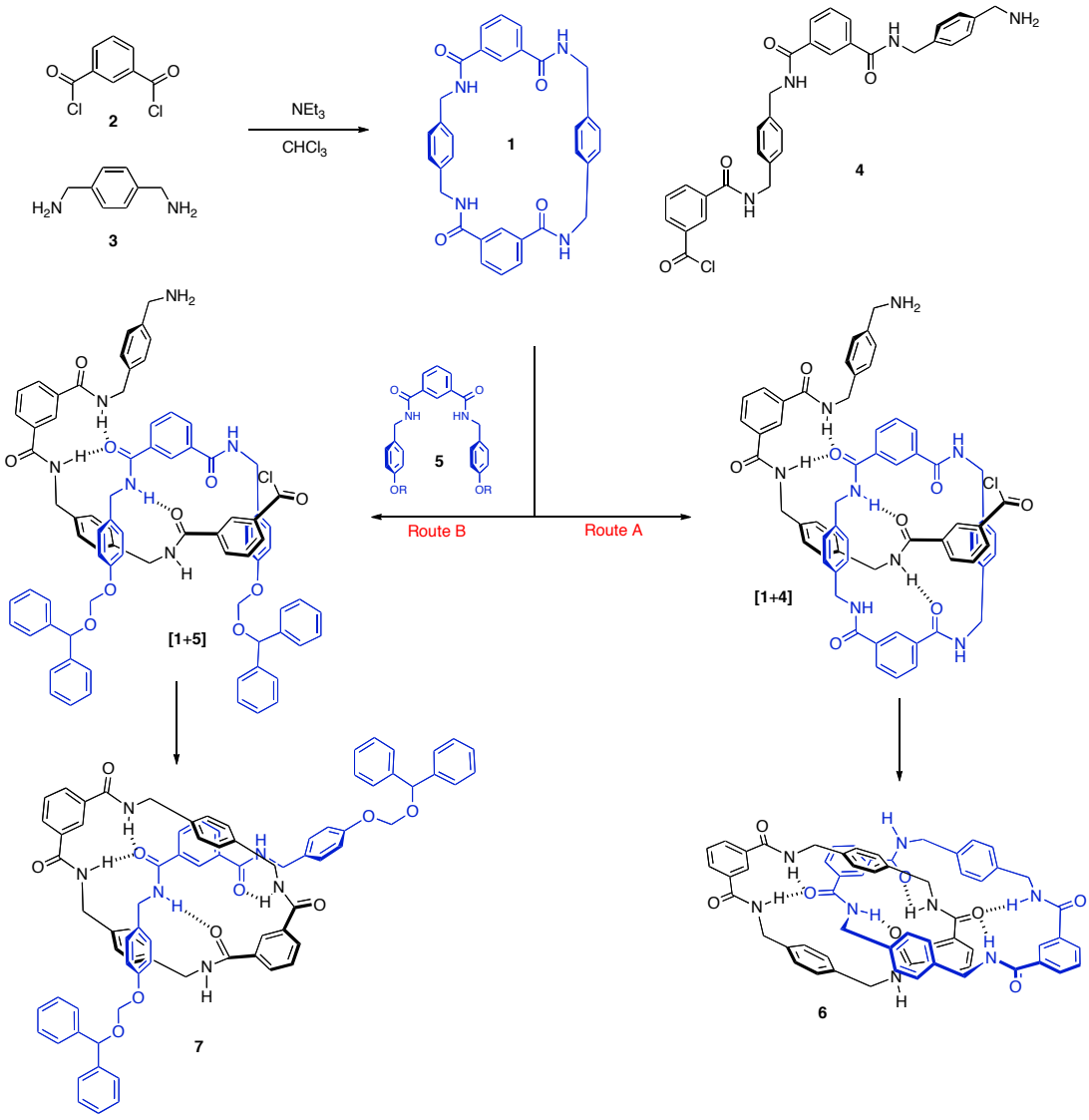

Scheme 3.3. Synthesis of Leigh's serendipitously discovered [2]catenane and [2]rotaxane and their supposed mechanism of formation.

It is assumed that, amongst other higher degree polymeric and macrocyclic adducts, free macrocycle **1** is formed and consequently bound by one equivalent of the macrocycle precursor **4** to form intermediate **[1+4]**. Subsequent intramolecular macrocyclization affords [2]catenane **6**.

Soon afterwards, it was demonstrated that, if the reaction was carried out in the presence of a suitably stoppered benzylic 1,3-diamide thread **5**, [2]rotaxanes could also be formed.[20] Similarly to [2]catenane, the formation of [2]rotaxane appears to involve the directed assembly of the preformed macrocycle precursor **[1+5]** around the two *E*-amide bonds of the thread.

Importantly, in 1997 Leigh and co-workers showed that, when glycylglycine was incorporated into thread **8**, formation of [2]rotaxane **9** occurred in yields of up to 62% (Scheme 3.4a).[21] By further preorganizing the orientation of the carbonyl groups using the fumaramide moiety **10**, [2]rotaxane **11** was assembled in a near quantitative 97% yield (Scheme 3.4b).[22]

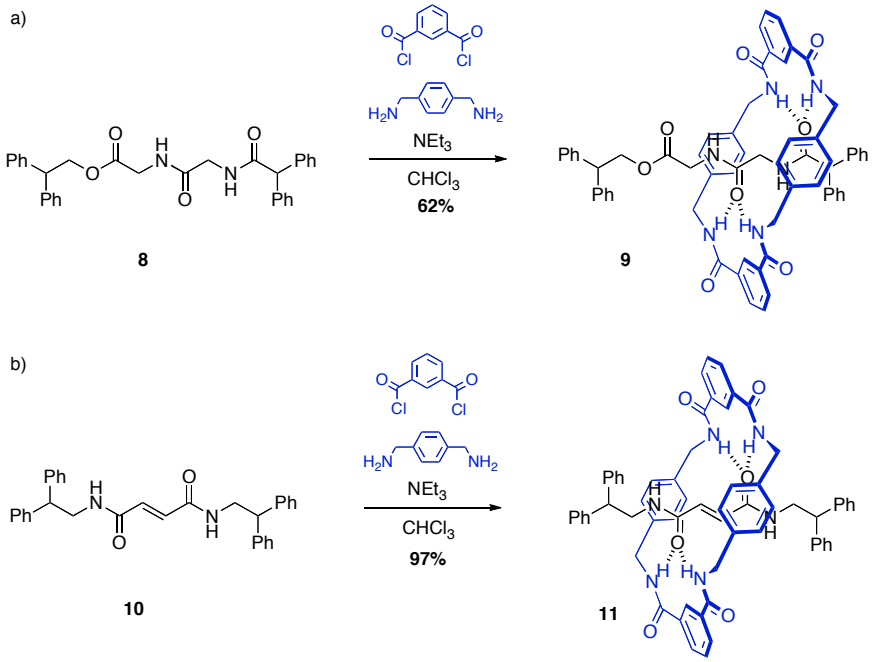

Scheme 3.4. Synthesis of a) glycylglycine [2]rotaxane, b) fumaric [2]rotaxane.

3.2.2 H-bond directed synthesis of molecular knots

Eight years after the publication of the first amide-based catenane by Hunter, the group of Vögtle discovered that a knotted structure was produced during the macrocyclization of U-shaped precursor **12** with pyridine dicarbonyl dichloride (Scheme 3.5).[23]

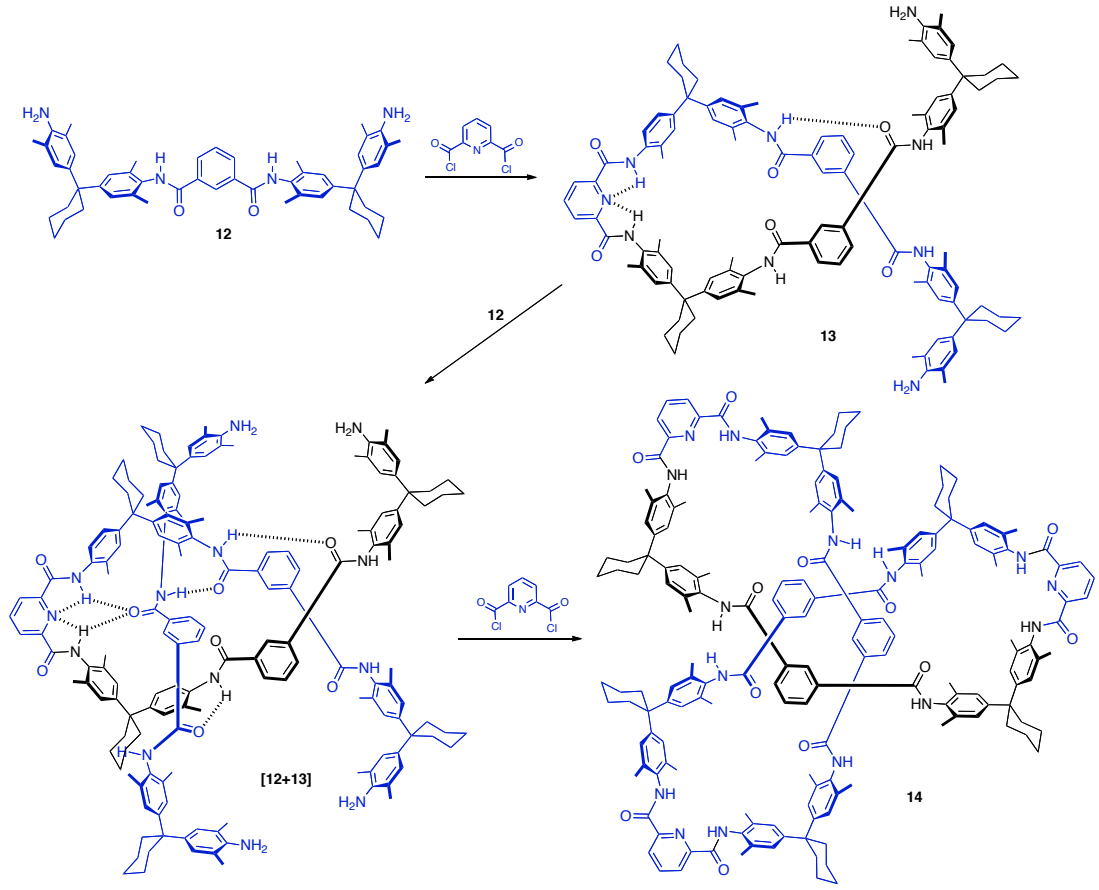

Scheme 3.5. Hydrogen bond-templated synthesis of a molecular knot. The assembly occurs through sequential, multiple self-assemby processes.

Producing knot in 20% yield, this impressive one step self-assembly was later rationalized, in a study supported by theoretical calculations.[24] The reactants were modified in order to evaluate the effect of structure on knot formation. One important feature is the presence of the pyridine unit in the backbone: replacing it with a phenyl group does not produce any knotted structure. The ability of the pyridine to form hydrogen bonds with its adjacent amide groups in a pyridine dicarboxamide moiety, spatially pre-organizes intermediate **13**. The pseudo-cavity thus formed is able to accommodate U-shape **12**. The entropy loss due to threading one molecule of U-shape **12** inside this arrangement is compensated by the enthalpy gain induced by the

formation of four hydrogen bonds between the two molecules in a comparable way as in formation of amide based catenanes and rotaxanes (intermediate **[12+13]**). The four terminal amines are now close in proximity to allow for fast reaction with dichloride in an intramolecular fashion. This last step traps intermediate **[12+13]** covalently leading to knot **14**.

3.2.3 Synthesis of peptide-containing [2]rotaxanes

The Leigh group has pioneered the field of synthetic interlocked architectures based on peptidic building blocks. As depicted in Scheme 3.4, the transoïd arrangement of the two adjacent carbonyl groups of a glycyl-glycyl sequence provides an excellent template for the formation of the benzylic amide macrocycle. [21]

In order to investigate the effect of the side chain substituents on the rotaxane forming reaction various dipeptidic threads were reacted under standard conditions, in a further study (Scheme 3.6).[26,27]

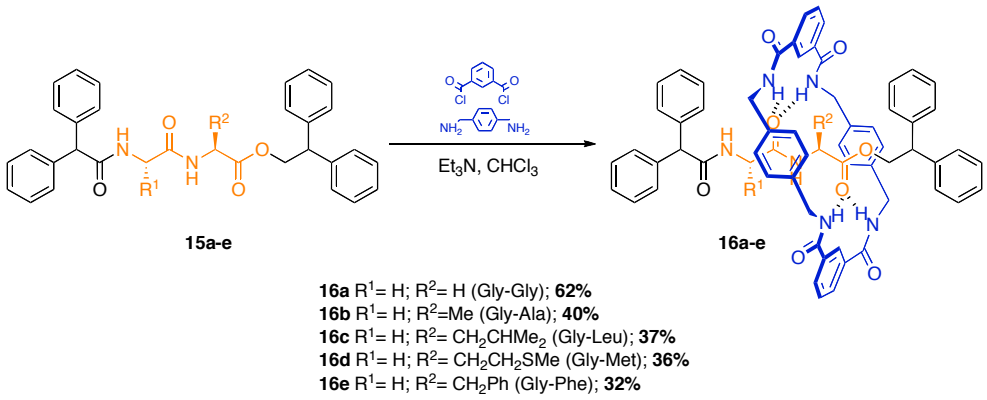

Scheme 3.6. Hydrogen bond-directed self-assembly of peptido[2]rotaxanes with various dipeptidic template units.

In most cases rotaxane was produced provided at least one of the two amino acids was a glycine. Yields varied according to the steric bulk of the side chain residues, but respectable yields were obtained in most cases.

Rotaxanes could also be formed, in moderate to good yields, with tripeptidic threads. The best yields were obtained when the thread contained two consecutive glycine residues. More than three amino acid in the thread gives yields of less than 5%, presumably due to the formation of intramolecular hydrogen bonds within the backbone, which disrupts the transoïd amide arrangement necessary to template the

rotaxane assembly. The poor solubility of long peptides in non-hydrogen bonding solvents (necessary conditions for efficient rotaxane formation) is also a limiting factor. Thus, Leu-enkephalin analogue **17**, despite containing the glycylglycyl template, only gives 1% yield when subjected to rotaxane forming conditions (Scheme 3.7).[27]

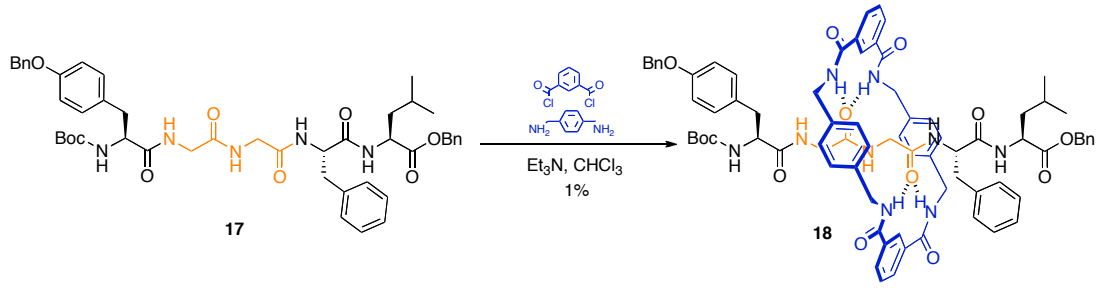

Scheme 3.7. Synthesis of a Leu-enkephalin analogue rotaxane via hydrogen bond-directed self-assembly.

3.2.4 Synthesis of rotaxanes of cyclic peptides

Using a fundamentally different approach the group of Leigh recently achieved the synthesis of [2] and [3]rotaxanes of cyclic peptides.[28] Contrary to the previous examples, the peptidic component is the macrocycle in this case (Scheme 3.8). Consisting of an eight or a ten amino acid repeating Gly-Pro unit, these macrocycles exhibit a strong affinity for metal cations and diammonium salts.[29] The geometry adopted by such rings in 1:2 host-guest ammonium complexes is cylindrical, with the glycine carbonyls rotated towards one face of the ring and the proline carbonyls toward the other face, with each set of carbonyls directed towards one ammonium group (Scheme 3.8). Binding occurs outwith the macrocycle.

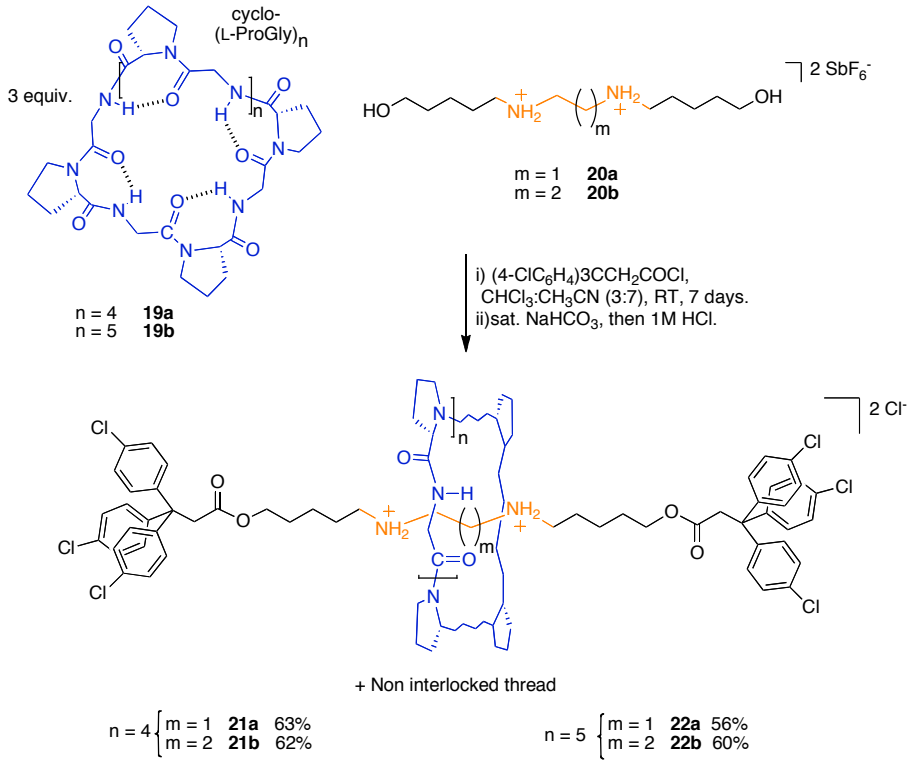

Scheme 3.8. Synthesis of rotaxanes of cyclic peptides. Atom labels are only shown for one repeat unit of the cyclopeptide in [2]rotaxanes.

This feature has been exploited to form rotaxanes by threading diammonium-based, linear molecules through the cavity of the macrocycle. In a typical procedure, an inclusion complex is prepared in situ by mixing an alkyl diamonium thread **20**, bearing free hydroxy groups at each end, with the cyclic peptide **19**. Reaction of the 1:1 complex with an acid chloride-functionalized stopper affords rotaxanes of cyclic peptides **21** and **22** in good yield. Similar yields were obtained with either Cyclo-L(Pro-Gly)$_4$ or Cyclo-L(Pro-Gly)$_5$, with two different diammonium threads (Scheme 3.8).

3.2.5 Synthesis of a p53-derived [2]catenane

In this unique example of a synthetic protein based catanane, the group of Dawson took advantage of the ability of tumour suppressor p53 protein to form entangled tetramers to direct catenation between two synthetic short analogues of p53.[30] The tetramerization domain of p53, characterized by X-ray crystallography,[31] is in fact a "dimer of dimers" in which each dimer consists of two monomeric fragments held together in an intertwined manner (Scheme 3.7).

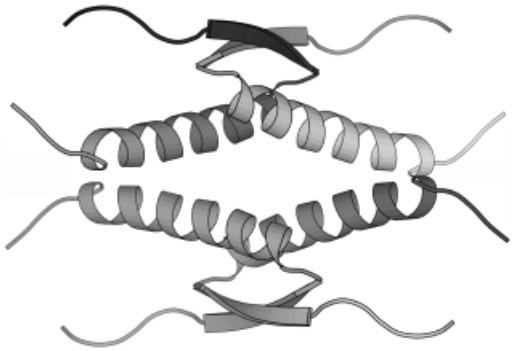

Figure 3.7. Structure of the tetramerization domain of the tumor suppressor protein p53. The backbone is represented as a ribbon to highlight the interlocked structure of the dimers. Reproduced with permission from WILEY-VCH Verlag GmbH.

A polypeptide corresponding to residues 325 to 361 (the dimerization domain of one monomeric unit of p53), with an additional CGG fragment at the N-terminus and a thioester at the C-terminus, was synthesized by solid phase peptide synthesis. The terminal cysteine and thioester allowed for intramolecular native chemical ligation after interlocked folding of two units of the polypetide had taken place (Scheme 3.9).

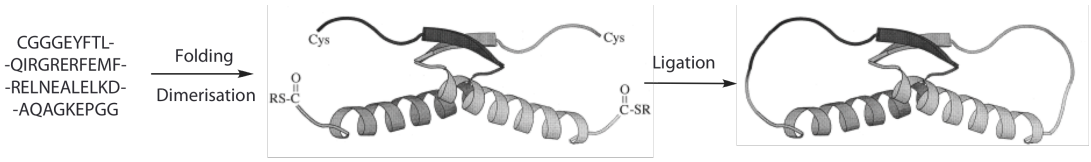

Scheme 3.9. Assembly of protein catenane. A synthetic analogue of the dimerization domain, functionalized at both ends, is macrocyclized after folding held the two monomers in interlocked manner. Adapted with permission from WILEY-VCH Verlag GmbH.

[2]-Catenane was isolated in an excellent 47% yield, and its interlocked structure was confirmed by single cleavage of the cysteine residue and mass spectrometry analysis of the cleavage products.

3.3 Mechanical encapsulation and applications

Since its inception, supramolecular chemistry has paved the way towards molecular encapsulation. Host-guest chemistry is, in fact, one of the first forms of molecular encapsulation. The first two-dimensional crown ethers capable of sequestering anions were soon extended to cryptands, compounds having a capsular or cage shape.[32] If these early systems were based on coordination interaction, they were soon complemented by more complex architectures, able to encapsulate various

substrates through hydrogen bond interaction, hydrophobic effect or Van der Waals forces.[33]

However, encapsulation in an interlocked system (or mechanical encapsulation) is a relatively recently developed concept.[34] It represents a novel and rather different approach to encapsulation: although the formation of the molecule is directed by a process relying on supramolecular interactions, the final guest is locked in the cavity of the host by a mechanical bond. A covalent bond has to be broken to release the guest, making these non-supramolecular entities very stable. This covalent bond breakage can be stimulus-triggered widening the scope of the systems to include the selective delivery of guests.

3.3.1 Cyclodextrin-based rotaxane-encapsulated dyes

Improving the properties of dyes by molecular encapsulation has recently attracted a great deal of attention from organic chemists. It has been found that rotaxanes, especially those based on cyclodextrins, can be very useful for dye encapsulation.[34] The group of Anderson has been one of the pioneers in demonstrating the dramatic change in properties that can arise from mechanical interlocking. In a recent report, they describe how an α-cyclodextrin (α-CD)-encapsulated azo dye had its resistance towards oxidation greatly improved as a results of encapsulation.[35] The synthesis of such rotaxanes has been achieved in very high yields on a gram scale, making it very appealing for potential applications. The structure of these rotaxane, an example of which is depicted in Figure 3.8, consist of a diazo moiety, which is threaded through the α-CD, and a chloro-1,3,5 triazine, necessary to attach the dye to a surface.

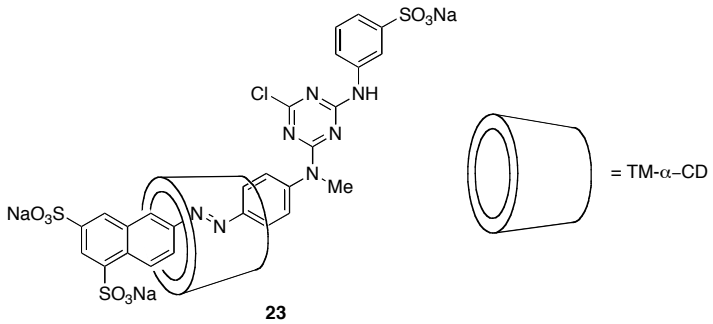

23

Figure 3.8. Anderson's encapsulation of a diazo dye. TM-α-CD corresponds to an α-cyclodextrin in which all free hydroxyl group have been methylated.

Several tests have been carried out with both interlocked and non-interlocked versions of the dye, all of them confirming the greater resistance to oxidation of the rotaxane compared to that of the free dye, both in solution and on a surface. A cotton sample dyed with rotaxane **23** showed increased resistance against bleaching than a sample dyed with the non-interlocked species.

Other examples have been published by Anderson and co-workers, in which mechanical encapsulation is reported to improve the properties of the molecule.[36]

3.3.2 Rotaxane-encapsulated squaraine dyes for *in vivo* imaging

The group of Smith has used rotaxane encapsulated squaraine dyes in *in vivo* and *in vitro* near infra-red (NIR) imaging. The squaraine motif, composed of a four-membered ring, substituted with two oxoanions, has interesting fluorescence properties. However, these properties can be altered by aggregation in solution (band broadening), and more importantly, by chemical decomposition (the highly electron deficient cyclobutene ring is readily attacked by nucleophiles, leading to the loss of the dye's colouration).

In a preliminary study,[37] Smith and co-workers demonstrated the ability of the squaraine motif to template the formation of a Leigh-type benzylic amide macrocycle around a thread-shaped dye, 'stoppered' at each end by benzylic groups. An example is shown in Figure 3.10.

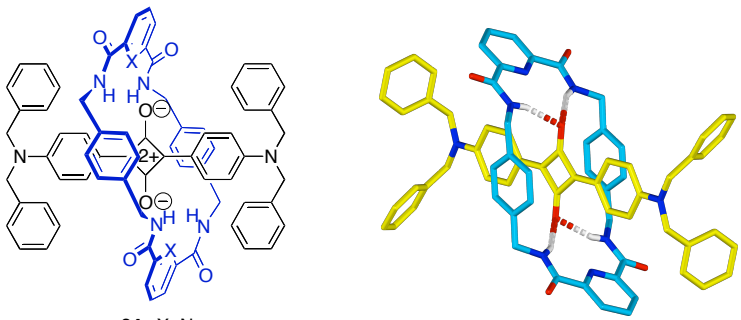

Scheme 3.10. Chemical structure of a rotaxane of a squaraine dye and its X-ray crystal structure.

Unlike the free dye, this molecule (**24a**) retained its absoption properties in the presence of strong nucleophiles. The macrocycle induces only a slight shift in the absorption and emission bands, but gives a slightly higher quantum yield and keeps

aggregation to a minimum, greatly improving the overall properties of the dye (Figure 3.10).

In a second report,[38] rotaxane-encapsulated squaraine dyes were applied *in vitro* and *in vivo*. As an example, *E.Coli* cells stained with a squaraine rotaxane could be monitored while cells underwent division. Subcutaneous injection of the stained bacterias in nude mice could be observed in a live mouse by irradiating the animal at the appropriate wavelength.

3.3.3 Rotaxane-encapsulated peptides

Mass spectrometry analysis of the first peptido[2]rotaxane synthesised by Leigh and co-workers strongly suggested that the macrocycle protects the thread from fragmention.[21] This apparent shielding effect was later confirmed and exploited to protect peptides against enzymatic cleavage. It was demonstrated that in the presence of α-chymotripsin, a pancreatic peptidase, rotaxane **26** (Scheme 3.11) had a significantly longer half-life than its non-interlocked counterpart. Boc-Leu-enkephalin **25** is cleaved within minutes, whereas rotaxane **26** shows complete stability over 24 hours (Scheme 3.11).[27]

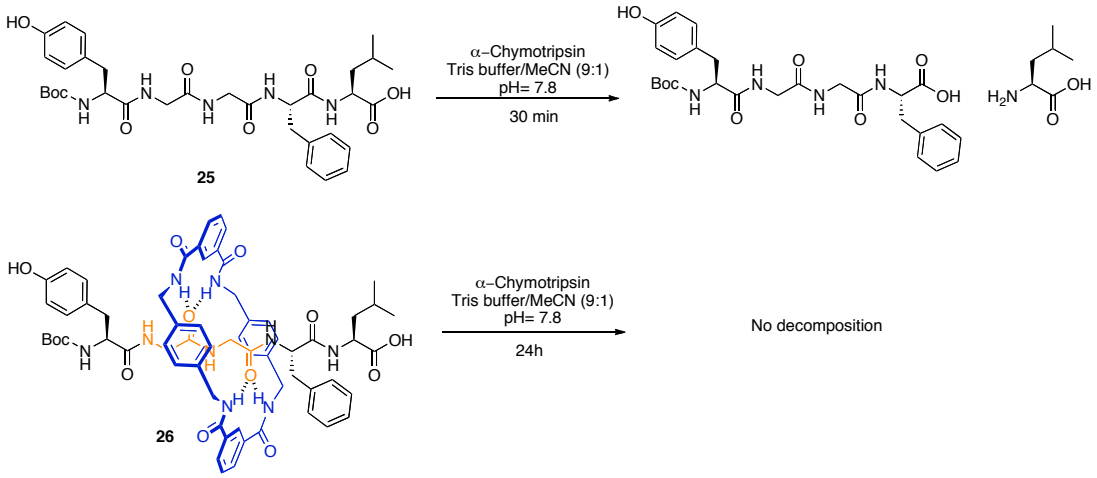

Scheme 3.11. The stability of a rotaxane-encapsulated Leu-enkephalin analogue towards α-chymotripsin compared to that of the parent peptide.

In addition, the binding affinity between the Boc-Leu-kephalin rotaxane **26** and opioid receptors was found to be significantly decreased compared to that of its

parent thread.[39] The additional lipophilic character given to the structure makes the concept of peptidorotaxanes very attractive for drug delivery, since it can provide an effective way to protect peptides against *in vivo* degradation, enhance intracellular transport and temporarily 'turn off' their activity during transport throughout the journey to the target.

3.4 Molecular carriers based on interlocked architectures

3.4.1 Polyrotaxane-based drug carriers

The first drug delivery devices based interlocked architectures were described by Yui *et al.*[40] In a series of different studies, they demonstrated the ability of multi α-CD-containing polyrotaxanes to be involved in various biological processes.[41,42] One of their first studies involved the design of a drug-polyrotaxane conjugate able to transport and deliver theophylline to a target organ. Scheme 3.12 depicts the model device, **27**, which consist of a polyethylene glycol chain (PEG) threaded through multiple α-CD rings. Each α-CD is functionalized by the active drug (theophylline), linked to the ring by a spacer.

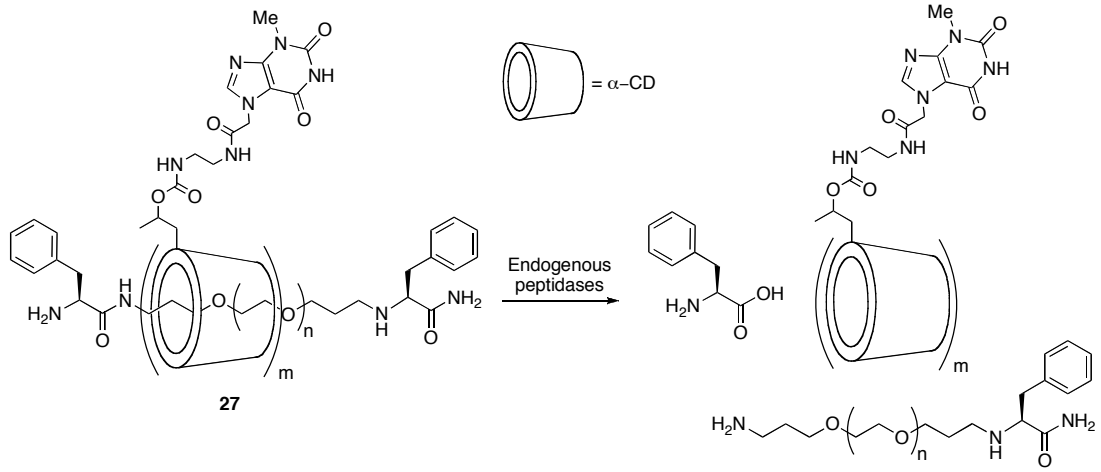

Scheme 3.12. Chemical structure and schematic representation for the operation of Yui's rotaxane based drug carrier.

The PEG thread is stoppered by a biodegradable moiety in such a way that it would be cleaved in the extracellular media, supposedly releasing the drug-functionalized rings in close proximity to the targeted cell. Stopper cleavage-mediated release of

the rings was assessed *in vivo* in the presence of both papain and α-chymotripsin and in both cases cleavage occurred, albeit very slowly (320 h and 150 h respectively).[43] Using similar structures Yui et al. designed a range of drug carrier systems[43,44] and have recently applied them to gene transfection.[45]

3.4.2 Host-guest rotaxane as cell membrane transporters

In a different approach, the group of Smithrud have shown that host-[2]rotaxanes can transport various compounds through the cell membrane.[46,47] The transporting device is composed of an ammonium containing thread, stoppered at one end with either a cyclophane pocket or an aromatic cleft, and a diarginine derivatized crown ether macrocycle. The various guests bind to the lipophilic pocket and the whole complex travels passively through the cell membrane. Host-[2]rotaxane **28** (Figure 3.9) is an example of such a device, which has been subjected to rigorous experiments in order to understand how it achieves intracellular transport.

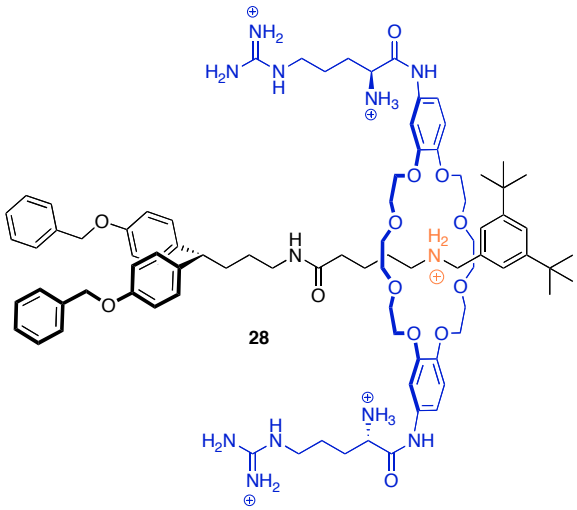

Figure 3.9. Smithrud's Host[2]rotaxane.

To evaluate the influence of the ring position on the binding affinity with the guest, an analogue of **28**, where the ring is locked away from the ammonium group (by acetylation of it), was synthesized and subjected to binding affinity experiments.[46] These revealed that ring motion along the thread is crucial in reaching maximal binding of the host-[2]rotaxane with the guest, promoting cell penetration. When moving from the aqueous media to the vey lipophilic cell membrane, the rotaxane carrier experiences a sudden change in polarity of its environment. The host-rotaxane

has the flexibility to alter its conformation through shuttling of the ring along the thread in order to maximize the binding free energy of host-guest association, and simultaneously minimize the environmental effects on the stability of the complex. In a polar medium the ring is expected to be separated in space from the polar ammonium group, whereas in the cell membrane the ring slides back over it to give a 'more lipophilic character' to the complex (Figure 3.10).

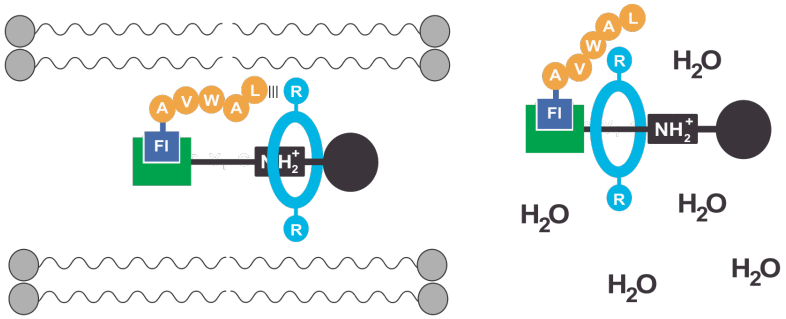

Figure 3.10. Representation of the host-[2]rotaxane-fluorescein-functionalized peptide complex crossing the cell membrane. The ring slides along the thread in order to maximize the binding free energy of the complex and minimize environmental effect.

3.4.3 Rotaxane-based nanovalves

In an approach combining nanofabrication and supramolecular assembly, the group of Stoddart and Zink first designed[48] drug carriers based on nanoporous silica nanoparticules derivatised with rotaxane or pseudo-rotaxanes gatekeepers.[49] The concept has attracted attention from other research groups over the last decade,[50] and various rotaxanes and pseudo-rotaxanes have been used as gatekeepers: paraquat (Scheme 3.13), crown ethers,[51] cyclodextrins,[52] and more recently cucurbiturils.[53] Silica-based nanoparticules of a 500 nm size range were used for the fabrication of the device. Within these particules 2-3 nm wide containers were carved using templating methods. Functionalization of the outer face of the pore by rotaxane- or pseudo-rotaxane-based stalks enables the system to function as a valve (Scheme 3.13). The pores can be selectively opened or closed by controlling the position of the macrocycle on the thread. When the macrocycle is located close to the pore opening, the pore is obstructed and the valve is said to be closed. Contrary, when the macrocycle is far away, the pore is less obstructed and the valve is opened. The device can then be loaded with guest molecules and subsequent closing traps them in until the appropriate stimuli is applied to open the valve and release them.

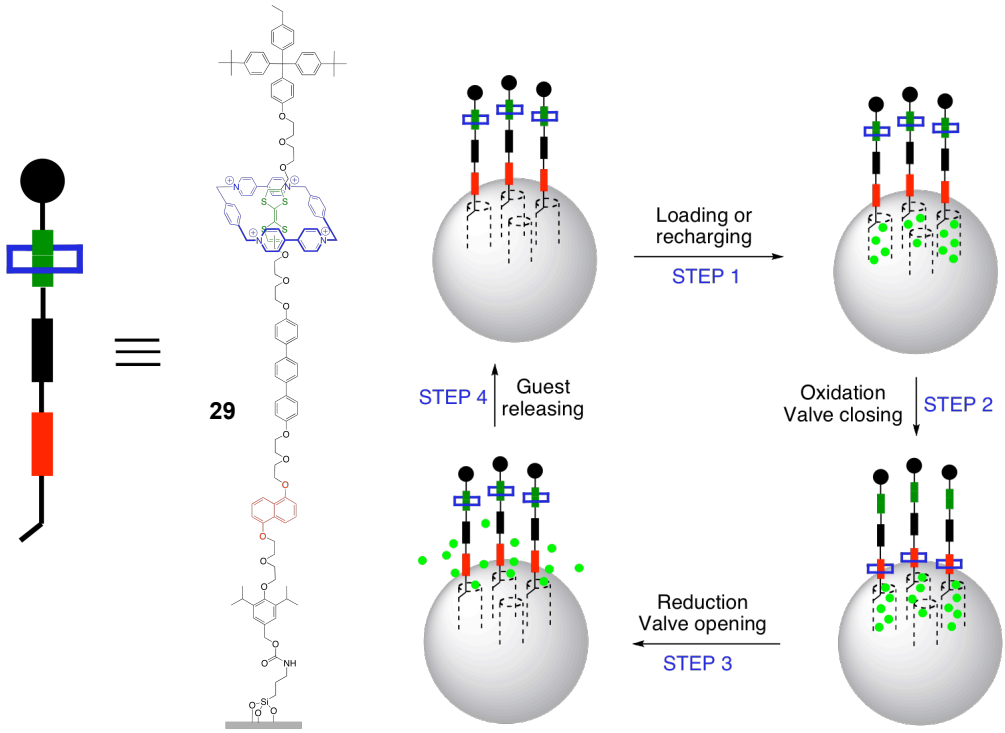

Scheme 3.13. a) The chemical structure of a bistable [2]rotaxane, **29** used as a valve. b) Schematic representation of the operating cycle of the nanovalve.

Scheme 3.13 shows the mechanism of action of a nanovalve described by Stoddart *et al.* The valve is based on the well studied bistable [2]rotaxane **29**, which is composed of a paraquat-based macrocycle ($CBPQT^{4+}$) and a combination of tetrathiafulvalene (TTF) and dioxynaphtalene (DNP) units on the thread. Chemical oxidation of TTF using $Fe(ClO_4)_3$ triggers displacement of the macrocycle from the preferred TTF station to the DNP station, closing the pores and trapping guest molecules inside. Opening of the valve is achieved by reducing the TTF^{2+} station with ascorbic acid, which releases the trapped molecules.

Simpler stimuli such as pH[51,53] or more recently enzymes,[52] have subsequently been used.

3.5 Design and outlook of the project

Designing nanodevices capable of transporting active chemicals safely and release them under controlled stimuli is no longer hypothetical. As has been discussed, complex supramolecular or mechanically linked architectures, capable of encapsulating guest molecules, have already been built and operated with great

success. The Leigh group has previously demonstrated that peptides (and bioactive peptide analogues) could be mechanically encapsulated as part of a rotaxane structure. However to perform a useful task, these devices should be able to deliver and release the encapsulated peptide to a given target. This aspect had not been investigated yet, and thus was the aim of the work presented in this thesis.

3.5.1 Design

In the transformation of these early peptidorotaxanes into real drug carriers, there are several factors to take in to account. As well as protecting the backbone against peptidase hydrolysis, the potential peptide carriers should be able to release the active peptide in a controlled manner (*i.e.* at a specific location, under a specific stimulus). A logical way to proceed towards achieving this goal would be to adapt the prodrug approach[54] to the specific release of the mechanically encapsulated peptide. Accordingly, the function of the nanodevice is to improve the peptide's administration properties, mainly low bioavailability and poor membrane transport, as well as significantly decreasing its activity and toxicity during transport to the target.

In a similar way as Yui's carriers,[42] the encapsulated peptide should be 'sandwiched' between two stoppers, which are cleaved by a specific enzyme, triggering slipping of the macrocycle component and release of the peptide from its protective capsule. This means that the *N*-terminus amine and the *C*-terminus carboxylic acid are restored after cleavage has occurred (Scheme 3.14).

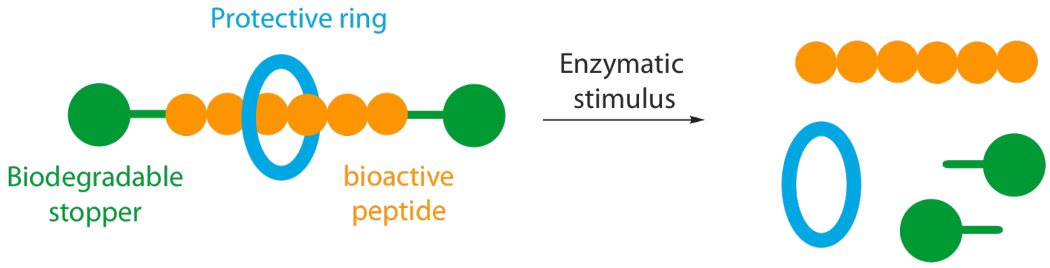

Scheme 3.14. Schematic representation of a universal rotaxane peptide carrier.

In order to efficiently protect the peptide against proteolysis, the macrocycle should be able to explore the whole backbone through random Brownian motion (*i.e.* its

cavity should be large enough to accommodate each residue). It is difficult to predict the maximum length that could be protected through random shuttling of the ring along the peptide, however as a result from a previous study by Anderson it can be accepted that to be the most efficient, the macrocycle has to reside over or in very close proximity of the residues prone to hydrolysis for as long a period of time as possible.[55] In his study, Anderson shows that when the macrocycle constituent of a rotaxane is concealed in proximity to a specific peptidic bond, the latter is not cleaved by α-chymotrypsin. If, however, the macrocycle is free to move along the whole thread, the peptidic bond is readily hydrolyzed by the enzyme (Scheme 3.15).

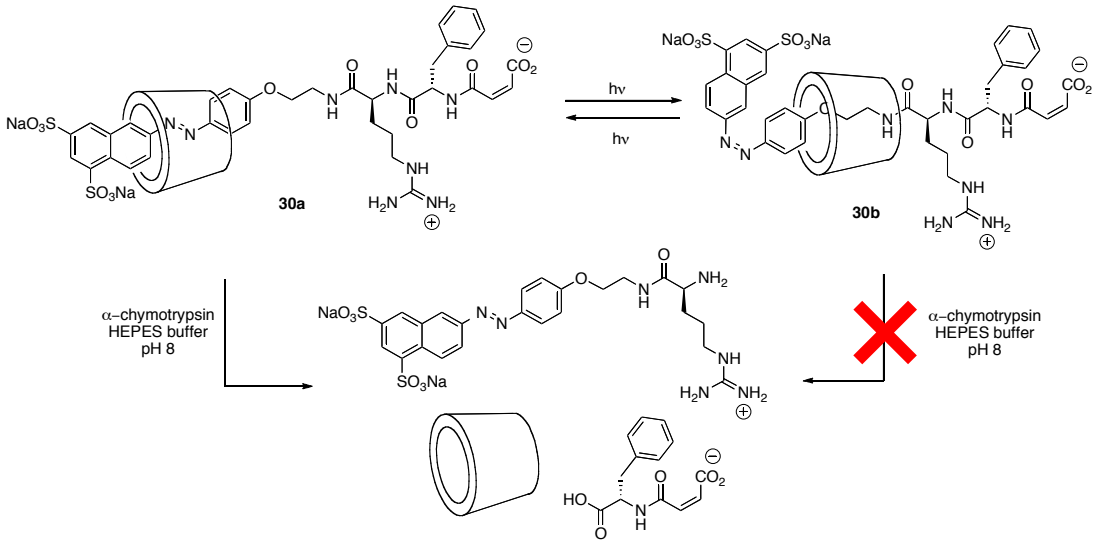

Scheme 3.15. Anderson's enzymatic cleavage of a peptide-linked rotaxane. When the α-CD is concealed in proximity to the Arg-Phe residues (**30b**) , the rotaxane is not cleaved by α-chymotrypsin. If, however, the macrocycle is free to move along the whole thread (**30a**), the Arg-Phe linkage is readily hydrolyzed by the enzyme.

In most common proteolytic enzymes only one or two residues are sufficient for substrate recognition (hydrolysis will occur after or between these residues). For example, α-chymotrypsin is very specific to one Leu, Phe or Tyr residue but is not demanding concerning the remaining amino acids of the sequence.[56] This somewhat low specificity of peptidases explains why, even though the macrocycle constituent of the peptidorotaxane is proximity to the hydrolysis position, this may not be a sufficient condition to interfere with enzyme recognition. Hence it is important that for maximum protection efficiency the macrocycle is statistically located over the side chain of each amino acid for as long a period of time as possible (determined by the length of the peptide). Thus in the case of a wholly peptidic thread, to protect

every peptidic bond in the sequence, the ring should reside over each residue for a statistically equal length of time. The faster the ring shuttles from on end of the thread to the other the better both aforementioned conditions will be fulfilled.[57]

As well as functioning as a protective shield the ring can be functionalized to perform additional tasks. For example, solubility of the device can be fine tuned, therapeutic targeting can be achieved by attaching ligands specific to a certain type of cell, active intracellular transport can also be triggered by selecting ligands that provoke endocytosis. One can also envisage functionalizing the macrocycle with bioactive molecules, which once delivered, could act complementarily to the bioactive peptide, or have a similar activity to enhance therapy efficiency (Scheme 3.16).

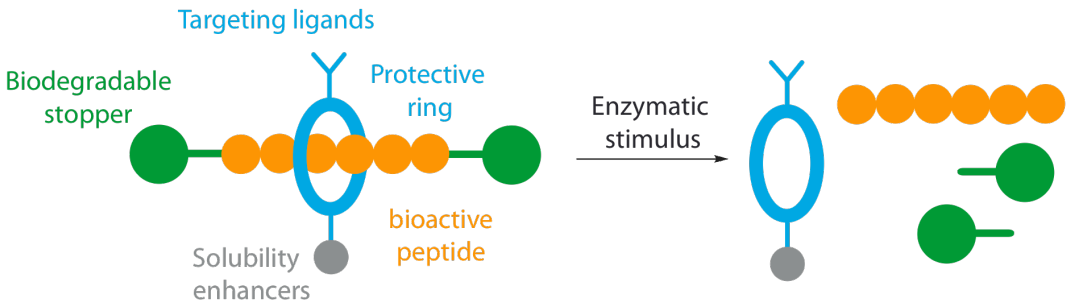

Scheme 3.16. Schematic representation of a universal rotaxane peptide carrier for targeted therapy and enhanced pharmacological properties.

3.5.2 Outlook

The conditions mentioned above, constitute the requirements for the construction of a universal peptide carrier, which, by definition, could be adapted to any type of peptide and to any type of therapeutic target. There is no doubt that such devices will be accessible in the near future, but to approach this design one has to adopt a stepwise strategy. Thus, in the following chapters, some elements of the design (size of the macrocycle, type of biodegradable stoppers) are based on previous studies. In summary:

i) The cavity of the benzylic amide macrocycle used in previous peptide rotaxanes is not sufficiently large to accommodate all proteinogenic amino acids. However, it constitutes the key element of peptide mechanical

encapsulation and as such no attempt was be made in this study to find a larger substitute

ii) Biodegradable stoppers were elaborated for tumour-triggered release of peptides and were designed, as a first example, for the N-terminus of the peptide only.

This thesis will describe, in the first place, the optimization of a methodology for the synthesis of peptido-rotaxanes of long peptides (Chapter 4). The use of this methodology to build an anti-cancer therapy compatible peptide rotaxane carrier will be described in Chapter 5. Finally, Chapter 6 will describe the development of biodegradable stoppers and the functionalization of the macrocycle constituent of peptide carrier models for anti-cancer therapy.

3.6 References and notes

[1] D. A. Clayton, J. Vinograd, *Nature,* **1967**, *216*, 652-657; B. Hudson, J. Vinograd, *Nature,* **1967**, *216*, 647-652.

[2] D. B. Amabilino, J. F. Stoddart, *Chem. Rev.,* **1995**, *95*, 2725-2828.

[3] J. F. Conway, R. L. Duda, N. Cheng, R. W. Hendrix, A. C. Steven, *J. Mol. Biol. ,* **1995**, *253*, 86-99; R. L. Duda, **1998**, *94*, 55-60; R. W. Hendrix, R. L. Duda, K. Maramorosch, F. A. Murphy, J. S. Aaron, *Advances in Virus Research*, Academic Press: **1998**; Vol. 50, p 235-288.

[4] W. R. Wikoff, L. Liljas, R. L. Duda, H. Tsuruta, R. W. Hendrix, J. E. Johnson, *Science,* **2000**, *289*, 2129-2133.

[5] P. D. Ross, N. Q. Cheng, J. F. Conway, B. A. Firek, R. W. Hendrix, R. L. Duda, A. C. Steven, *EMBO J.,* **2005**, *24*, 1352-1363.

[6] Another type of knot, sometimes referred as ‘open knot’ present in some proteins (mostly enzymes) has been defined recently [W. R. Taylor, Nature, 2000, 406, 916-919.]. This intertwining pattern, which is similar to a laces knot (one end of the protein backbone threaded into a loop formed by the other part of the backbone) does not constitute either a topological or a mechanical link. For recent reviews see; [W. R. Taylor, *Comput. Biol. Chem.*, **2007**, 31, 151-162; A. L. Mallam, *FEBS J.*, **2009**, 276, 365-375].

[7] P. K. Pallaghy, K. J. Nielsen, D. J. Craik, R. S. Norton, *Protein Sci.,* **1994**, *3*, 1833-1839; D. J. Craik, N. L. Daly, J. Mulvenna, M. R. Plan, M. Trabi, **2004**, *5*, 297-315; D. J. Craik, N. L. Daly, M. R. Plan, A. A. Salim, L. Sando, *J. Toxicol.: Toxin Rev.,* **2002**, *21*, 229 - 271; D. J. Craik, M. Cemazar, N. L. Daly, *Curr. Opin.*

Drug Discovery Dev., **2007**, *10*, 176-184; C. W. Gruber, M. Cemazar, M. A. Anderson, D. J. Craik, *Toxicon,* **2007**, *49*, 561-575; P. B. Pelegrini, B. F. Quirino, O. L. Franco, *Peptides,* **2007**, *28*, 1475-1481; H. Kolmar, *FEBS J.,* **2008**, *275*, 2684-2690.

[8] D. J. Craik, N. L. Daly, C. Waine, *Toxicon,* **2001**, *39*, 43-60.

[9] M. Čemažar, D. Craik, *Int. J. Pept. Res. Ther.,* **2006**, *12*, 253-260.

[10] P. Escoubas, L. Rash, *Toxicon,* **2004**, *43*, 555-574.

[11] L. Gran, *Acta. Pharmacol.Toxicol.,* **1973**, *33*, 400-408.

[12] M. Cemazar, C. W. Gruber, D. J. Craik, *Antioxid. Redox Signaling* **2008**, *10*, 103-111.

[13] Y. E. Rita Vos, *Photochem. Photobiol.,* **1994**, *60*, 24-32; D. Frechet, J. D. Guitton, F. Herman, D. Faucher, G. Helynck, B. Monegier du Sorbier, J. P. Ridoux, E. James-Surcouf, M. Vuilhorgne, *Biochemistry,* **1994**, *33*, 42-50; K. L. Constantine, M. S. Friedrichs, D. Detlefsen, M. Nishio, M. Tsunakawa, T. Furumai, H. Ohkuma, T. Oki, S. Hill, R. E. Bruccoleri, P.-F. Lin, L. Mueller, *J. Biomol. NMR,* **1995**, *5*, 271-286; R. Katahira, K. Shibata, M. Yamasaki, Y. Matsuda, M. Yoshida, *Bioorg. Med. Chem.,* **1995**, *3*, 1273-1280; R. Katahira, M. Yamasaki, Y. Matsuda, M. Yoshida, *Bioorg. Med. Chem.,* **1996**, *4*, 121-129; K. Yano, S. Toki, S. Nakanishi, K. Ochiai, K. Ando, M. Yoshida, Y. Matsuda, M. Yamasaki, *Bioorg. Med. Chem.,* **1996**, *4*, 115-120; T. A. Knappe, U. Linne, S. Zirah, S. Rebuffat, X. Xie, M. A. Marahiel, *J. Am. Chem. Soc.,* **2008**, *130*, 11446-11454.

[14] S. Rebuffat, A. Blond, D. Destoumieux-Garzon, C. Goulard, J. Peduzzi, *Curr. Protein Pept. Sci. ,* **2004**, *5*, 383-391.

[15] M. J. Bayro, J. Mukhopadhyay, G. V. T. Swapna, J. Y. Huang, L.-C. Ma, E. Sineva, P. E. Dawson, G. T. Montelione, R. H. Ebright, *J. Am. Chem. Soc.,* **2003**, *125*, 12382-12383; K. J. Rosengren, R. J. Clark, N. L. Daly, U. Goransson, A. Jones, D. J. Craik, *J. Am. Chem. Soc.,* **2003**, *125*, 12464-12474; K.-A. Wilson, M. Kalkum, J. Ottesen, J. Yuzenkova, B. T. Chait, R. Landick, T. Muir, K. Severinov, S. A. Darst, *J. Am. Chem. Soc.,* **2003**, *125*, 12475-12483.

[16] S. Duquesne, D. Destoumieux-Garzon, S. Zirah, C. Goulard, J. Peduzzi, S. Rebuffat, *Chem. Biol.,* **2007**, *14*, 793-803.

[17] C. A. Hunter, *J. Am. Chem. Soc.,* **1992**, *114*, 5303-5311.

[18] F. Vogtle, S. Meier, R. Hoss, *Angew. Chem., Int. Ed.,* **1992**, *31*, 1619-1622.

[19] A. G. Johnston, D. A. Leigh, R. J. Pritchard, M. D. Deegan, *Angew. Chem. Int. Ed.,* **1995**, *34*, 1209-12.

[20] A. G. Johnston, D. A. Leigh, A. Murphy, J. P. Smart, *Bull. Soc. Chim. Belg.* **1996**, *105*, 721-727.

[21] D. A. Leigh, A. Murphy, J. P. Smart, A. M. Z. Slawin, *Angew. Chem., Int. Ed. ,* **1997**, *36*, 728-732.

[22] F. G. Gatti, D. A. Leigh, S. A. Nepogodiev, A. M. Z. Slawin, S. J. Teat, J. K. Y. Wong, *J. Am. Chem. Soc.,* **2001**, *123*, 5983-5989.

[23] O. Safarowsky, M. Nieger, R. Fröhlich, F. Vögtle, *Angew. Chem., Int. Ed.,* **2000**, *39*, 1616-1618.

[24] C. A. Schalley, W. Reckien, S. Peyerimhoff, B. Baytekin, F. Vögtle, *Chem.--Eur. J.,* **2004**, *10*, 4777-4789.

[25] A. G. Johnston, D. A. Leigh, A. Murphy, J. P. Smart, M. D. Deegan, *J. Am. Chem. Soc.,* **1996**, *118*, 10662-10663; A. G. Johnston, D. A. Leigh, L. Nezhat, J. P. Smart, M. D. Deegan, *Angew. Chem. Int. Ed. Engl.,* **1995**, *34*, 1212-16.

[26] G. Brancato, F. Coutrot, D. A. Leigh, A. Murphy, J. K. Y. Wong, F. Zerbetto, *Proc. Natl. Acad. Sci. U. S. A.,* **2002**, *99*, 4967-4971.

[27] S. Van Meurs, *PhD thesis*, University of Warwick, 2001.

[28] V. Aucagne, D. A. Leigh, J. S. Lock, A. R. Thomson, *J. Am. Chem. Soc.,* **2006**, *128*, 1784-1785.

[29] Y.-Y. Chiu, L. D. Brown, W. N. Lipscomb, *J. Am. Chem. Soc.,* **1977**, *99*, 4799-4803; C. M. Deber, E. R. Blout, *J. Am. Chem. Soc.,* **1974**, *96*, 7566-7568; V. Madison, C. M. Deber, E. R. Blout, *J. Am. Chem. Soc.,* **1977**, *99*, 4788-4798.

[30] P. E. D. Liang Z. Yan, *Angew. Chem., Int. Ed.,* **2001**, *40*, 3625-3627.

[31] P. Jeffrey, S. Gorina, N. Pavletich, *Science,* **1995**, *267*, 1498-1502.

[32] *Comprehensive Supramolecular Chemistry*, (G. W. Gokel Ed., Pergamon Press: Cambridge, **1996**, Vol. 1.

[33] *Comprehensive Supramolecular Chemistry*, (F. Vögtle Ed., Pergamon Press: Cambridge, **1996**, Vol. 2; *Comprehensive Supramolecular Chemistry*, (Pergamon Press: Cambridge, **1996**, Vol. 3.

[34] C. C. Forbes, E.Arunkumar, B. D. Smith, *Eur. J. Org. Chem. ,* **2005**, 4051-4059.

[35] M. G. H. Michael R. Craig, Tim D. W. Claridge, Harry L. Anderson,, *Angew. Chem., Int. Ed.,* **2001**, *40*, 1071-1074.

[36] J. E. H. Buston, F. Marken, H. L. Anderson, *Chem. Commun.,* **2001**, 1046-1047; J. E. H. Buston, J. R. Young, H. L. Anderson, *Chem. Commun.,* **2000**, 905-906; M. R. Craig, T. D. W. Claridge, M. G. Hutchings, H. L. Anderson, *Chem. Commun.,* **1999**, 1537-1538; F. Cacialli, J. S. Wilson, J. J. Michels, C. Daniel, C. Silva, R. H. Friend, N. Severin, P. Samori, J. P. Rabe, M. J. O'Connell, P. N. Taylor, H. L. Anderson, *Nat. Mater.,* **2002**, *1*, 160-164.

[37] E. Arunkumar, C. C. Forbes, B. C. Noll, B. D. Smith, *J. Am. Chem. Soc.,* **2005**, *127*, 3288-3289.

[38] J. R. Johnson, N. Fu, E. Arunkumar, W. M. Leevy, S. T. Gammon, D. Piwnica-Worms, B. D. Smith, *Angew. Chem., Int. Ed. ,* **2007**, *46*, 5528-5531.

[39] Unpublished results, Glakso-Smith-Kline

[40] T. Ooya, H. Mori, M. Terano, N. Yui, *Macromol. Rapid Commun.,* **1995**, *16*, 259-263.

[41] T. Ooya, N. Yui, *Crit. Rev. Ther. Drug. Carrier. Syst.,* **1999**, *16*, 289-330.

[42] N. Yui, T. Ooya, *J. Artif. Organs,* **2004**, *7*, 62-8.

[43] T. Ooya, N. Yui, *J. Controlled Release,* **1999**, *58*, 251-269.

[44] W. Kamimura, T. Ooya, N. Yui, *J. Controlled Release,* **1997**, *44*, 295-299; N. Yui, T. Ooya, T. Kumeno, *Bioconjugate Chem.,* **1998**, *9*, 118-125; T. Ooya, M. Eguchi, N. Yui, *Biomacromolecules,* **2001**, *2*, 200-203; T. Ooya, N. Yui, *J. Controlled Release,* **2002**, *80*, 219-228; N. Yui, T. Ooya, T. Kawashima, Y. Saito, I. Tamai, Y. Sai, A. Tsuji, *Bioconjugate Chem.,* **2002**, *13*, 582-587; M. Eguchi, T. Ooya, N. Yui, *J. Controlled Release,* **2004**, *96*, 301-307.

[45] T. Ooya, H. S. Choi, A. Yamashita, N. Yui, Y. Sugaya, A. Kano, A. Maruyama, H. Akita, R. Ito, K. Kogure, H. Harashima, *J. Am. Chem. Soc.,* **2006**, *128*, 3852-3853; A. Yamashita, N. Yui, T. Ooya, A. Kano, A. Maruyama, H. Akita, K. Kogure, H. Harashima, *Nat. Protoc.,* **2006**, *1*, 2861-2869; A. Yamashita, D. Kanda, R. Katoono, N. Yui, T. Ooya, A. Maruyama, H. Akita, K. Kogure, H. Harashima, *J. Controlled Release,* **2008**, *131*, 137-144.

[46] X. Bao, I. Isaacsohn, A. F. Drew, D. B. Smithrud, *J. Am. Chem. Soc.,* **2006**, *128*, 12229-12238.

[47] V. Dvornikovs, B. E. House, M. Kaetzel, J. R. Dedman, D. B. Smithrud, *J. Am. Chem. Soc.,* **2003**, *125*, 8290-8301; X. Y. Wang, X. F. Bao, M. McFarland-Mancini, I. Isaacsohn, A. F. Drew, D. B. Smithrud, *J. Am. Chem. Soc.,* **2007**, *129*, 7284-7293; D. W. Zehnder, D. B. Smithrud, *Org. Lett,* **2001**, *3*, 2485-2487; J. Zhu, B. E. House, E. Fleck, I. Isaacsohn, A. F. Drew, D. B. Smithrud, *Bioorg. Med. Chem. Lett.,* **2007**, *17*, 5058-5062; J. Zhu, M. McFarland-Mancini, A. F. Drew, D. B. Smithrud, *Bioorg. Med. Chem. Lett.,* **2009**, *19*, 520-523; J. Zhu, D. B. Smithrud, *Org. Biomol. Chem.,* **2007**, *5*, 2992-2999.

[48] R. Hernandez, H. R. Tseng, J. W. Wong, J. F. Stoddart, J. I. Zink, *J. Am. Chem. Soc.,* **2004**, *126*, 3370-3371.

[49] S. Saha, K. C.-F. Leung, T. D. Nguyen, J. F. Stoddart, J. I. Zink, *Adv. Funct. Mater.,* **2007**, *17*, 685-693.

[50] K. O. Chiyoung Park, Sang Cheon Lee, Chulhee Kim,, *Angew. Chem., Int. Ed.,* **2007**, *46*, 1455-1457.

[51] K. C.-F. Leung, T. D. Nguyen, J. F. Stoddart, J. I. Zink, *Chem. Mater.,* **2006**, *18*, 5919-5928; T. D. Nguyen, K. C. F. Leung, M. Liong, C. D. Pentecost, J. F. Stoddart, J. I. Zink, *Org. Lett.,* **2006**, *8*, 3363-3366.

[52] K. Patel, S. Angelos, W. R. Dichtel, A. Coskun, Y.-W. Yang, J. I. Zink, J. F. Stoddart, *J. Am. Chem. Soc.,* **2008**, *130*, 2382-2383.

[53] S. Angelos, Y.-W. Yang, K. Patel, J. F. Stoddart, J. I. Zink, *Angew. Chem., Int. Ed.,* **2008**, *47*, 2222-2226.

[54] This simple approach, widely used in the pharmaceutical industry, consists of modifying the active drug while maintaining its inherent pharmacological properties. The parent drug is released *in vivo* after chemical or enzymatic transformation of the prodrug. The prodrug, composed of the active drug and the pro-moiety, should be cleaved only after all bioavailability barriers have been crossed. These barriers can be numerous and include aqueous solubility, chemical instability, insufficient oral absorption, rapid pre-systemic metabolism, inadequate brain penetration, toxicity and local irritation. It is important to note that the toxicity of the drug should be diminished in the prodrug version in order to improve drug targeting and administration quantities. Cleavage of the pro-moiety is usually achieved by enzymes specifically located at the periphery of the target organ. For a recent review see: [J. Rautio, H. Kumpulainen, T. Heimbach, R. Oliyai, D. Oh, T. Jarvinen, J. Savolainen, *Nat. Rev. Drug. Discov.*, **2008**, 7, 255-270.]

[55] A. G. Cheetham, M. G. Hutchings, T. D. W. Claridge, H. L. Anderson, *Angew. Chem., Int. Ed.,* **2006**, *45*, 1596-1599.

[56] For an account on proteolytic enzymes specificity see: R. Beynon, J. S. Bond *Proteolytic Enzymes*; Second ed.; Oxford university press: Oxford, 2001.

[57] Even though it seems that fast shuttling rates will decrease the time that the ring spends on each residue, over a longer period of time the ring is statistically uniformly distributed over the whole surface of the peptide backbone. Shielding effects will then be at a maximum.

CHAPTER FOUR

A new methodology for the synthesis of natural peptide-based rotaxanes

Acknowledgments

Most of the practical work described in this chapter was originally carried out by Stéphanie Potok. However, it was found that several final compounds contained considerable amounts of epimerization adducts. With the aim of submitting this work for publication, some key coupling reactions were optimized, and enantiomerically pure final rotaxanes were isolated and characterized (**16** to **28**). Dr. Anthony Fernandes and Dr. Vincent Aucagne are also greatly acknowledged for their valuable help in synthesizing peptide fragment **25** and peptide **28**, respectively.

4 Synopsis

Although rotaxanes of dipeptidic fragments have previously been synthesized using the Leigh-type direct self-assembly of benzylic amide rotaxanes, longer peptidic sequences have so far failed to afford rotaxanes in respectable yield under the same conditions. There are two main reasons for this. Firstly, long peptide threads are only poorly soluble under the strictly non-protic solvent conditions necessary for rotaxane formation. Secondly and most importantly, long peptidic backbones self-satisfy in terms of hydrogen bonds and fold up on themselves, resulting in disruption of the transoïd arrangement between carbonyl groups necessary to template the formation of rotaxane.

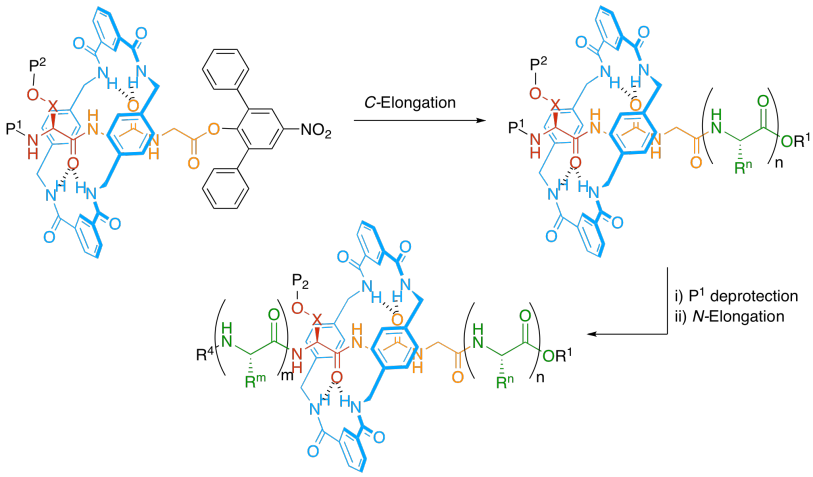

In the following chapter, the synthesis of wholly proteinogenic peptide rotaxanes via the elongation of lateral chains of short peptide rotaxane precursors is described. These pre-activated rotaxane building blocks consist of a Leigh-type benzylic amide macrocycle around a three amino acid long thread, bearing a set of N and side chain bulky protecting groups at the N-terminus and a sterically blocking activated para-nitrophenol ester at the C-terminus. Reaction of theses precursors with the nucleophilic amine of a stoppered peptidic fragment gives C-elongated adducts in good to excellent yields. Subsequent deprotection at the N^{α} allows reaction with the free carboxylic acid of an N-stoppered peptidic fragment under phosphonium-type coupling conditions. This method is the only method to date leading to rotaxanes in which the thread is made out of exclusively proteinogenic amino acids.

4.1 Introduction

Since amino acids are one of the main constituents of the human body, most biological processes are regulated by the endogenous production of specific peptides or proteins. Hence peptide-based drugs offer the possibility of highly efficacious interaction with many biological processes. Unfortunately, however, peptide-based drugs suffer from several severe drawbacks, of which the most significant are their very low bioavailability (they are rapidly decomposed by peptidases *in vivo*) and their very low membrane-crossing ability (due to their highly polar nature). The metabolism of peptides and proteins has been studied extensively,[1] and a number of proteolytic enzymes found in various part of the human body break down proteins and peptides into smaller peptidic fragments or single amino acids.

Backbone chemical modification has been the major technique used in order to get around these issues. L to D amino acid substitution, N and C-terminus modification and liposome encapsulation are probably the most significant examples of methods used in development laboratories. These methods give variable levels of success and often require a high degree of optimization.[2]

Mechanical encapsulation proved to be a viable alternative to the degradation of peptides *in vivo* (Chapter 3). The evidence suggests that the macrocycle constituent protects the backbone in a rotaxane-encapsulated peptide but the range of peptides that can be encapsulated is so far still limited. A new methodology needs to be developed to derivatize peptides into a rotaxane-encapsulated form.

4.1.1 Background

The original synthesis of interlocked architectures using an amide-based hydrogen bond template as the recognition motif for their self-assembly dates back to the early 1990's.[3] A few years later, following the serendipitous discovery of benzylic amide [2]catenanes by Leigh and co-workers,[4] it was demonstrated that rotaxanes could also be easily synthesized in a similar way using a stoppered thread containing pre-organized amide groups.[5-7] Two consecutive glycines were shown to adopt the

prerequisite transoïd conformation between the two carbonyls of the peptidic backbone to template the formation of rotaxane in 62% yield (Scheme 4.1).[6]

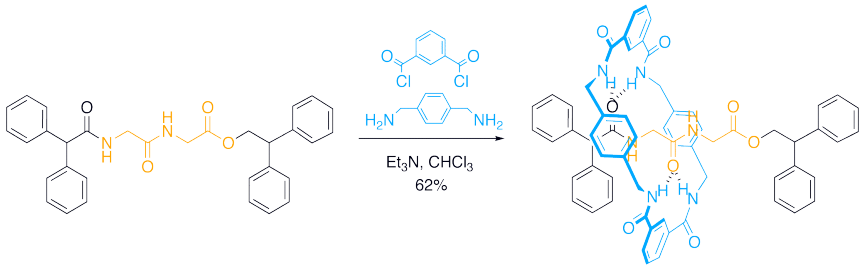

Scheme 4.1. Templated assembly of [2]Rotaxane around a glycylglycyl fragment.

Since this discovery, the Leigh group has investigated the effect of mechanical interlocking on different peptide backbones.[8] Although the macrocycle plays a crucial role in the stability and the solubility of the ensemble, the synthesis of peptide rotaxanes is however limited to threads containing five consecutive amino acids and practically viable only for sequences not longer than three amino acids.[8] The predisposition of the peptide backbone to fold due to intramolecular hydrogen-bonding is detrimental for the integrity of the transoïd arrangement between the carbonyl groups necessary to template the assembly. This effect is more prevalent with longer peptide sequences and is apparently emphasized in non-polar solvents, which are essential for the rotaxane-forming reaction. It appeared to us that a solution to circumvent this apparent conundrum was to build up longer peptide rotaxanes by elongation of short-sequence building blocks.

The feasibility of such strategy was in fact demonstrated in a report from Stoddart *et al*. a few years ago, in which the Authors used phosphorus ylide rotaxane building blocks to synthesize rotaxane polymers and molecular shuttles via a Wittig elongation reaction.[9] Soon afterwards, the group of Smithrud described a rather similar elongation strategy (Scheme 4.2),[10] which, despite having the merit of creating a peptidic bond within an interlocked structure, has never been applied to the synthesis of natural peptide rotaxanes.

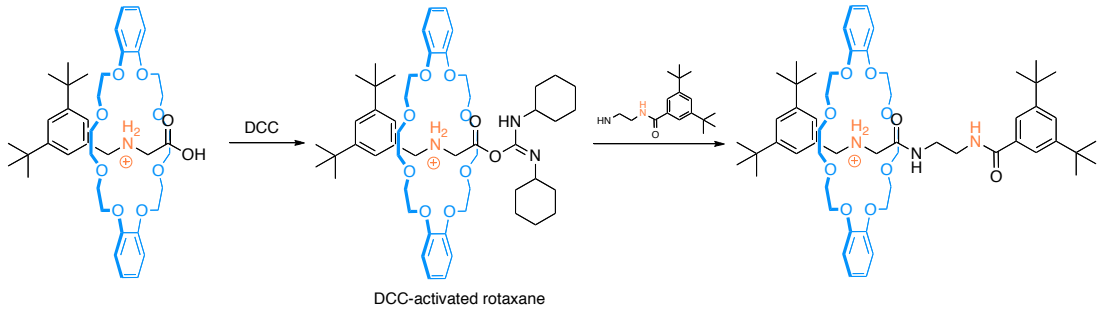

Scheme 4.2. Smithrud elongation of DCC- activated rotaxanes

Using Smithrud's approach, the terminal carboxylic acid of an ammonium-crown ether pseudo-rotaxane is treated with DCC to form a bulky *O*-acylurea, preventing the structure from de-threading. The resulting activated rotaxane is isolated and further elongated by displacement of the reactive *O*-acylurea with an amine-based suitably stoppered half-thread (Scheme 4.2).

However. to be adapted to the synthesis of peptide rotaxanes such method would require that a DCC-activated short peptidic thread is converted into a rotaxane under our 'clipping' conditions. Unfortunately, the large excess of *para*-xylylenediamine (15 equivalents compared to the thread) required during the rotaxane-forming step would undoubtedly quickly consume the highly reactive *O*-acylurea and mostly lead to undesired products.

4.1.2 Active esters

The high reactivity exhibited by *O*-acylureas is generally regarded as a drawback for the formation of an amide bond. In particular, when an amide bond is to be formed between peptidic fragments directly from *O*-acylurea, numerous side reactions (particularly epimerization) are likely to occur.[11] The mechanisms of these unwanted reactions are well established and peptide chemists have spent the past four decades tackling this issue. Wünsch and Weygand first developed a protocol,[12] which was the foundation of a nowadays generally-used procedure. In their original work, whilst attempting to synthesize glucagon and calcitonin, one equivalent of DCC and two equivalents of *N*-hydroxysuccinimide (HOSu) were applied concomitantly. During the course of the reaction the HOSu additive intercepts the highly reactive *O*-acylurea before it undergoes side reactions, thereby forming an OSu active ester, which is lower in reactivity but still reactive enough to be displaced by the amino

acid to be coupled. Since then, extensive research has focused on the elaboration of a variety of active esters in order to obtain the best reactivity to side reaction ratio.

According to a general assumption, the electrophilicity of an ester is related to the pK_a of the parent alcohol and increases as the pK_a decreases.[13] The benchmark has been centred on 1-hydroxybenzotriazole (HOBt) (Table 4.1), which is by far the most frequently used activating agent in peptide syntheses. It is either used in combination with a DCC type carbodiimide reagent or formed *in situ* from phosphonium (*e.g.* BOP, PyBOP) or uronium coupling reagents (*e.g.* HBTU, TBTU). Reactions employing a combination of diimide reagent and HOBt are typically complete in less than an hour in solution or on solid phase, and epimerization and/or side reactions are generally suppressed.

Table 4.1. Selected coupling additives and their pK_a values.

	HOAt	HOBt	HOSu	ONp
Structure	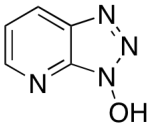	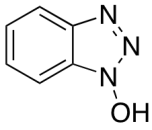	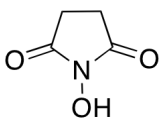	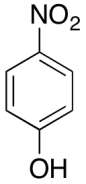
pK_a[14]	3.47	4.57	6.0	7.15

The ability of such activated esters to decrease the reactivity of the *O*-acylurea intermediate could be exploited in the elongation of short peptide rotaxanes. Exchange of stoppers in rotaxanes involving ester groups has been described[15] and the fact that active esters can be isolated and are stable towards hydrolysis motivated us to adopt this strategy (Scheme 4.3).

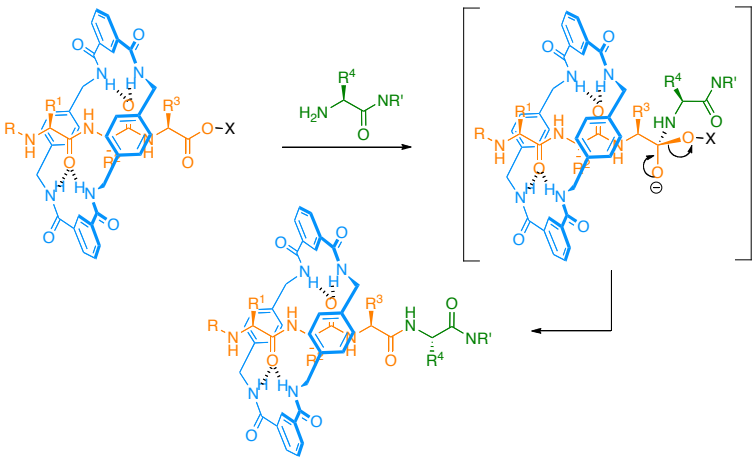

Scheme 4.3. Elongation mechanism of ester-activated peptidorotaxanes. The group X should be bulky enough to avoid dethreading. The tetrahedral intermediate allows the rotaxane to be elongated without potential dethreading

The challenge, in this particular case, was to find an appropriate type of active ester, which would be unreactive towards the excess of amine needed for the rotaxane forming step, but that could subsequently be activated for the coupling of the elongation segment.[16] To fulfill these requirements, the parent alcohol should have a significantly higher pK_a value than HOBt, given the fast rate of aminolysis exhibited by HOBt esters at room temperature. HOSu ($pK_a = 6$) is expected to be just over 25 times less reactive than HOBt ($pK_a \approx 4.6$), and would not be sufficiently inactivated (Table 4.1).

An initial screening of the pK_a values of the some common activating agents led us to *para*-nitrophenol (ONp) (Table 4.1), a less frequently used additive but known to give a slower rate of reaction.[17,18,19] With a pK_a of 7.15, the latter can be expected to be over 300 times less reactive than HOBt at room temperature. Chemical functionalization of the phenyl ring is straightforward and appropriate *ortho* substitution could be used to tune the reactivity of the ester. Adding electron withdrawing groups would decrease the pK_a of the phenol, rendering the corresponding ester a better leaving group, whereas adding bulky donating groups would have the opposite effect. This rather 'unreactive' ester could then be 'turned on' at higher temperatures to allow for reaction with terminal amines, after rotaxane has been formed at room temperature.

Commercial diphenyl-*para*-nitrophenol seemed a perfect candidate for a first trial. Molecular modeling (CPK) showed that the two *ortho*-phenyl groups are large enough to avoid slippage of the ring in a Leigh-type rotaxane structure. The two

ortho-phenyl groups would certainly add a significant increase in pK_a, ensuring that the ester would be robust enough for the rotaxane-forming step. Additionally, once formed, the macrocycle should have a shielding effect on the thread and protect the active ester from further reaction.

4.1.3 Design

To assess the inertness of the *para*-nitrophenol unit under rotaxane-forming conditions and its reactivity toward aminolysis at elevated temperatures, we designed a dipeptidic model thread stoppered at its C-terminus by 2,6-diphenyl *para*-nitrophenol ester. Rotaxane was formed in good yield and elongation by various peptide fragments proved the method to be very efficient.

A universal method for the synthesis of theoretically unlimited length peptido[2]rotaxanes was then developed, in which the threads are made out of exclusively proteinogenic amino acids. The process for the construction of such original interlocked architectures relies on the C-elongation of rotaxane building blocks via nitrophenol ester stopper aminolysis and N-elongation via peptide coupling chemistry. Figure 4.1 gives a schematic representation of such building blocks, which are stoppered at the N-terminus, by a bulky protecting group (P_2) attached to the side chain of an amino acid. Once C-elongated, the rotaxane is N^{α} deprotected and further N-elongation is achieved under standard peptide coupling conditions.[20]

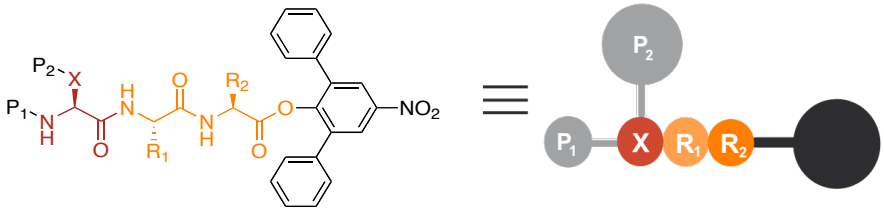

Figure 4.1. Structure of tripeptide precursors: The side chain at the N-terminus bears a bulky protecting group (P_2) that acts as a stopper while the two following amino acids (R_1 and R_2) template the rotaxane assembly.

4.2 Results and discussion

4.2.1 Design and synthesis of activated rotaxane building block

To test whether the nitrophenol group is suitable for rotaxane elongation, a model thread was designed and the elongation of rotaxane was assessed under various conditions and using various peptide fragments. The synthesis of activated thread and rotaxane is depicted in scheme 4.4. For comparison reasons, the activated thread was made out of the same glycylglycyl fragment (**4**, Scheme 4.2) previously reported by Leigh and coworkers (Scheme 4.1).

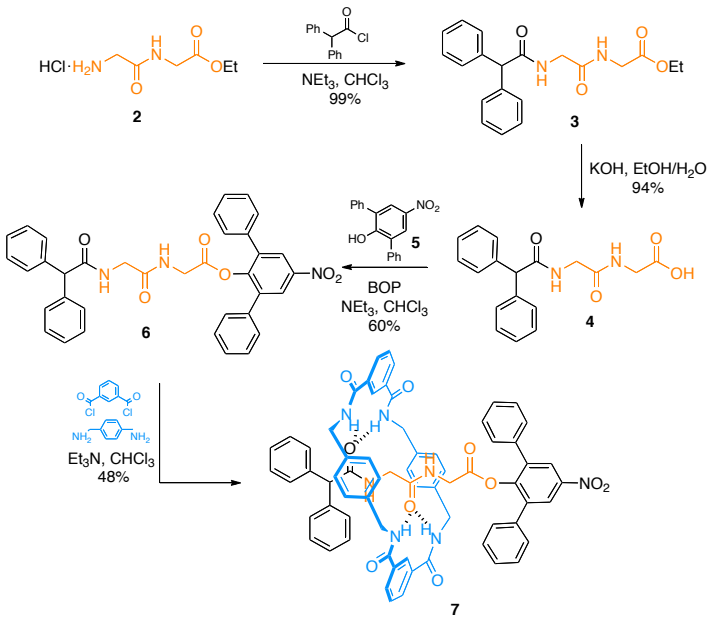

Scheme 4.4. Synthesis of the dipeptide activated ester thread and of rotaxane building block.

The nitrophenol moiety was incorporated after basic hydrolysis of known ester **3** using BOP as the coupling agent (Scheme 4.4). A 5-fold excess of **5** was necessary to obtain a satisfactory yield of coupling and unreacted **5** could be easily recoved during chromatography purification of the product. Formation of rotaxane **7** was carried out using a slightly modified procedure from the one initially reported by Leigh (where equimolar quantities of isophthaloyl dichloride and *para*-xylylenediamine are simultaneously added to a solution of thread in $CHCl_3$ containing an excess of NEt_3). To avoid any premature decomposition of the thread,[21] NEt_3 was mixed with *para*-xylylenediamine prior to addition allowing it to be immediately consumed by the HCl produced during the course of the reaction.

Filtration of the crude mixture left a solution containing mainly peptido[2]rotaxane **7** and unreacted thread **6**, together with catenated and polymeric species. Purification by flash column chromatography led to rotaxane **7** in 48% yield, which is comparable to the 62% obtained with the non-activated thread in Scheme 4.1. Although one can suspect partial nucleophilic attack of *para*-xylylenediamine on the activated carbonyl to be responsible for this slight decrease in yield, reaction of the diamine with the dichloride is essentially favoured. Importantly, rotaxane **7** proved to be stable in air for months without any sign of decomposition.

4.2.2 Elongation of activated rotaxane

Elongation of activated rotaxane building blocks was carried out according to Scheme 4.5.

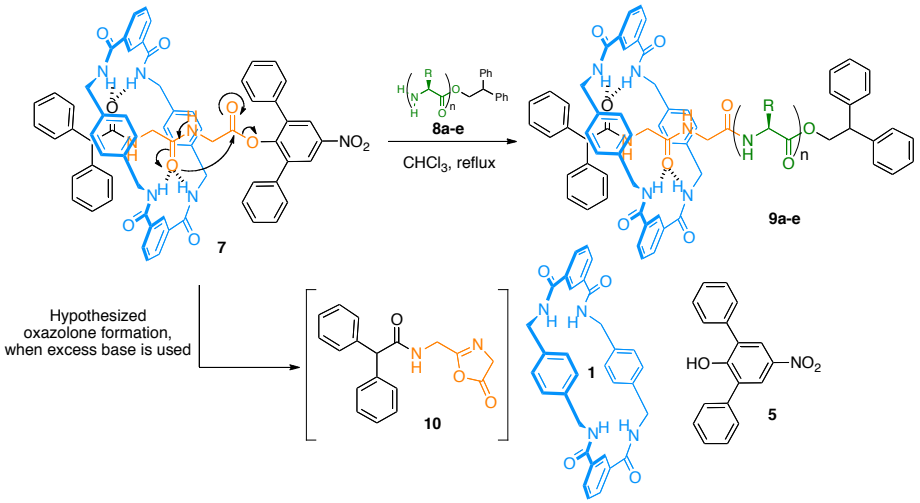

Scheme 4.5. Elongation of the activated rotaxane by different peptide fragments and the suggested mechanism for the formation of free macrocycle.

As expected, rotaxane **7** did not react with the primary amine of stoppered amino acids at room temperature (Table 4.2, Entry 1). This lack of reactivity is believed enhanced by the shielding effect of the macrocycle. In a first attempt, rotaxane **7** was heated at reflux in $CHCl_3$ with the trifluoroacetate salt of stoppered glycine **8a** and an excess of NEt_3 (Table 4.2, Entry 2). Pleasingly, after a few hours, TLC analysis showed the slow disappearance of **7** and the appearance of new compounds. Isolation of the major compound by flash chromatography afforded tripeptido[2]rotaxane **9a** in 61% yield. Together with **9a,** the eliminated nitrophenol stopper **5** and other

unknown by-products, we were surprised to isolate a fair amount of free macrocycle **1**. Originally thought to be produced *via* hydrolysis of the activated ester by residual water,[22] this was better rationalized by the intramolecular formation of an undesired oxazolone ring, **10**, at the C-terminus, causing de-threading. (Scheme 4.5).[23]

The formation of this intermediate is often observed in peptide couplings and can expected to be favoured by the use of excess of base and high temperatures.[11,18,24] In the hope of minimizing undesired side reactions, the elongation was performed without the addition of base. The best results were then obtained when a mixture of rotaxane **7** and at least two equivalents of peptide as the free amine were heated at reflux in $CHCl_3$. A series of mono- to tri-peptide half-stoppered threads have been reacted under these optimized conditions. Peptido[2]rotaxanes were isolated in good to excellent yields (Table 4.2).

Table 4.2. Effect of stoichiometry, reaction time, and reaction conditions on the C-elongation of model rotaxane **7.** [a] The TFA salt of the substrate was used.

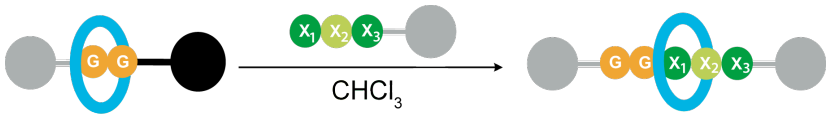

Entry	Substrate				equiv.	NEt_3 (equiv.)	temp.	time (h)	product		yield (%)
	X_1	X_2	X_3								
1	G	-	-	**8a**	2	1	RT	24	GGG	**9a**	0
2	G	-	-	**8a** [a]	2	2	reflux	24	GGG	**9a**	61
3	G	-	-	**8a**	2	0	reflux	24	GGG	**9a**	91
4	A	-	-	**8b**	2	0	reflux	24	GGA	**9b**	88
5	L	-	-	**8c**	2	0	reflux	24	GGL	**9c**	78
6	F	-	-	**8d**	5	0	reflux	52	GGF	**9d**	74
7	A	G	G	**8e**	2	0	reflux	72	GGAGG	**9e**	55

Although reactivity drops according to the bulkiness of the substrate, the reaction could easily be forced towards completion by increasing the load of reactant or by extending the reaction time (Table 4.2, Entries 6 and 7). The excess of peptide fragments could be recovered in each case during purification of the elongated rotaxanes.

4.2.3 Synthesis of a Leu-enkephalin rotaxane

Rotaxane of the biologically active pentapeptide Leu-enkephalin (YGGFL), whose synthesis had previously been unsuccessfully attempted in our group by direct formation of rotaxane using the pentapeptide (1% yield),[8] has the right structural requirements to be synthesized via the new approach expounded above. The first three amino acids of the sequence (YGG) will indeed adopt the correct orientation to template the formation of the macrocycle as internal hydrogen bonding will be minimal (Scheme 4.6).

Scheme 4.6. C-elongation strategy applied to the synthesis of a Leu-enkephalin analogue rotaxane

A permanent N^{α} protecting group is needed to stopper the assembly as the tyrosine is not large enough on its own, whereas the consecutive phenyalanyl and leucyl residues will provide an appropriate stopper at the other end after being incorporated into the thread by elongation.

The phenol of the tyrosine and the carboxylate of the terminal leucine were both protected by benzyl groups, which can be selectively cleaved in the last step, leaving the Boc group intact. The synthesis of Boc-Leu-enkephalin rotaxane is depicted in Scheme 4.7.

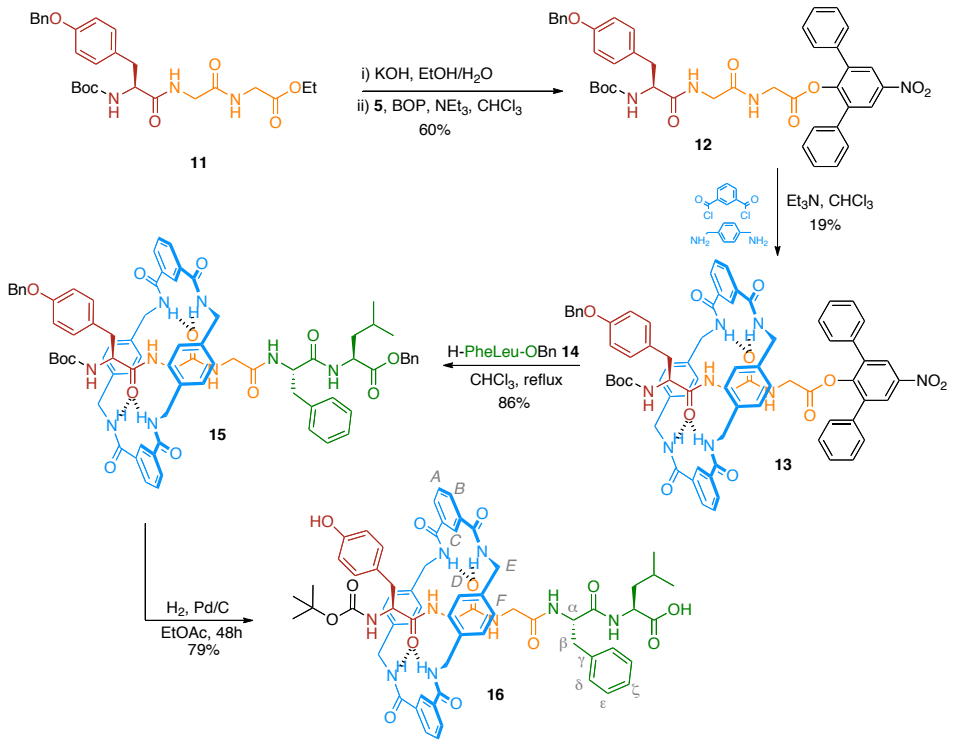

Scheme 4.7. Synthesis of Leu-enkephalin analogue rotaxane.

Starting from known[25] ester **11**, the tripeptide activated thread **12** was prepared in two steps in 60% overall yield (Scheme 4.7). Rotaxane formation was carried out using the procedure described earlier, producing rotaxane **13** in an isolated yield of 19%, after purification by flash chromatography on silica gel without any sign of decomposition. This activated rotaxane proved to be stable in air at room temperature for several months. The key elongation step was achieved in very good yield (86%) using an excess of commercial nucleophile **14** under the optimized conditions described above. Finally, deprotection of the two benzyl groups – carried out with H_2 and Pd/C as catalyst – appeared to be sluggish but finally reached completion after 48 hours. LCMS analysis of the final product showed the presence of one major compound (> 92%, HPLC purity), whose *m/z* of 1188 corresponded to the expected $[M+H]^+$.

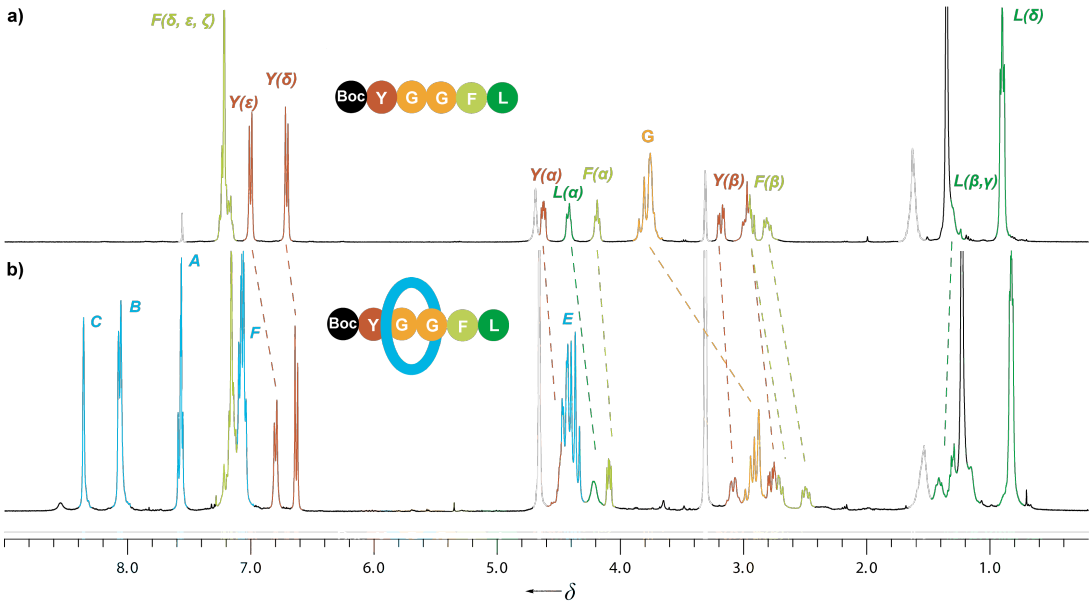

Figure 4.2. ^{1}H NMR spectra (400 MHz, $CDCl_3$-CD_3OD (1:1), 300 K) of a) Boc-Leu-enkephalin, b) Boc-Leu-enkephalin rotaxane **16**. The assignments and colouring of signals correspond to that shown in Scheme 4.7. Residual solvent peaks are shown in grey.

^{1}H NMR spectra of rotaxane **16** and of Boc-Leu-enkephalin are shown in Figure 4.2. The spectrum of the rotaxane shows upfield shifts of several signals with respect to the non-interlocked counterpart. Such shielding is typical of interlocked architectures where the aromatic rings of one component are positioned face on with another component. They are most intense for the protons of the two glycines (H_G) indicating that the macrocycle is mostly located over that portion, on the NMR timescale. The signals of the eight methylene protons (H_E) from the macrocycle display a high multiplicity pattern (*i.e.* the eight methylene protons belong to magnetically distinct environments), indicating that the macrocycle experiences rather slow pirouetting on the NMR timescale.[7] The availability of many hydrogen bond donors within the structure and the confinement of the macrocycle within a restricted area (*i.e.* over the two glycines) are both likely to be the factors affecting the pirouetting rate.

4.2.4 N and C-elongation: synthesis of a wholly proteinogenic peptide rotaxane

4.2.4.1 Design and synthesis of a ready-to-elongate building block

To complete this study, we extended the methodology to the synthesis of more challenging structures where the thread is of a wholly peptidic nature, without additional protecting groups and of a greater length. The key step to accessing longer peptide rotaxanes is the combination of the C-elongation described earlier together with an N-elongation procedure. To allow for extension at the N-terminus the side-chain of the *N*-terminal amino acid has to bear a large enough protecting group to prevent the structure falling apart after deprotection of its N^{α} (**24**, Scheme 4.8). In addition, both elongation fragments should comprise two consecutive large amino acids to prevent the final assembly from dissociating.

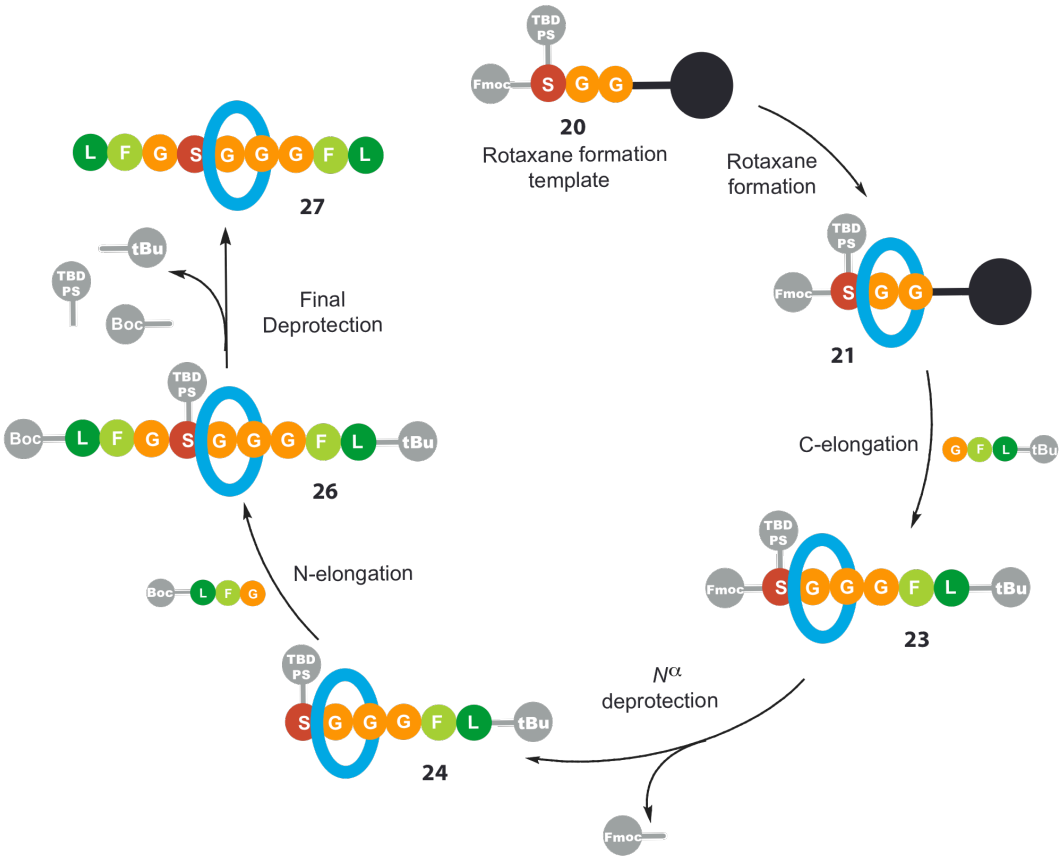

Scheme 4.8. Combined N- and C-elongation strategy in the synthesis of petido[2]rotaxanes containing only proteinogenic amino acids.

We initially considered extending this N-elongation approach to a slightly modified version of the tyrosylglycylglycyl fragment **13** (Scheme 4.7) where the tyrosyl residue would bear a bulky diphenylmethyl (Dpm) group instead of a benzyl group. While Dpm is cleaved under the same conditions as the latter, the N^{α} of the N-elongation fragment would optimally require a Cbz-type protecting group to fit in this H_2-labile protecting groups scheme. Although final hydrogenolysis should in this case afford the fully deprotected product, the slow reaction times upon hydrogenation observed in the previous example suggested that a one-pot deprotection of a Dpm, Bn and Cbz groups could be rather challenging. More importantly, Dpm groups are not resistant under classical Boc cleavage conditions (10% TFA in CH_2Cl_2),[26] and as a result, the N^{α}-protecting group of the rotaxane building block would have to be substituted by an non-acid-labile protecting group.

To circumvent such concerns, we opted for a variation of the classical Fmoc synthesis approach, routinely used in solid phase peptide synthesis (SPPS). This universally approved approach takes advantage of the base-labile Fmoc protecting group at the N-terminus while side-chain and C-terminus deprotections are accomplished under acidic conditions.[11] A bulky, acid labile silyl group such as TBDPS on the side chain would then be appropriate, while a *tert*-butyl (*t*-Bu) protecting group at the C-terminus of the C-elongation fragment and a Boc at the N-terminus of the N-elongation fragment would suit these requirements perfectly (Scheme 4.8). Additionally, switching from a tyrosine to a serine for the seemed a wise choice to us as acid mediated deprotection of TBDPS-protected primary alcohols are several orders of magnitude faster than the corresponding reaction with phenols[27] (Scheme 4.9).

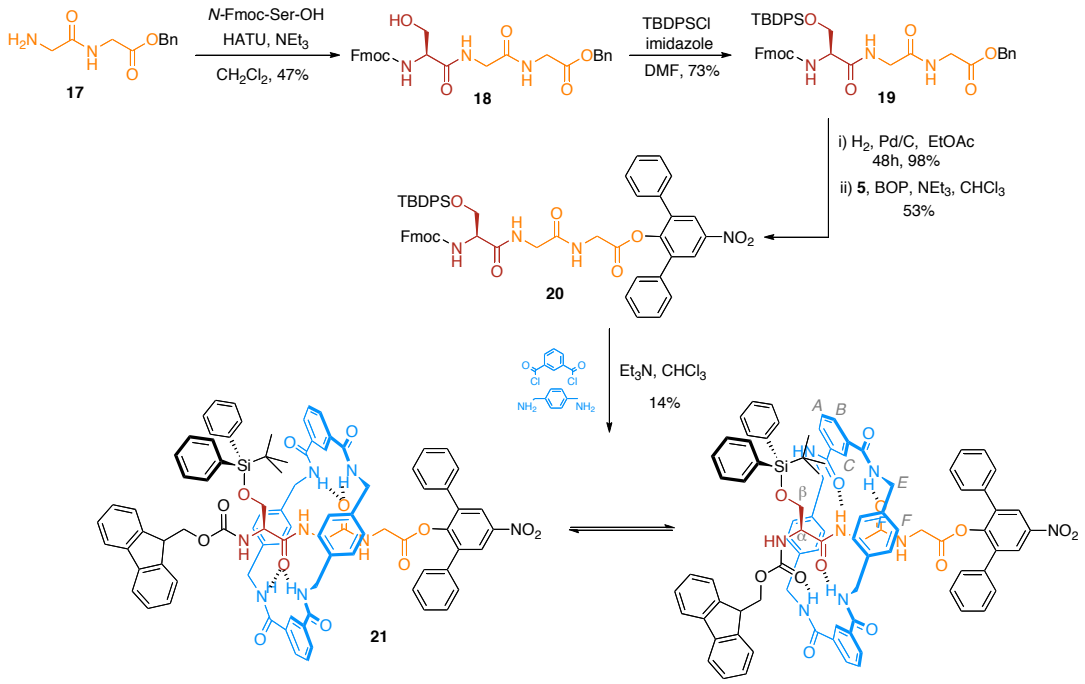

Scheme 4.9. Synthesis of the ready-to-elongate precursor.

Hence, the synthesis of the ready-to-elongate rotaxane was carried out according to Scheme 4.9, where it was obtained in four steps, starting from precursor **17**. The serine was then coupled to this glycylglycyl-benzylated fragment **18** under HATU-mediated coupling conditions. A moderate yield was obtained although examples in the literature report higher yields for the coupling of non-alcohol-protected amino acids.[28] A comparable yield was obtained using EDC together with HOBt, whereas a significant drop in yield occurred under BOP or TBTU conditions.

C-terminus deprotection, activation and rotaxane formation gave the ready-to-elongate rotaxane **21** in 15% yield which, given the steric hindrance around the template, is very remarkable.

The ^{1}H NMR spectrum of building block rotaxane **21** shows the peaks of the macrocycle with those of the thread shifted upfield, characteristic of an interlocked architecture (Figure 4.3). Surprisingly, the two β protons of the serine residue in rotaxane **21** exhibit a significant upfield shift (~1 ppm) compared to the parent thread, indicating that the macrocycle is predominantly located over the bulky N-terminus end of the peptide chain. This feature is confirmed by the chemical shift of the α protons of the same amino acid. It appears to us that to minimize the steric clash at the N-terminus, the carbamate moiety of the Fmoc group adopts a cisoïd conformation relative to the adjacent carbonyl of the peptidic bond (Scheme 4.9).

The carbonyl of the carbamate group is then accessible by the macrocycle, whose amides groups form a hydrogen bond with it.

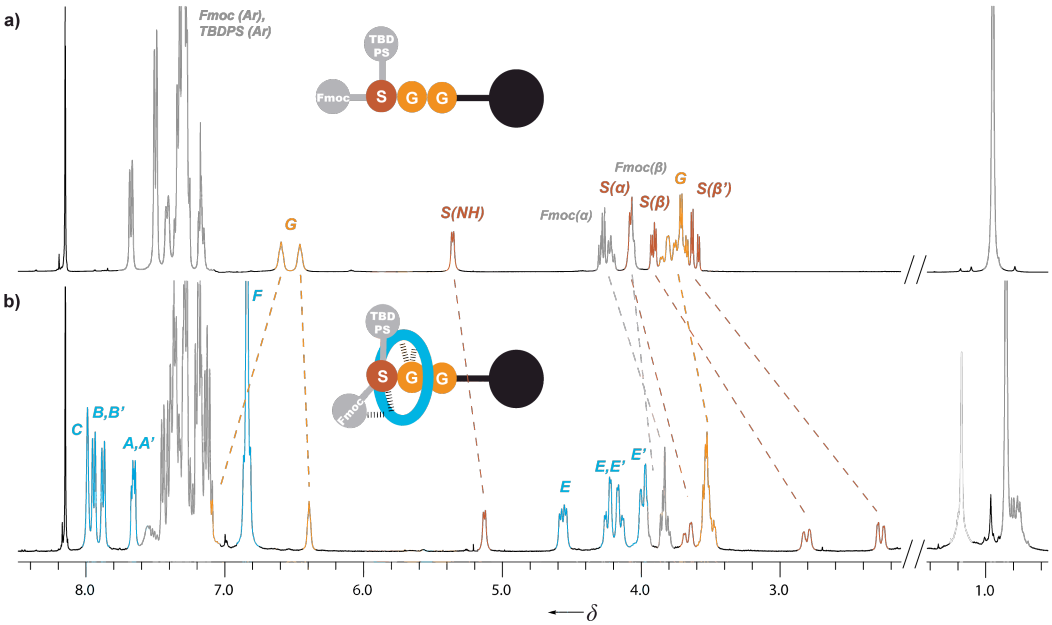

Figure 4.3. Partial ^{1}H NMR spectra (400 MHz, $CDCl_3$, 300 K) of a) thread **20**, b) Ready-to-elongate precursor rotaxane **21**. The assignments and colouring of signals correspond to that shown in Scheme 4.9. Residual solvent peaks are shown in light grey.

Furthermore, one of the -NH signals of the glycines is greatly deshielded compared to the non-interlocked thread suggesting that this proton is involved in hydrogen bonding, probably to a carbonyl of the macrocycle, which adopts a twisted conformation (Scheme 4.9). The high multiplicity signal of the methylene protons of the macrocycle (H_E) is also an indication of an unusually unsymmetrical environment and a rather rigid conformation. The double set of protons given by H_A and H_B shows that the upper and bottom half of the macrocycle are not equivalent on the NMR timescale, implying that pirouetting is also fairly slow.

4.2.4.2 C- and N-elongation of the building block

C- and N-elongation of building block **21** were performed with three amino acid long peptide fragments. Both fragments contained two consecutive terminal leucyl and phenylalanyl residues to stopper the assembly. According to the planned strategy (Scheme 4.8), the C-elongation fragment was *t*-Bu protected at its C-terminus and

the N-elongation fragment was Boc protected at its N-terminus, both of which allow for a final acidic cleavage (Scheme 4.10).

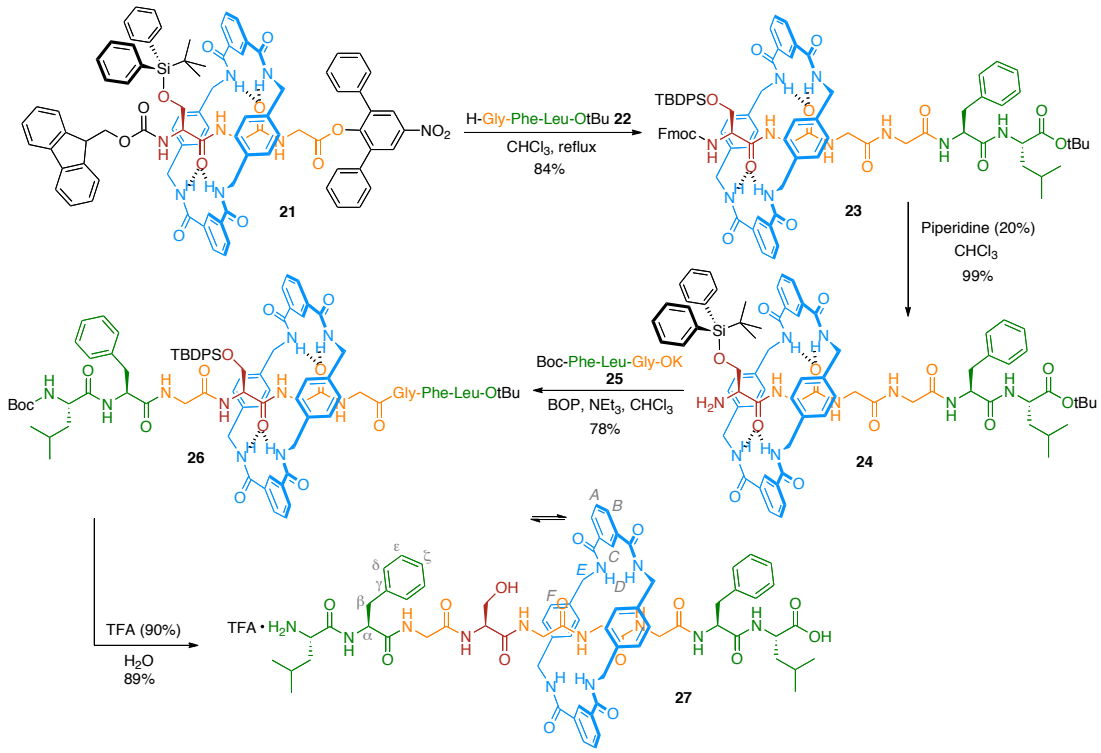

Scheme 4.10. Synthesis of nona-peptido[2]rotaxane via C- and N-elongation.

Rotaxane **21** and 5 equivalents of the amine **22** were then stirred in $CHCl_3$ under reflux overnight to give **23** in very good yield (Scheme 4.10). Cleavage of the Fmoc protecting group with piperidine gave a quantitative yield of the free amine **24**, which was further elongated under BOP coupling conditions. A good yield of rotaxane was obtained using only 2 equivalents of peptide **25**, suggesting that the terminal amine was less shielded by the macrocycle than originally expected. This could be due to the fact that the thread comprises four accessible binding sites of equivalent affinity on which the macrocycle spends a statistically equal amount of time, leaving the terminal amine less shielded by the macrocycle and thus more prone to react.

Final lateral and side chain deprotections were achieved with TFA/H_2O (9:1), which (after evaporation and precipitation of the supernatant in Et_2O) led to peptido[2]rotaxane **27** as its TFA salt. A pure sample of **27** was analyzed by LCMS. The chromatogram confirmed the presence of one major compound (> 95% HPLC purity) whose *m/z* of 1386 corresponded to the expected $[M+H]^+$.

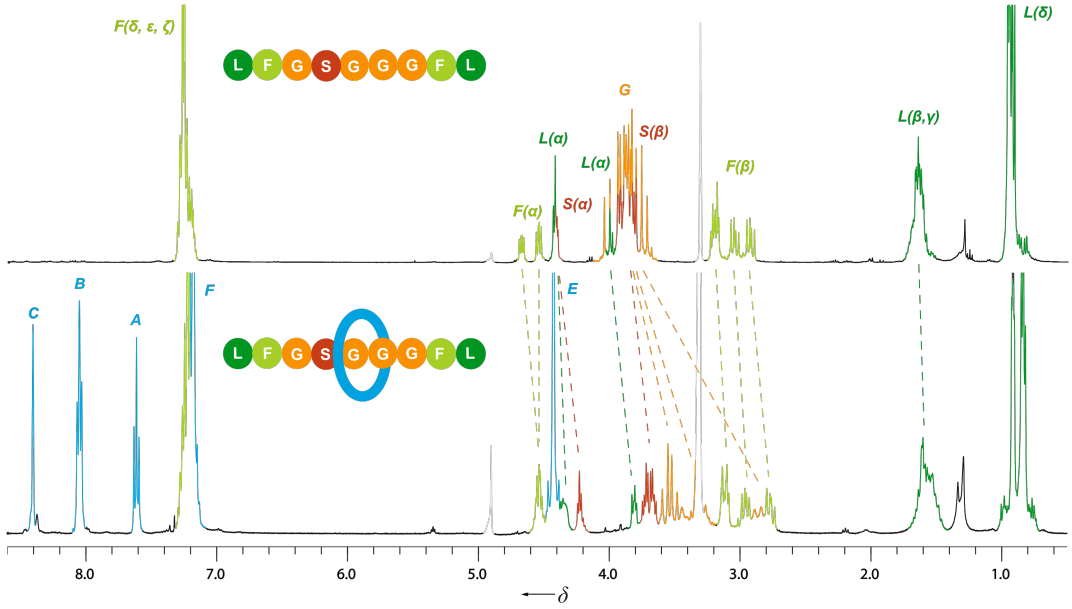

Figure 4.4. ^{1}H NMR spectra (400 MHz, CD_3OD, 300 K, H_2O suppression) of a) nona-peptide thread **28**, b) nona-peptido[2]rotaxane **27**. The assignments and colouring of signals correspond to that shown in Scheme 4.10. Residual solvent peaks are shown in grey.

The ^{1}H NMR spectrum of rotaxane **27** is shown in Figure 4.4, together with a spectrum of the analogous non-interlocked thread **28** prepared by standard Fmoc/*t*-Bu automated solid phase synthesis. The chemical shift differences observed in the spectrum of the rotaxane compared to the thread follow the usual trend (upfield shift) but to a lesser extent than seen previously. The signals are indeed less shifted (≤1 ppm) and this seems consistent with the fact that the structure is much less constrained than in earlier examples. The peptide backbone consists of multiple adjacent binding sites of similar affinities (each one being two consecutive carbonyls in a transoid conformation): the macrocycle is then able to 'travel' freely from one end of the thread to the other, spending an approximately equal amount of time over each fragment of the thread. The sharp signal given by the protons H_E of the macrocycle is strong evidence for such a 'free' macrocycle and for a fast rate of pirouetting.

4.3 Conclusion

In conclusion, an efficient and versatile methodology for assembling interlocked molecular architectures where the thread is made entirely out of proteinogenic amino acids has been described. These architectures are, to best of our knowledge, the first examples of synthetic rotaxanes were the thread is entirely made of fully deprotected proteinogenic amino acids.

The C-elongation method described is readily accessible from commercial 2,6-diphenyl-*para*-nitrophenol whereas N-elongation simply requires a protected side chain amino acid. The majority of proteinogenic amino acids are suitable for this task, since most of them contain a heteroatom of some sort on their side chain that can be substituted with a temporary blocking group. The synthesis of short peptide rotaxane building blocks requires a certain level of pre-organization in the template, but a combination of side chain protected amino acids and two consecutive amino acids of moderate bulkiness are the only prerequisites for the synthesis of such architectures.

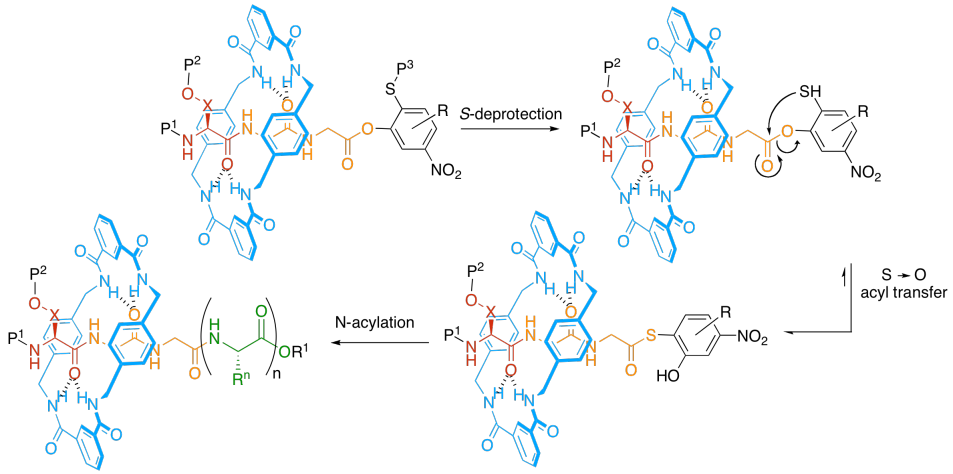

Scheme 4.11. A potential C-elongation strategy for improved coupling efficiency and milder reaction conditions.

Future work could be to consider an alternative to the somewhat high temperatures required to 'turn on' the active ester for C-elongation. An intramolecular acyl-transfer, in a similar way as Danishefsky has recently described, could be a viable option.[29] In this ingenious system, resembling native chemical ligation, an *S*-protected mercaptophenol ester substituted at the 4-position by the fragment to be ligated is 'turned on' for coupling when the thiol is deprotected. Deprotection

triggers S → O acyl transfer, transforming the phenol ester into a thioester, which is a much better leaving group than the former. Subsequent N → S acyl transfer terminates the coupling sequence. Using a similar idea, a bulky nitromercaptophenol could serve the purpose of elongating rotaxane building blocks with longer sequences at significantly lower temperatures (Scheme 4.11).

4.4 Experimental section

4.4.1 General methods

General method A: Formation of 2-6 diphenyl-*p*-nitrophenol esters

To a solution of carboxylic acid (3.2 mmol, 1.0 equiv.), NEt_3 (48 mmol, 15.0 equiv.) and BOP (4.8 mmol, 1.5 equiv.) in $CHCl_3$ (70 mL), was added 2-6 diphenyl-*p*-nitrophenol (16 mmol, 5.0 equiv.). The reaction mixture was stirred for 4 hours at room temperature. An aqueous solution (1M) of HCl (50 mL) was added. The layers were separated and the aqueous layer was extracted with CH_2Cl_2 (2 × 40 mL). The combined organic fractions were washed with an aqueous saturated solution of $NaHCO_3$ (2 × 40 mL), followed by H_2O (1 × 50 mL), dried ($MgSO_4$) and concentrated under reduced pressure. Purification by flash column chromatography on silica gel afforded pure activated ester.

General method B: Benzylic amide rotaxane-forming reaction

To a vigorously stirred solution of thread (1.91 mmol, 1.0 equiv.) in dry $CHCl_3$ (100 mL) under nitrogen, was simultaneously added a solution of *p*-xylylenediamine (15.6 mmol, 15 equiv.) and NEt_3 (39.3 mmol, 30 equiv.) in $CHCl_3$ (50 mL) and a solution of isophthaloyl dichloride (15.6 mmol, 15 equiv.) in $CHCl_3$ (50 mL) over a period of 3 hours using motor-driven syringe pumps. The reaction mixture was stirred for another 2 hours, filtered over a Celite® pad and the filtrate was concentrated under reduced pressure. The resulting orange solid was purified by flash column chromatography on silica gel.

General method C: C-elongation of 2-6 diphenyl-*p*-nitrophenol esters [2]rotaxanes

A solution of activated [2]rotaxane (79 µmol, 1 equiv.) and the stoppered nucleophile (158-395 µmol, 2 to 5 equiv.) in $CHCl_3$ (20 mL) was heated at reflux for 24-72 hours. The solvent was removed under reduced pressure and the resulting yellow oil was directly purified by flash column chromatography on silica gel to give in order of elution 2,6-diphenyl-*p*-nitrophenol, and the elongated [2]rotaxane.

4.4.2 Characterization of Boc-Leu-enkephalin rotaxane (16)

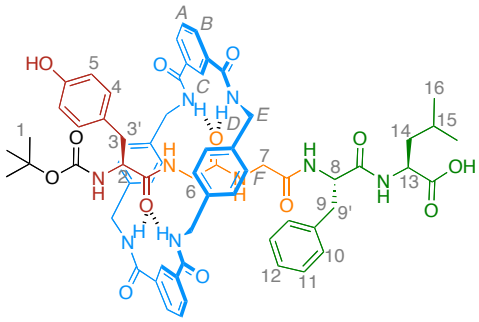

16

A solution of **15** (17.5 mg, 12.8 mmol, 1 equiv.) and palladium (10%) on carbon (60 mg) in AcOEt (500 mL) was purged with H_2 by means of three vacuum/H_2 cycles and the mixture was stirred at room temperature for 48 hours. The solid was filtered off with Celite® and AcOEt was evaporated under reduced pressure. The resulting yellow oil was purified by preparative TLC on silica gel with acetone-CH_2Cl_2 (10:90, 3 runs) as eluent to give **16** as a light yellow solid (12 mg, 10.1 µmol, 79%); **^{1}H-NMR (400 MHz, $CDCl_3$-CD_3OD [1:1]):** δ = 8.36 (s, 2H, H_C), 8.06 (d, 4H, *J* = 9.5 Hz, H_B), 7.57 (t, 2H, *J* = 9.1 Hz, H_A), 7.28-6.9 (m, 17H, H_F, H_4, H_5, H_{10}, H_{11}, and H_{12}), 6.80 (d, 2H, *J* = 8.2 Hz, H_5), 6.65 (d, 2H, *J* = 8.4 Hz, H_4), 4.54-4.03 (m, 9H, H_E, and H_2), 4.28-4.17 (m, 1H, H_{13}), 4.09 (dd, 1H, *J* = 5.4 Hz, *J* = 8.8 Hz, H_8) 3.18-3.02 (m, 2H, H_3), 3.02-2.83 (m, 4H, H_6 and H_7), 2.78 (dd, 1H, *J* = 5.4 Hz, *J* = 14.0 Hz, $H_{3'}$ or $H_{9'}$), 2.71 (dd, 1H, *J* = 10.0 Hz, *J* = 14.0 Hz, $H_{3'}$ or $H_{9'}$), 2.50 (dd, 1H, *J* = 8.8 Hz, *J* = 13.8 Hz, H_9), 1.45-1.10 (m, 3H, H_{14} and H_{15}), 0.94-0.70 (m, 6H, H_{16}); **^{13}C-NMR (100 MHz, CD_3OD):** δ = 172.5, 172.4, 171.4, 169.1, 168.2, 167.3, 167.2, 157.6, 155.8, 137.2, 136.8, 136.4, 135.2, 134.0, 133.9, 131.3, 131.22, 130.2, 129.9, 129.2, 129.0, 128.7, 131.7, 131.6, 130.9, 130.8, 130.7, 129.9, 129.8, 128.2, 116.5,

58.2, 57.4, 56.4, 48.8, 45.9, 43.5, 42.4, 39.9, 29.0, 23.7, 22.5, 22.3; **LRESI-MS:** *m/z* = 1188 $[M+H]^+$, **ESI-HRMS** : *m/z* = 1205.5677 $[M+NH_4]^+$ (calc. for $C_{65}H_{77}O_{13}N_{10}$ 1205.5666 $[M+NH_4^+]$).

4.4.3 Experimental procedures for the synthesis of nonapeptide rotaxane (27)

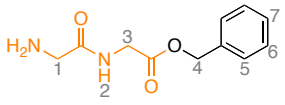

17

To a solution of Boc-Gly-Gly-OBn (126 mg, 0.39 mmol, 1 equiv.) in CH_2Cl_2 (10 mL) at 0°C was added Trifluoroacetic acid (1.65 mL, 0.22 mol, 45.0 equiv.) drop-wise. After 30 minutes at 0°C, the solution was stirred a further 1.5 hours at room temperature and then cooled to 0°C. After neutralization with a saturated solution of $NaHCO_3$, the mixture was extracted with a $CHCl_3$/*i*PrOH (3/1, v/v) mixture, dried and concentrated under reduced pressure to give **17** (34 mg, 0.15 mmol, 39%) as a light yellow wax. **^{1}H-NMR (400 MHz, $CDCl_3$):** δ = 7.31-7.18 (m, 6H, H_2, H_5, H_6 and H_7), 5.08 (s, 1H, H_4), 4.50 (bs, 2H, N*H*$_2$), 3.95 (s, 2H, H_1), 3.24 (bs, 1H, H_3); **^{13}C-NMR (100 MHz, $CDCl_3$):** δ = 173.7, 169.4, 134.7, 127.9, 127.8, 127.6, 126.6, 126.3, 66.5, 66.5, 43.2, 40.3; **LRFAB-MS:** *m/z* = 223 $[M+H]^+$

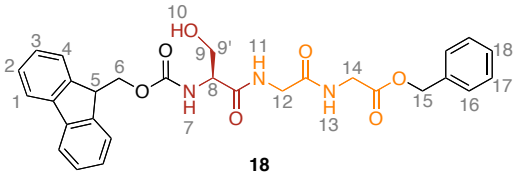

18

To a solution Fmoc-Ser-OH (200 mg, 0.58 mmol, 1 equiv.), NEt_3 (180 µL, 1.29 mmol, 2.2 equiv.) and HATU (331 mg, 0.87mmol, 1.5 equiv.) in CH_2Cl_2 (15 mL) at 0°C, was added **17** (193 mg, 0.87 mmol, 1.5 equiv.). The reaction mixture was left to warm up to room temperature and stirred overnight. An aqueous solution (1M) of HCl (15 mL) was added, the layers were separated and the aqueous layer was extracted with $CHCl_3$ (3 × 15 mL). The combined organic fractions were washed with an aqueous saturated solution of $NaHCO_3$ (2 × 20 mL) followed by H_2O (1 × 40 mL), dried ($MgSO_4$) and concentrated under reduced pressure. The resulting brown residue was purified by flash column chromatography on Silica gel with CH_2Cl_2-

MeOH (98:2 to 92:8) as eluent to afford pure **18** as a white solid (145 mg, 0.27 mmol, 47%). **M.p.** 130-133°C; $[\alpha]_D$ -4.4 (*c* 0.05 in $CHCl_3$); **^{1}H-NMR (400 MHz, $CDCl_3$):** δ = 7.73 (d, 2H, *J* = 7.6 Hz, H_1), 7.57-7.24 (m, 13H, H_2, H_3, H_4, H_{10}, H_{12}, H_{15}, H_{16} and H_{17}), 6.12 (d, 1H, *J* = 6.4 Hz, H_7), 5.12 (s, 2H, H_{14}), 4.38 (d, 2H, *J* = 7.0 Hz, H_6), 4.33-4.26 (m, 1H, H_8), 4.16 (t, 1H, *J* = 7.0 Hz, H_5), 4.05-3.91 (m, 5H, H_9, H_{11} and H_{13}), 3.70-3.63 (m, 1H, $H_{9'}$), 2.04-1.93 (m, 1H,); **^{13}C-NMR (100 MHz, $CDCl_3$):** δ = 170.9, 170.1, 169.5, 158.0, 143.6, 141.3, 134.8, 128.6, 128.6, 128.3, 127.8, 127.1, 125.0, 120.0, 67.4, 67.2, 62.9, 56.3, 47.0, 43.0, 41.2; **LRFAB-MS:** *m/z* = 554 $[M+Na]^+$, **HRFAB-MS** : *m/z* = 554.19050 $[M+Na]^+$ (calc. for $C_{29}H_{29}N_3O_7Na$ 554.19035 $[M+H]^+$).

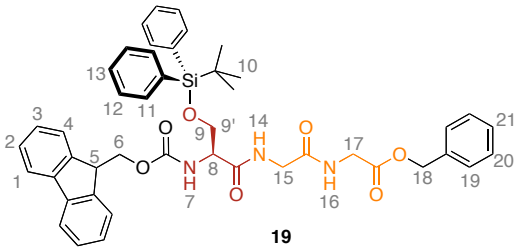

19

To a solution of **18** (1.89 g, 3.55 mmol, 1 equiv.) and imidazole (609 mg, 8.95 mmol, 2.5 equiv.) in dry DMF (5 mL) under nitrogen was added TBDPSCl (4.5 mL, 17.58 mmol, 5 equiv.) and the solution was stirred at room temperature for 24 hour. The solvent was evaporated under reduced pressure and the resulting yellow oil was purified by flash column chromatography on Silica gel with CH_2Cl_2-MeOH (98:2) as eluent to afford pure **19** as a white solid (2.06 g, 2.67 mmol, 73%); **M.p.** 153-156°C; **^{1}H-NMR (400 MHz, $CDCl_3$):** δ = 7.76 (d, 2H, *J* = 7.2 Hz, H_1), 7.64-7.23 (m, 21H, H_2, H_3, H_4, H_{11}, H_{12}, H_{13}, H_{19}, H_{20} and H_{21}), 7.05 (bt, 1H, H_{14} or H_{16}), 6.97 (bt, 1H, H_{14} or H_{16}), 5.63 (d, 1H, *J* = 6.0 Hz, H_7), 5.11 (s, 2H, H_{18}), 4.46-4.35 (m, 2H, Fmoc H_6), 4.31-4.25 (m, 1H, H_8), 4.19 (t, 1H, *J* = 6.8 Hz, H_5), 4.09-3.93 (m, 5H, H_9, H_{15} or H_{17}), 3.84 (dd, 1H, *J* = 5.2 Hz, *J* = 10.4 Hz, $H_{9'}$), 1.05 (s, 9H, H_{10}); **^{13}C-NMR (100 MHz, $CDCl_3$):** δ = 169.1, 169.0, 168.2, 157.9, 141.3, 135.5, 135.4, 134.8, 130.1, 128.6, 128.5, 128.4, 128.0, 127.8, 127.1, 125.1, 124.9, 120.0, 80.0, 68.0, 67.41, 67.2, 57.1, 56.1, 43.1, 41.2, 26.8; **LRFAB-MS:** *m/z* = 770 $[M+H]^+$, **HRFAB-MS** : *m/z* = 770.32591 $[M+H]^+$ (calc. for $C_{45}H_{48}N_3O_7Si$ 770.32616 $[M+H]^+$).

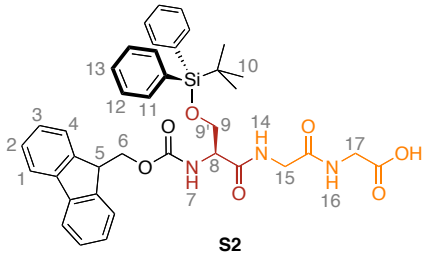

S2

A solution of **19** (2.34 g, 3.04 mmol, 1 equiv.) and palladium (10% wt) on carbon (345 mg) in AcOEt (80 mL) was purged with H_2 by means of three vacuum/H_2 cycles and the mixture stirred at room temperature for 4 hours. The solid was filtered off with Celite® and AcOEt was evaporated under reduced pressure to afford **S2** as a white solid. (2.06 g, 3.05 mmol, 100%); **M.p.** 80-83°C; **^{1}H-NMR (400 MHz, $CDCl_3$):** δ = 7.73 (d, 2H, *J* = 6.8 Hz, H_1), 7.58 (d, 2H, *J* = 6.8 Hz, H_2), 7.42-7.24 (m, 15H, H_3, H_4, H_{11}, H_{12}, H_{13} and H_{14} or H_{16}), 7.15 (bt, 1H, H_{14} or H_{16}), 5.71 (d, 1H, *J* = 6.4 Hz, H_7), 4.39-4.31 (m, 3H, H_6 and H_8), 4.19-4.11 (m, 2H, H_5 and H_9), 3.99 (bd, 2H, H_{15} or H_{17}), 3.93 (bd, 2H, H_{15} or H_{17}), 3.82 (dd, 1H, *J* = 4.8 Hz, *J* = 9.6 Hz, H_9), 1.02 (s, 9H, H_{10}); **^{13}C-NMR (100 MHz, $CDCl_3$):** δ = 172.0, 170.8, 169.5, 156.6, 143.7, 143.5, 141.2, 135.4, 134.8, 132.4, 130.0, 129.6, 127.9, 127.9, 127.8, 127.7, 127.1, 126.9, 125.1, 125.0, 120.0, 119.8, 80.1, 67.4, 63.8, 56.6, 46.9, 42.9, 41.2, 26.7; **LRFAB-MS:** *m/z* = 680 $[M+H]^+$, **HRFAB-MS** : *m/z* = 680.27965 $[M+H]^+$ (calc. for $C_{38}H_{42}N_3O_7Si$ 680.27921 $[M+H]^+$).

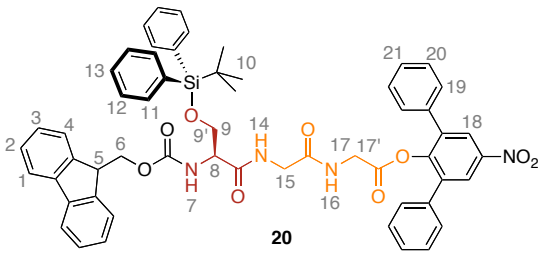

20

Using general method **A**, carboxylate **S2** (2.06 g, 3.04 mmol, 1.0 equiv.), DIPEA (530 µL, 3.04 mmol, 1.0 equiv.), 2-6 diphenyl-*p*-nitrophenol **5** (1.77 g, 6.08 mmol, 2.0 equiv.) and BOP (2.02 g, 4.56 mmol 1.5 equiv.) in $CHCl_3$ (60 mL) afforded crude material which was purified by flash column chromatography on silica gel with AcOEt/cyclohexane (1:2 to 1:1) as eluent to give **20** as a yellow solid (1.53 g, 1.61 mmol, 53%). **M.p.** 103-105°C; **^{1}H-NMR (400 MHz, $CDCl_3$):** δ = 8.24 (s, 2H, H_{18}), 7.76 (d, 2H, *J* = 7.6 Hz, H_1), 7.61-7.22 (m, 26H, H_2, H_3, H_4, H_{11}, H_{12}, H_{13}, H_{19},

H_{20} and H_{21}) 6.57 (bt, 1H, H_{14}), 6.44 (bt, 1H, H_{16}), 5.37 (d, 1H, *J* = 5.2 Hz, H_7), 4.38 (dd, 1H, *J* = 6.4 Hz, *J* = 10.4 Hz, H_6), 4.30 (dd, 1H, *J* = 6.4 Hz, *J* = 10.4 Hz, $H_{6'}$), 4.18-4.10 (m, 2H, H_5 and H_8), 4.00 (dd, 1H, *J* = *4.8* Hz, *J* = 10.8 Hz, H_9), 3.88 (dd, 1H, *J* = 5.2 Hz, *J* = 18.8 Hz, H_{17}), 3.82-3.73 (m, 3H, H_{14} and $H_{9'}$), 3.69 (dd, 1H, *J* = 4.8 Hz, *J* = 18.8 Hz, $H_{17'}$), 1.03 (s, 9H, H_{10}); **^{13}C NMR (100 MHz, $CDCl_3$):** δ = 171.1, 167.8, 166.9, 157.7, 149.2, 145.9, 143.6, 141.3, 137.4, 135.5, 135.4, 135.2, 130.1, 128.8, 128.8, 128.7, 128.0, 128.0, 127.9, 127.8, 127.1, 127.0, 125.0, 124.9, 124.8, 120.0, 80.7, 67.2, 63.3, 56.9, 47.0, 42.8, 40.8, 26.8; **FAB-HRMS:** *m/z* = 953.35770 $[M+H]^+$ (calc. for $C_{56}H_{53}N_4O_9Si$ 953.35818 $[M+H]^+$).

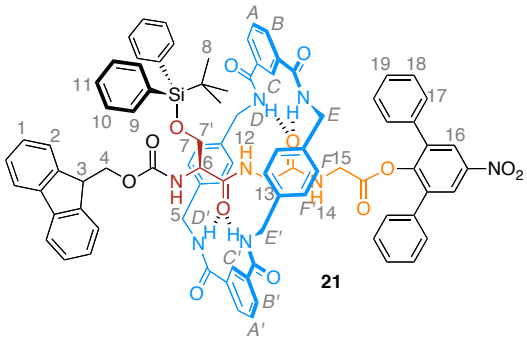

Using general method **B**, thread **20** (495 mg, 0.52 mmol, 1.0 equiv.), *p*-xylylenediamine (1.135 g, 8.35 mmol, 15 equiv.), isophthaloyl dichloride (1.69 g, 8.35 mmol, 15 equiv.), NEt_3 (2.32 mL, 16.68 mmol, 30.0 equiv.) in $CHCl_3$ (90 mL) afforded crude material which was purified by flash column chromatography on silica gel with cyclohexane-EtOAc (1:1) and $CHCl_3$/MeOH (98:2) as eluent to give **21** as a light yellow solid (108 mg, 0.073 mmol, 14%); **M.p.** 144°C; $[\alpha]_D$ -29.1 (*c* 0.01 in $CHCl_3$); **^{1}H NMR (400 MHz, $CDCl_3$):** δ = 8.23 (s, 2H, H_2, H_{16}), 8.07 (s, 2H, H_C and $H_{C'}$), 8.03 (d, 2H, *J* = H_B), 7.96 (d, 2H, *J* = 7.8 Hz, $H_{B'}$), 7.77-7.60 (m, 2H, H_A and $H_{A'}$), 7.60-7.17 (m, 33H, H_1, H_2, H_9, H_{10}, H_{11}, H_{12}, H_{17}, H_{18}, H_{19}, H_D and $H_{D'}$), 6.94 (m, 4H, H_F and $H_{F'}$), 6.48 (bs, 1H, H_{14}), 5.22 (d, 1H, *J* =*6.0* Hz, H_5), 4.65 (dd, 2H, *J* = 6.0 Hz, *J* = 13.6 Hz, H_E), 4.33 (dd, 2H, *J* = 4.4 Hz, *J* = 14.2Hz, H_E), 4.24 (dd, 2H, *J* = 4.8 Hz, *J* = 14.2 Hz, $H_{E'}$), 4.12-4.02 (m, 4H, $H_{E'}$ and H_3), 3.93 (m, 2H, *J* = 6.8 Hz, H_4), 3.75 (m, 1H, H_6), 3.67-3.53 (m, 4H, H_{13} and H_{15}), 2.90 (bd, 1H, H_7), 2.36 (bd, 1H, $H_{7'}$), 0.99 (s, 9H, H_8); **^{13}C NMR (100 MHz, $CDCl_3$):** δ = 169.20, 168.12, 167.02, 166.86, 166.20, 158.1, 149.1, 146.1, 141.2, 137.4, 137.3, 137.1, 133.9, 132.4, 132.2, 131.3, 131.2, 130.9, 130.2, 129.2, 128.9, 128.8, 128.7, 128.6, 128.5, 128.0, 127.9, 127.8, 127.1, 127.0, 125.1, 125.0, 124.9, 120.0, 81.0, 67.6, 62.4,

52.4, 47.0, 44.3, 44.1, 42.7, 40.7, 26.7; **FAB-HRMS:** *m/z* = 1485.56038 $[M+H]^+$ (calc. for $C_{88}H_{81}N_8O_{13}Si$ 1485.56924 $[M+H]^+$).

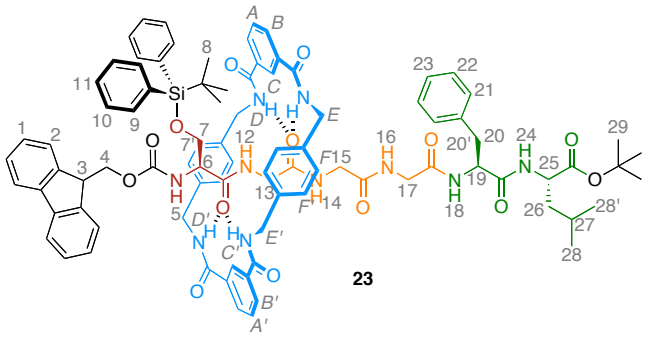

23

Using general method **C**, activated rotaxane **21** (69 mg, 46.7 µmol, 1.0 equiv.) and H-Phe-Leu-OtBu **22** (79 mg, 233 µmol, 5.0 equiv.) in $CHCl_3$ (5 mL) for 24 hours afforded crude material which was purified by flash column chromatography on silica gel with CH_2Cl_2-MeOH (98:2 to 10:90) as eluent to give **23** as a white foam (74 mg, 46.6 µmol, 98%); **^{1}H NMR (400 MHz, $CDCl_3$):** δ = 8.27 (s, 1H, H_C), 8.22 (s, 1H, $H_{C'}$), 8.02 (d, 2H, *J* = 7.8 Hz, H_B), 7.98 (d, 2H, *J* = 7.8 Hz, $H_{B'}$), 7.86 (bt, 2H, H_D), 7.79 (bt, 2H, $H_{D'}$), 7.74-7.15 (m, 29 H, H_1, H_2, H_9, H_{10}, H_{11}, H_{21}, H_{22}, H_{23}, H_{14}, H_{16}, H_{18}, H_{24} and H_A), 7.10 (s, 4H, H_F), 7.09 (s, 4H, $H_{F'}$), 6.56 (bs, 1H, H_{12}), 5.58 (d, 1H, *J* = 6.8 Hz, H_5), 4.62-4.43 (m, 5H, H_E and H_{19}), 4.38-4.21 (m, 7H, $H_{E'}$, H_4 and H_{25}) , 4.19-3.97 (m, 2H, H_6 and H_3), 3.80 (dd, 1H, *J* = 5.6 Hz, *J* = 10.2 Hz, H_7), 3.75 (dd, 1H, *J* = 5.2 Hz, *J* = 10.2 Hz, $H_{7'}$), 3.25 (dd, 1H, *J* = 4.8 Hz, *J* = 16.8 Hz, H_{13} or H_{15} or H_{17}), 3.17-3.05 (m, 2H, H_{13} or H_{15} or H_{17}), 2.99 (dd, 1H, *J* = 4.0 Hz, *J* = 16.8 Hz, H_{13} or H_{15} or H_{17}), 2.95-2.89 (m, 2H, H_{20} and H_{13} or H_{15} or H_{17}), 2.84 (dd, 1H, *J* = 7.6 Hz, J = 13.6 Hz, $H_{20'}$), 2.60 (dd, 1H, *J* = 4.4 Hz, *J* = 17.2 Hz, H_{13} or H_{15} or H_{17}), 1.50-1.33 (m, 12H, H_{26}, H_{27} and H_{29}) , 1.00 (s, 9H, H_8), 0.81 (d, 3H, *J* = 5.8 Hz, H_{28}), 0.78(d, 3H, *J* = 5.8 Hz, $H_{28'}$); **^{13}C NMR (100 MHz, $CDCl_3$):** δ = 171.5, 170.5, 170.3, 170.1, 169.2, 168.2, 167.3, 167.2, 143.6, 141.2, 137.3, 136.3, 136.1, 135.4, 134.4, 134.2, 132.5, 132.4, 131.1, 131.0, 130.1, 129.3, 129.2, 129.0, 128.9, 128.8, 128.7, 128.6, 128.2, 127.9, 127.8, 127.1, 127.1, 125.7, 125.4, 125.0, 120.0, 82.1, 82.0, 67.3, 63.2, 56.4, 54.8, 51.7, 46.9, 44.4, 44.2, 42.7, 42.2, 41.8, 41.3, 38.4, 28.0, 26.7, 24.8, 22.5; **FAB-HRMS:** *m/z* = 1585.73695 $[M+H]^+$ (calc. for $C_{91}H_{101}N_{10}O_{14}Si$ 1585.72680 $[M+H]^+$).

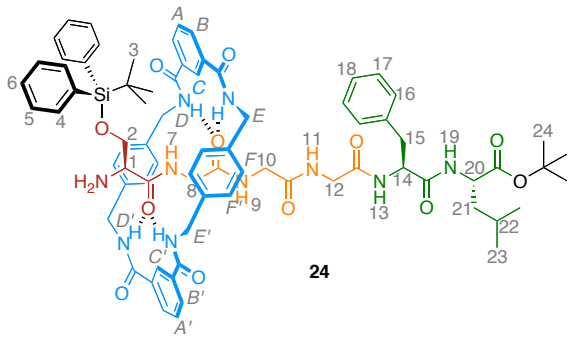

24

Rotaxane **23** (74 mg, 46.5 µmol, 1 equiv.) was dissolved in 2 mL piperidine/$CHCl_3$ (1:3) and was stirred at room temperature for 2 hours. The solvent was removed under reduced pressure and the crude material was purified by flash column chromatography on silica gel with $CHCl_3$-MeOH (96:4) as eluent to give **24** as a white foam (50 mg, 36.6 µmol, 78%); **^{1}H NMR (400 MHz, $CDCl_3$):** δ = 8.30 (s, 2H, H_C and $H_{C'}$), 8.10(d, 2H, *J* = 8.6 Hz, H_B), 8.07 (d, 2H, *J* = 8.6 Hz, $H_{B'}$), 7.69-7.57 (m, 4H, H_D and $H_{D'}$), 7.56-7.13 (m, 19 H, H_4, H_5, H_6, H_7, H_9, H_{16}, H_{17}, H_{18}, and H_A), 7.09 (s, 8H, H_F and $H_{F'}$), 6.92 (d, 1H, *J* = 7.2 Hz, H_{11} or H_{13} or H_{19}), 6.85 (bt, 1H, H_{11} or H_{13} or H_{19}), 6.46 (d, 1H, *J* = 7.6 Hz, H_{11} or H_{13} or H_{19}), 4.60-4.42 (m, 5H, H_E and H_{14}), 4.41-4.25 (m, 5H, H_E and H_{20}), 3.72-3.63 (m, 1H, H_1), 3.47-3.37 (m, 2H, H_8 or H_{10} or H_{12}), 3.36-3.24 (m, 3H, H_{15}, H_{21} and H_8 or H_{10} or H_{12}), 3.11 (dd, 1H, *J* = 3.2 Hz, *J* = 16.4 Hz, H_{14}), 3.06-2.98 (m, 2H, H_2 and H_8 or H_{10} or H_{12}), 2.97-2.84 (m, 2H, H_8 or H_{10} or H_{12}), 1.86-1.65 (m, 2H, NH_2), 1.58-1.46 (m, 1H, H_{22}), 1.45-1.33 (m, 11H, H_{21} and H_{24}), 1.00 (s, 9H, H_3), 0.85 (m, 6H, H_{23}); **^{13}C NMR (100 MHz, $CDCl_3$):** δ = 172.0, 171.6, 170.3, 170.2, 169.9, 168.8, 167.9, 166.8, 137.4, 137.4, 136.2, 136.1, 135.4, 135.4, 133.9, 132.8, 131.4, 131.3, 130.1, 130.0, 129.3, 129.1, 129.0, 128.6, 128.5, 127.8, 127.1, 127.0, 124.6, 124.5, 82.1, 82.0, 65.6, 56.4, 54.5, 51.7, 44.1, 42.5, 42.4, 41.4, 41.2, 38.8, 38.6, 28.0, 26.8, 24.8, 22.5, 22.1; **FAB-HRMS:** *m/z* = 1363.65512 $[M+H]^+$ (calc. for $C_{76}H_{91}N_{10}O_{12}Si$ 1363.65872 $[M+H]^+$).

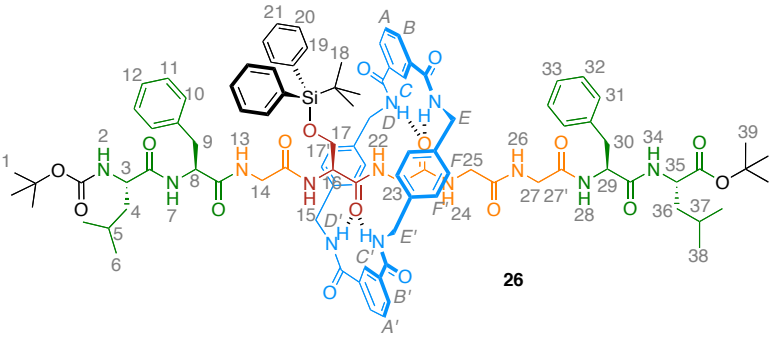

26

To a solution of rotaxane **24** (49 mg, 36.0 µmol, 1 equiv.), Boc-Leu-Phe-Gly-OK **25** (35 mg, 72.1 µmol, 2 equiv.) and NEt_3 (11 µL, 79.2 µmol, 2.2 equiv.) in $CHCl_3$ (10 mL), was added BOP (17 mg, 38 µmol, 1 equiv.) and the reaction mixture was stirred overnight at room temperature. The solvent was removed under reduced pressure and the crude material was purified by flash column chromatography on silica gel with CH_3Cl-MeOH (98:2 to 86:14) as eluent to give **26** as a white foam (54 mg, 84%); $[\alpha]_D$ -89.1 (*c* 0.009 in $CHCl_3$); **^{1}H NMR (400 MHz, $CDCl_3$):** δ = 8.30 (s, 2H, H_C and $H_{C'}$), 8.06 (d, 4H, J = 7.2 Hz, H_B and $H_{B'}$), 7.90 (bt, 2H, H_D), 7.85 (bt, 2H, $H_{D'}$), 7.60-7.00 (m, 32H, H_{10}, H_{11}, H_{12}, H_{19}, H_{20}, H_{21}, H_{31}, H_{32}, H_{33}, H_F, $H_{F'}$, H_A, and $H_{A'}$), 6.90 (bt, 1H, H_{15} or H_{22} or H_{24} or H_{26} or H_{28}), 6.79 (d, 1H, J = 7.2 Hz, H_{15} or H_{22} or H_{24} or H_{26} or H_{28}), 6.63 (bd, 1H, H_{15} or H_{22} or H_{24} or H_{26} or H_{28}), 6.54 (bs, 1H, H_{15} or H_{22} or H_{24} or H_{26} or H_{28}), 6.47 (bs, 1H, H_{15} or H_{22} or H_{24} or H_{26} or H_{28}), 6.13 (d, 1H, J = 6.8 Hz, H_2), 5.92 (d, 1H, J = 8.0 Hz, H_{13}), 4.92 (bd, 1H, H_{34}) 4.76-4.54 (m, 4H, H_E), 4.50-4.43 (m, 1H, H_8), 4.39-4.14 (m, 8H, $H_{E'}$, H_{29}, H_{35}, $H_{14'}$, and $H_{16'}$), 3.93-3.86 (m, 1H, H_3), 3.83-3.78 (m, 1H, H_{14}), 3.74-3.62 (m, 1H, $H_{27'}$), 3.51-3.14 (m, 2H, H_{25}), 3.25 (dd, 1H, J = 6.8 Hz, J = 17.2 Hz, H_{23}), 3.20-3.14 (m, 1H, $H_{23'}$), 3.10-2.96 (m, 3H, H_9, $H_{17'}$ and H_{27}), 2.89-2.76 (m, 3H, $H_{9'}$,H_{17} and H_{30}), 2.65-2.62 (m, 1H, H_9), 1.57-1.47 (m, 1H, H_{37}), 1.43-1.32 (m, 22H, H_1, H_4, H_{36}, and $H_{3\ 9}$), 1.00 (s, 9H, H_{18}), 0.86-0.75 (m, 6H, H_{38}); **^{13}C NMR (100 MHz, $CDCl_3$):** δ = 173.2, 172.5, 171.7, 171.4, 170.7, 170.4, 170.1, 169.6, 167.8, 167.3, 167.1, 157.4, 137.3, 137.2, 136.1, 136.0, 135.5, 134.4, 134.1, 132.8, 132.6, 131.2, 131.0, 129.9, 129.3, 129.2, 129.0, 128.9, 128.8, 128.6, 127.8, 127.3, 127.3, 127.1, 127.0, 125.6, 81.9, 81.2, 81.0, 55.1, 54.8, 54.6, 54.4, 51.8, 51.6, 44.6, 44.4, 43.9, 42.7, 42.2, 41.3, 41.0, 40.3, 38.7, 36.7, 28.2, 28.0, 26.8, 24.8, 22.8, 22.5, 22.0, 21.9, 21.6; **FAB-HRMS:** *m/z* = 1781.88738 $[M+H]^+$ (calc. for $C_{98}H_{122}N_{13}O_{17}Si$ 1781.88845 $[M+H]^+$).

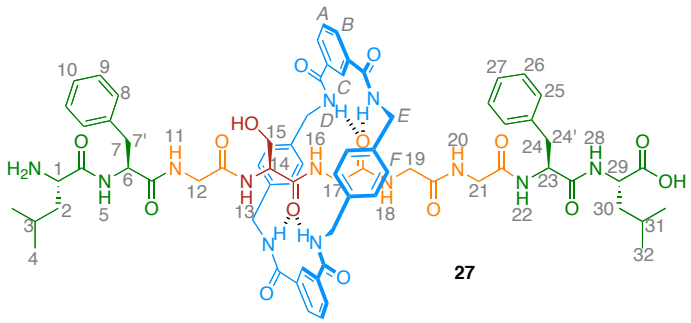

27

Rotaxane **26** (0.019 g, 0.010 mmol) was dissolved in a H_2O:TFA (1:9) solution (5 mL). The reaction mixture was stirred overnight at room temperature and then concentrated under reduced pressure. A solution of Et_2O:$CHCl_3$ (3:1) was added (5mL), the solid was sonicated for 10 min, filtered and washed with Et_2O:$CHCl_3$ (3:1) (3 × 5 mL) to give **27** as a white solid (0.014 g, 89%); **^{1}H NMR (400 MHz, MeOD-*d*$_4$):** δ = 8.40 (s, 2H, H_C), 8.05 (m, 4H, H_B), 7.61 (t, 2H, *J* = 7.5 Hz, H_A), 7.41-7.18 (m, 10H, H_8, H_9, H_{10}, H_{19}, H_{25}, H_{26} and H_{27}), 7.16 (s, 8H, H_F), 4.59-4.49 (m, 2H, H_6 and H_{23}), 4.47-4.39 (bs, 8H, H_E), 4.37-4.35 (m, 1H, H_1), 4.22 (t, 1H, *J* = 5.6 Hz, H_{14}), 3.91 (dd, 1H, *J* = 6.9 Hz, *J* = 9.0 Hz, H_{29}), 3.60 (dd, 1H, *J* = 5.6 Hz, *J* = 11.3 Hz, H_{15}), 3.57 (dd, 1H, *J* = 5.5 Hz, *J* = 11.2 Hz, $H_{15'}$). 3.56-3.20 (m, 8H, H_{17}, H_{19} and H_{21}), 3.09-2.94 (t, 1H, *J* = 6.0 Hz, H_7 and H_{24}), 2.86 (dd, 1H, *J* = 9.1 Hz, *J* = 14.0 Hz, $H_{7'}$ or $H_{24'}$), 2.86-2.67 (m, 2H, H_{12}), 2.67 (dd, 1H, *J* = 10.3 Hz, *J* = 14.0 Hz, $H_{7'}$ or $H_{24'}$), 1.67-1.41 (m, 6H, H_2, H_3, H_{30} and H_{31}), 0.86-0.77 (m, 12H, H_3, H_4, H_{31} and H_{32}); **^{13}C NMR (100 MHz, MeOD):** δ = 175.6, 173.8, 173.5, 172.6, 172.2, 171.6, 171.1, 170.4, 170.2, 169.3, 169.1, 138.6, 138.6, 138.4, 138.2, 135.6, 135.6, 131.8, 131.7, 130.4, 130.3, 130.2, 130.1, 129.9, 129.6, 129.5, 128.9, 128.6, 128.0, 128.0, 127.9, 62.8, 56.8, 56.1, 56.0, 52.7, 52.2, 45.4, 45.3, 45.3, 43.4, 43.2, 42.4, 41.6, 41.4, 39.2, 38,1, 26.7, 25.9, 25.2, 23.3, 21.9, 21.5; **FAB-HRMS:** *m/z* = 1386.65029 $[M+H]^+$ (calc. for $C_{73}H_{88}N_{13}O_{15}$ 1386.65229 $[M+H]^+$).

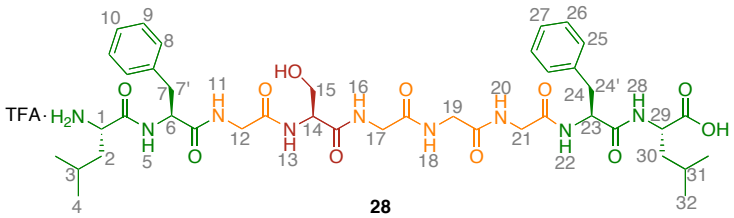

28

The peptide sequence (LFGSGGGFL) was assembled on Fmoc-Leu-Wang resin (0.62 mmol/g) *via* the Fmoc solid-phase peptide synthesis strategy on a 433A Applied Biosciences automated peptide synthesizer using Fmoc/tBu strategy, with HBTU/HOBt as coupling reagents, DIPEA as a base and NMP as the reaction solvent. The coupling sequence was carried out on a 0.1 mmol scale with the "Fastmoc" program supplied by the manufacturer, consisting in a single coupling followed by capping with an acetic anhydride solution then a deprotection with 20% piperidine in NMP. 10-Fold excess was used for protected amino acids and coupling reagents and 20-fold excess for DIPEA. Serine was introduced as its t-butyl ether Fmoc-Ser(tBu)-OH.

Peptidylresin was washed with CH_2Cl_2 and treated with TFA/H_2O/PhOH/iPr_3SiH (88.5:5:5:2.5) for 2h. The crude product was then precipitated by slow addition of the supernatant into ice-cold Et_2O and washed twice with the same solvent to afford **28** as a white solid. $[\alpha]_D$ -41.8 (*c* 0.02 in MeOH); **^{1}H NMR (400 MHz, MeOD-*d*$_4$):** δ = 7.38-7.11 (m, 10H, H_8, H_9, H_{10}, H_{19}, H_{25}, H_{26} and H_{27}), 4.68 (dd, 2H, 1H, *J* = 4.6 Hz, *J* = 9.4 Hz, H_6 or H_{23}), 4.68 (dd, 2H, 1H, *J* = 6.1 Hz, *J* = 9.2 Hz, H_6 or H_{23}), 4.47-4.38 (m, 2H, H_{14} and H_1 or H_{29}), 4.09-4.66 (m, 1H, H_{12}, H_{15}, H_{17}, H_{19}, H_{21} and H_1 or H_{29}), 3.21 (t, 1H, *J* = 6.0 Hz, H_7 or H_{24}), 3.18 (t, 1H, *J* = 6.2 Hz, H_7 or H_{24}), 3.04 (dd, 1H, *J* = 9.2 Hz, *J* = 13.9 Hz, $H_{7'}$ or $H_{24'}$), 2.92 (dd, 1H, *J* = 9.4 Hz, *J* = 14.0 Hz, $H_{7'}$ or $H_{24'}$), 1.57-1.55 (m, 6H, H_2, H_3, H_{30} and H_{31}), 1.02-0.86 (m, 12H, H_3, H_4, H_{31} and H_{32}); **^{13}C NMR (100 MHz, MeOD):** δ = 173.7, 173.5, 172.4 (2×), 172.2 (2×), 172.0 (2×), 171.4, 138.4, 138.3, 130.4, 130.3, 129.6, 129.5, 129.5, 128.0, 127.8, 62.7 (2×), 57.3, 57.1, 56.0, 52.8, 52.4, 43.9, 43.6, 43.3, 41.6, 38.8, 37.8, 26.0, 25.3, 23.4, 23.3, 21.9, 21.6; **ESI-HRMS:** *m/z* = 854.4411 $[M+H]^+$ (calc. for C_{41} H_{60} O_{11} N_9 854.4407 $[M+H]^+$).

4.5 References and notes

[1] *Peptide-Based Drug Design: Controlling Transport and Metabolism*; M. D. Taylor, G. L. Amidon, Eds., American Chemical Society: Washington DC, **1995**.

[2] R. Krishnamoorthy, A. Mitra, *Peptide-Based Drug Design: Controlling Transport and Metabolism* (M. D. Taylor, G. L. Amidon, Eds.), American Chemical Society: Washington DC, **1995**, p 63-65; J. Moss, *Peptide-Based Drug Design: Controlling Transport and Metabolism* (M. D. Taylor, G. L. Amidon, Eds.), American Chemical Society: Washington DC, **1995**, p 423-448; J. J. Nestor Jr., *Peptide-Based Drug Design: Controlling Transport and Metabolism* (M. D. Taylor, G. L. Amidon, Eds.), American Chemical Society: Washington DC, **1995**, p 449-471; T. K. Sawyer, *Peptide-Based Drug Design: Controlling Transport and Metabolism* (M. D. Taylor, G. L. Amidon, Eds.), American Chemical Society: Washington DC, **1995**, p 387-422.

[3] C. A. Hunter, *J. Am. Chem. Soc.,* **1992**, *114*, 5303-5311; F. Vogtle, S. Meier, R. Hoss, *Angew. Chem., Int. Ed.,* **1992**, *31*, 1619-1622.

[4] A. G. Johnston, D. A. Leigh, L. Nezhat, J. P. Smart, M. D. Deegan, *Angew. Chem. Int. Ed. Engl.,* **1995**, *34*, 1212-16; A. G. Johnston, D. A. Leigh, R. J. Pritchard, M. D. Deegan, *Angew. Chem. Int. Ed.,* **1995**, *34*, 1209-12.

[5] A. G. Johnston, D. A. Leigh, A. Murphy, J. P. Smart, M. D. Deegan, *J. Am. Chem. Soc.,* **1996**, *118*, 10662-10663; A. M. Brouwer, C. Frochot, F. G. Gatti, D. A. Leigh, L. Mottier, F. Paolucci, S. Roffia, G. W. H. Wurpel, *Science,* **2001**, *291*, 2124-2128; F. G. Gatti, D. A. Leigh, S. A. Nepogodiev, A. M. Z. Slawin, S. J. Teat, J. K. Y. Wong, *J. Am. Chem. Soc.,* **2001**, *123*, 5983-5989; E. Arunkumar, C. C. Forbes, B. C. Noll, B. D. Smith, *J. Am. Chem. Soc.,* **2005**, *127*, 3288-3289.

[6] D. A. Leigh, A. Murphy, J. P. Smart, A. M. Z. Slawin, *Angew. Chem., Int. Ed. ,* **1997**, *36*, 728-732.

[7] V. Bermudez, N. Capron, T. Gase, F. G. Gatti, F. Kajzar, D. A. Leigh, F. Zerbetto, S. Zhang, *Nature,* **2000**, *406*, 608-611.

[8] S. Van Meurs, *Phd thesis*, University of Warwick, 2001.

[9] S. J. Rowan, S. J. Cantrill, J. F. Stoddart, A. J. P. White, D. J. Williams, *Org. Lett.,* **2000**, *2*, 759-762; S. J. Rowan, J. F. Stoddart, *J. Am. Chem. Soc,* **2000**, *122*, 164-165.

[10] D. W. Zehnder, D. B. Smithrud, *Org. Lett,* **2001**, *3*, 2485-2487.

[11] N. Sewald, H.-D. Jakubke, *Peptides: Chemistry and Biology*; Wiley-VCH: Weinheim, 2002.

[12] F. D. Erich Wünsch, *Chem. Ber.,* **1966**, *99*, 110-120; F. Weygand, D. Hoffmann, E. Wunsch, *Z. Naturforsch. ,* **1966**, *B 21*, 426-&.

[13] I. Koppel, J. Koppel, I. Leito, V. Pihl, L. Grehn, U. Ragnarsson, *J. Chem. Res.,* **1993**, 446.

[14] I. E. Pop, B. P. Deprez, A. L. Tartar, *J. Org. Chem.,* **1997**, *62*, 2594-2603.

[15] J. S. Hannam, S. M. Lacy, D. A. Leigh, C. G. Saiz, A. M. Z. Slawin, S. G. Stitchell, *Angew. Chem., Int. Ed.,* **2004**, *43*, 3260-3264.

[16] It is assumed that the active ester in question will be modified with bulky groups in order to avoid slippage of the macrocyle.

[17] M. Bodanszky, *Nature,* **1955**, *175*, 685-685; M. Bodanszky, V. Du Vigneaud, *Nature,* **1959**, *183*, 1324-1325; M. Bodanszky, K. W. Funk, *J. Org. Chem.,* **1973**, *38*, 1296.

[18] E. Valeur, M. Bradley, *Chem. Soc. Rev.,* **2009**, *38*, 606-631.

[19] ONp active esters were in fact one of the first active esters to be investigated for the coupling of peptides (ref [17]). They proved efficient in both solution and solid phase synthesis in conjunction with carbodiimide reagents, but are nowadays rarely used. Noteworthy, the ONp group has been recently incorporated in phosphonium-type reagents (ref [18]).

[20] S. Potok, *Phd thesis*, University of Edinburgh, **2004**.

[21] Although no decomposition was observed in this particular case, this measure was taken as a preventive measure to avoid potential cleavage of any base-labile protecting groups that would be present in the peptidic backbone (for example the Fmoc group in thread **20** (Scheme 4.9).

[22] The presence of macrocycle **1** in the crude mixture was also observed when great care was taken to remove any trace of residual water from the reaction.

[23] Formation of a byproduct arising from intramolecular cyclization, similar to the oxazolone hypothesized in Scheme 4.5, is observed in Smithrud's example. This compound was isolated in up to 61% yield in their case, see ref [10].

[24] C. A. G. N. Montalbetti, V. Falque, *Tetrahedron,* **2005**, *61*, 10827-10852.

[25] M. T. K. Clausen, S.-O. Lawesson, A. F. Spatola, *J. Chem. Soc., Perkin Trans. 1,* **1984**, 785 - 798.

[26] C. Froussios, M. Kolovos, *Synthesis,* **1987**, *1987*, 1106-1108.

[27] T. W. Greene, W. P. G. M., *Protective groups in organic synthesis* Third edition ed., John Wiley & sons, Inc.: New York, **1999**, p 114.

[28] K. W. Li, J. Wu, W. Xing, J. A. Simon, *J. Am. Chem. Soc.,* **1996**, *118*, 7237-7238; T. J. Greshock, D. M. Johns, Y. Noguchi, R. M. Williams, *Org. Lett.,* **2008**, *10*, 613-616.

[29] J. D. Warren, J. S. Miller, S. J. Keding, S. J. Danishefsky, *J. Am. Chem. Soc.,* **2004**, *126*, 6576-6578; G. Chen, J. D. Warren, J. Chen, B. Wu, Q. Wan, S. J. Danishefsky, **2006**, *128*, 7460-7462.

CHAPTER FIVE

Synthesis and in vitro assays of a Met-enkephalin rotaxane carrier for use in ADEPT anti-cancer therapy

Published in Angewandte Chemie as "*Rotaxane-Based Propeptides: Protection and Enzymatic Release of a Bioactive Pentapeptide*":
Anthony Fernandes, Aurélien Viterisi, Frédéric Coutrot, Stéphanie Potok, David A. Leigh, Vincent Aucagne and Sébastien Papot, **2009**, 48, 6443-6447.

Acknowledgments

The work described in this chapter was shared equally between the author and Dr. Anthony Fernandes, whose contribution is gratefully acknowledged. The synthesis of propeptide **27** and rotaxane propeptide **2** was entirely carried out by Dr. Anthony Fernandes. Preparative HPLC purifications of the final compounds, β-galactosidase hydrolysis studies, proteolysis studies, solubility measurements and plasma stability assessments were carried out entirely by the author.

5 Synopsis

The rotaxanation of peptides has already shown great potential for protecting peptides against the action of endogenous peptidases. The ring component of the assembly induces remarkable changes in the peptides' properties. Solubility and lipophilicity can be greatly influenced by this encapsulation method. Importantly, it has been shown that the activity of the peptide in question is completely inhibited when encapsulated within a rotaxane structure. Although theses structures display optimal properties to act as peptide drug carriers, future functional devices able to carry and selectively release bioactive peptides are still a long way off.

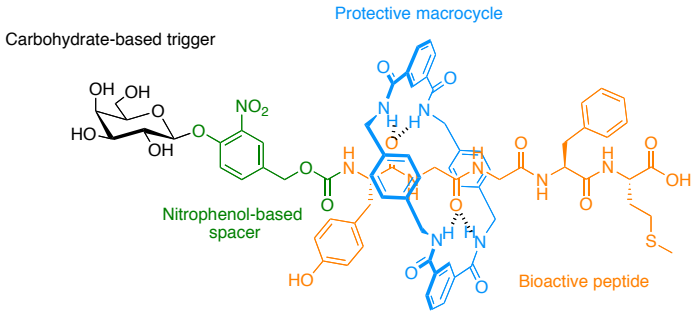

Herein we describe how, in collaboration with the group of Gesson, we combined his prodrug approach with the peptide rotaxanes of Leigh, to synthesize nanodevices capable of protecting, transporting and releasing an anti-cancer peptide. This device consists of an ADEPT (Antibody directed enzyme prodrug therapy) specific prodrug of Met-enkephalin (YGGFM), mechanically encapsulated into a Leigh type rotaxane assembly. The mechanism of release of the so-called rotaxane propeptide is dictated by the action of a specific β-galactosidase enzyme located around cancer cells (via Antibody-enzyme conjugates bound to cancer cells) whose action provokes hydrolysis and self-immolation of the stopper with immediate disassembly of the architecture.

The device has been successfully synthesized using the C-elongation methodology optimized in Chapter 2. β-Galactosidase triggered release has been studied in vivo, as well as resistance against endogenous peptidases. Finally its half-life in human plasma was measured.

5.1 Introduction and background

5.1.1 Opioids as anti-cancer agents

Opioid peptides, discovered in the mid-1970's, belong to a small family of peptides derived from three different precursor proteins. They are produced in the brain periphery and are involved in several physiological processes such as nociception, cognition, release of hormones and neurotransmission. However, a few decades ago, opioid peptides were also found in a wide variety of human and animal tumours in neural and nonneuronal tissues.[1,2] These studies suggested that opioid peptides are integral components of most tumour cells. Further studies showed that they are located in the cytoplasm of tumour cells suggesting that they are either produced or sequestered in malignant cells.[2] Met-enkephalin is one of these opioid peptides, whose sequence varies from Leu-enkephalin by only the last residue, and has been studied extensively regarding its anti-tumour properties. Zagon and co-workers have identified it as a negative cell growth regulator and termed it OGF (opioid growth factor).[3] It has been demonstrated that cell proliferation is inhibited when a specific receptor located at the nucleus periphery is blocked. The proteomic nature of this receptor is distinctly different from classical opioid receptors and has been named OGF receptor (OGFr) by Zagon *et al*.[4] Cell replication is interrupted by OGF at the G_0-G_1 phase of the cell cycle and recent studies proved that OGF uses the p16 and p21 pathways to restrict cell proliferation.[5]

If these recent results showed the great potential of Met-enkephalin as an anti-tumour agent, the very few *in vivo* tests performed to date, with human tumours-implanted mice do not seem to follow the same trend as the *in vitro* experiments.[6] The stability of the peptide in biological fluids seems to be the main limiting factor,[7,8] along with cell penetration.[9] Several reports have shown conclusively that both Leu and Met-enkephalin have very short half-lives in both mouse and human plasma.[10] The group of Horvat has recently brought valuable evidence to light that suggests that cell penetration is also likely to be one of these limiting factors, by synthesizing a lipophilic analogue showing higher activity than OGF.[9]

In the hope of improving its pharmacokinetics, two examples of OGF prodrugs have already been reported. The first one proved to be resistant only to aminopeptidases

and was rapidly decomposed by endopeptidases in human plasma[11] while the second, despite having shown good stability in human plasma, has not found any applications to date (probably due to its non specific mode of release).[12]

5.1.2 Prodrugs and anti-cancer therapy

The prodrug strategy is particularly useful in anti-cancer therapy since it represents an efficient way to get around the lack of specificity exhibited by anti-tumour agents towards tumour cells. In order to minimize side effects, it is important to design anti-cancer prodrugs in such a way that the active drug is delivered and activated only at the tumour site. Additionally, chemical modification of the drug should be performed so as to decrease toxicity in its prodrug version to minimize side effects due to non-specific cell targeting.

In anti-cancer therapy using prodrugs, three main approaches are possible. In the simplest case the prodrug is selectively activated by endogenous enzymes in tumour tissues (tumour-activated prodrugs; TAP) (Scheme 5.1a).[13,14] To be efficient, this method requires that the level of the chosen enzyme is significantly higher in tumour tissues that in tumour-free tissues. Several enzymes fulfill this requirement to various extents, the most studied belong to three main classes: oxidoreductases, transferases and hydrolysases.

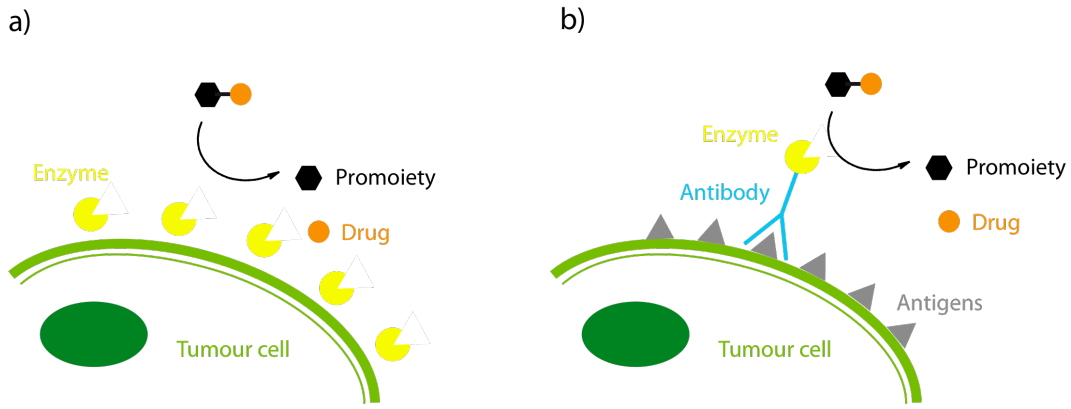

Scheme 5.1. Treatment of a tumour over the course of a) TAP, b) ADEPT

The second alternative to achieve local activation of prodrugs is the use of enzyme immunoconjugates. In this, strategy termed Antibody-Directed Enzyme Prodrug Therapy (ADEPT),[14,15] specific antigens expressed in tumour cells are used to target

enzymes to the tumour (Scheme 5.1b). A specific antibody-enzyme conjugate that binds exclusively to tumour cells is administered to the patient before treatment. After the excess of unbound conjugates has left the blood stream (several days) the prodrug is administered and selectively activated by the conjugate extracellularly. The main advantage of ADEPT is the potential to use prodrugs activated by non-human enzymes, which are introduced into the body *via* the Antibody-enzyme conjugate. The third strategy (originally designed to circumvent the immunogenic issues of ADEPT) utilizes targeted delivery of genetic material encoding for prodrug-activating enzymes to tumour cells. This approach can be divided into two subclasses termed Gene-directed Enzyme Prodrug Therapy (GDEPT) and Virus-directed Enzyme Prodrug Therapy (VDEPT).[14,16] In the former, the gene is delivered *via* non-viral vectors whereas in the latter method this task is accomplished by viral vectors. These two techniques have the advantage of avoiding the immunogenic side effects of ADEPT caused by the injection of animal-produced antibody-enzyme conjugates. In further contrast to ADEPT, drug activation is performed intracellularly and the prodrug must therefore penetrate the cell before activation.

5.1.3 Gesson's approach to anti-cancer prodrugs

Over the past few decades, the Gesson group have elaborated prodrugs of various known anti-cancer drugs that are selectively activated *via* ADEPT or PMT (Prodrug Mono Therapy). The latter method is of the TAP type and relies on abnormally high β-glucuronidase activity in the necrotic tissue of solid tumours.[17,18] Thus the Poitiers group, in collaboration with Hoechst-Marion-Roussel and the group of Monneret, have extensively investigated the β-glucuronidase-mediated release of anti-cancer drugs, under PMT.[18,19]

The mere functionalization of anti-cancer agents by glucuronic acid does not produce fast enough rates of cleavage *in vitro* to expect the dug to be released in sufficient amount around the tumour site *in vivo*.[20] Linking the glucuronic acid (called the "trigger") to the drug *via* a spacer group, which self-immolates once the β-glucosidic linkage is hydrolyzed, gives much faster rates of release (Scheme 5.2).[21] The glucuronide, now more distant from the anti-cancer drug, is better recognized by the

enzyme. Scheme 5.2 shows Gesson's most optimized system, which underwent phase-I clinical trials, along with its mechanism of drug release.[22]

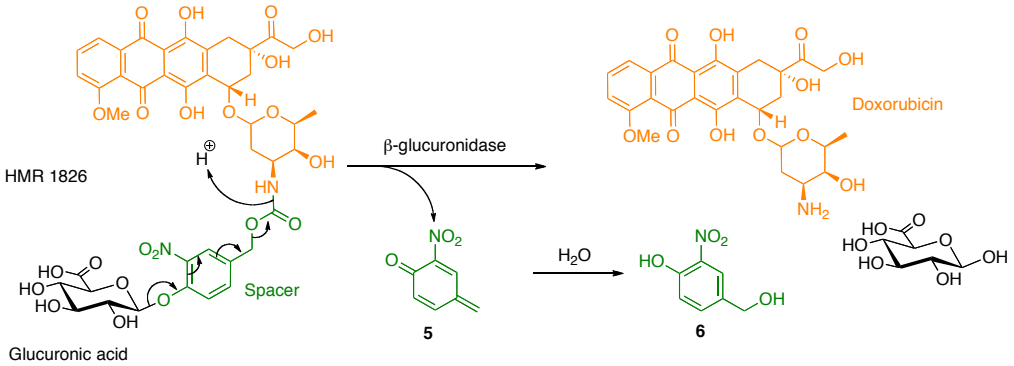

Scheme 5.2. Gesson's HMR 1826 prodrug of doxorubicin and its mechanism of release under PMT anti-cancer treatment.

Hydrolysis of the glucuronic bond forms the unstable phenolate ion, whose elimination, driven by the production of CO_2, produces a highly reactive quinone methide intermediate, **5**. The surrounding water quenches this intermediate very quickly, giving rise to the re-aromatized nitrophenol **6**.

5.1.4 The design of a Met-enkephalin rotaxane propeptide for ADEPT strategy

As a first step toward the realization of drug carriers, a few systems made from interlocked structures that disassemble in the presence of an enzymatic stimulus have already been described. Yui *et al*. first described rotaxane-based carriers where the stopper is made out of two consecutive amino acids.[23] Under a proteolytic enzymatic stimulus, the stopper is hydrolyzed, triggering the release of the constituents of the interlocked architecture. Anderson also utilized a proteolytic enzyme to cleave the stopper of a cyclodextrin-based rotaxane, although the design and the function of his system are fundamentally different from that of Yui.[24,25] In a more applied manner, Stoddart and Zink reported an enzyme-responsive molecular silica nanocontainer capable of carrying drugs.[26] Molecules trapped in the pores of silica nanoparticles by means of rotaxane-based stalks covalently bound to the nanoparticles, are released upon esterase-triggered disassembly of the rotaxane structure.

If these systems bring valuable information on how rotaxane-based drug carriers should operate, they are still elementary and the aspect of specificity is omitted in the design. Proteolytic enzymes and esterases as used by Yui and Stoddart, are by no means specific to only one substrate and since they are found in various places in the human body, cannot be used to target a precise location *in vivo*.

To achieve specificity, the target has to be well known and well studied, and thus in the present chapter we describe how (in collaboration with the group of Gesson, whose prodrugs have already been shown to be successful in phase-I clinical trials) we applied Leigh-type rotaxanes to the specific delivery of Met-enkephalin.

The previously described elongation method for the synthesis of peptidorotaxanes (Chapter 4) was used to build a Met-enkephalin rotaxane carrier, consisting of a Gesson-type prodrug of Met-enkephalin, topologically encapsulated within a rotaxane structure (termed a Rotaxane propeptide) (Figure 5.1).

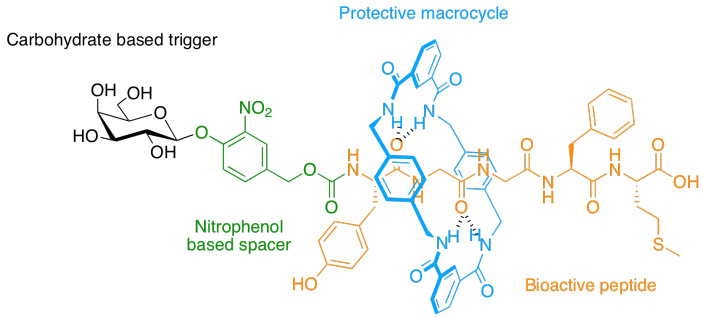

Figure 5.1. Chemical structure of a Met-enkephalin rotaxane propeptide

In the same way as the Boc-Leu-enkephalin rotaxane, the assembly was stoppered at the C-terminus by two consecutive Phe and Met residues. At the N-terminus though, 'stoppering' was ensured by the trigonal arrangement between the trigger-spacer unit and the adjacent Tyrosine residue. The operation of this nanodevice should be simple and only requires, in theory, a tumour treated under PMT or ADEPT. The β-glycosidic linkage is cleaved in the presence of the appropriate enzyme, allowing the decarboxylation driven elimination to occur. Once the spacer has undergone elimination, the whole assembly dissociates, releasing the active peptide (scheme 5.3).

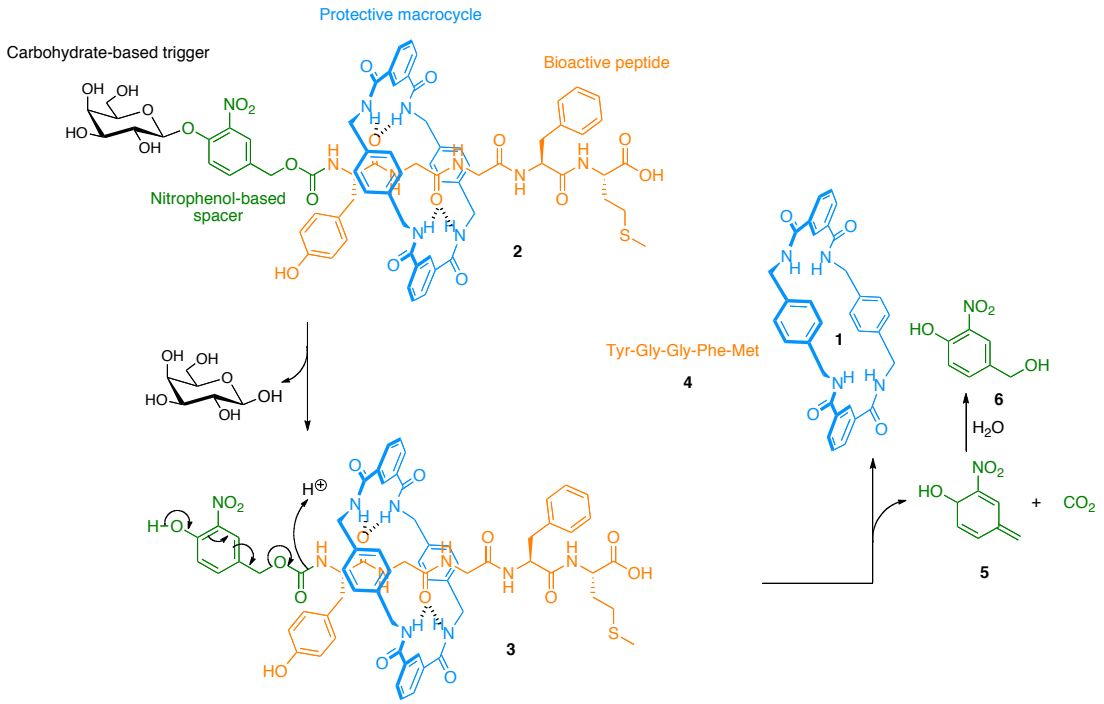

Scheme 5.3. Operation of Met-enkephalinephalin rotaxane propeptide.

5.2 Results and discussion

5.2.1 Design and synthesis

In order to maximize the chances of success we selected Gesson's most studied trigger-spacer combination (Scheme 5.2). We swapped the glucuronic acid trigger for a galactose-based trigger to avoid the tricky final deprotection of the acid group of the glucuronide.[27] This does not affect the system's applicability to anti-cancer treatment, as galactose is compatible with ADEPT. Given the similarity between Met-enkephalin and Leu-enkephalin, it was straightforward to adapt the synthesis of the Leu-enkephalin rotaxane to our device. The synthesis was carried out in a convergent manner, the key step being a C-elongation of the pre-activated rotaxane precursor.

The synthesis of the self-immolative moiety was carried out according to a know procedure (Scheme 5.4).[28]

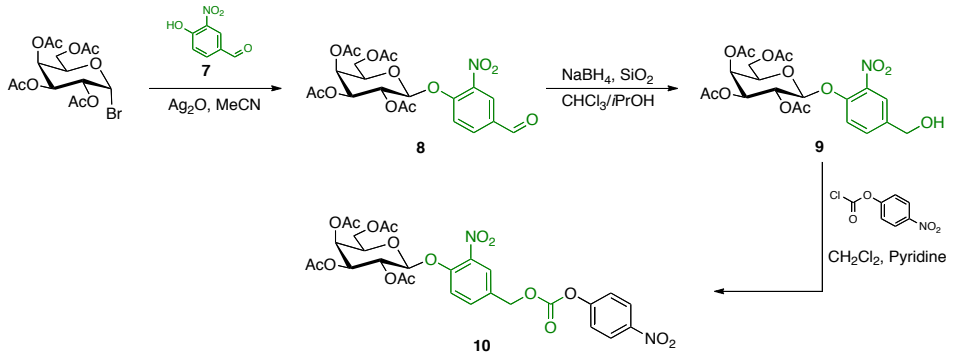

Scheme 5.4. Synthesis of the galactose-based trigger-spacer unit.

Commercial acetylated bromogalactose was coupled to commercially available aldehyde **7** under Konigs-Knorr conditions and subsequently reduced and activated. The activated trigger-spacer unit **10** was reacted with the three amino acid fragment **15** whose synthesis is depicted in Scheme 5.5.

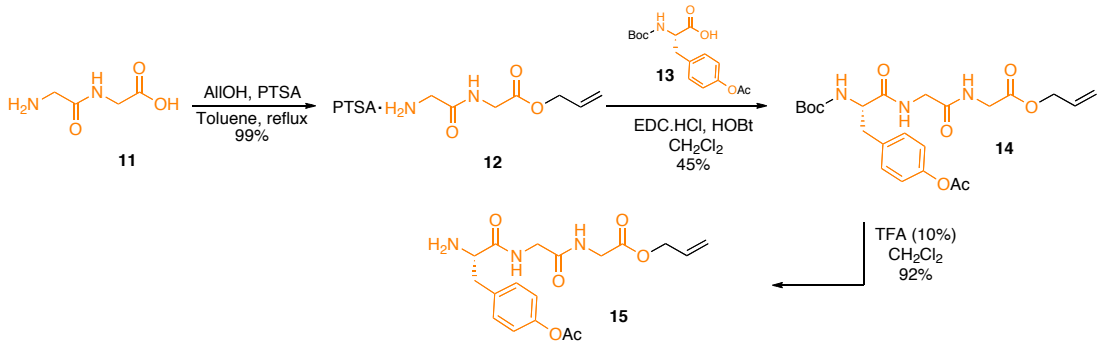

Scheme 5.5. Synthesis of the rotaxane-forming template fragment

This three amino acid moiety was synthesized from commercial fragments **11** and **13**, using common peptide coupling chemistry and a Boc protection scheme. The C-terminus of the peptidic fragment was protected with an allyl ester, orthogonal to the Boc and acetyl groups, whereas the phenol moiety of the tyrosine residue was protected with an acetyl group. Fragment **15** was obtained in good overall yield, and stirring it overnight in MeCN in the presence of **10** and pyridine afforded the trigger-spacer-peptide precursor **16** (Scheme 5.6).

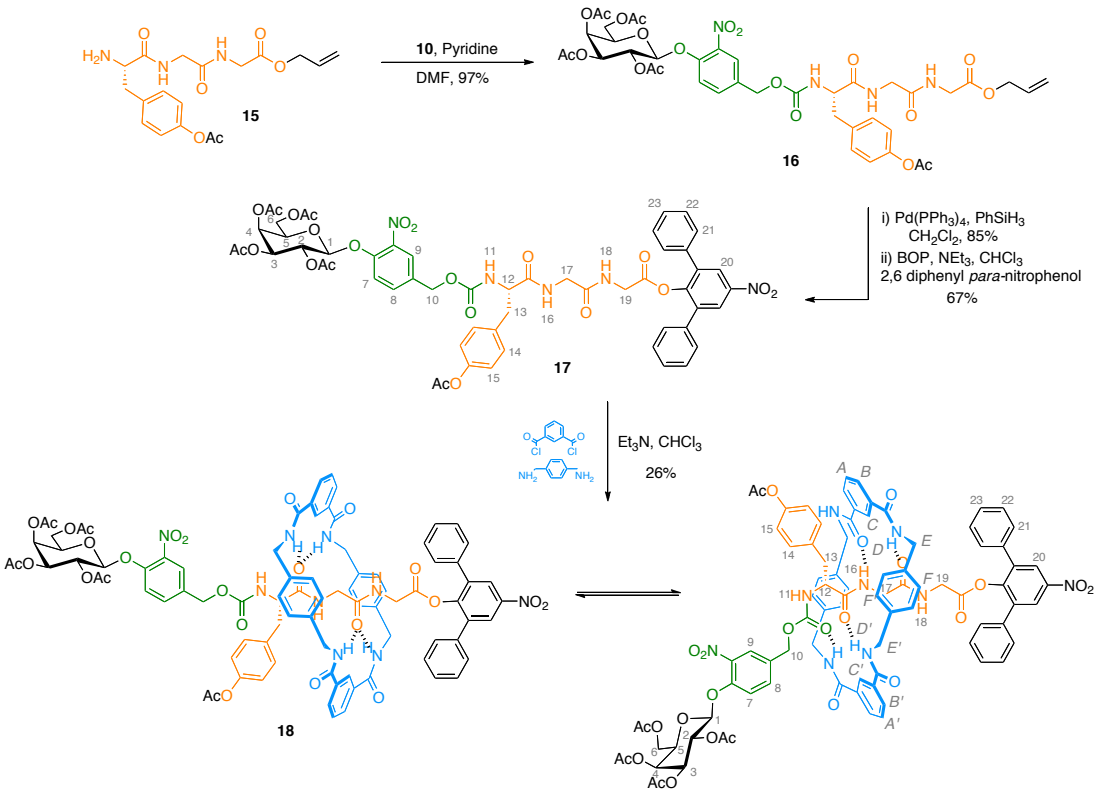

Scheme 5.6. Synthesis of activated rotaxane building block

Activation using BOP chemistry gave similar yields of **17** to those reported in the previous chapter.[25] Finally, the rotaxane forming-reaction (using the 'standard' 16 fold excess of macrocycle precursors) proceeded in slightly better yield (26%) than for the Leu-enkephalin analogue. This shows that the numerous acetyl groups and the nitro group in the molecule do not interfere with template recognition and are stable towards the excess of *para*-xylylenediamine. In fact the less bulky acetyl group on the tyrosine residue leads to higher yields of rotaxane than does the benzyl group previously used (chapter 4). Purification of rotaxane **18** from the starting thread was not possible *via* silica gel flash chromatography, but size exclusion chromatography proved to be a good alternative.

The ^{1}H NMR spectrum of rotaxane-activated ester **18** (Figure 5.2) shows the interlocked nature of the molecule unambiguously, with most resonances of the thread shifted upfield in the rotaxane. According to the chemical shifts of protons H_7, H_8 and H_9 of the spacer, the macrocycle has access to the part of the thread beyond the tyrosine residue, showing the importance of the orthogonal arrangement of the latter with respect to the spacer, in order to effectively stopper the assembly.

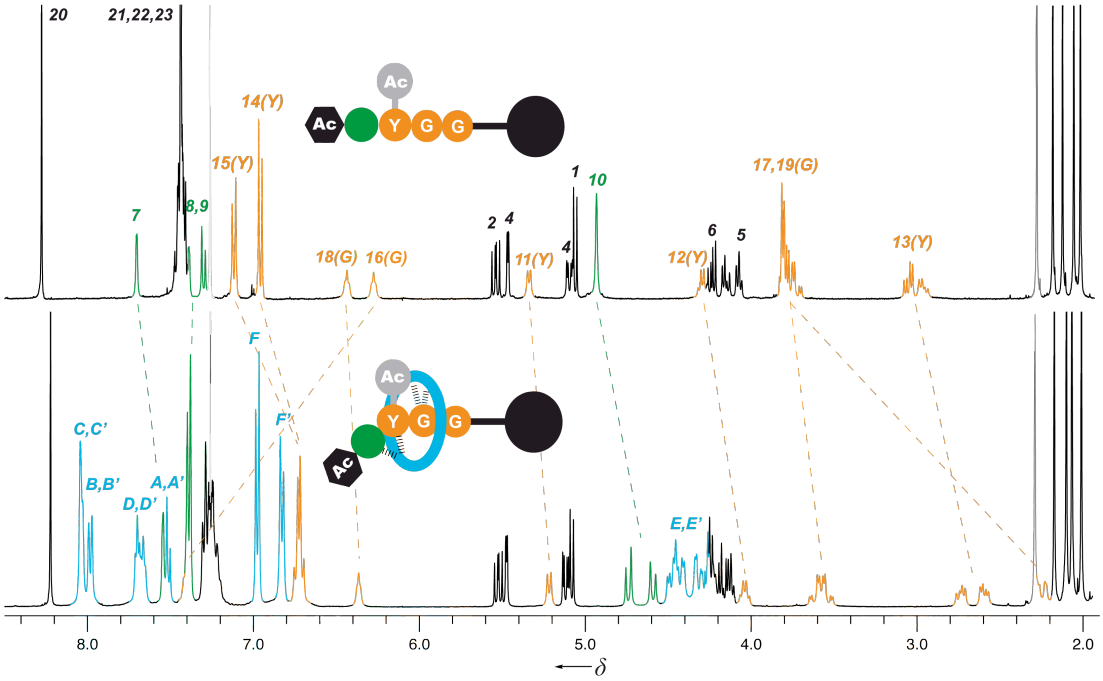

Figure 5.2. ^{1}H NMR spectra (400 MHz, $CDCl_3$, 300K) of a) thread **17**, b) Rotaxane propeptide activated building block **18**. The assignments and colouring of signals correspond to the lettering shown in scheme 5.6.

The downfield shift of the amide proton of the glycine residue (H_{16}) is indicative of a hydrogen bond to a carbonyl from the macrocycle, confirmed by the high multiplicity of the signal for H_E (due to the restricted motion of the ring in the NMR timesale) and by the large upfield shift of an signal from a glycine residue, supposedly H_{17}, indicating that the macrocycle spends most of its time over that residue. The molecule is then likely to adopt the conformation shown in scheme 5.6, which predominates on the NMR timescale.

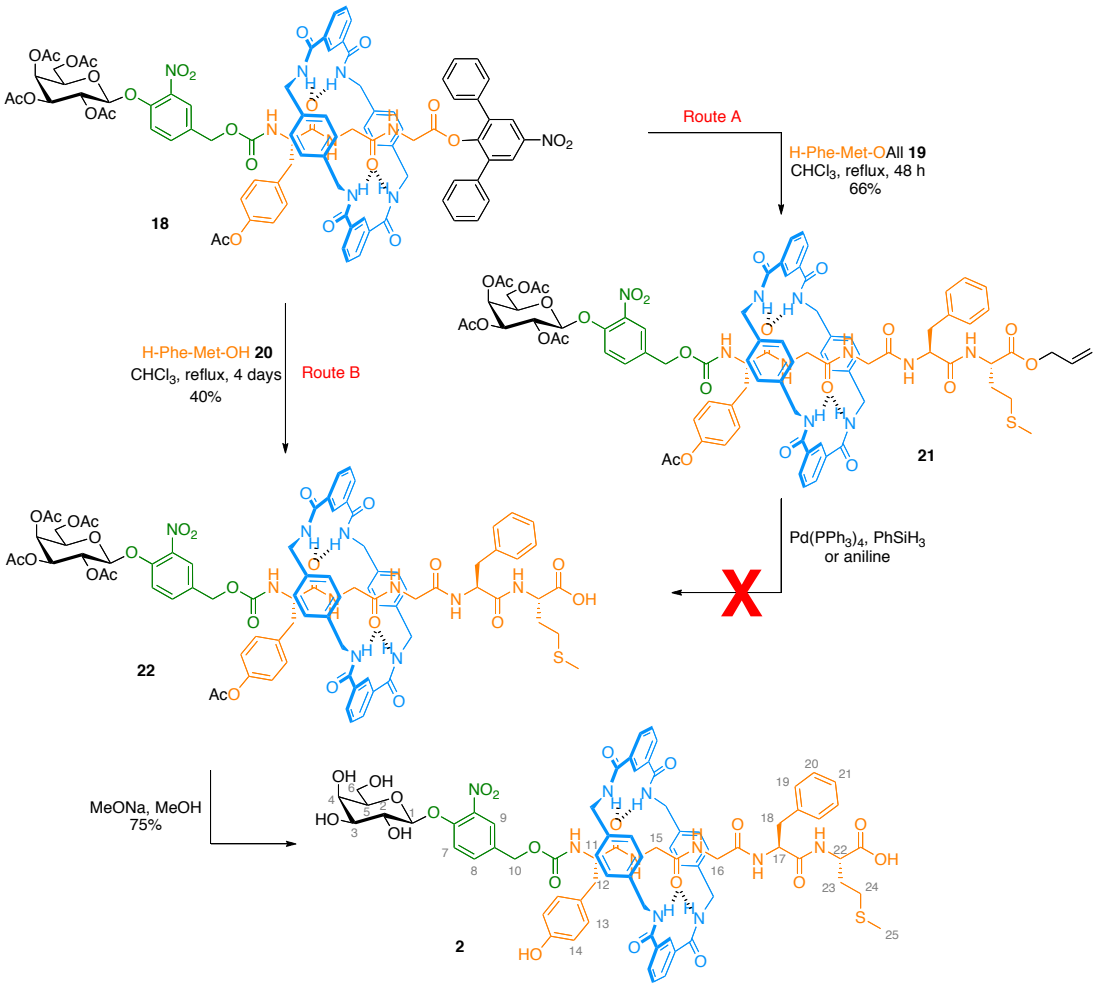

Scheme 5.7. C-elongation of rotaxane building block **16** by allyl-protected and non-protected Phe-Met fragments. Protecting group cleavage leads to the rotaxane propeptide.

C-elongation using the allyl-protected dipeptidic residue **19** was rather slow (using 5 equivalents of dipeptide), but reached an acceptable yield of 66% if left for an extended period of time (48 h) (Scheme 5.7, Route A). Surprisingly, cleavage of the C-terminal ally group of **21** could not be accomplished due to the gelation effect displayed by the molecule: when dissolved in CH_2Cl_2, THF, DMF or MeCN, **21** formed a thick gel preventing the cleavage reaction from occurring. Hence, elongation was performed using 5 equivalents of the non-protected Phe-Met residue **20** (Scheme 5.7, Route B), which displayed comparable kinetics to the allyl-protected analogue **19**. Elongated rotaxane **22** was isolated in 40% yield (59 % of unreacted **20** recovered from the reaction). The final cleavage of the acetyl groups afforded a quantitative amount of rotaxane propeptide **2**. Purification by preparative HPLC gave **2** in high purity (> 95%).

For the purposes of comparison, the non-rotaxane encapsulated propeptide was also synthesized, starting from building block **24**, obtained earlier from de-allylation of **16** (Scheme 5.6). The coupling step of the last two amino acid fragments proved to be troublesome, but was not optimized further as the final product could be isolated in sufficient quantity for enzymatic assays (Scheme 5.8).

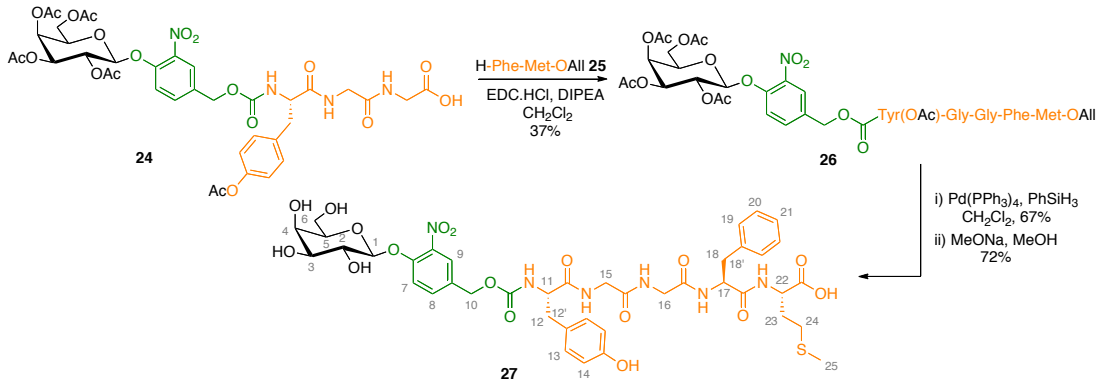

Scheme 5.8. Synthesis of free the propeptide (**27**)

The ^{1}H NMR spectra of both thread (**27**) and rotaxane (**2**) in CD_3OD are shown in Figure 5.3. Apart from the signals corresponding to the carbohydrate protons (shown in black), most of the resonances in the thread are shifted upfield in the rotaxane indicating that the macrocycle is able to (and does) move beyond the original template. Although the rotaxane Gly-Gly methylene protons H_{15} and H_{16} are the most shielded, indicating the macrocycle spends most of its time in this region, various peptide protons near the C-terminus (e.g. H_{24}) and protons in the nitrophenol spacer near the N-terminus are shielded to some extent by the aromatic rings of the macrocycle.

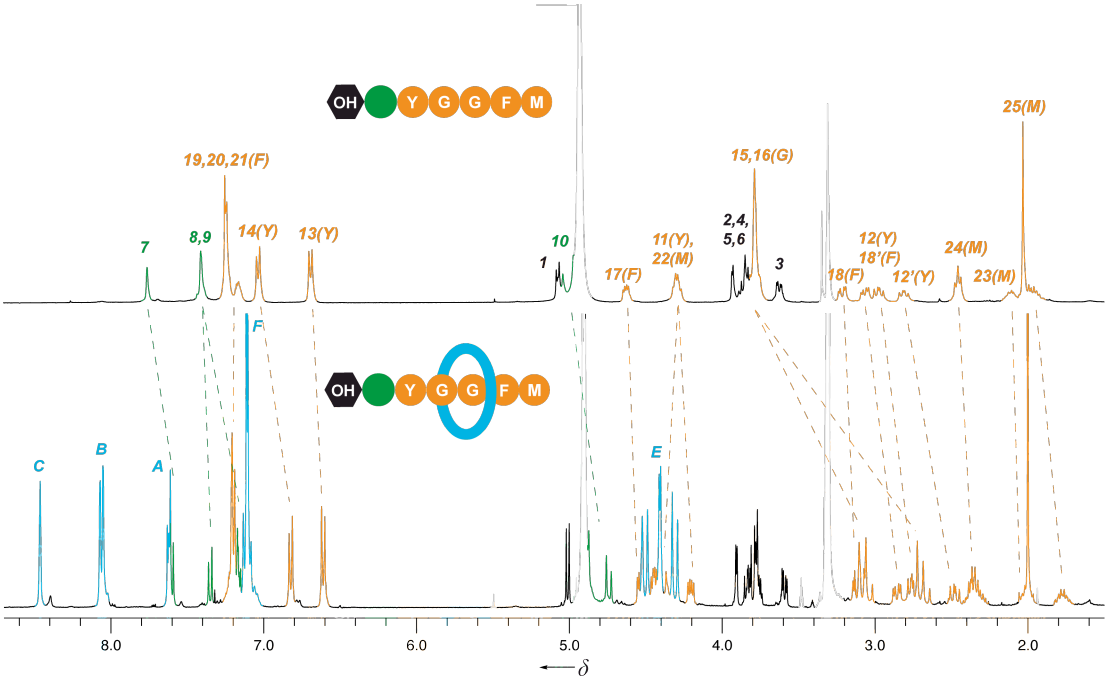

Figure 5.3. ^{1}H NMR spectra (400 MHz, CD_3OD, 300K) of a) propeptide **27**, b) Rotaxane propetide **2**. The assignments and colouring of signals correspond to the lettering shown in schemes 5.7 and 5.8. Residual solvent peaks are shown in grey.

5.2.2 *In vitro* β-galactosidase triggered release of Met-enkephalin

In order to assess the efficiency of our system, beta galactosidase assays were conducted on both the non-rotaxane-protected propeptide and on the rotaxane propeptide. Prior to enzymatic cleavage, some basic solubility tests in water were carried out with the thread and the rotaxane. HPLC comparison of saturated solution of each compound in water with a solution of the same compound of a known concentration in DMSO/water, gave a solubility of 2.2 g/L ($2.3 \cdot 10^{-3}$ mol/L) for propeptide **27** and 670 mg/L for rotaxane propeptide **2** ($4.6 \cdot 10^{-4}$ mol/L). As expected, the lypophilic character of the macrocycle is transmitted to the rotaxane, whose solubility in water decreases of a few orders of magnitude, being about 10 times less soluble in water than the parent thread **2**. Although this value is in the lower limit of drug administration standards, it is still higher than several commercial drugs.

To carry out enzymatic tests with β-galactosidase, however, a solution containing 2.5% DMSO was used in order to reach higher concentrations, allowing us to compare the rate of hydrolysis with reported data.[29] Thus mixing a solution of thread in phosphate buffer/DMSO with a solution of β-galactosidase at 37 °C gave, almost

instantly, an intense yellow coloration characteristic of the nitrophenolate spacer adduct **6** (Figure 5.4). Pleased by this preliminary result, the course of the hydrolysis was followed by HPLC for both thread and rotaxane (Figure 5.4).

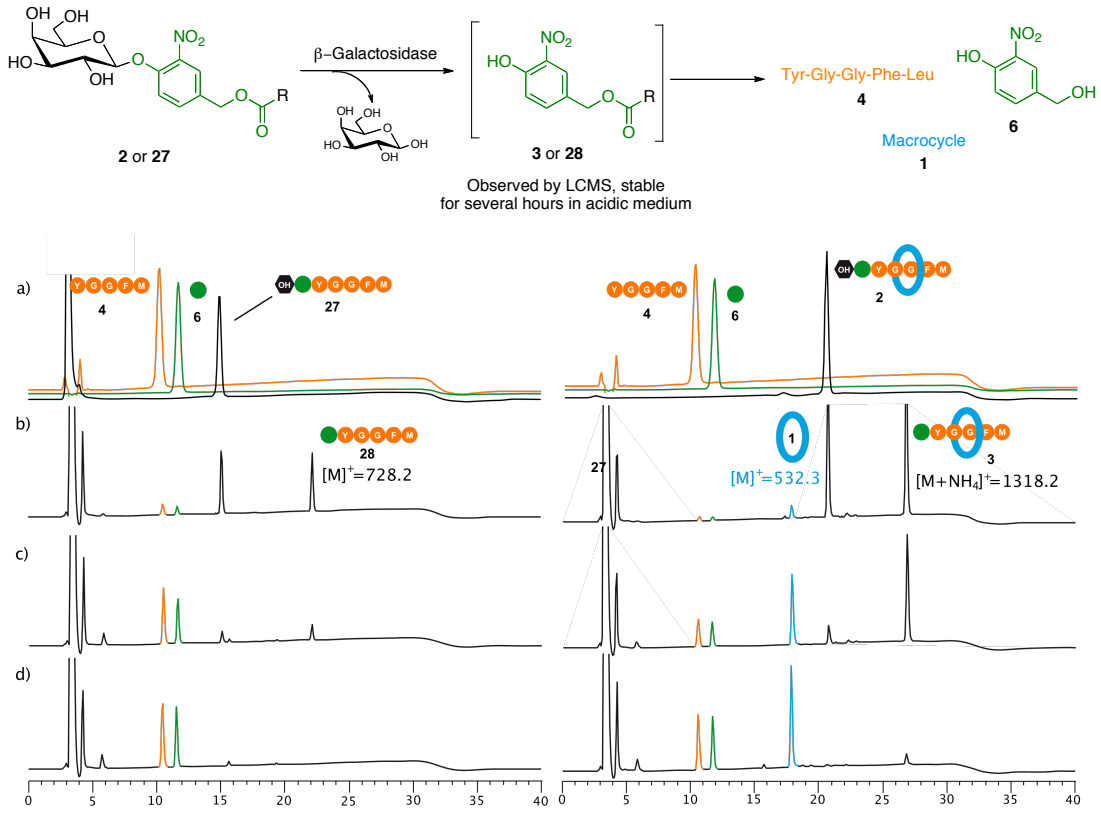

Figure 5.4. HPLC traces of hydrolysis of propeptide **27** (left) and rotaxane propeptide **2** (right), with *E. coli* β-galactosidase in 97.5 % phosphate buffer (0.02 M, pH 7.0), 2.5 % DMSO, at 37 °C using 10 U/μmol of substrate (substrate concentration 0.33 mM): a) references of individual components **2**, **4**, **6** and **27**, after b) t = 2min., c) t =5 min., d) t =10 min

Hydrolysis of both compounds was carried out at the same concentration and temperature and aliquots were withdrawn from the media at the same time intervals. Commercial Met-enkephalin and spacer hydrolysis adduct **6** were used as references. Cleavage of either the thread or rotaxane propeptide proceeded at almost the same rate with complete release of Met-enkephalin after 10 and 15 minutes[30] respectively and the amount of Met-enkephalin released proved quantitative for both species (by HPLC) (Scheme 5.4).

Interestingly, the starting propeptides are almost totally consumed within two minutes after addition of the enzyme, producing the intermediate species **3** and **28** (characterized by LCMS) (Scheme 5.1 and Figure 5.4),[31] demonstrating that elimination of CO_2 is the rate limiting step. This also gives strong evidence that the

macrocycle does not have any negative effects on substrate recognition, since the galactose unit is hydrolyzed equally as fast in both thread and rotaxane. However, the rate of CO_2 elimination is determined by the ability of the carbamate group to adopt a perpendicular conformation with respect to the plane of the phenyl ring (assuming that the elimination cascade is of the E_2 type). This occurs slightly slower in the rotaxane, presumably because of the restricted conformational freedom of the thread caused by its encapsulation within the macrocycle.

5.2.3 *In vitro* stability tests

5.2.3.1 Stability toward pancreatic enzymes

As the main barrier to peptide drug administration is of a proteolytic nature, we were interested in placing our rotaxane in contact with a set of relevant enzymes to evaluate its potential to increase the pharmacokinetics of the encapsulated peptide. If a drug is to be administered orally, several types of proteases will be encountered along the metabolic pathway. Careful analysis of specificity of the most common pancreatic enzymes revealed that α-chymotrypsin (an endopeptidase) and carboxypeptidase A (a metallo-exopeptidase) readily hydrolyze Met-enkephalin.[32] According to previous reports on the digestion of enkephalins,[33,34] α-Chymotrypsin shows a strong preference for both aromatic residues whereas carboxypeptidase A, belonging to the exopeptidase family, will only cleave the C-terminus residue (Scheme 5.9).

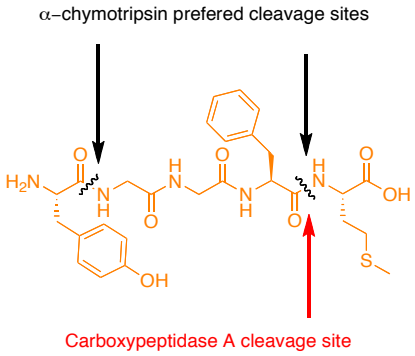

Scheme 5.9. Selectivity of α-chymotrypsin and carboxypeptidase A towards Met-enkephalin (**4**)

Accordingly, experiments were set up in which the three compounds, Met-enkephalin (**4**), non-rotaxane encapsulated propeptide **27** and rotaxane propeptide **2** were placed in the presence of α-chymotrypsin and carboxypeptidase A. Rates of cleavage were analyzed by HPLC (by plotting the absolute area of the peak displayed by the starting material) and the amount of enzyme was adjusted in order to be able to compare the rates of cleavage of the three species relative to one another. Under these conditions (see Experimental section), complete digestion of Met-enkephalin with either α-chymotrypsin or carboxypeptidase A occurred in less than 6 hours. Free propeptide **27** exhibited slower kinetics with both enzymes but was completely hydrolyzed in less than 24 hours. LCMS data carried out on the non-protected propeptide was in accordance with the predicted selectivity of the enzymes (Scheme 5.10).

Rotaxane propeptide **2** showed an improvement compared to the non-protected propeptide with both enzymes, being completely cleaved in less than 48 hours (about 8 times slower than Metenkephalin), however this improvement (relative to free Metenkephalin) is not high enough to be exploited for oral drug administration.[35] The rate difference observed for all three species proves that the structural change has an impact on substrate recognition, but not to the expected extent. The selectivity of both enzymes suggests that only the last peptidic bond of the peptide is vulnerable to hydrolysis. It is however impossible to conclude on the ability of the macrocycle to protect the adjacent bonds since cleavage by α-chymotrypsin could also occur, in theory, between Tyr and Gly (scheme 5.10).

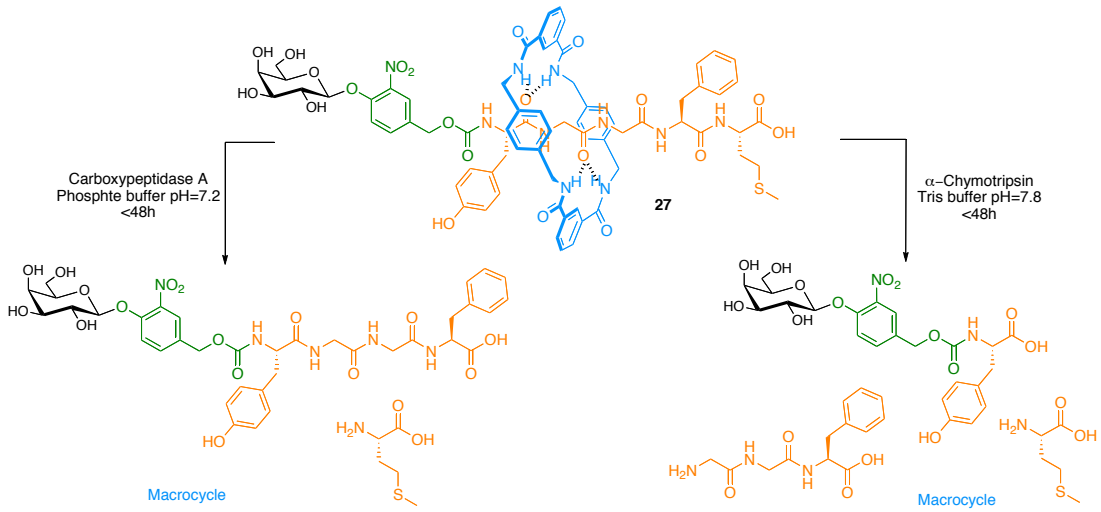

Scheme 5.10. Carboxypeptidase A and α-chymotrypsin cleavage of rotaxane propeptide **2** and the potential fragments (as deduced from LCMS studies on the cleavage of free propeptide **27**).

Although rotaxane propeptide **2** was expected to show comparable resistance to α-chymotrypsin as that observed with the (structurally very similar) Boc-Leu-enkephalin rotaxane (Chapter 3),[36] previous work from Anderson demonstrates that little structural or positional changes in the rotaxane can affect the recognition by the proteolytic enzyme. In a study, they show, that α-chymotrypsin cleavage of a rotaxane stoppered by two consecutive amino acids (Arg-Phe) can be either inhibited (as with Boc-Leu-enkephalin rotaxane) or even accelerated (compared to enzymatic cleavage of the parent thread) depending on the position of the ring on the thread. In this example, when the α-cyclodextrin ring is forced (*via* isomerization of a double bond) to reside close to the terminal Arg-Phe residues, cleavage is not observed (even though the ring does not sit over these residues). However, when the macrocycle has access to the whole thread, hydrolysis is even faster than for the non-interlocked thread! (see Chapter 3) This effect is believed to be due to activating interactions between the ring and the enzyme, and seems to be in accordance with Smithrud's observations on host-guest rotaxanes (see Chapter 3).[37] Hence, when the ring is not blocked in one location, a rotaxane structure has the ability to rearrange dynamically with the ring shuttling along the thread in order to maximize the binding free energy of the substrate-enzyme complex and hydrolysis could be favoured. In our case, the macrocycle is believed to have sufficient freedom of movement so that the above-mentioned phenomenon applies to our system.

These preliminary assays confirm the necessity of the macrocycle to sit over the residues prone to hydrolysis for as long a period of time as possible (See Chapter 3), in order for the rotaxane structure to be as efficient as possible for protecting the peptide.

5.2.3.2 Stability in human plasma

Previous results motivated us to investigate on the stability of propeptides toward enzymes present in the systemic circulation. Aminopeptidase M and the Angiotensin Converting Enzyme (ACE) have both been identified to be responsible for enkephalins hydrolysis in human and animal plasma. Hydrolysis studies on Met-enkephalin revealed that the peptide is cleaved between theTyr-Gly, Gly-Gly by Amino peptidase M, and between the Gly-Phe residues by ACE (Scheme 5.11).[7,10,38]

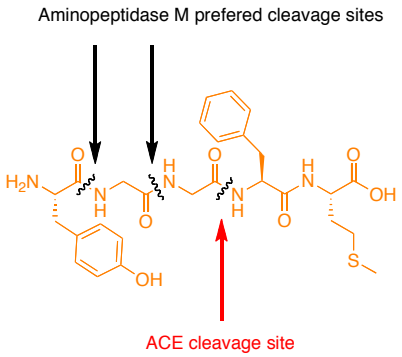

Scheme 5.11. Selectivity of Aminopeptidase M and ACE towards Met-enkephalin

Aminopeptidase M requires, by definition,[34] a free terminal amine for substrate recognition, and should not hydrolyze **2** or **27**; conversely, ACE will provide information on the ability of the macrocycle to protect the peptide at the Gly-Phe linkage.

To test these assumptions, all three substrates were incubated with either Aminopeptidase M or ACE for 50 hours. The quantity of enzyme used was arbitrarily chosen in order to measure a half-life time accurately for all species; their rates of hydrolysis were measured by HPLC (Figure 5.5 anf 5.6). In both cases, rotaxane **2** exhibited very high stability compared to Met-enkephalin. Measured half-life times were much greater than 60 hours with both Aminopeptidase M and ACE, which represents a greater than a 100-fold increase in stability.

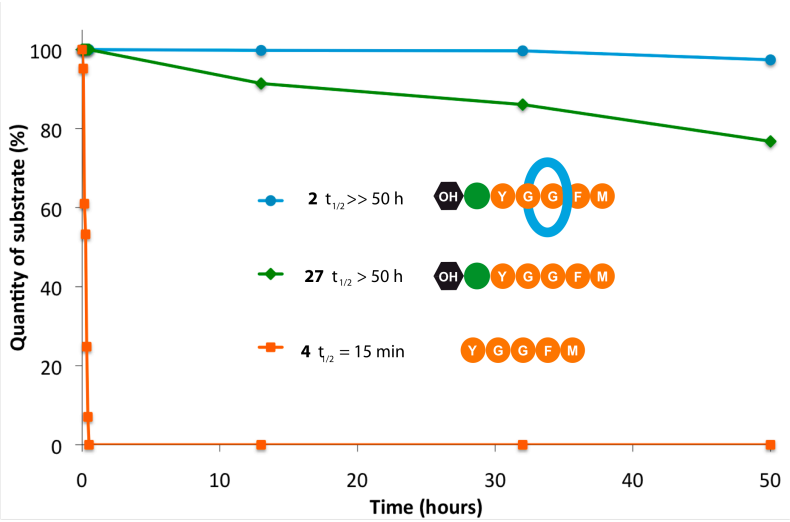

Figure 5.5. Enzymatic digestion of (i) rotaxane propeptide **2** (blue circles), (ii) thread **27** (green diamonds) and (iii) Met-enkephalin **4** (orange squares) with porcine kidney aminopeptidase M. Reactions were carried out at 25 °C in 95 % phosphate buffer (0.05 M, pH 7.2), 5 % DMSO, using 0.005 U/μmol of substrate. 0.0025 U/μmol of enzyme was added every 12 hours. [39]

Free propeptide **27** shows reasonable stability under Aminopeptidase M conditions as expected, but slow decomposition can still be observed, however.[40] In the presence of ACE, the resistance of **27** against proteolysis is only slightly higher than Met-enkephalin, demonstrating that the macrocycle protects the peptide efficiently up to the Gly-Phe linkage.

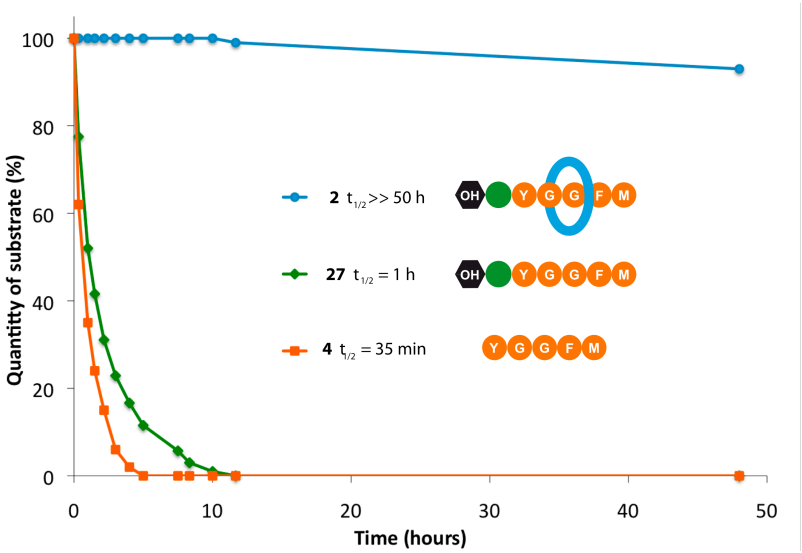

Figure 5.6. Enzymatic digestion of (i) rotaxane propeptide **2** (blue circles), (ii) thread **27** (green diamonds) and (iii) Met-enkephalin **4** (orange squares) with rabbit lung angiotensin converting enzyme (ACE). Reactions were carried out at 25 °C in 95 % HEPES buffer (0.05 M, pH 8.3), 5 % DMSO, 0.3 M NaCl, using 0.8 U/μmol of substrate. 0.4 U/μmol of enzyme was added every 12 hours.

Improved pharmacokinetics could therefore be expected if the rotaxane propeptide was to be administered intravenously, since Aminopeptidase M and ACE are the only two enzymes responsible for Met-enkephalin breakdown in human plasma.

Although the galactose-nitrophenol unit is believed to be stable for several hours in biological fluids when incorporated to prodrug systems, as an ultimate proof of stability, our nanodevice was incubated in human plasma as along with species **27** and **4**.

Hence, commercial human plasma was reconstituted in phosphate buffer and samples were incubated at 37°C for several days. Aliquots were withdrawn periodically and (after the proteins had been precipitated) the rate of decomposition was measured in the same way as described above. The concentration of incubated substrate was based on the dose of Met-enkephalin that has been administered to mice during anti-tumour assays (10 mg/Kg).[34] This dose was adjusted to a hypothetical adult human of weight 70 Kg, with a blood volume of roughly 5 L, and this quantity was translated

to 100 μL sample experiments. **2** and **27** could be monitored easily under these conditions, whereas Met-enkephalin **4** did not show a high enough UV-absorbance maximum to be monitored at that concentration. The quantity of Met-enkephalin **4** was thus increased 20-fold, but its rate of decomposition (supposedly diminished by this increase) was still much faster than for rotaxane **2** (Figure 5.7).

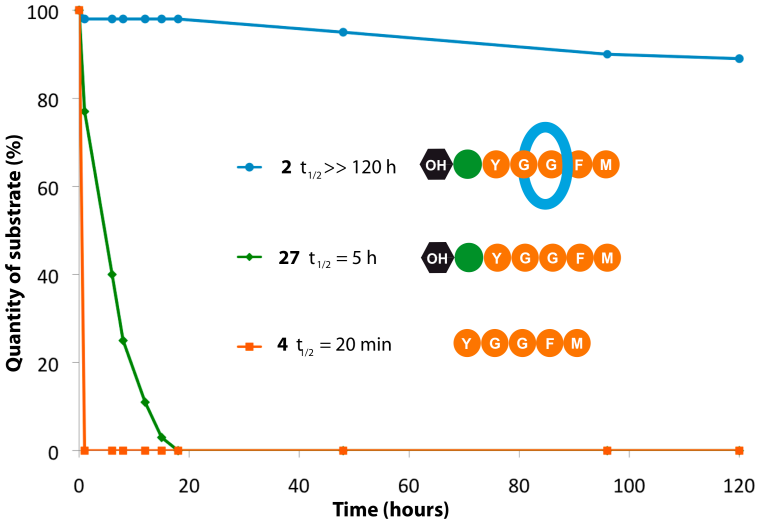

Figure 5.7. Stability of (i) rotaxane propeptide **2** (blue circles), (ii) thread **27** (green diamonds) and Met-enkephalin **4** (orange squares) in human plasma, reconstituted from lyophilized powder with 0.01 M Tris buffer at pH 7.4, at 37 °C.

The half-life time of rotaxane **2** is in the range of highly stable drugs, showing less than 10% decomposition after 4 days incubation in human plasma, whereas the non-rotaxane-protected species are metabolized very rapidly.

5.3 Conclusion

From a practical point of view, the synthesis of the first peptide carrier based on topological encapsulation has been achieved. Although not optimized yet, the synthesis is based on simple and readily available building blocks and could lead to rotaxane propeptides on the gram scale without the need for extended purification procedures. Preliminary results on β-galactosidase mediated drug release are very encouraging, as the rate of peptide release is of the same order of magnitude as that already reported in the literature for anti-cancer prodrugs. β-Galactosidic linkage cleavage proceeds in a clean manner, with quantitative release of the peptide (by

HPLC). Stability studies of the device in human plasma are very promising regarding the potential applications of rotaxane propeptides in ADEPT anti-cancer treatment strategies.

On a purely scientific level, this study has provided valuable insight into the applicability of mechanical encapsulation to the specific delivery of bioactive peptides. The device presented in this Chapter represents a potential breakthrough in the way drugs are designed, and further advanced biological assessment would hopefully confirm it.

The studies on proteolytic cleavage have confirmed the hypothesis of Chapter 3. The ring is effective at protecting the amino acids over which it spends the most time, but the intermittent presence of the ring in proximity to the last two residues is insufficient to avoid the formation of a substrate-enzyme complex that leads to hydrolysis of the peptidic bond between these last two residues. This issue highlights the limitations of the system and, as stated earlier, the elaboration of a carrier device where the peptide can be completely concealed by the ring would be a major advance.

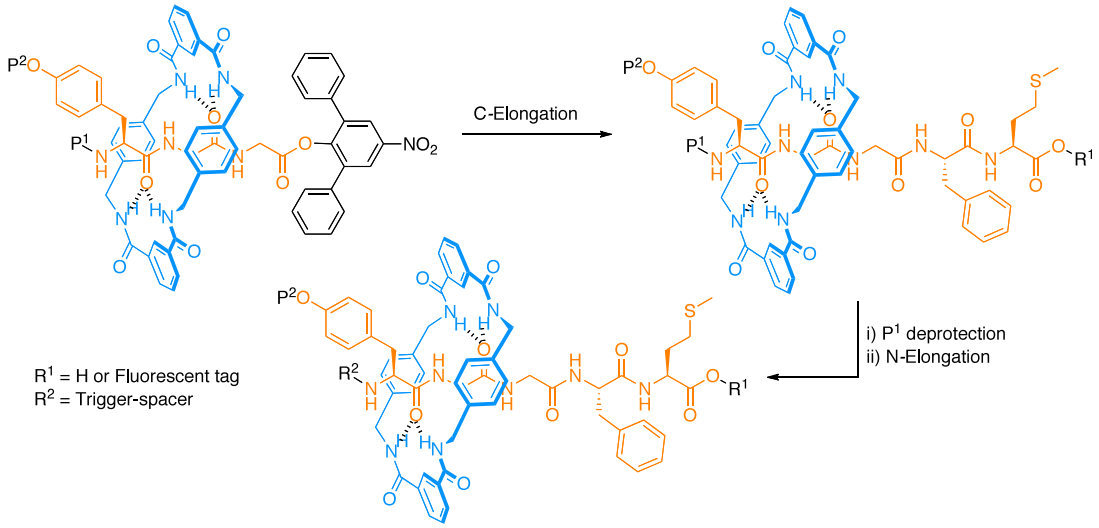

Scheme 5.12. Proposed synthesis of future nanodevices by successive C- and N-elongation of activated rotaxane precursors

Although the synthesis of the first generation rotaxane-encapsulated propeptides expounded above has been carried out in a stepwise fashion, the next generation could be synthesized in a convergent manner using the successive N and C-elongation methods developed in Chapter 4. This would allow for late stage diversification, and the synthesis of any combination of trigger, spacer and peptide

starting from a single building block would be possible (scheme 5.12). Thus, the addition of the last two amino acids of the sequence and the trigger-spacer unit at a late stage could lead to a library of close analogues for screening with various tumour treatments. Furthermore, by varying the trigger unit, a fluorescent version of the chosen trigger-spacer-peptide combination could be synthesized for use in biological assays (*e.g. in vivo* distribution).

5.4 Experimental section

***E. coli* β-Galactosidase enzymatic cleavage**

Enzymatic hydrolysis was carried out with commercial β-galactosidase from *Escherichia coli* E.C. 3.2.1.23 (1000 units/mg protein (biuret), aqueous glycerol suspension (1:1), 10 mM Tris buffer salts and 10 mM magnesium chloride, pH 7.3). Substrates were incubated at 37°C with the enzyme (10 Units/μmol of substrate) in 20 mM Phosphate buffer at pH 7.0 containing 2.5% (v/v) DMSO (concentration of substrate 0.1 mmol/L). Aliquots (20 μL) were periodically withdrawn from the medium and diluted into a solution of TFA (0.1%) in H_2O (40 μL). The rate of hydrolysis was monitored by analytical HPLC and LCMS.

Enzymatic stability toward α-Chymotrypsin

Digestions were carried out with commercial α-Chymotrypsin from bovine pancreas (59 units/mg, lyophilised powder). Solution of the enzyme in Tris buffer 50 mM, pH 7.8, containing 10 mM $CaCl_2$, were freshly prepared before use. Substrates were incubated at 25°C with the enzyme (5 Units/μmol of substrate) in Tris buffer 50 mM, pH 7.8, containing 10 mM $CaCl_2$ and 10% (v/v) MeCN (concentration of substrate 1 mmol/L). Aliquots (10 μL) were periodically withdrawn from the medium and diluted into a solution of TFA (0.1%) in H_2O (20 μL). The rate of decomposition was measured by plotting the absolute area of the peak of interest against time.

Enzymatic stability toward Carboxypeptidase A

Digestions were carried out with commercial Carboxypeptidase A from bovine pancreas (Type II-PMSF treated, 73 units/mg protein, aqueous suspension with

toluene added). Substrates were incubated at 25°C with the enzyme (5 Units/μmol of substrate) in 20 mM Phosphate buffer at pH 7.0 containing 5% (v/v) DMSO (concentration of substrate 0.25 mmol/L). Aliquots (10 μL) were periodically withdrawn from the medium and diluted into a solution of TFA (0.1%) in H_2O (20 μL). The rate of decomposition was measured by plotting the absolute area of the peak of interest against time.

Enzymatic stability toward Aminopeptidase M

Digestions were carried out with commercial microsomal Leucine Aminopeptidase (Aminopeptidase M), from porcine kidney, type IV-S, E.C. 3.4.11.2 (24 units/mg protein (Bradford), suspension in 3.5 M $(NH_4)_2SO_4$ solution, pH 7.7, containing 10 mM $MgCl_2$). Substrates were incubated at 25°C (to minimize loss of activity) with the enzyme (5.10^{-3} Units/μmol of substrate) in 50 mM Phosphate buffer at pH 7.2 containing 5% (v/v) DMSO (concentration of substrate 0.25 mmol/L). Enzyme was added to the medium every 12 hours to compensate for loss of activity ($2.5.10^{-3}$ Units/μmol of substrate). Aliquots (5 μL) were periodically withdrawn from the medium and directly used for analytical HPLC monitoring. The rate of decomposition was measured by plotting the absolute area of the peak of interest against time.

Enzymatic stability toward Angiotensin Converting Enzyme

Digestion were carried out with commercial Angiotensin Converting Enzyme from rabbit lung (3.92 units/mg protein (modified Warburg-Christian), lyophilized powder). The enzyme was kept in a solution of 10 mM potassium phosphate buffer, pH 7.0, containing 0.5 M NaCl (Concentration: 1 mg of enzyme/mL) and stored at -20°C [Stewart, T. A., et al., Human Peptidyl Dipeptidase (Converting Enzyme, Kininase II). *Meth. Enzymol.*, **80**, 450-460 (1981).]. Substrates were incubated at 25°C (to minimize loss of activity) with the enzyme (0.8 Units/μmol of substrate) in 50 mM HEPES buffer at pH 8.3 containing 0.3 M NaCl and 5% (v/v) DMSO (concentration of substrate 0.125 mmol/L). Enzyme was added to the medium every 12 hours to compensate for loss of activity (0.4 Units/μmol of substrate). Aliquots (5 μL) were periodically withdrawn from the medium and directly used for analytical HPLC monitoring. The rate of decomposition was measured by plotting the absolute

area of the peak of interest against time.

Stability in human plasma

Stability in human plasma was carried out with commercial lyophilized human plasma reconstituted by dissolving the solid in the appropriate volume of 0.01 M Tris buffer at pH 7.4. Substrates were incubated at 37°C in the freshly prepared solution (0.150 μmol of substrate/mL). Aliquots (50 μL) were periodically withdrawn from the medium, poured into cold MeOH (50 μL) to precipitate the proteins and cooled on ice. After 30 min., the sample was centrifuged (17 000 g, 2 min) and the supernatant analyzed by analytical HPLC. The rate of decomposition was measured by plotting the absolute area of the peak of interest against time.

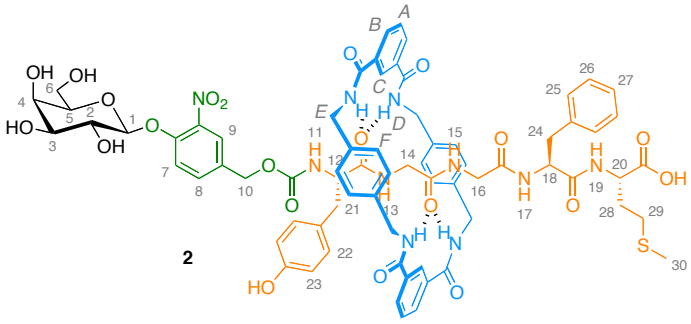

2

To a solution of **22** (31 mg, 0.019 mmol) in MeOH (5 mL) at 0°C was added drop-wise a solution of MeONa (10 mg, 0.19 mmol, 10.0 equiv.) in MeOH (3 mL). The mixture was stirred for 1 hour at 0°C, neutralized with Amberlite IR-120 and filtered. MeOH was then evaporated to afford **2** (29 mg, 0.019 mmol, quant.) as a pale brown solid which was then purified by preparative RP-HPLC using a linear gradient (58 to 80% in 20 min) of MeCN in H_2O at a flow rate of 10 mL/min to give rotaxane **1** as a pale yellow solid. Purity (HPLC): >95%. **M.p.** 172-174°C; **^{1}H NMR (400 MHz, CD_3OD):** δ = 8.46 (s, 2H, H_C), 8.06 (d, 4H, *J* = 8.0 Hz, H_B), 7.63-7.59 (m, 3H, H_9 and H_A), 7.35 (d, 1H, *J* = 8.8 Hz, H_7), 7.23-7.08 (m, 16H, H_8, H_{25}, H_{26}, H_{27} and H_F), 6.82 (d, 2H, *J* = 8.4 Hz, H_{22}), 6.61 (d, 2H, *J* = 8.4 Hz, H_{23}), 5.01 (d, 1H, *J* = 8.0 Hz, H_1), 4.95-4.73 (m, 2H, H_{10}), 4.56-4.29(m, 10H, H_{18}, H_{20} and H_E), 4.21 (dd, 1H, *J* = 9.6 Hz, *J* = 4.8 Hz, H_{12}), 3.91 (d, 1H, *J* = 3.2 Hz, H_4), 3.85-3.74 (m, 4H, H_2, H_5 and H_6), 3.59 (dd, 1H, *J* = 9.6 Hz, *J* = 3.2 Hz, H_3), 3.15-3.02 (m, 3H, H_{16} and H_{24}), 2.86 (dd, 1H, *J* = 14.0 Hz, *J* = 5.2 Hz, H_{21}), 2.78-2.64 (m, 3H, H_{14} and H_{24}), 2.48 (dd, 1H, *J* = 14.0 Hz, *J* = 10 Hz, H_{21}), 2.39-2.28 (m, 2H, H_{29}), 2.06-1.97 (m, 1H, H_{28}), 2.00 (s,

3H, H_{30}), 1.83-1.72 (m, 1H, H_{28}); **^{13}C NMR (100 MHz, CD_3OD):** δ = 174.8, 174.2, 173.9, 170.7, 170.0, 169.2, 169.1, 157.8, 157.1, 156.7, 151.0, 141.5, 138.6, 138.5, 138.4, 135.6 (x2), 134.1, 132.4, 132.0, 131.4, 130.4, 130.2 (x2), 130.0, 129.6, 129.2, 128.0, 127.9, 125.3, 125.2, 118.7, 116.2, 102.9, 77.4, 74.9, 72.0, 70.2, 65.8, 62.5, 57.6, 56.2, 52.8, 45.4, 45.3, 43.2, 42.4, 39.2, 37.9, 31.9, 31.2, 30.8, 15.2; **LRFAB-MS (3-NOBA matrix):** *m/z* 1463 $[M+H]^+$, 1485 $[M+Na]^+$; **LRESI-MS:** *m/z* 1463 $[M+H]^+$; **HRESI-MS:** *m/z* 1463.5122 (calcd. for $C_{73}H_{79}N_{10}O_{21}S$ 1463.5136 $[M+H^+]$).

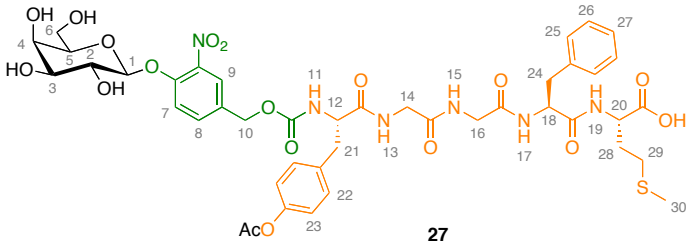

27

To a solution of **26** (54 mg, 0.047 mmol, 1 equiv.) in MeOH (7 mL) at 0°C was added a solution of MeONa (26 mg, 0.47 mmol, 10.0 equiv.) in MeOH (4 mL) dropwise. The mixture was stirred for one hour at 0°C, neutralized with Amberlite IR-120, filtered. And concentrated under reduced pressure. Purification by flash column chromatography on silica gel with CH_2Cl_2-MeOH (9:1 to 1:1) to afford **27** (38 mg, 0.041 mmol, 87%) as a pale brown solid which was then re-purified by preparative RP-HPLC using a linear gradient (27 to 45% in 15 min) of MeCN in H_2O at a flow rate of 10 mL/min to give rotaxane **27** as a white solid. Purity (HPLC): >98%. **M.p.** 158-160°C; **^{1}H NMR (400 MHz, CD_3OD):** δ = 7.76 (bs, 1H, H_9), 7.41 (bs, 2H, H_7 and H_8), 7.26-7.24 (m, 4H, H_{25} and H_{26}), 7.19-7.16 (m, 1H, H_{27}), 7.04 (d, 2H, *J* = 8.0 Hz, H_{22}), 6.69 (d, 2H, *J* = 8.0 Hz, H_{23}), 5.08 (d, 1H, *J* = 7.6 Hz, H_1), 5.09-4.94 (m, 2H, H_{10}), 4.63 (dd, 1H, *J* = 9.2 Hz, *J* = 4.4 Hz, H_{18}), 4.30 (m, 2H, H_{12} and H_{20}), 3.93 (d, 1H, *J* = 3.2 Hz, H_4), 3.89-3.75 (m, 8H, H_2, H_5, H_6, H_{14} and H_{16}), 3.63 (dd, 1H, *J* = 9.6 Hz, *J* = 3.2 Hz, H_3), 3.21 (dd, 1H, *J* = 14.4 Hz, *J* = 4.4 Hz, H_{24}), 3.07 (dd, 1H, *J* = 13.6 Hz, *J* = 5.6 Hz, H_{21}), 2.98 (dd, 1H, *J* = 14.0 Hz, *J* = 9.6 Hz, H_{24}), 2.81 (dd, 1H, *J* = 13.6 Hz, *J* = 9.2 Hz, H_{21}), 2.46 (t, 2H, *J* = 8.0 Hz, H_{29}), 2.13-2.10 (m, 1H, H_{28}), 2.03 (s, 3H, H_{30}), 2.00-1.93 (m, 1H, H_{28}); **^{13}C NMR (100 MHz, CD_3OD):** δ = 177.6, 175.2, 172.8, 172.2, 171.6, 170.0, 158.4, 157.3, 151.0, 141.7, 138.7, 134.3, 132.6, 131.4, 130.4, 129.5, 129.1, 127.8, 125.3, 118.8 , 116.3, 102.9, 77.2, 74.8, 72.0, 70.2, 66.1, 62.4, 58.6, 56.5, 55.4, 43.9, 43.4, 38.4, 37.9, 33.6, 31.2, 15.3; **LRESI-MS:** *m/z*

953 $[M+Na]^+$; **LRESI-MS (negative mode):** *m/z* 929 $[M-H]^-$; **HRESI-MS**: *m/z* 948.3287 (calcd. for $C_{41}H_{54}N_7O_{17}S$ 948.3297 $[M+NH_4]^+$)

5.5 References and notes

[1] J. M. Lundberg, B. Hamberger, M. Schultzberg, T. Hokfelt, P. O. Granberg, S. Efendic, L. Terenius, M. Goldstein, R. Luft, *Proc. Natl. Acad. Sci. U. S. A.,* **1979**, *76*, 4079-4083.

[2] I. S. Zagon, P. J. McLaughlin, S. R. Goodman, R. E. Rhodes, *J. Natl. Cancer. Inst.,* **1987**, *79*, 1059-1065.

[3] I. S. Zagon, M. F. Verderame, P. J. McLaughlin, *Brain Res. Rev.,* **2002**, *38*, 351-376.

[4] I. S. Zagon, S. R. Goodman, P. J. McLaughlin, *Brain Res.,* **1993**, *605*, 50-6; I. S. Zagon, P. J. McLaughlin, *Brain Res.,* **1993**, *630*, 295-302; I. S. Zagon, P. J. McLaughlin, *Growth Factors,* **1993**, 171-80.

[5] F. Cheng, I. S. Zagon, M. F. Verderame, P. J. McLaughlin, *Cancer Res.,* **2007**, *67*, 10511-10518; F. Cheng, P. McLaughlin, M. Verderame, I. Zagon, *Molecular Cancer,* **2008**, *7*, 5; F. Cheng, P. J. McLaughlin, M. F. Verderame, I. S. Zagon, *Mol. Biol. Cell,* **2009**, *20*, 319-327.

[6] I. S. Zagon, S. D. Hytrek, J. P. Smith, P. J. McLaughlin, *Cancer Lett.,* **1997**, *112*, 167-175; P. J. McLaughlin, R. J. Levin, I. S. Zagon, *Cancer lett.,* **2003**, *199*, 209-217; P. J. McLaughlin, B. C. Stack, Jr., K. M. Braine, J. D. Ruda, I. S. Zagon, *Int. J. Oncol.,* **2004**, *24*, 227-232; J. P. Smith, R. L. Conter, S. I. Bingaman, H. A. Harvey, D. T. Mauger, M. Ahmad, L. M. Demers, W. B. Stanley, P. J. McLaughlin, I. S. Zagon, *Anticancer Drugs,* **2004**, *15*, 203-209.

[7] M. R. Boarder, W. McArdle, *Biochem. Pharmacol.,* **1986**, *35*, 1043-1047.

[8] S. Horvat, M. Kralj, M. Perc, I. Jeric, L. Varga-Defterdarovic, A. Jakas, M. Roscic, L. Suman, M. Gredicak, *Chem. Biol. Drug Des.,* **2009**, *73*, 253-257.

[9] S. Horvat, K. Mlinaric-Majerski, L. Glavas-Obrovac, A. Jakas, J. Veljkovic, S. Marczi, G. Kragol, M. Roscic, M. Matkovic, A. Milostic-Srb, *J. Med. Chem.,* **2006**, *49*, 3136-3142.

[10] M. Marini, A. Urbani, E. Trani, L. Bongiorno, L. G. Roda, *Peptides* **1997**, *18*, 741-748; M. Marini, G. Roscetti, L. Bongiorno, A. Urbani, L. G. Roda, *Neurochem. Res.,* **1990**, *15*, 61-7; S. Shibanoki, S. B. Weinberger, K. Ishikawa, J. L. Martinez, Jr., *Regul. Pept.,* **1991**, *32*, 267-78; S. Shibanoki, S. B. Weinberger, K. Ishikawa, J. L. Martinez, Jr., *Prog. Clin. Biol. Res.,* **1990**, *328*, 253-6.

[11] A. Bak, M. Fich, B. D. Larsen, S. Frokjaer, G. J. Friis, *Eur. J. Pharm. Sci.,* **1999**, *7*, 317-323.

[12] G. J. Rasmussen, H. Bundgaard, *Int. J. Pharm.,* **1991**, *76*, 113-22.

[13] A. K. Sinhababu, D. R. Thakker, *Adv. Drug Delivery Rev.,* **1996**, *19*, 241-273; W. A. Denny, *Eur. J. Med. Chem.,* **2001**, *36*, 577-595.

[14] M. Rooseboom, J. N. M. Commandeur, N. P. E. Vermeulen, *Pharmacol. Rev.,* **2004**, *56*, 53-102.

[15] G. M. Dubowchik, M. A. Walker, *Pharmacol. Ther.,* **1999**, *83*, 67-123; I. Niculescu-Duvaz, C. J. Springer, *Adv. Drug Delivery Rev.,* **1997**, *26*, 151-172; R. F. Sherwood, *Adv. Drug Delivery Rev.,* **1996**, *22*, 269-288.

[16] O. Greco, G. U. Dachs, *J. Cell. Physiol.,* **2001**, *187*, 22-36; M. Aghi, F. Hochberg, X. O. Breakefield, *J. Gene. Med.,* **2000**, *2*, 148-164.

[17] K. Bosslet, J. Czech, D. Hoffmann, *Tumor. Target.,* **1995**, *1*, 45-50; B. Sperker, T. E. Murdter, M. Schick, K. Eckhardt, K. Bosslet, H. K. Kroemer, *J. Pharmacol. Exp. Ther.,* **1997**, *281*, 914-920; M. deGraff, E. Boven, H. Scheeren, W., H. Haisma, J., H. Pinedo, M., *Curr. Pharm. Des.,* **2002**, *8*, 1391-1403.

[18] K. Bosslet, R. Straub, M. Blumrich, J. Czech, M. Gerken, B. Sperker, H. K. Kroemer, J.-P. Gesson, M. Koch, C. Monneret, *Cancer Res.,* **1998**, *58*, 1195-1201.

[19] M. Azoulay, J. C. Florent, C. Monneret, J. P. Gesson, J. C. Jacquesy, F. Tillequin, M. Koch, K. Bosslet, J. Czech, D. Hoffman, *Anti Canc. Drug Des.,* **1995**, *10*, 441-50; J.-C. Florent, X. Dong, G. Gaudel, S. Mitaku, C. Monneret, J.-P. Gesson, J.-C. Jacquesy, M. Mondon, B. Renoux, S. Andrianomenjanahary, S. Michel, M. Koch, F. Tillequin, M. Gerken, J. Czech, R. Straub, K. Bosslet, *J. Med. Chem.,* **1998**, *41*, 3572-3581; J. C. Florent, X. Dong, G. Gaudel, S. Mitaku, C. Monneret, J. P. Gesson, J. C. Jacquesy, M. Mondon, B. Renoux, S. Andrianomenjanahary, S. Michel, M. Koch, F. Tillequin, M. Gerken, J. Czech, R. Straub, K. Bosslet, *J. Med. Chem.,* **1998**, *41*, 3572-81.

[20] H. J. Haisma, M. Van Muijen, H. M. Pinedo, E. Boven, *Cell. Biophys.,* **1994**, *24-25*, 185-192; H. J. Haisma, E. Boven, M. Van Muijen, J. de Jong, W. J. F. van der Vijgh, H. M. Pinedo, *Br. J. Cancer,* **1992**, *66*, 474-478.

[21] I. Tranoy-Opalinski, A. Fernandes, M. Thomas, J. P. Gesson, S. Papot, *Anticancer Agents Med. Chem.,* **2008**, *8*, 618-37.

[22] T. E. Murdter, B. Sperker, K. T. Kivisto, M. McClellan, P. Fritz, G. Friedel, A. Linder, K. Bosslet, H. Toomes, R. Dierkesmann, H. K. Kroemer, *Cancer Res.,* **1997**, *57*, 2440-2445.

[23] T. Ooya, H. Mori, M. Terano, N. Yui, *Macromol. Rapid Commun.,* **1995**, *16*, 259-263.

[24] A. G. Cheetham, M. G. Hutchings, T. D. W. Claridge, H. L. Anderson, *Angew. Chem., Int. Ed.,* **2006**, *45*, 1596-1599.

[25] S. Potok, *Phd thesis*, University of Edinburgh, 2004.

[26] K. Patel, S. Angelos, W. R. Dichtel, A. Coskun, Y.-W. Yang, J. I. Zink, J. F. Stoddart, *J. Am. Chem. Soc.,* **2008**, *130*, 2382-2383.

[27] Final deprotection of the glucuronide's acid group via basic hydrolysis often leads to an unwanted 4,5-dehydro side product arising from elimination of the proton α to the carbonyl group. For recent examples see: A. El Alaoui, F. Schmidt, C. Monneret, J.-C. Florent, *J. Org. Chem.*, **2006**, 71, 9628-9636; J. Senn-Bilfinger, J. R. Ferguson, M. A. Holmes, K. W. Lumbard, R. Huber, K. Zech, R.-P. Hummel, P. J. Zimmermann, *Tetrahedron Lett.*, **2006**, 47, 3321-3323.

[28] Ahmed Kamal, Venkatesh Tekumalla, Anita Krishnan, Manika Pal-Bhadra, Utpal Bhadra, *ChemMedChem,* **2008**, *3*, 794-802.

[29] R. Madec-Lougerstay, J.-C. Florent, C. Monneret, *J. Chem. Soc., Perkin Trans. 1,* **1999**, 1369-1375.

[30] It is important that under these conditions (established by the group of Gesson) the peptide is released over the course of only a few minutes. One of the main parameters limiting the ADEPT strategy is the amount of enzyme available at the tumour site to activate the prodrug. Indeed, when the enzyme-antibody conjugate is injected into the patient, the unbound conjugates have to be cleared from the blood stream before the prodrug is administered (in order to prevent uncontrolled activation of the prodrug). This clearance is often very slow (several days) and during this time the concentration of enzyme-conjugated antibodies fixed on the tumour decreases as well. Although the enzyme is usually in excess compared to the prodrug concentration at the tumour site, it is important to keep the rate of drug release to a minimum so that that a maximum amount of prodrug is activated before it leaves the tumour site.

[31] Intermediates **3** and **28** are only stable for a few minutes at pH 7 at 37 °C, However, they survive for hours at pH 2 at room temperature (the equilibrium between the phenol and phenolate forms is shifted towards the phenol and elimination occurs only slowly). In the β-galactosidase catalyzed reactions, aliquots were withdrawn from the reaction medium and diluted with a solution of TFA (to pH 2) before being injected into the HPLC with the mobile phase buffered at pH 2 (see Experimental Section).

[32] The specificity of peptidases is defined as follows by Beynon and Bond: [R. Beynon, J. S. Bond *Proteolytic Enzymes*; Second ed.; Oxford University Press: Oxford, **2001**.] "*Crystallographic structures show that the active site of a peptidase is commonly located in a groove on the surface of the molecule between adjacent structural domains, and the substrate specificity is dictated by the properties of binding sites arranged along the groove on one or both sides of the catalytic site that is responsible for the hydrolysis of the peptide bond. Accordingly, the specificity of a peptidase is described by use of a conceptual model in which each specificity subsite is able to accommodate the side chain of an amino acid residue. The sites are numbered from the catalytic site, S1, S2,…Sn towards the N-terminus and S1', S2', …Sn' towards the C-terminus. The amino acids they accommodate are numbered, P1, P2,…Pn and P1', P2', …Pn' respectively*." In most common proteolytic enzymes, just one or two sites are sufficient for substrate recognition. For example,

α-chymotripsin is very specific to Leu, Phe or Tyr residues as P1 but does not require any specific residues at the other sites. Similarly, Carboxypeptidase A is particularly specific to Phe residues as P1, but it is not demanding concerning the remaining amino acids of the sequence. This somewhat low specificity of peptidases explains why - even though the ring constituent of the peptidorotaxane is in an adjacent position to P1 (say over P2) - hydrolysis might still possibly occur.

[33] R. Van Breemen, M. Bartlett, Y. Tsou, C. Culver, H. Swaisgood, S. Unger, *Drug Metab. Dispos.,* **1991**, *19*, 683-690; R. Beynon, J. S. Bond, *Proteolytic Enzymes*; Second ed.; Oxford University Press: Oxford, 2001.

[34] P. D. Boyer, *Hydrolysis: Peptide bonds*; Third ed.; Academic press: New York, 1971; Vol. III.

[35] *In vivo* half-life of enkephalins in rat stomach has shown to be less than five minutes (see, N. W. Bunnett, J. H. Walsh, H. T. Debas, *Am. J. Physiol. Gastrointest. Liver Physiol.*, **1990**, 258, G143-151). Based on these results a 100-fold decrease in cleavage rate of rotaxane propeptide by pancreatic proteases was assumed to be a minimum value to expect significantly improved pharmacokinetics of the rotaxane compared to Met-enkephalin

[36] S. Van Meurs, *Phd thesis*, University of Warwick, 2001.

[37] X. Bao, I. Isaacsohn, A. F. Drew, D. B. Smithrud, *J. Am. Chem. Soc.,* **2006**, *128*, 12229-12238.

[38] S. Shibanoki, S. B. Weinberger, G. Schulteis, K. Ishikawa, J. L. Martinez, Jr., *Life Sci.,* **1992**, *50*, 667-75; G. Schulteis, W. A. Rodriguez, S. B. Rodriguez, J. L. Martinez, Jr., *Peptides,* **1993**, *14*, 1083-9.

[39] A control experiment was carried out where **4** was incubated with a solution of enzyme in buffer that had been left 24 hours at room temperature prior usage. The recorded half-life was approximatively increased by 25% compared with the one measured when using freshly prepared enzyme solution.

[40] A control experiment where **27** was placed in the initial buffer conditions (phosphate buffer/DMSO (5%) at pH 7.2) showed that the propeptide decomposes slowly in solution

CHAPTER SIX

Towards a universal peptide rotaxane carrier for ligand-targeted anti-cancer therapy.

Acknowledgments

The work described in this chapter was shared equally between the author and Dr. Anthony Fernandes, whose contribution is gratefully acknowledged. Synthesis of trigger-spacer units **8**, **18** and **29** and synthesis of rotaxanes **38**, **42**, **43a-c** and **48a-c** was carried out by Dr. Anthony Fernandes. Synthesis of peptides **4** and **34**, alkynes **45**, **46**, **47** and synthesis of rotaxanes **51**, **52a-c** and isolation macrocycles **53a-c** was carried out by the author. All preparative HPLC purifications, β-galactosidase hydrolysis assays and solubility measurements were performed by the author.

6 Synopsis

The design, synthesis and operation of a model rotaxane peptide carrier are described. This novel device, which operates autonomously, has been adapted to anti-cancer treatment. Selective targeting of tumour cells is achieved by functionalizing of the macrocycle constituent of the device with targeting ligands. Release of the hypothetic drug is achieved via enzymatic cleavage of a self-immolative stopper. Binding of the targeting ligands to their specific receptors should trigger endocytosis-mediated internalization of the whole device and metabolism by tumour-specific enzymes will release the active peptide into the cytoplasm.

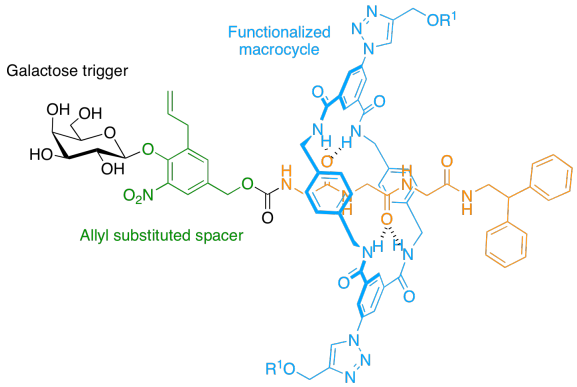

Model rotaxane propeptides in which the hypothetic bioactive peptide consists of a di or triglycil fragment were synthesized. The self-immolative stopper is a variation of Gesson's HMR 1826 original trigger-spacer unit used in chapter 5, bearing an allyl group on the nitrophenol moiety. The latter group is large enough to avoid slippage of the macrocycle without the need for an adjacent side chain amino acid (see chapter 5). Carbohydrate groups were attached to the macrocycle constituent as a model for targeting ligands and to improve aqueous solubility of the molecule. Methodology was developed to isolate the corresponding macrocycles, with the aim of subjecting them to biological assays. Solubility of rotaxanes and macrocycles were measured and enzymatic release of peptide was assessed.

6.1 Introduction

6.1.1 Ligand targeted therapy

Selectivity is by far the most important aspect of anti-cancer therapy. Under ADEPT this aspect is addressed by the use of antibody-enzyme conjugate targeting combined with a specific mode of drug release. Although this method has led to some encouraging results, it suffers from highly demanding practical procedures. To tackle this issue, conceptually similar approaches have been developed alongside ADEPT, where the active drug is directly attached to a monoclonal Antibody (mAb), or where mAbs are used as single agents.[1,2] Here specific targeting is achieved by binding to specific antigens, as with ADEPT.

A somewhat related but simpler approach has recently become popular. The idea is to specifically target cancer cells *via* the binding of a ligand to tumour-associated receptors, rather than antigens. These receptors, which are over expressed in cancer cells, are numerous and ligands can vary from high to low molecular weight compounds depending on the receptor targeted.[2,3] Many receptors that bind relatively small molecules have been investigated, such as the epidermal growth factor receptor (EGFr),[4] the folate receptor,[5] glucose uptake receptors (GLUTs),[6] galectins[7] and the asialoglycoprotein receptor.[8]

Targeting is then accomplished by designing ligand-prodrug conjugates that display high affinity for the targeted receptor. This ligand-functionalized prodrug binds to the individual receptor and is subsequently internalized *via* receptor-mediated endocytosis or through passive facilitated transport (*e.g.* in the case of GLUTs). Metabolism in the endosomes or lysosomes releases the active drug directly into the cytoplasm (scheme 6.1).

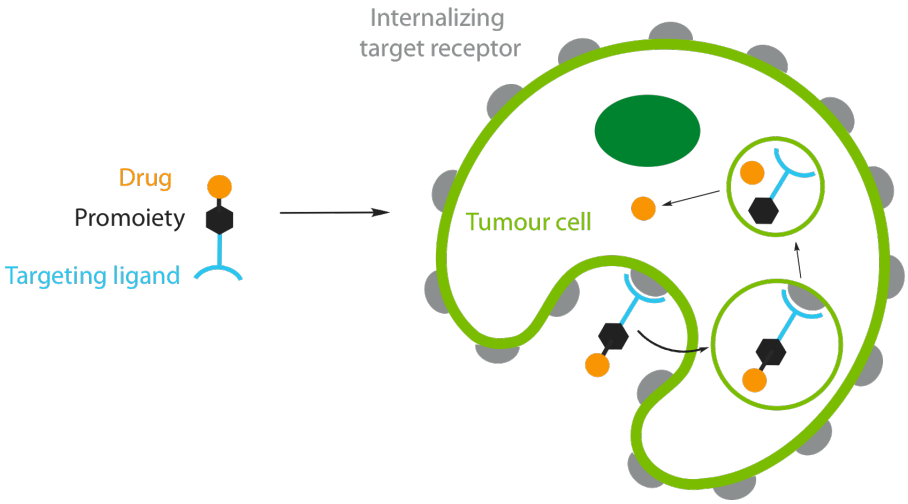

Scheme 6.1. General principle of ligand targeted therapy. Binding of the ligand to the receptor triggers endocytosis-mediated internalization. Metabolism in the endosomes or lysosomes releases the active drug inside the cell.

6.1.2 Towards ligand targeting rotaxane propeptides

Ligand targeted therapy has a great advantage over anti-cancer therapies that rely on antigen targeting in that the drug can be directed to the tumour site without the need for sophisticated bioengineering. Attaching a targeting ligand to a prodrug is sufficient to convey the drug directly into the malignant cell.

Therefore, as opposed to the Met-enkephalin rotaxane propeptide (Chapter 5), designed solely for ADEPT, a new device based on ligand targeting would have the advantage of carrying the drug into the cytoplasm before release. This aspect is of capital importance since passive transport of peptides through the cell membrane is usually very poor. This is also an opportunity to fully exploit the interlocked nature of the carrier device, since now the macrocycle constituent can serve not only to protect the peptide against degradation, but also act to target the drug to the desired site. Yui and coworkers have already demonstrated that ligand-functionalized rotaxanes bind to various receptors,[9] for example polyrotaxanes where the macrocycle constituents are functionalized by small peptides[10] or carbohydrates[11] showed improved binding strength over non-interlocked analogues.

According to these results, functionalization of our macrocycle with a ligand with affinity for the desired target should in theory convey the peptide directly into cancer

cells. The release of the bioactive molecule inside the cell could be realized by enzymes specific to cancer cells.[12]

A generic device would be designed as in scheme 6.1 where the macrocycle constituent is substituted with targeting ligands and the biodegradable stopper would be cleaved inside the cell – after receptor mediated-endocytosis – by over-expressed enzymes (scheme 6.1).

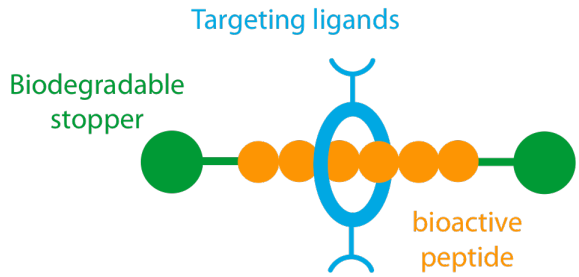

Figure 6.1. A generic design for an autonomous ligand-targeted peptide carrier.

6.1.3 Design of a model rotaxane carrier for ligand-targeted therapy

The first step toward the development of an autonomous and universal device for peptide delivery, as stated in chapter 3, is the creation of a universal type of biodegradable stopper. This means that, as opposed to the Met-enkephalin rotaxane in Chapter 3, the biodegradable stopper should be able to prevent slipping of the macrocycle without the need for an adjacent amino acid side chain. To achieve this task, it was a rational choice to build on the already well-established trigger-spacer combination of Gesson. While the trigger unit cannot easily be modified without interfering with enzyme recognition, the spacer can be decorated with blocking groups that will act as stoppers (Figure 6.2).

As the trigger unit, β-galactosidase was deemed a good choice for an initial model compound. Indeed, lysosomal β-galactosidase activity can be exploited for intracellular drug release in a ligand-targeted scheme. The enzyme is present in several mammalian cells and is over-expressed in a range of tumour cells.[13] As with ADEPT, the rate of drug release should be as high as possible and this rate will be the major parameter which is taken into account when assessing the suitability of potential spacers. Such new spacers would allow the use of di- and tri-glycyl diphenylethyl stoppered peptides to be used as models (because of their efficient

templating ability, see chapter 4) for the assessment of trigger-spacer biodegradation properties (Figure 6.2).

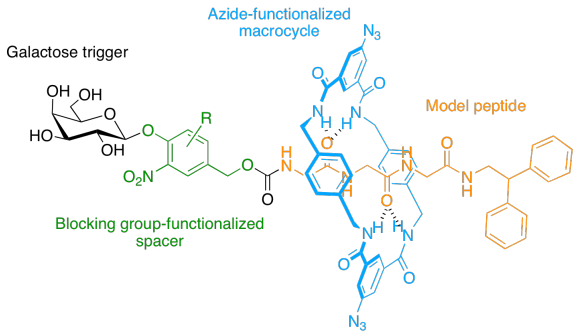

Figure 6.2. A model rotaxane peptide carrier.

In the second part of this chapter, a general methodology for the attachment of functional groups to the macrocycle constituent of the device will be developed.

To be able to screen the future carrier rotaxanes against a wide range of targets, it is desirable to build libraries of devices comprising the same bioactive peptide but bearing different sets of targeting ligands. Hence attachment of the functional groups has to occur at as late a stage in the synthesis as practically possible. An excellent tool to accomplish this task is the so-called 'click' concept promulgated by Sharpless recently. Compatible with highly functionalized molecules, giving high yields of pure product, the ever-popular CuAAC 'click' reaction concurrently discovered by Meldal and Fokin,[14-16] seemed to be the reaction of choice. Already used in the Leigh group to attach highly functional groups to the macrocycle constituent of rotaxanes,[17] it seemed straightforward to adapt it to our system (Figure 6.2).

For a first trial, the groups attached to the rotaxane were chosen in such a way as to enhance solubility of the whole device, in addition to providing a model for a targeting ligand.

Knowing that several receptors display high affinity for carbohydrates (Glucose uptake transporters (GLUTs), galectins or asialoglycoprotein receptors), and can induce endocytosis upon binding (galectins or asialoglycoprotein receptors), it was a rational choice to take advantage of their highly hydrophilic character to simultaneously ameliorate the solubility of the device in aqueous media. The improved binding capacity of carbohydrate-containing polyrotaxanes to lectin receptors observed by Yui and co-workers also motivated this choice.[9,11] The

requirements when designing ligands that bind to these receptors vary considerably from one receptor to another. Monosaccharides (for GLUTs),[18] high molecular weight oligosaccharides[19] or saccharide cross-linked polymers.[20] could potentially be used as ligands. No attempt to design a specific ligand was made here, but emphasis was given to enhancing the aqueous solubility of the devices.

6.2 Result and discussion

6.2.1 Assessment of Gesson's nitrophenyl-malonaldehyde-based system as a self-immolative stopper

In a first attempt to build an autonomus anticancer device, a previously published trigger-spacer combination was used, which theoretical models (CPK) showed to be bulky enough to stopper a rotaxane assembly (Scheme 6.2).

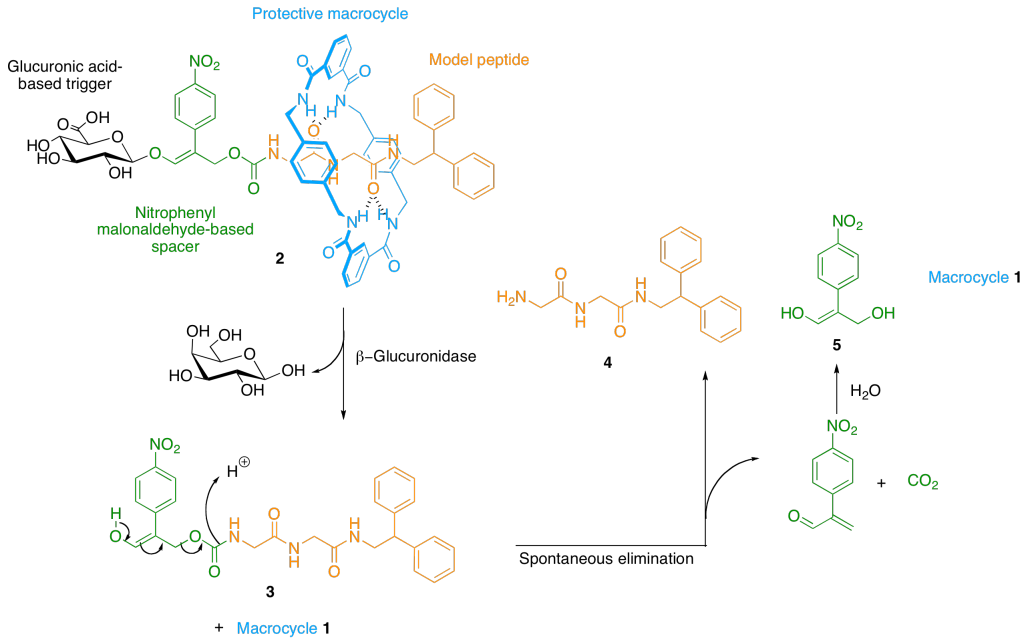

Scheme 6.2. Design of a nitrophenyl-malonaldehyde-based rotaxane propeptide model and its mechanism of drug release.

The trigger consists of the typical carbohydrate unit of Gesson's systems, whereas the spacer consists of a nitrophenyl-malonaldehyde-based unit, whose β-glucuronidase triggered-elimination is similar to that of the phenol-based spacer used in chapter 5. In this case, the trigonal arrangement of the sugar unit and the nitrophenyl group (present in the Met-enkephalin rotaxane propeptide *via* the Tyrosine residue) act as a stopper for the structure. Cleavage of the sugar moiety will

disrupt this arrangement and the macrocycle will slip over that end of the molecule. For initial studies, a sample of the imidazole-activated glucuronic acid version of the trigger-spacer building block **8** (Scheme 6.4) was provided by the group of Gesson,[21] and was successfully coupled to the glycylglycyl stoppered model peptide **4**.

Synthesis of **4** was carried out using conventional peptide chemistry, under 'activated' (EDCI and DMAP) coupling conditions (Scheme 6.3).

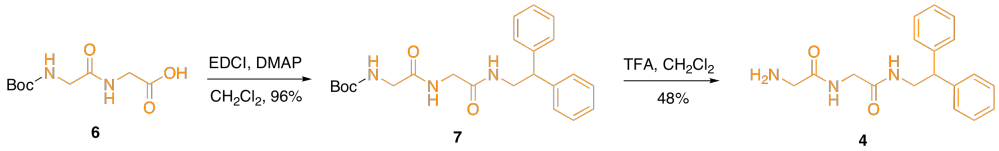

Scheme 6.3. Synthesis of model peptide fragment

Although the coupling step did not pose any problem (no risk of epimerization due to the presence of exclusively glycines), the final cleavage of the Boc protecting group was particularly laborious and **4** was obtained in reasonable purity only after several purification steps. Undesired DKP formation, often observed in peptide synthesis involving glycylglycine fragments,[22] was suspected to dominate the reaction, although none of the side products could be indentified. Subsequent coupling of **4** to the trigger-spacer group **8** proceeded with good conversion (Scheme 6.4), but unfortunately purification of the product was very difficult. Slow eluting silica gel chromatography column afforded thread **9** in sufficient purity to carry out the rotaxane formation step under the conditions mentioned previously.

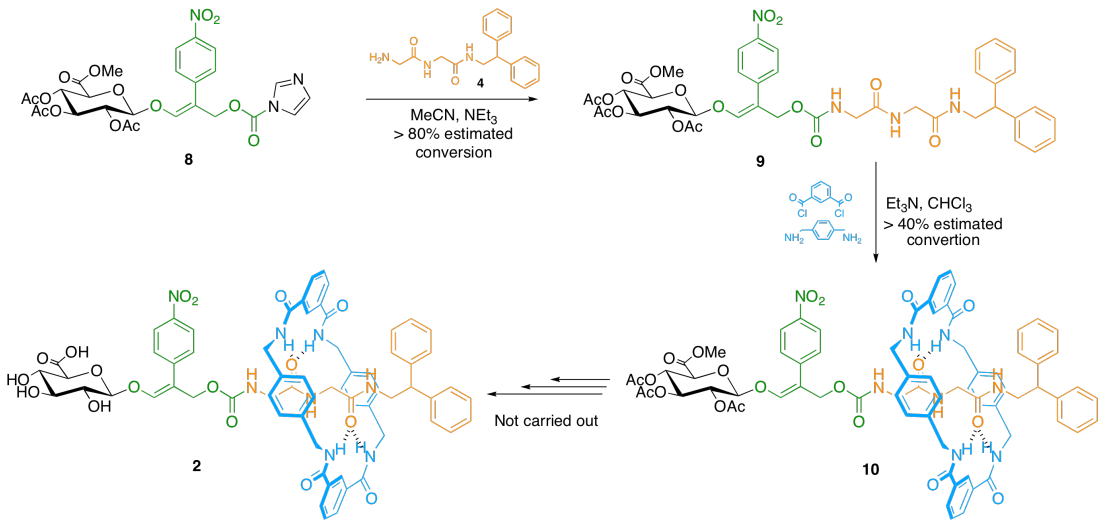

Scheme 6.4. Attempted synthesis of model rotaxane propeptide

The ^{1}H NMR spectrum of the crude mixture revealed good conversion to rotaxane **10** compared to the thread (~50%), but once again purification was difficult by any means attempted (silica gel, alumina or gel permeation chromatography). A relatively pure sample of rotaxane was obtained after purification by preparative TLC. Even though rotaxane **10** was not fully characterized, ^{1}H NMR analysis confirmed its structure. Unfortunately, leaving the sample in $CHCl_3$ over extended periods of time (approximatively 24 hours) resulted in high degree of decomposition to side products (revealed by ^{1}H NMR), preventing further synthetic steps. Qualitative assays later showed that light is the main factor affecting the stability of the molecule. Although never observed before (neither in the Met-enkephalin rotaxane propeptide nor by Gesson's research team), this fast rate of decomposition was attributed to the highly UV absorbing nitroaromatic unit combined to the hydrogen bonding effect of the macrocyclic amides.[23]

6.2.2 A bis-galactose-based self-immolative stopper

6.2.2.1 Design and synthesis

Despite synthetic setbacks, this initial trial set up the requirements for the design of the next generation propeptide models. Therefore, although the apparently unstable nitro group of the spacer could be replaced by a halogen atom,[24] substitution with a halogen would result in significantly slower elimination of the spacer than with a nitro group. However, as the spacer used in the Met-enkephalin rotaxane propeptide has proved stable when incorporated into a rotaxane structure, it was jugged sensible to develop on that same trigger-spacer core instead, substituting the aromatic ring to provide a similar trigonal junction as that in rotaxane **2**. A straightforward solution provided by the team of Gesson relied on a slightly modified version of this spacer where the position *para* to the nitro group is substituted by a second sugar unit (Scheme 6.5).

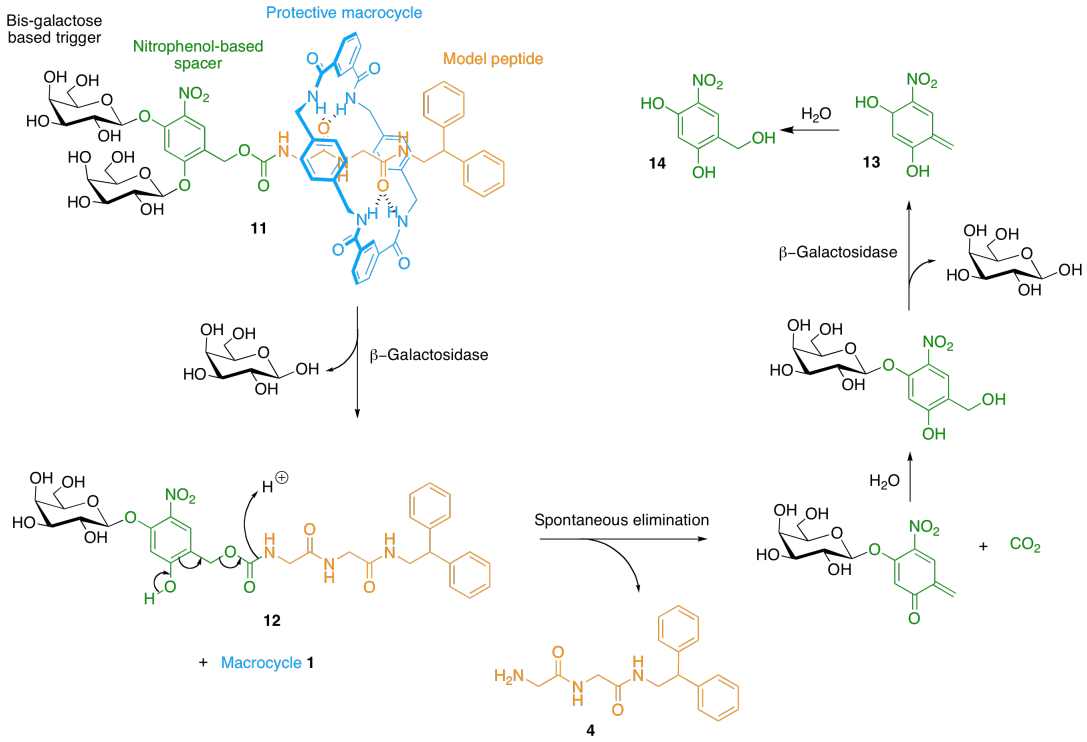

Scheme 6.5. Design of a bis-galactose based rotaxane propeptide model and its mechanism of peptide release

The advantage of such a system is that only one sugar unit has to be cleaved to allow for the quinone methide formation-decarboxylation cascade to occur, and dethreading can take place as soon as one sugar unit is cleaved (Scheme 6.5).

The synthesis of the trigger-spacer group shown, in β-galactose series, in Scheme 6.6 was based on a similar strategy to the one previously mentioned for Met-enkephalin propeptide spacer (Chapter 5).

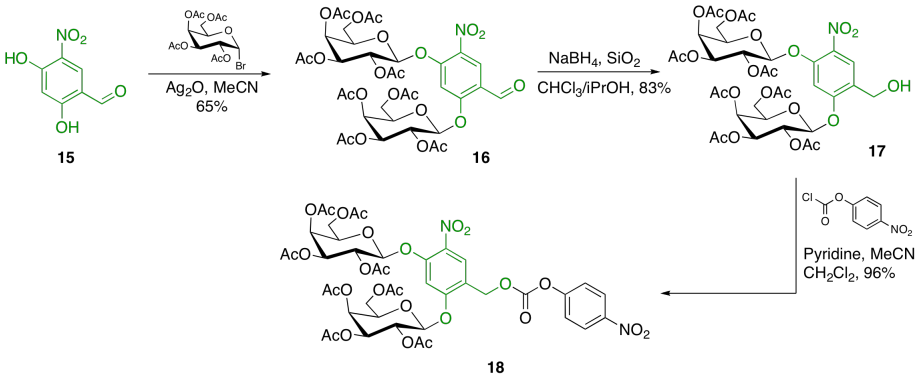

Scheme 6.6. Synthesis of bis-galactose based spacer

Starting from commercial aldehyde **15**, double Konigs-knorr reaction afforded precursor **16** in good yield which, after $NaBH_4$ reduction, furnished the activated carbonate **18** ready to be coupled to the peptide fragment.

Reacting model peptide **4** with the activated trigger-spacer unit **18** in MeCN overnight afforded thread **19** in good yield (Scheme 6.7). Rotaxane-forming reaction using the standard 16-fold excess of macrocycle precursors gave **21** in 43% yield, which was purified from the unreacted thread by gel permeation chromatography. Cleavage of the acetyl protecting groups finally afforded model rotaxane propeptide **11**. Precipitation in Et_2O gave a sufficiently pure batch of product to attempt preliminary enzymatic trials.

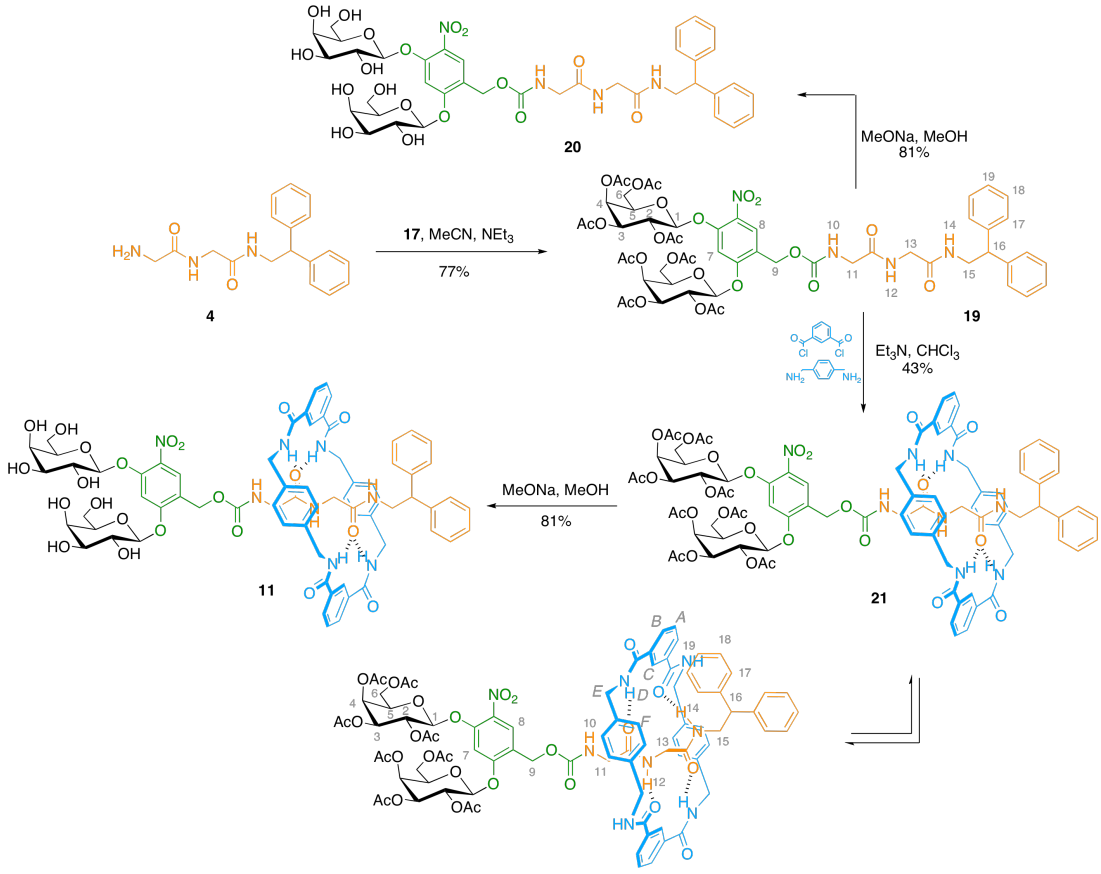

Scheme 6.7. Synthesis bis-galactose based rotaxane propeptide model

The ^1H NMR spectrum of the acetyl-protected rotaxane **21**, together with the spectrum of the non-interlocked thread, are shown in Figure 6.3. The spectrum shows the characteristic shifts of an interlocked structure. The strong upfield shift of the glycine proton signals indicates that the macrocycle predominantly resides over the peptide backbone. However, it can readily access the nitrophenyl core of the spacer unit, manifested in the upfield shift exhibited by signals of protons H_8 and H_9.

Downfield shift of the signals given by protons H_{12} and H_{14} are indicative of hydrogen bonding to the macrocycle, which adopts a twisted conformation (Scheme 6.7).

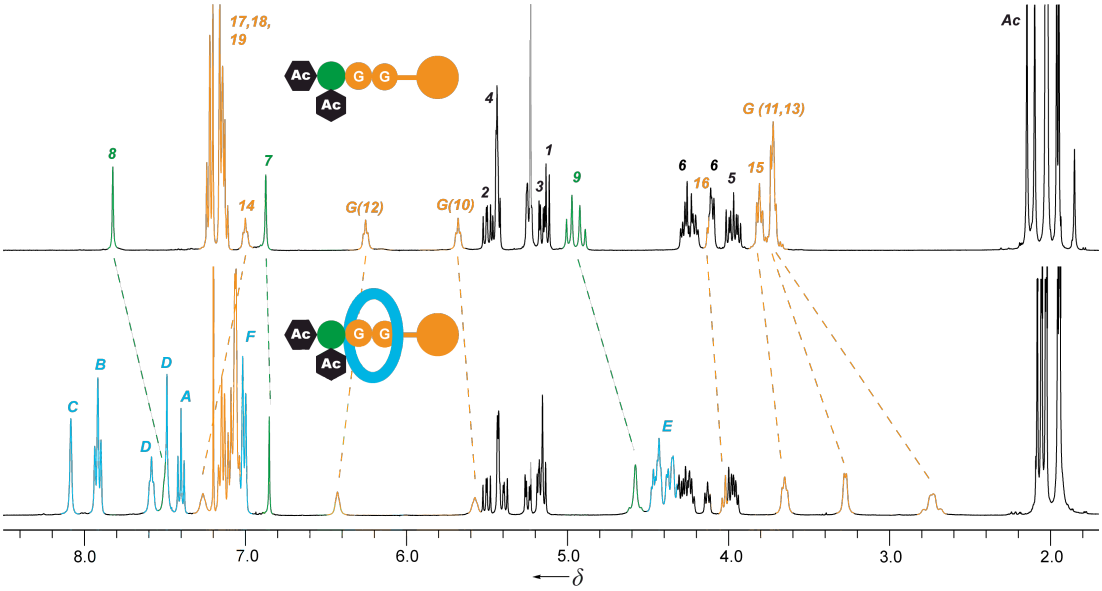

Figure 6.3. ^{1}H NMR spectra (400 MHz, $CDCl_3$, 300K) of a) propeptide **20**, b) Rotaxane propetide **21**. The assignments and colouring of signals correspond to that shown in Scheme 6.7. Residual solvent peaks are shown in grey.

6.2.2.2 *In vitro* trials

Preliminary enzymatic assessments with β-galactosidase on the rotaxane-encapsulated model propeptide could, unfortunately, not be carried out in satisfactory solubility conditions. Although the presence of two galactose units in the structure were expected to greatly enhance solubility in aqueous media, rotaxane **11** showed very poor solubility in purely aqueous buffer. This trend was found to be only slightly improved in a 1:1 mixture of phosphate buffer/DMSO. In these dilute and very high DMSO-content solutions, almost no cleavage could be observed in the presence of β-galactosidase, even using a very high enzyme/substrate ratio.

Nevertheless, hydrolysis studies on the non-rotaxane protected thread **20** has enabled the evaluation of the new trigger-spacer group. It, indeed, exhibited higher solubility than its interlocked analogue, and β-galactosidase assays could be carried out under satisfactory dilution conditions.

It was therefore surprising to find that when thread **20** is in the presence of the enzyme, the cleavage of the galactose trigger was rather messy, although some

peptide is released. A chromatogram of the enzymatic hydrolysis of thread **20** after 45 minutes is shown in Figure 6.4.

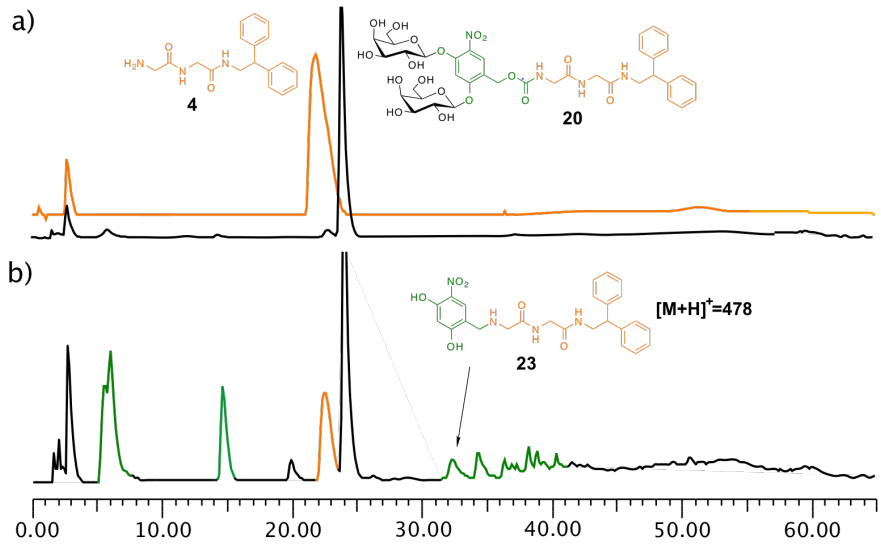

Figure 6.4. HPLC traces of hydrolysis of propeptide **20**, with *E. coli* β-galactosidase in phosphate buffer (0.02 M, pH 7.0), at 37 °C using 80 U/μmol of substrate (substrate concentration 0.5 mM): a) references of individual components **4** and **20**, after b) t = 45 min., The peaks coloured in green are those observed when the chromatogram is recorded at 420 nm.

As well as peaks due to the released peptide and remaining starting material several additional peaks were observed, in contrast to the only-expected spacer elimination adduct **14** (Scheme 6.5). Identification of **14** failed using several methods. In order to produce a reference, synthesis of **14** was attempted by reduction of commercial aldehyde **15**. The use of either $NaBH_4$ or $LiAlH_4$ as reducing agents led to decomposition of starting material, unfortunately.

Nevertheless, some valuable information could be drawn from the chromatogram recorded at 420 nm, the wavelength where the nitrophenol core exhibits a characteristic absorption (giving an intense yellow colour). At this wavelength, only the compounds containing the nitrophenol core are expected to appear. Surprisingly, most of the peaks of the by-products detected at 254 nm appeared in the trace recorded at 420 nm (shown in green in the chromatogram recorded at 254 nm, Figure 6.4b), meaning that these compounds very likely have the nitrophenol group in their structure.

To gain a better understanding of how these by-products are formed, LCMS was carried out using the electrospray ionization technique. Unfortunately, both positive

and negative ionization mode gave only the ion peak of one species (Figure 6.4b) and the expected elimination adduct **14** could not be identified.[25] The peak at Rt = 32 min ($[M+H]^+$ = 478) corresponding to compound **23** (Figure 6.4b), which is the product of nucleophilic attack of the released peptide on the quinone methide intermediate **13** (Scheme 6.5), confirms our hypothesis.

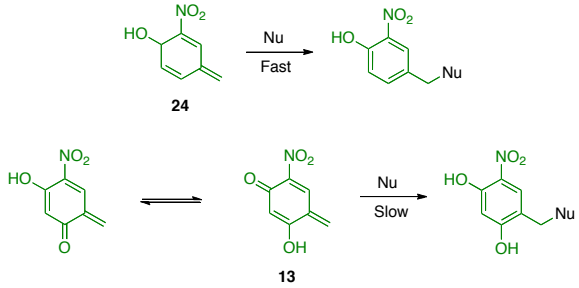

Scheme 6.8. Reaction of quinone methide **13** and its tautomer with nucleophiles.

With these data in hand, it was possible to rationalize the production of side products during enzymatic cleavage by the attack of nucleophiles (other than water) on the quinone methide intermediate **13**. Indeed, a recent study[26] shows that quinone methides substituted with electron-donating groups are much less reactive than those unsubstituted or substituted with electon-withdrawing groups. Thus, the presence of the extra donating OH group in intermediate **13** presumably renders it less reactive than its analogue **24** (produced in the study of chapter 5, Scheme 6.8). The kinetics of the reaction of **13** with the surrounding water to produce **14** will be inherently slower. Nucleophilic attack on the Michael acceptor by stronger nucleophiles present in solution will then be favourable (confirmed by the presence of **23**, figure 6.4). The side products observed can thus derive from oligomerization of **13**, for example, or from attack of some nucleophilic residues of the enzyme.[27] Carrying out the enzymatic hydrolysis in varying concentrations confirmed this hypothesis as the degree of side product produced increased with substrate concentration. Diluting the reaction medium led to less side products but extended reaction times, and the conditions in Figure 6.4 were found to be optimum, although reaction did not reach completion after several hours and many side products were detected. Unfortunately even under these optimized conditions the behaviour of this new trigger-spacer combination is very far from reaching the minimum standard for targeted drug release and had to be abandoned.

6.2.3 The serendipitous discovery of an allyl-substituted nitrophenol spacer

6.2.3.1 Synthesis

While looking for new alternatives of self-immolative spacers, an intriguing side product was produced from the allyl-protection reaction leading to **25** (Scheme 6.9). What was found to be the product of a Claisen rearrangement, **26**, showed to our surprise that, in combination with a sugar unit would act as suitable stopper (by CPK models). Although substitution of the position *ortho* to the phenoxy group can, in some cases, be detrimental to substrate recognition by the enzyme, it is likely that an allyl group would have only a minor effect.

Optimization of the Claisen rearrangement led to a good yield of allyl-substituted precursor from allyl-protected nitrophenol **25** (Scheme 6.9). Coupling with peracetylated bromogalactose afforded – after $NaBH_4$ reduction, and subsequent activation – the trigger-spacer, ready to couple to the model peptide.

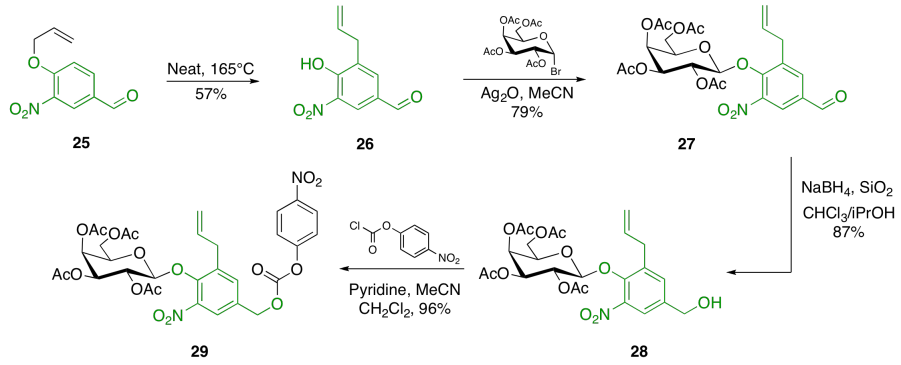

Scheme 6.9. Synthesis and activation of the Trigger-spacer unit

To be able to produce a large quantity of peptide, the low yielding synthesis of the glycylglycyl model **4** was abandoned in favour of synthesis of the tripeptidic analogue **34**, using a CbZ protecting group scheme. The potential formation of DKP adducts is now avoided and final deprotection using H_2 over Pd/C afforded pure **34** in good overall yield (Scheme 6.10).

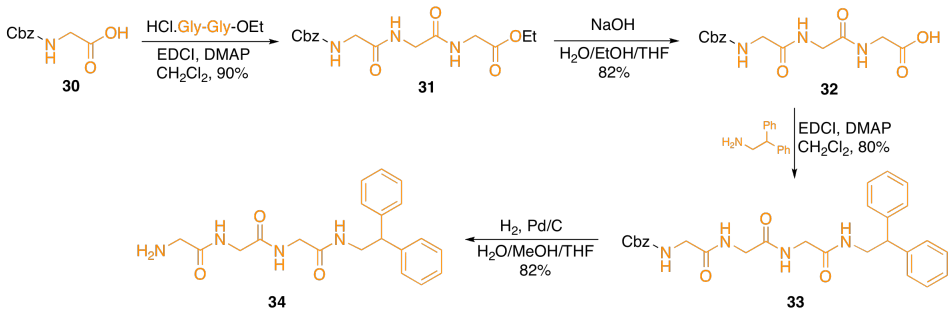

Scheme 6.10. Synthesis of model peptide drug

The assembly of the rotaxane propeptide was carried out under previously described conditions. Scheme 6.11 shows the synthesis of rotaxane **38**, together with its corresponding thread, necessary for enzymatic comparative studies. Final rotaxane and thread were purified by preparative RP-HPLC.

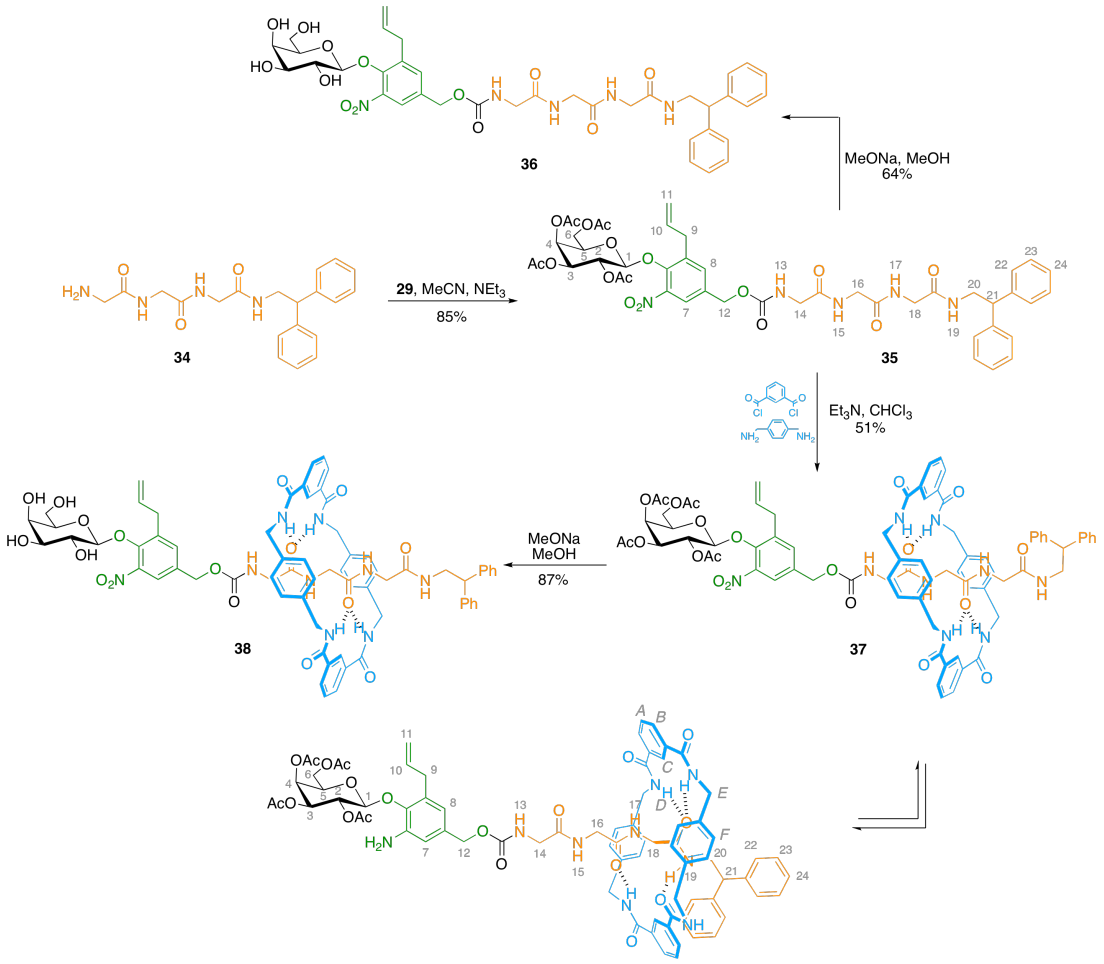

Scheme 6.11. Synthesis of model rotaxane propeptide and thread propeptide.

6.2.3.2 *In vitro* β-galactosidase assays

Preparative HPLC afforded thread **36** and rotaxane **38** in high enough purity to subject them to β-galactosidase assays. The mechanism of peptide release is shown in Scheme 6.12.

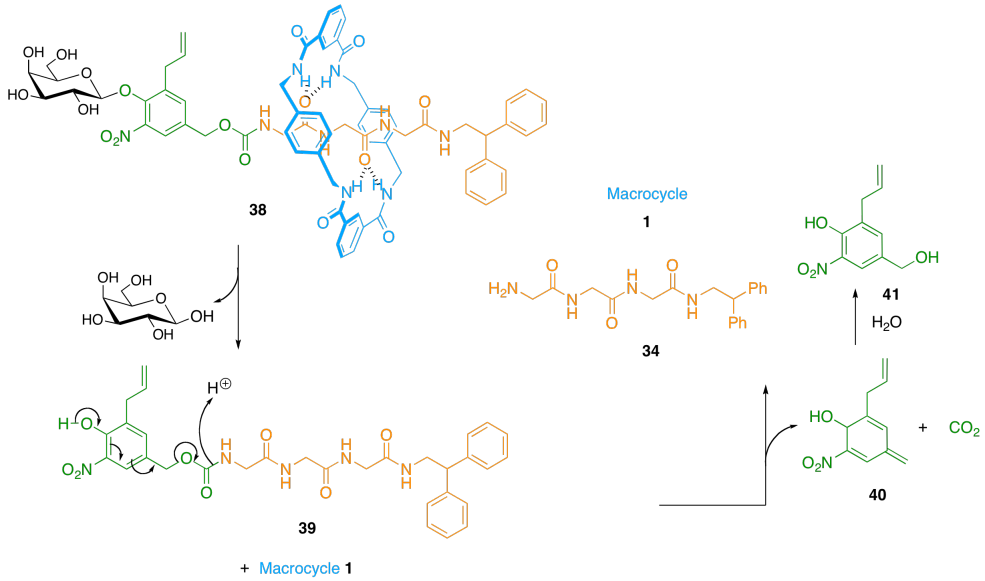

Scheme 6.12. Mechanism of peptide release

Again, rotaxane **38** displayed very poor solubility in purely aqueous media (Table 6.1) and a high volume of DMSO was necessary to solubilize it in a phosphate buffer solution. As expected, under these conditions, the assay did not give any meaningful results.

Nevertheless, thread **36** was sufficiently soluble in a 9:1 mixture of phosphate buffer/DMSO and enzymatic hydrolysis was found to reach an acceptable rate using a 10 fold excess of enzyme compared to that used with the Met-enkephalin rotaxane studied previously. As shown in Figure 6.5, peptide release reached completion after 1 h 30 min and was achieved in quantitative yield (measured by HPLC).

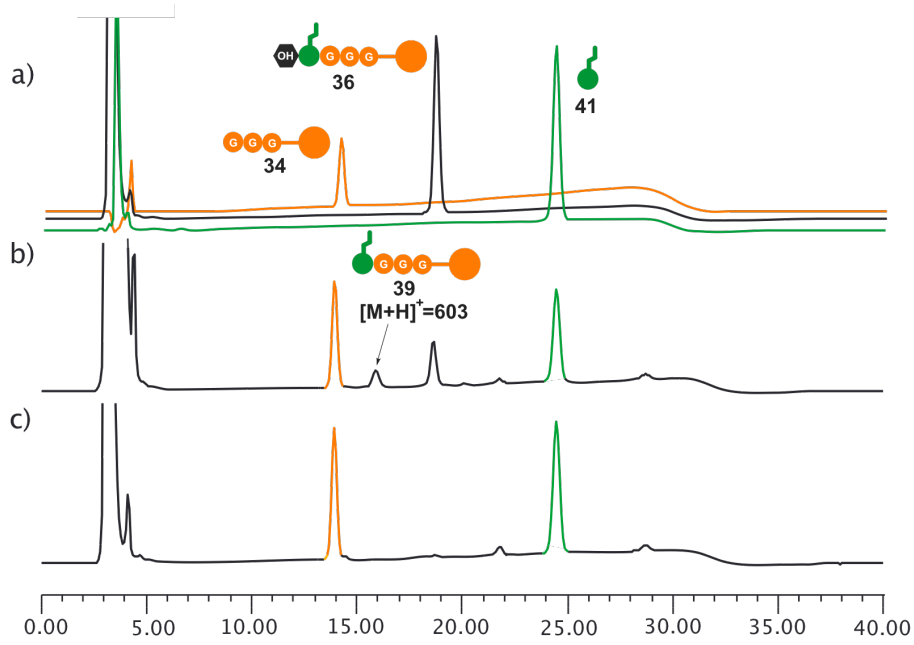

Figure 6.5. HPLC traces of hydrolysis of propeptide **36**, with *E. coli* β-galactosidase in 90 % phosphate buffer (0.02 M, pH 7.0), 10 % DMSO, at 37 °C using 100 U/μmol of substrate (substrate concentration 0.2 mM): a) references of individual components **34**, **36** and **41**, after b) t = 1 h, c) 1 h 30 min.[28]

It is worthy to note that the intermediate arising from hydrolysis of the sugar before the spacer undergoes elimination (**39**, Scheme 6.12) is observed here as well (Figure 6.5). Interestingly, contrary to the Met-enkephalin rotaxane propeptide, the ratio between intermediate **39** and propeptide **36** appears to be much less significant[29] and, more importantly, as opposed to Met-enkephalin rotaxane propeptide, the starting thread **36** is not totally consumed before intermediate **39** is consumed. Hence, in this case, the limiting step is not the elimination of the spacer but the hydrolysis of the carbohydrate unit by the enzyme (see chapter 5). This is in accordance with the expected weaker affinity of β-galactosidase for this new galactose-allylnitrophenol unit (due to substitution at the *ortho* position). Overall, even though it exhibits slower hydrolysis kinetics, the allyl-based spacer was jugged to be a good starting point for the assessment of the enzymatic cleavage of rotaxane propeptide models solely stoppered by a trigger-spacer unit.

6.2.4 Funtionalization of the macrocycle with glucose-based groups

To be able to enhance solubility of the rotaxane propeptide and at the same time produce a model for ligand-targeted therapy, it was decided, as a first step, to attach two glucose groups to the macrocycle constituent. To assess the effect of this on solubility, two different rotaxanes were synthesized in which the glucose groups were linked to the structure either directly or via an intercalating tetraethyleneglycol (TEG) group. A third rotaxane, functionalized solely by the TEG linker, was also synthesized in order to determine the influence of this linker on the solubility of the rotaxane (Scheme 6.13).

To link the glucose groups to the macrocycle, the popular concept of 'click' chemistry[30] was found to be the perfect tool to obtain high yields of pure products. The highly tolerant and high yielding 'click' CuAAC (Copper-catalyzed Alkyne-Azide Cycloaddition) reaction – popularized by Meldal and Fokin[14,15] – allows for very late stage diversification starting from an easy to prepare azide-functionalized rotaxane. Following precedent from the Leigh group,[17] a rotaxane, **42**, bearing a bis-azide functionalized macrocycle was synthesized from 5-azidoisophthaloyl dichloride and *para*-xylylenediamine (Scheme 6.13). The yield was surprisingly high, and, more interestingly, purification by ordinary silica gel flash chromatography was possible without the need to carry out an additional gel permeation chromatography purification step. The reaction could be easily scaled up, and a large batch of rotaxane **42** allowed for CuAAC reaction trials.

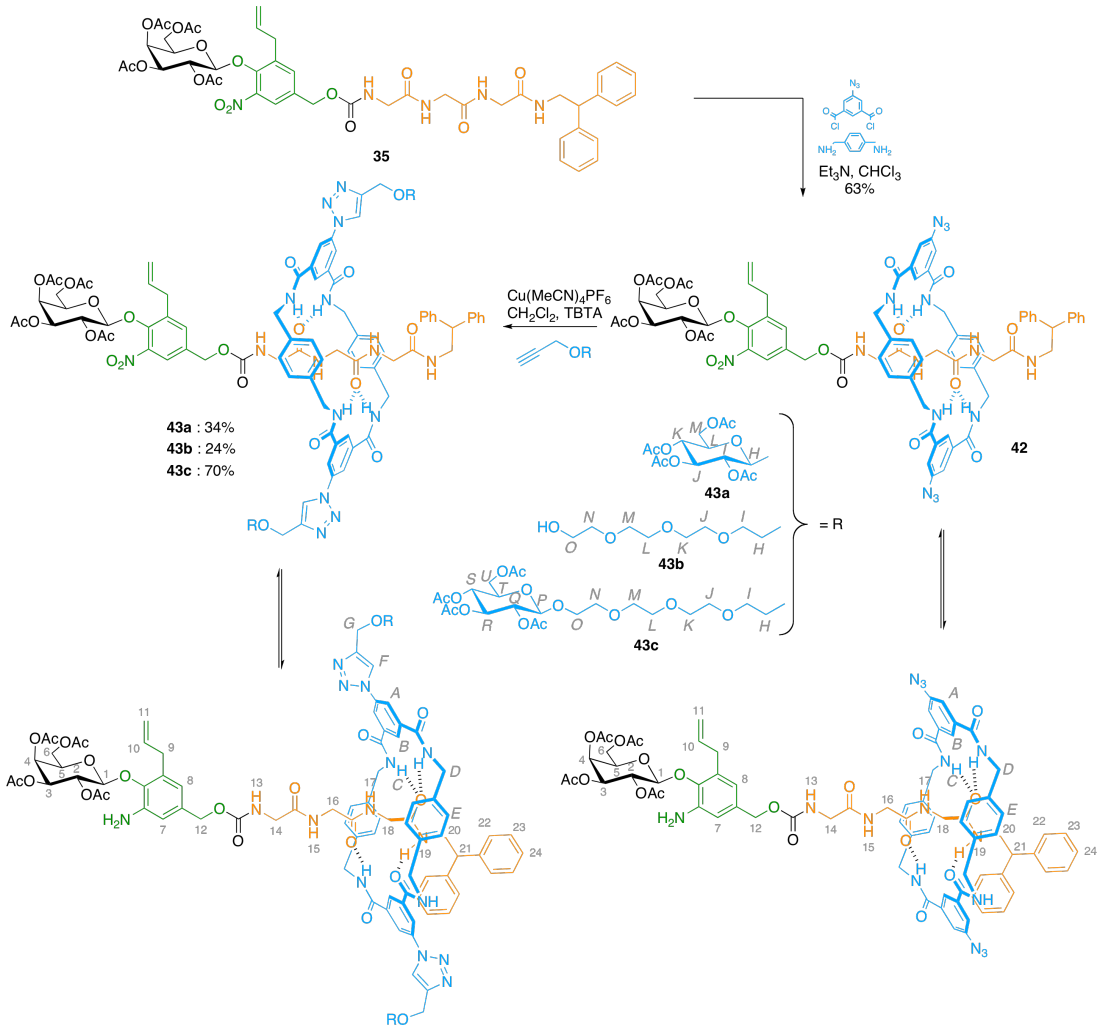

Scheme 6.13. Synthesis of functionalized rotaxane propeptide models.

Meanwhile, the three alkyne fragments were prepared. The synthesis was based on well-known chemistry, starting from cheap, commercially available starting materials (Scheme 6.14). The alkyne functionality was introduced by linking of a propargyl unit. Following literature procedures,[31] propargyl alcohol was coupled to peracetylated β-glucose **44**, to yield fragment **45**. TEG was desymmetrized using propargyl bromide, affording fragment **46**,[32] which was used to prepare the mixed TEG-glucose derivative **47**. The glucose units were left protected for the CuAAC reaction and were deprotected, together with the galactose from the thread, at the very last step.

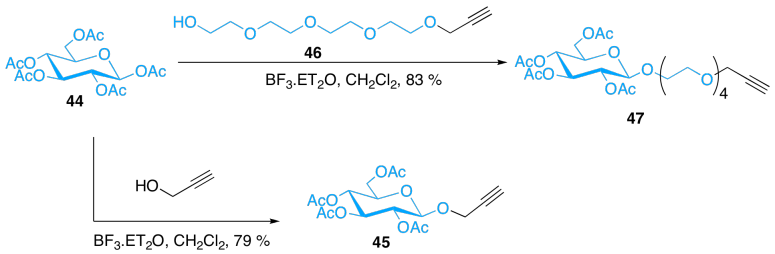

Scheme 6.14. Synthesis of hydrophilic targeting ligand models

The CuAAC reaction trials were primarily performed using procedures described by the Leigh group.[17,33] Stirring a mixture of rotaxane **42** with alkyne **45**, **46** or **47** in the presence of a catalytic amount of copper salt and Et_3N in dry CH_2Cl_2 overnight afforded the desired product in apparent good conversion (seen by NMR analysis of the reaction mixture) (Scheme 6.13). However, upon purification by flash chromatography, the yield dropped considerably (<35%, for all three rotaxanes). In each case, purification proved very difficult due to a co-eluting spot of very similar R_F value to that of the product. Reaction conditions were modified in an attempt to circumvent this purification issue. Adding TBTA [34,35] to the reaction mixture did not show any notable improvement and carrying out the reaction under Fokin's original conditions[15] failed to produce any product presumably due to poor solubility of the substrates in the aqueous-based solvent mixture.

Examination of the reaction of rotaxane **42** with fragment **47**, after extensive purification by preparative TLC, revealed that pure product could be isolated in 70% yield. Isolation and ^{1}H NMR analysis of the side product suggested a compound similar to **43c**, however its exact structure could not be elucidated. A mono-substituted adduct was, however, ruled out by mass spectrometry.

According to the latter result, it then appears that the low isolated yields obtained for **43a** and **43b** were as well due to purification issues. Side products are presumably formed by Cu(II)-promoted side reactions and screening of different Cu(I) stabilizing ligands would allow for the reaction conditions to be optimized. However, this work is not described here.

The synthesis of model rotaxane propeptides was completed by the acetyl-deprotection of the carbohydrate units, which proceeded smoothly in MeONa/MeOH (Scheme 6.15).

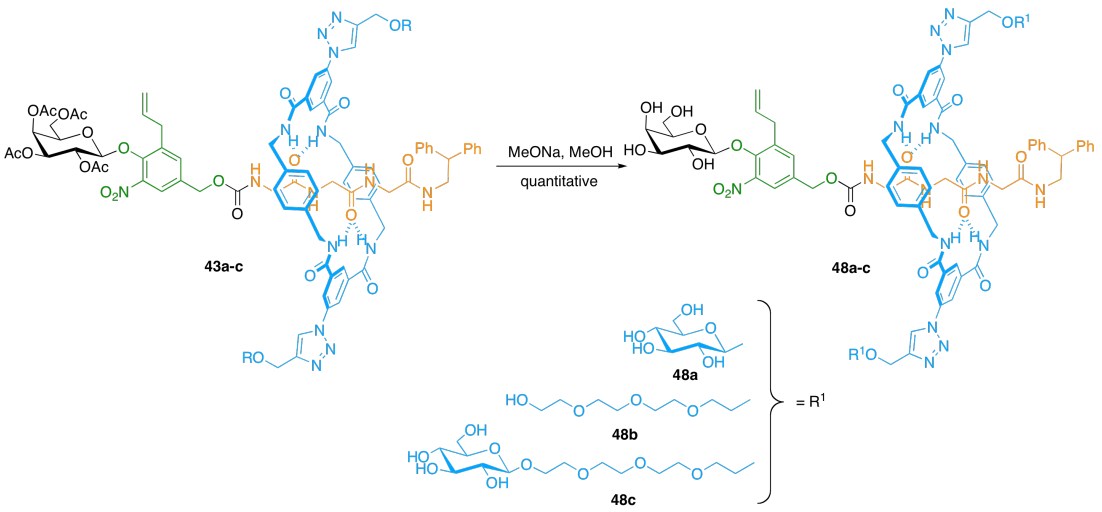

Scheme 6.15. Final cleavage of the acetyl protecting groups

6.2.5 Isolation of macrocycles *via* rotaxane synthesis followed by controlled dethreading

One issue that arises from the release of the peptide *in vivo*, is that of the fate of the remaining components of the rotaxane, released concomitantly. If the biological activity of the peptide is supposed to be known, the toxicity and metabolism of the spacer adduct and of the macrocycle would have to be studied additionally. To do so, it is necessary to develop a general method to isolate the macrocycle constituent of the rotaxanes synthesized.

The release of the macrocycle alongside the peptide could also be exploited for the delivery of an additional bioactive compound to the same target. Thus, functionalization of the macrocycle with bioactive compounds would give one more function to the macrocycle, aside from protecting the peptide, targeting it and improving the solubility of the rotaxane.[36] This functionalization will not be discussed here, but the isolation of the free macrocycles synthesized as part of our rotaxane propeptide models will be described. Their solubility in aqueous media will be measured.

As previously reported, the synthesis of benzylic amide macrocycles *via* the direct condensation of the corresponding diacyl chlorides and *para*-xylylenediamine leads predominantly to [2]catenanes.[37] The isolation of the macrocycle was, however, proved possible by hydrolysis of an ester-stoppered rotaxane.[38] Similarly, using the more efficient fumaramide template and the commercially available acid **49**, thread

50 was synthesized (Scheme 6.16), which, after rotaxane formation and attachment of the appropriate hydrophilic groups, could be hydrolyzed to release the corresponding macrocycles **53a**, **53b** and **53c** (Scheme 6.16).

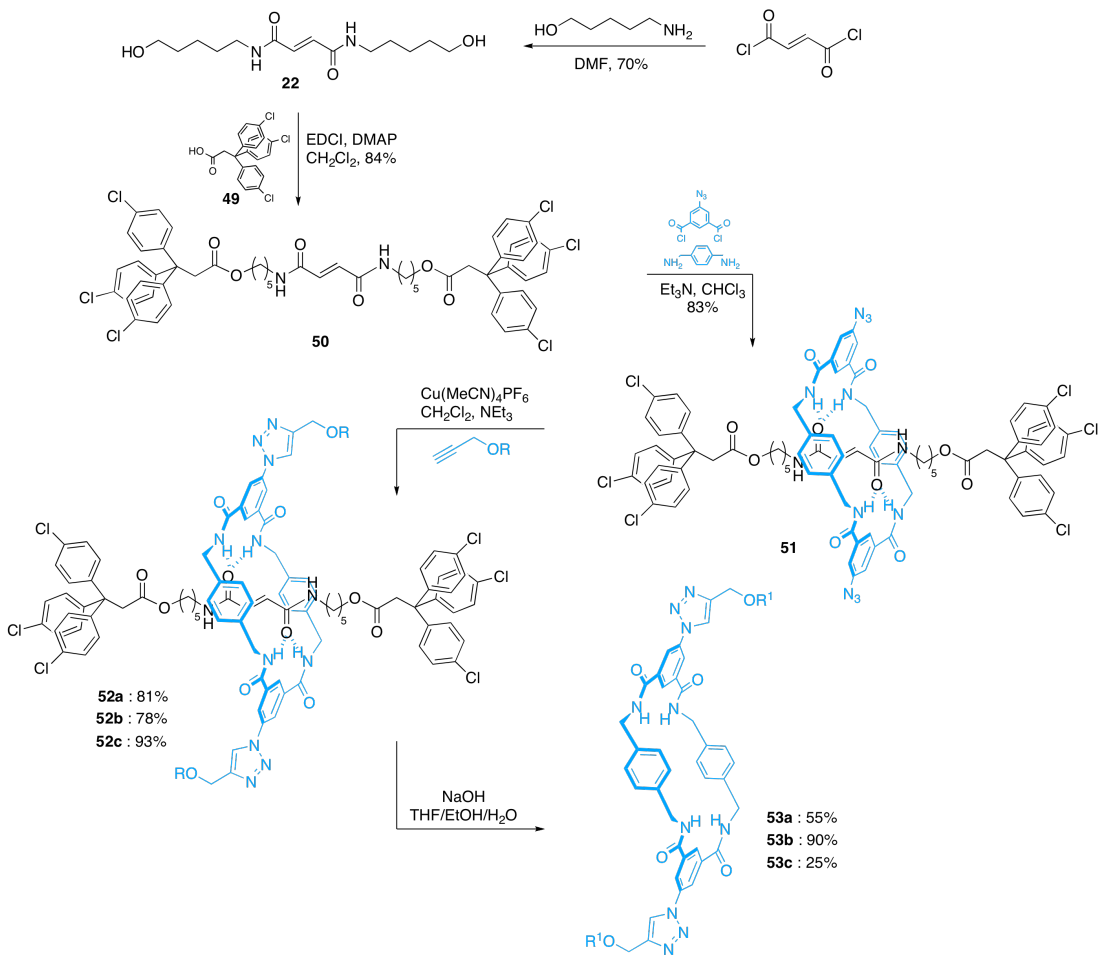

Scheme 6.16. Synthetic pathway for the isolation of functionalized macrocycles. Groups R and R^1 correspond to those depicted in Schemes 6.13 and 6.15 respectively.

The hydrolysis step proved to be capricious and did not give good results using similar conditions to that reported in the literature.[39] The desired products were obtained by carrying the reaction out in a concentrated solution of NaOH in a mixture of THF/EtOH/H_2O over extended periods of time. Free macrocycles were isolated with their carbohydrate residues fully deprotected. **53a** precipitated out from solution and was pure enough, after several washings. **53b** and **53c** were further purified by preparative RP-HPLC.

6.2.6 Solubility of rotaxane propeptides

To assess the effect of the hydrophilic groups on the solubility of the rotaxanes and the free macrocycles, quantitative solubility measurements in water were carried out. A known quantity of each compound was dissolved in a known volume of DMSO/X/H_2O (X= MeOH, EtOH or MeCN) and the solution was analyzed by HPLC. The absolute area of the peak of interest was then compared with the area of the peak produced by a saturated solution of the same compound in pure water at 20°C. The solubility of some of the propeptides synthesized thus far, together with that of the free macrocycles is reported in Table 6.1.

Table 6.1. Solubility of rotaxanes propeptide and free propeptides

Compound	Solubility in water (at 20°C, in mol/L)	Solubility in water (at 20°C)
Propeptide **36**	$8.6 \cdot 10^{-4}$	663mg/L
Rotaxane propeptide **38**	$3.8 \cdot 10^{-7}$	<500ug/L
Rotaxane propeptide **48a**	$3.0 \cdot 10^{-7}$	555ug/L
Rotaxane propeptide **48b**	$6.0 \cdot 10^{-6}$	11mg/L
Rotaxane propeptide **48c**	$2.2 \cdot 10^{-2}$	49.1g/L
Macrocycle **53a**	$4.7 \cdot 10^{-7}$	<500ug/L
Macrocycle **53b**	$1.7 \cdot 10^{-5}$	18mg/L
Macrocycle **53c**	$1.7 \cdot 10^{-4}$	236mg/L
Met-enkephalin propeptide	$2.3 \cdot 10^{-3}$	2.2g/L
Met-enkephalin rotaxane propeptide	$4.6 \cdot 10^{-4}$	674mg/L

The solubility of the rotaxanes was seen to increase with the flexibility of the structure. Surprisingly, rotaxane **48a** was almost completely insoluble in water, despite containing two polar hydrophilic glucose groups on the macrocycle and one galactose on the thread. The flexibility of the less polar TEG groups on rotaxane **48b**, accounts for its slightly higher solubility (11mg/L). A combination of both flexibility

and hydrophylicity is exhibited by rotaxane **48c**, which shows an exceptionally high solubility (49g/L), compared to rotaxane **48a** and **48b**. This clearly demonstrates the need for both flexibility and hydrophilicity in the molecule.

The same trend is followed by the free macrocycles, but to a lesser extent. The highest solubility is seen for macrocycle **53c** (236 mg/L), as expected. Macrocycle **53b**, although not very soluble in water, shows high solubility in a wide range of organic solvents. This is not the case for **53a** however; even though it contains two carbohydrate hydrophilic groups, it displays a similar solubility to that of the original non-substituted macrocycle (<500 mg/L).

6.2.7 ^{1}H NMR spectra of Ally-nitrophenol-based rotaxane propeptides

The ^{1}H NMR spectra of rotaxanes **37**, **42** and **43a-c** are shown in scheme 6.6, together with the spectrum of the non-interlocked thread **35**. They all show the common features of interlocked molecules, with the signals of the thread counterpart shifted upfield in the rotaxanes. The Glycine residues' signals are shifted furthest upfield, which is evidence for a slight preference of the macrocycle for the peptidic fragment over the rest of the molecule (due to the high number of consecutive carbonyl groups). The aromatic protons of the spacer, H_7, H_8 and H_{11} are considerably shielded showing that the macrocycle is accessing this part of the thread. All rotaxanes, without exception, have their terminal amide proton, H_{19}, shifted downfield which is characteristic of a hydrogen bonded amide. The high multiplicity of the splitting due to H_E of the macrocycle, is a sign of slow pirouetting. This gives strong evidence that H_{19} is hydrogen bonded to a carbonyl of the macrocycle, through a twisted conformation (Scheme 6.11 and 6.13).

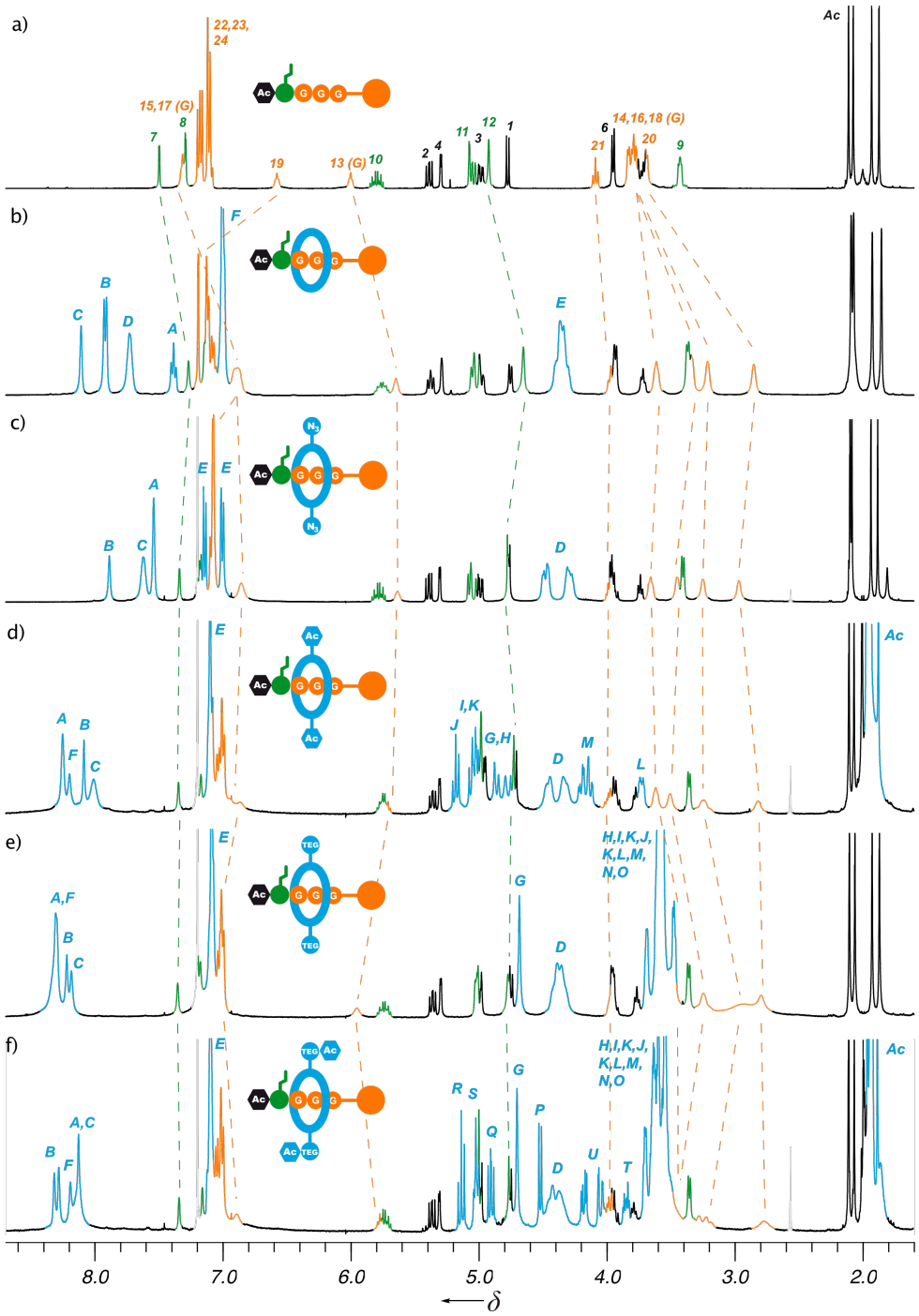

Figure 6.6. ^{1}H NMR spectra (400 MHz, $CDCl_3$, 300K) of a) propeptide **35**, b) Rotaxane propeptide **37**, c) Rotaxane propeptide **42**, d) Rotaxane propeptide **43a**, e) Rotaxane propeptide **43b**, f) Rotaxane propeptide **43c.** The assignments and colouring of signals correspond to that shown in Scheme 6.11 and 6.13. Residual solvent peaks are shown in grey.

6.2.8 *In vitro* β-galactosidase assays

All three rotaxanes were tested for β-galactosidase hydrolysis. The solubility of **48c** in neat phosphate buffer was optimum and was then used for preliminary trials. Unfortunately it was found that with the same substrate/enzyme ratio used for the non-interlocked thread, the reaction was very slow and almost not noticeable. Increasing the amount of enzyme ten fold (1000 U enzyme/μmol substrate) showed clean cleavage and quantitative release of peptide (by HPLC), but the process was complete only after 10 hours (Figure 6.7).

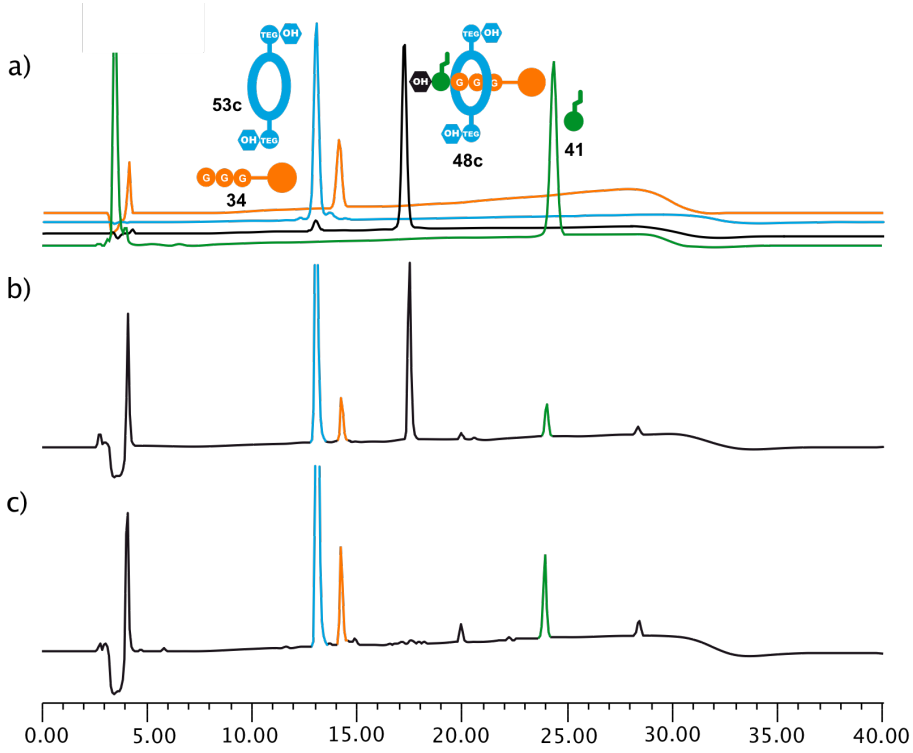

Figure 6.7. HPLC traces of hydrolysis of propeptide **48c**, with *E. coli* β-galactosidase in phosphate buffer (0.02 M, pH 7.0), at 37 °C using 1000 U/μmol of substrate (substrate concentration 0.2 mM): a) references of individual components **34**, **41**, **48c** and **53c**, after b) t = 2 h, c) 10 h.

Rotaxanes **48a** and **48b** were very difficult to solubilize under the assay conditions even in a solution containing more than 10% DMSO. Turbid solutions of both rotaxanes in a DMSO/phosphate buffer (1:9) solution were used in the same concentration conditions as above but, as expected, did not give great results. Cleavage of rotaxane **48b** did not reach completion even after 24 hours with the

same substrate/enzyme ratio as above (Figure 6.8). This slower rate of hydrolysis is most probably related to its poor solubility.

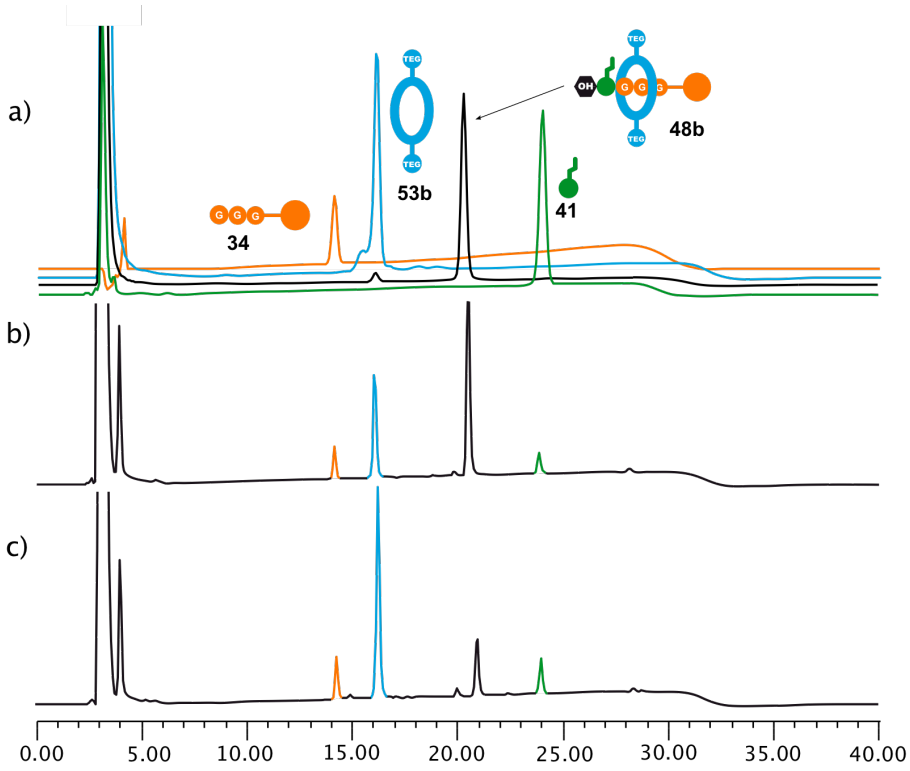

Figure 6.8. HPLC traces of hydrolysis of propeptide **48b**, with *E. coli* β-galactosidase in 90 % phosphate buffer (0.02 M, pH 7.0) and 10% DMSO, at 37 °C using 1000 U/μmol of substrate (substrate concentration 0.2 mM): a) references of individual components **34**, **41**, **48b** and **53b**, after b) t = 8 h, c) 24 h.

Rotaxanes stoppered with the allyl-based spacer exhibited a rate of hydrolysis greater than 100 times inferior to that of Met-enkephalin rotaxane. This decrease in rate compared to the free propeptide **36** is mainly due to the fact that the macrocycle can reach the spacer end of the thread to a considerable extent, interfering with the substrate/enzyme complex formation.

6.3 Conclusion

In conclusion, the development of a model for the construction of autonomous rotaxane carriers has been successful. It has been demonstrated that the attachment of functional groups on the macrocycle constituent of the device at a late stage in the synthesis is possible, and a small library of compounds has been prepared. Although the CuAAC reaction did permit the isolation of functionalized rotaxanes in high

yields in all cases, optimization of the reaction conditions by the screening of Cu(I) stabilization additives would improve this key step. Once optimized, the attachment of dendritic polysaccharides could be studied as a practical example of a targeting ligand.

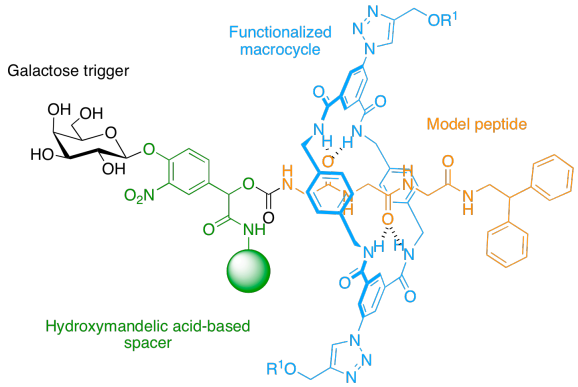

Figure 6.9. A new type of spacer in which blocking of the macrocycle is accomplished further away from the carbohydrate unit.

Furthermore, the development of peptide carriers solely stoppered by a self-immolative spacer has proved feasible. Although the rate of hydrolysis is presumably too slow to be practically useful in anti-cancer therapy, it has been demonstrated that this is partially due to the *ortho* substitution of the nitrophenol, and to a larger extent the fact that the macrocycle is accessing the spacer end of the molecule, interfering with enzyme recognition. To remedy this problem, a spacer with a blocking group attached further away from the carbohydrate unit may prevent the macrocycle accessing the recognition site. A recent example from Shabat, based on a hydroxymandelic acid core, where the blocking group is attached to the carbon α to the carbamate group, holds great potential for the development of new self-immolative stoppers (Figure 6.9).[40]

6.4 Experimental section

6.4.1 General methods

β-galactosidase enzymatic cleavage

Enzymatic galactose hydrolysis was carried out with commercial β-galactosidase from *Escherichia coli* E.C. 3.2.1.23 (1000 units/mg protein (biuret), aqueous glycerol suspension (1:1) in 10 mM Tris buffer salts containing 10 mM magnesium chloride, pH 7.3). Prodrugs were incubated at 37°C with the enzyme (10-100 Units/0.1 μmol of substrate) in 20 mM Phosphate buffer containing 2.5-10% (v/v) DMSO at pH 7.0 (concentration of substrate 0.2 mmol/L). Aliquots (20 μL) were periodically withdrawn from the medium and diluted into a solution of TFA (0.1%) in H_2O (40 μL). Hydrolysis was monitored by analytical HPLC and LCMS.

General method A: Benzylic amide rotaxane formation

To a vigourously stirred solution of thread (0.462 mmol, 1 equiv.) and NEt_3 (16.2 mmol, 35 equiv.) in 150 mL of dry $CHCl_3$ under nitrogen, was simultaneously added a solution of *p*-xylylenediamine (7.40 mmol, 16 equiv.) in $CHCl_3$ (50 mL) and a solution of isophthaloyl dichloride (7.40 mmol, 16 equiv.) in $CHCl_3$ (50 mL) over a period of 3 hours using motor-driven syringe pumps. The reaction mixture was stirred for a further 2 hours and filtered over a Celite® pad. The solid was washed with $CHCl_3$/MeOH 2 % (3 x 100mL) and the combined filtrates were concentrated under reduced pressure.

General method B: CuAAC coupling of model ligands on azide functionalized macrocycles

To a solution of rotaxane (0.035 mmol, 1.0 equiv.), alkyne (0.070 mmol, 2.0 equiv.), and $[Cu(CH_3CN)_4](PF_6)$ (0.017 mmol, 0.5 eq) in dry CH_2Cl_2 (5 mL) and under N_2 at room temperature was added NEt_3 (0.077 mmol, 2.2 equiv.) and the mixture was stirred overnight. Air was bubbled through the mixture for 15 minutes then a saturated solution of NH_4Cl was added (15 mL). The layers were separated and the aqueous layer was extracted with CH_2Cl_2 (1 × 10 mL). The combined organic

fractions were washed with a 1M solution of EDTA/K_2CO_3 (2 × 10 mL) and brine (10 mL), then dried ($MgSO_4$) and concentrated under reduced pressure.

General method C: Acetyl groups cleavage

To a solution of rotaxane or thread (0.025 mmol, 1 equiv.) in MeOH (5 mL) at 0°C was added drop-wise a solution of MeONa (0.25 mmol, 10 equiv.) in MeOH (1.5 mL) and the mixture was stirred for 1 hour at 0°C. The solution was neutralised with IRC-50 resin and filtered and the solvent was evaporated under reduced pressure.

6.4.2 Experimental procedure for the synthesis of bis-galactose-based propeptides

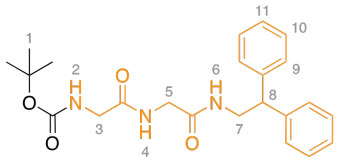

7

To a solution of *t*Boc-glycylglycine (2.63 g, 9.1 mmol, 1.0 equiv.), EDCI.HCl (2.09 g, 10.9 mmol, 1.2 equiv.) and DMAP (1.32 g, 10.9 mmol, 1.2 equiv.) in CH_2Cl_2 (100 mL) at room temperature, was added 2,2-diphenylethanamine (1.70 g, 8.6 mmol, 0.95 equiv.) and the reaction mixture was stirred overnight. An aqueous solution of HCl (1M) (150 mL) was added. The layers were separated and the aqueous layer was extracted with CH_2Cl_2 (3 × 50 mL). The combined organic fractions were washed with H_2O (50mL), dried ($MgSO_4$) and concentrated under reduced pressure. The crude solid was dissolved in CH_2Cl_2 (10 mL) and Et_2O (150 mL) was added. The resulting white precipitate was sonicated for 5 minutes and filtered by gravity to give **7** as a white solid (3.59 g, 8.7 mmol, 96%). **M.p. 142-144 °C**; **^{1}H-NMR (400 MHz, $CDCl_3$, 298 K):** δ = 7.35 (m, 1H, H_2 or H_4), 7.260-7.134 (m, 10H, H_9, H_{10} and H_{11}), 6.98 (m, 1H, H_6), 5.71 (m, 1H, H_2 or H_4), 4.152 (t, J = 8.5 Hz, 1H, H_8), 3.80 (d, J = 8.0 Hz, 2H, H_7), 3.691 (s, 2H, H_3 or H_5), 3.634 (s, 2H, H_3 or H_5), 1.40 (s, 9H, H_1); **^{13}C-NMR (100 MHz, $CDCl_3$, 298 K):** δ = 170.4, 168.9 (× 2), 141.6, 128.4, 127.8, 126.6, 80.2, 50.2, 43.6, 42.3 (× 2), 28.1; **LRESI-MS:** m/z = 412 $[M+H]^+$; **HRESI-MS :** m/z = 412.2230 $[M+H]^+$ (calc. for $C_{23}H_{30}O_4N_3$ 412.2231 $[M+H]^+$).

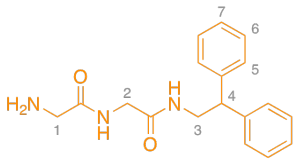

4

Compound **7** (133 mg, 0.43 mmol) was dissolved in a 15% (v/v) solution of TFA in CH_2Cl_2 (15 mL) and the mixture was stirred overnight at room temperature. Solvents were evaporated under reduced pressure. To the crude oil was added Et_2O (30 mL) and the resulting white precipitate was sonicated for 10 minutes and filtered by gravity. The solid was re-dissolved in CH_2Cl_2 (50mL), an aqueous saturated solution of $NaHCO_3$ (20 mL) was added, the layers were separated and the aqueous layer was extracted with CH_2Cl_2 (5 × 50 mL). The combined organic fractions were dried ($MgSO_4$) and concentrated under reduced pressure to afford pure **4** as a light yellow oil (48%). **^{1}H-NMR (400 MHz, $CDCl_3$/CD_3OD (3:1), 298 K):** δ = 7.31-7.12 (m, 10H, H_5, H_6 and H_7), 4.26-4.12 (m, 3H, H_3 and H_1 or H_2), 3.83 (d, J = 8.0 Hz, 2H, H_4), 3.72 (s, 2H, H_1 or H_2); **^{13}C-NMR (100 MHz, $CDCl_3$/CD_3OD (3:1), 298 K):** δ = 173.4, 169.8, 142.1, 128.8, 128.2, 127.0, 50.6, 44.1 (× 2), 42.6; **LRESI-MS:** *m/z* = 312 $[M+H]^+$; **HRESI-MS:** *m/z* = 312.1705 $[M+H]^+$ (calc. for $C_{18}H_{22}O_2N_3$ 312.1707 $[M+H]^+$).

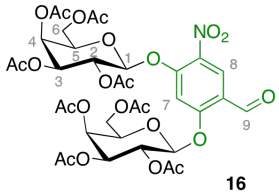

16

To a solution of α-D-galactopyranosyl bromide-2,3,4,6-tetraacetate (3.3 g, 8.38 mmol, 2.1 equiv.) in CH_3CN (30 mL) at 0°C was added 2,4-dihydroxy-5-nitrobenzaldehyde (730 mg, 3.99 mmol, 1 equiv.) and Ag_2O (2.3 g, 9.97 mmol, 2.5 equiv.). The mixture was stirred at room temperature over night, filtered through silica, washed with ethyl acetate and concentrated under reduced pressure. Purification by flash column chromatography on silica gel with petrol.-EtOAc (1:1 to 10:11) as eluent gave **16** as a white solid (2.2 g, 2.61 mmol, **65%**). **M.p.** 192-194°C; **^{1}H NMR (300 MHz, $CDCl_3$):** δ = 10.22 (s, 1H, H_9), 8.43 (s, 1H, H_8), 6.91 (s, 1H, H_7), 5.44 (d, 1H, J = 7.9 Hz, H_1), 5.65-5.28 (m, 6H, H_2, H_3 and H_4), 5.35 (d, 1H, J = 8.2 Hz, H_1), 4.41-4.26 (m, 4H, H_5 and H_6), 4.05-3.95 (m, 2H, H_6), 2.23-1.99 (m,

24H, *H*-Ac); **^{13}C NMR (75 MHz, $CDCl_3$):** δ = 186.1, 171.3, 171.1, 170.3 (x2), 170.2, 170.1, 169.4, 169.3, 161.2, 154.8, 135.7, 126.9, 120.2, 103.4, 99.1, 97.8, 71.2, 71.0, 70.5, 70.3, 68.0, 67.5, 67.0, 66.9, 61.3, 61.2, 20.8, 20.6 (x2), 20.5; **LRFAB-MS (3-NOBA matrix):** ***m/z*** 866.5 $[M+Na]^+$; **HRFAB-MS (3-NOBA matrix):** ***m/z*** 866.19582 (calcd. for $C_{35}H_{41}NO_{23}Na$ 866.19616 $[M+Na]^+$).

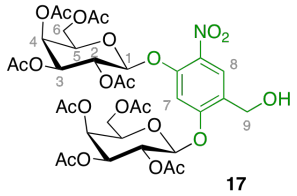

17

To a solution of **16** (2.0 g, 2.37 mmol, 1 equiv.) in $CHCl_3$/*i*PrOH (16 mL/11 mL) was added silica (1.8 g). The mixture was cooled to 0°C and $NaBH_4$ (1.1 g, 12 equiv.) was added portion-wise. After 3h at 0°C, the solution was allowed to warm up to room temperature and filtered through Celite®. Solvents were evaporated under reduced pressure and purification by flash column chromatography on silica gel with petrol.-EtOAc (4:6 to 3:7) as eluent gave **17** as a white solid (1.7 g, 1.97 mmol, **83%**). **M.p.** 124-126°C; $[\alpha]_D$ +44.8 (*c* 0.07 in $CHCl_3$); **^{1}H NMR (300 MHz, $CDCl_3$):** δ = 7.95 (s, 1H, H_8), 6.91 (s, 1H, H_7), 5.61-5.48 (m, 4H, H_2 and H_4), 5.35-5.31 (m, 2H, H_1 and H_3), 5.20-5.19 (m, 2H, H_1 and H_3), 4.64-4.57 (d, 2H, *J* = 13.9 Hz, H_9), 4.38-4.27 (m, 3H, H_5 and H_6), 4.20-4.13 (m, 1H, H_5), 4.05-3.98 (m, 2H, H_6), 2.62 (bs, 1H, O*H*), 2.23-2.02 (m, 24H, *H*-Ac); **^{13}C NMR (75 MHz, $CDCl_3$):** δ = 171.0, 170.8, 170.4, 170.3, 170.2 (x2), 170.0, 169.5, 157.5, 150.4, 135.3, 126.4, 126.1, 104.9, 100.0, 98.1, 71.1, 71.0, 70.6, 70.3, 68.5, 67.8, 67.0, 66.8, 61.2, 61.1, 59.8, 20.9 (x2), 20.8, 20.7, 20.6; **LRFAB-MS (3-NOBA matrix):** ***m/z*** 868.2 $[M+Na]^+$.

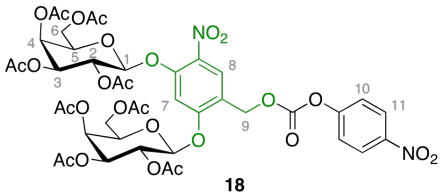

18

To a solution of 17 (700 mg, 0.83 mmol, 1 equiv.) in CH_2Cl_2 (15 mL) was added p-nitrophenyl chloroformiate (370 mg, 1.82 mmol, 2.2 equiv.) and pyridine (170 µL, 2.5 equiv.) and the reaction mixture was stirred overnight. Water was added, the

layers were separated and the aqueous layer was extracted with CH_2Cl_2 (3 × 15 mL). The combined organic fractions were washed with H2O (50mL), dried (MgSO4) and concentrated under reduced pressure. Purification by flash column chromatography on silica gel with petrol.-EtOAc (7:3 to 65:35) as eluent gave 18 as a white waxy solid (803 mg, 0.80 mmol, 96%). 1H NMR (300 MHz, CDCl3): δ 968.29 (d, 2H, J = 9.2 Hz, H11), 8.07 (s, 1H, H8), 7.43 (d, 2H, J = 9.2 Hz, H10), 6.94 (s, 1H, H7), 5.63-5.50 (m, 4H, H2 and H4), 5.36-5.14 (m, 6H, H1, H3 and H9), 4.38-4.22 (m, 4H, H5 and H6'), 4.07-3.98 (m, 2H, H6), 2.23-2.02 (m, 24H, H-Ac); 13C NMR (75 MHz, CDCl3): δ.2171.1, 170.4, 170.3, 170.2, 170.1, 169.7, 169.5, 158.3, 155.5, 152.4, 151.8, 145.7, 135.0, 128.5, 125.5, 122.0, 118.8, 104.3, 99.5, 98.1, 71.1, 71.0, 70.5, 70.4, 68.0, 67.7, 67.0, 66.9, 64.6, 61.2, 61.1, 21.0 (x2), 20.8 (x3), 20.7; LRESI-MS: m/z 1033.2, 1034.2, 1035.2 $[M+Na]^+$.

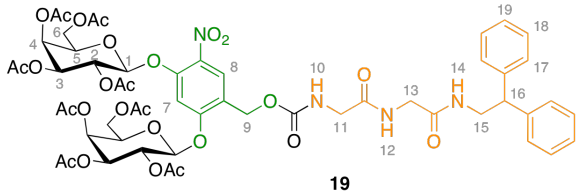

19

To a solution of **18** (780 mg, 0.77 mmol, 1 equiv.) in CH_3CN (40 mL) was added peptide **4** (286 mg, 0.92 mmol, 1.2 equiv.) and Et_3N (0.3 mL, 1.92 mmol, 2.5 equiv.) and the reaction mixture was stirred for 19 hours. Water was added, the layers were separated and the aqueous layer was extracted with EtOAc (3 × 40 mL). The combined organic fractions were washed with H_2O (50mL), dried ($MgSO_4$) and concentrated under reduced pressure. Purification by flash column chromatography on silica gel with petrol.-EtOAc (4:6 to 2:8) then CH_2Cl_2-MeOH (9:1) as eluent gave **19** as a white waxy solid (699 mg, 0.59 mmol, **77%**). **M.p.** 128-130°C; $[\alpha]_D$ +22.3 (*c* $1.7 \cdot 10^{-2}$M in $CHCl_3$); **^{1}H NMR (400 MHz, $CDCl_3$):** δ = 7.89 (s, 1H, H_8), 7.31-7.18 (m, 10H, H_{17}, H_{18} and H_{19}), 7.07 (bt, 1H, *J* = 4.8 Hz, H_{14}), 6.94 (s, 1H, H_7), 6.32 (bt, 1H, *J* = 5.6 Hz, H_{12}), 5.75 (bt, 1H, *J* = 5.2 Hz, H_{10}), 5.57 (dd, 1H, *J* = 8.0 Hz, *J* = 10.4 Hz, H_2), 5.51-5.49 (m, 3H, H_2 and H_4), 5.32-5.30 (m, 3H, H_1 and H_3), 5.23 (dd, 1H, *J* = 3.2 Hz, *J* = 10.4 Hz, H_3), 5.19 (d, 1H, *J* = 8.0 Hz, H_1), 5.06-4.98 (d, 2H, *J* = 13.9 Hz, H_9), 4.37-4.26 (m, 3H, H_5 and H_6), 4.20-4.16 (m, 2H, H_5 and H_{16}), 4.09-4.00 (m, 2H, H_6), 3.88 (t, 2H, *J* = 6.4 Hz, H_{15}), 3.81-3.78 (m, 4H, H_{11} and H_{13}), 2.22-2.02 (m, 24H, *H*-Ac); **^{13}C NMR (100 MHz, $CDCl_3$):** δ = 170.9, 170.7, 170.2, 170.1, 170.0,

169.9, 169.7, 169.3 (x2), 168.6, 157.2, 156.1, 150.6 , 141.7, 141.6, 135.0, 128.7, 127.9, 126.8, 126.3, 121.2, 104.9, 99.6, 98.0, 70.9, 70.4, 70.2, 68.1, 67.5, 66.8, 66.7, 61.0 (x2), 60.7, 50.3, 44.3, 43.7, 43.0, 20.8 (x2), 20.7 (x3), 20.6; **LRFAB-MS (3-NOBA matrix):** ***m/z*** 1183.7 $[M+H]^+$, 1205.7 $[M+Na]^+$; **HRFAB-MS (3-NOBA matrix):** ***m/z*** 1183.37652 (calcd. for $C_{54}H_{63}N_4O_{26}$ 1183.37305 $[M+H]^+$)

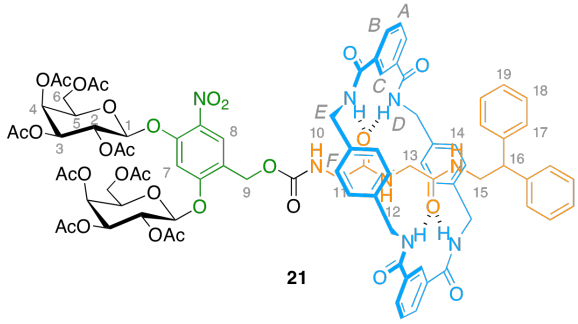

21

Using general method **A**, thread **19** (200 mg, 0.17 mmol, 1 equiv.), *p*-xylylenediamine (377 mg, 16 equiv.), isophthaloyl dichloride (563 mg, 16 equiv.) and Et_3N (0.9 mL, 35 equiv.) in CHCl3 (100 mL) gave crude **21** as an orange solid. Purification by flash column chromatography on silica gel with $CHCl_3$-MeOH (99:1 to 93:7) as eluent gave a mixture of thread **19** and rotaxane **21**. This mixture was resolved by size exclusion chromatography using $CHCl_3$/MeOH (50/50: v/v) as eluent to give rotaxane **21** as a white solid (93 mg, 0.05 mmol, **31%**). **M.p.** 164-166°C; $[\alpha]_D$ +12.9 (*c* 0.05 in $CHCl_3$) **^{1}H NMR (400 MHz, $CDCl_3$):** δ = 8.15 (s, 2H, H_C), 7.98 (t, 4H, *J* = 7.6 Hz, H_B), 7.64 (t, 2H, *J* = 4.4 Hz, H_D), 7.55 (bs, 3H, H_8 and H_D), 7.46 (t, 2H, *J* = 8.0 Hz, H_A), 7.32 (ls, 1H, H_{14}), 7.23-7.06 (m, 18H, H_{17}, H_{18}, H_{19} and H_F), 6.91 (s, 1H, H_7), 6.49 (bs, 1H, H_{12}), 5.64 (bs, 1H, H_{10}), 5.56 (dd, 1H, *J* = 8.0 Hz, *J* = 10.4 Hz, H_2), 5.49 (d, 2H, *J* = 3.2 Hz, H_4), 5.46 (dd, 1H, *J* = 8.0 Hz, *J* = 10.4 Hz, H_2), 5.31 (dd, 1H, *J* = 3.6 Hz, *J* = 10.4 Hz, H_3), 5.23 (dd, 1H, *J* = 10.4 Hz, *J* = 3.2 Hz, H_3), 5.21 (t, 2H, *J* = 8.0 Hz, H_1), 4.64 (bs, 2H, H_9), 4.54-4.49 (m, 8H, H_E), 4.45-4.27 (m, 3H, H_5 and $H_{6'}$), 4.19 (t, 1H, *J* = 6.4 Hz, H_5), 4.10-4.00 (m, 3H, H_6 and H_{16}), 3.71 (t, 2H, *J* = 6.0 Hz, H_{15}), 3.34 (d, 2H, *J* = 5.2 Hz, H_{11}), 2.80 (bdd, 2H, *J* = 22.4 Hz, *J* = 17.2 Hz, H_{13}), 2.14-2.02 (m, 24H, *H*-Ac); **^{13}C NMR (100 MHz, $CDCl_3$):** δ 170.9, 170.8, 170.1 (x2), 170.0, 169.9, 169.5, 169.5, 169.4, 168.4, 166.9, 166.8, 157.2, 156.2, 156.1, 150.6, 141.4, 137.3, 137.2, 134.8, 134.0, 133.9, 131.0, 130.8, 128.9, 128.7, 127.8, 126.9, 126.3, 124.8, 120.8, 105.6, 99.5, 98.2, 77.2, 70.9, 70.3, 70.1, 68.1, 67.6, 66.8, 61.0, 60.4, 44.3, 44.1, 41.8, 29.6, 20.8 (x2), 20.7, 20.6,

20.5; **LRFAB-MS (3-NOBA matrix):** ***m/z*** 1716.8 $[M+H]^+$ **HRFAB-MS (3-NOBA matrix):** ***m/z*** 1715.57894 (calcd. for $C_{86}H_{91}N_8O_{30}$ 1715.58411 $[M+H]^+$).

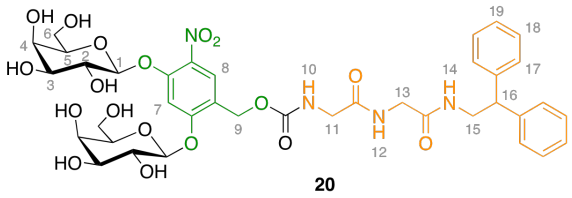

20

Using general method **C**, thread **19** (250 mg, 0.21 mmol, 1 equiv.) and MeONa (228 mg, 4.2 mmol, 20 equiv.) at 0°C in MeOH (12 mL) gave crude **20** as yellow solid. Purification by flash column chromatography on silica gel with CH_2Cl_2-MeOH (8:2 to 1:1) as eluent gave **20** as a yellow solid (144 mg, 0.17 mmol, **81%**). **M.p.** 135-137°C; **^{1}H NMR (400 MHz, $CDCl_3$):** δ = 7.98 (s, 1H, H_8), 7.30-7.15 (m, 11H, H_7, H_{17}, H_{18} and H_{19}), 5.18 (m, 2H, H_9), 5.14 (d, 1H, *J* = 8.0 Hz, H_1), 5.09 (d, 1H, *J* = 8.0 Hz, H_1), 4.27 (t, 1H, *J* = 8.0 Hz, H_{16}), 4.03 (dd, 2H, *J* = 4.0 Hz, *J* = 8.0 Hz, H_5), 3.91-3.72 (m, 16H, H_2, H_4, H_6, H_{11}, H_{13} and H_{15}); **^{13}C NMR (100 MHz, CD_3OD):** δ = 172.8, 171.6, 170.4, 160.7, 153.7, 143.8, 134.7, 129.6, 129.2, 127.7, 127.6 , 120.4, 104.7, 102.3, 102.1, 77.7, 74.9, 74.8, 71.9 (x2), 70.6, 63.1 (x2), 62.2, 51.7, 49.9, 45.1, 43.4; **LRFAB-MS (3-NOBA matrix):** ***m/z*** 847.1 $[M+H]^+$; 869.1 $[M+Na]^+$ **HRFAB-MS (3-NOBA matrix):** ***m/z*** 869.26978 (calcd. for $C_{38}H_{46}N_4O_{18}Na$ 869.26993 $[M+Na]^+$).

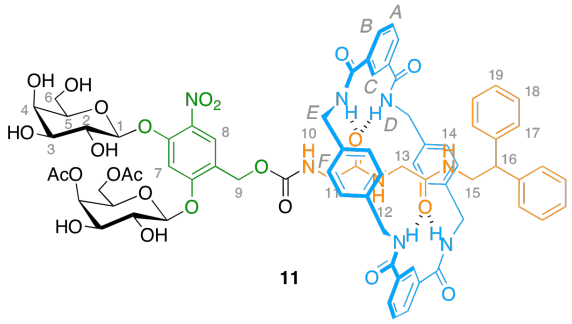

11

Using general method **C**, rotaxane **21** (43 mg, 0.025 mmol, 1 equiv.) and MeONa (27 mg, 0.5 mmol, 20 equiv.) at 0°C in MeOH (5 mL) gave crude **11** as yellow solid. Purification by flash column chromatography on silica gel with CH_2Cl_2-MeOH (9:1 to 1:1) as eluent gave **11** as a yellow solid (33 mg, 0.022 mmol, **88%**). **M.p.** decomposition; **^{1}H NMR (400 MHz, CD_3OD):** δ = 8.27 (bs, 2H, H_C), 8.01 (dd, 4H, *J* = 7.6 Hz, *J* = 1.6 Hz, H_B), 7.62-7.58 (m, 3H, H_8 and H_A), 7.21-7.12 (m, 15H, H_7,

H_{17}, H_{18}, H_{19} and H_F), 6.99-6.97 (m, 4H, H_F), 5.10 (d, 1H, J = 7.6 Hz, H_1), 4.98 (d, 1H, J = 8.0 Hz, H_1), 4.78-4.68 (d, 2H, J = 13.2 Hz, H_9), 4.33 (bs, 8H, H_E), 4.06-3.80 (m, 11H, H_2, H_4, H_5, H_6, H_{15} and H_{16}), 3.63 (dd, 1H, J = 9.6 Hz, J = 3.2 Hz, H_3), 3.57 (dd, 1H, J = 9.6 Hz, J = 3.2 Hz, H_3), 3.49-3.38 (m, 4H, H_6 and H_{13}), 2.78 and 2.65 (d, 2H, J = 16.4 Hz, H_{11}); **^{13}C NMR (100 MHz, CD_3OD):** δ 171.9, 170.3, 169.3, 160.4, 158.3, 153.6, 143.6, 138.6, 135.6, 135.5, 134.0, 131.8, 131.7, 130.1, 129.9, 129.8, 129.6, 129.0, 127.8, 127.7, 119.6, 104.3, 102.2, 102.1, 77.7, 77.6, 74.9, 74.8, 71.8, 71.7, 70.6, 70.5, 63.2, 63.1, 61.8, 49.9, 45.3, 45.2, 44.9, 44.8, 42.3; **LRESI-MS:** ***m/z*** 1401.8, 1402.8, 1403.8 $[M+Na]^+$; **LRFAB-MS (3-NOBA matrix):** ***m/z*** 1402.9 $[M+Na]^+$ **HRFAB-MS (3-NOBA matrix):** ***m/z*** 1379.50013 (calcd. for $C_{70}H_{75}N_8O_{22}$ 1379.49959 $[M+H]^+$).

6.4.3 Experimental procedures for the preparation of ally-nitrophenol-based propeptides

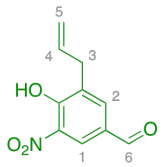

26

3-nitro-4-(2-propenyloxy)benzaldehyde (5.60 g, 27.05 mmol, 1 equiv.) was heated at 160-165°C over a period of 17 hours. After allowing the mixture to reach room temperature, aqueous HCl (1M) (50 mL) and CH_2Cl_2 (50 mL) were added. The layers were separated and the aqueous layer was extracted with CH_2Cl_2 (3 × 50 mL). The combined organic fractions were dried ($MgSO_4$) and concentrated under reduced pressure. Purification by flash column chromatography on silica gel with Petrol.-EtOAc (8:2 to 6:4) as eluent gave **26** as a yellow solid (3.20 g, 15.46 mmol, **57%**). **M.p.** 82-84°C; **^{1}H NMR (400 MHz, $CDCl_3$):** δ = 11.41 (bs, 1H, O*H*), 9.91 (s, 1H, H_6), 8.51 (d, 1H, J = 2.0 Hz, H_1), 8.01 (d, 1H, J = 2.0 Hz, H_2), 6.03-5.93 (m, 1H, H_4), 5.20-5.18 (m, 1H, H_5), 5.16 (dq, 1H, J = 11.2 Hz, J = 1.6 Hz, H_5), 3.53 (d, 2H, J = 6.8 Hz, H_3); **^{13}C NMR (100 MHz, $CDCl_3$):** δ 189.0, 157.7, 135.8, 134.1, 133.5, 133.3, 128.4, 126.9, 118.0, 33.7; **LRFAB-MS (3-NOBA matrix):** ***m/z*** 208 $[M+H]^+$

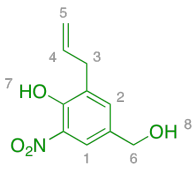

41

To a solution of **26** (100 mg, 0.48 mmol) in $CHCl_3$/*i*PrOH (2.4 mL/1.6 mL) was added silica (90 mg). The mixture was cooled 0°C and $NaBH_4$ (320 mg, 12 equiv.) was added portion wise. After stirring for 1 hour at 0°C, the solution was allowed to reach room temperature and filtered over Celite®. Concentration of the filtrate under reduced pressure and purification by flash column chromatography on silica gel with Petrol.-EtOAc (9:1 to 8:2) as eluent gave **41** as a yellow solid (40 mg, 0.19 mmol, **40%**). **M.p.** 40-42°C; **^{1}H NMR (400 MHz, $CDCl_3$):** δ = 10.92 (bs, 1H, H_7), 7.98 (d, 1H, *J* = 2.0 Hz, H_1), 7.48 (d, 1H, *J* = 2.0 Hz, H_2), 6.03-5.93 (m, 1H, H_4), 5.15 (t, 1H, *J* = 1.2 Hz, H_5), 5.12 (dq, 1H, *J* = 6.4 Hz, *J* = 1.2 Hz, H_5), 4.65 (s, 2H, H_6), 3.48 (d, 2H, *J* = 6.4 Hz, H_3), 1.91 (bs, 1H, H_8); **^{13}C NMR (100 MHz, $CDCl_3$):** δ 152.8, 136.4, 135.1, 133.3, 132.5, 131.9, 121.2, 117.2, 64.0, 33.9; **LRESI-MS (negative):** ***m/z*** 208 $[M-H]^-$

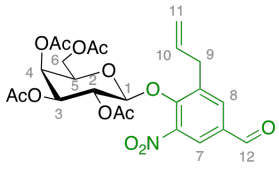

27

To a solution of **26** (570 mg, 2.75 mmol, 1.1 equiv.) in CH_3CN (30 mL) at 0°C was added α-D-galactopyranosyl bromide-2,3,4,6-tetraacetate (1.03 g, 2.51 mmol, 1 equiv.) and Ag_2O (872 mg, 4.12 mmol, 1.5 equiv.). The mixture was stirred at room temperature over night, filtered through silica, washed with ethyl acetate and concentrated under reduced pressure. Purification by flash column chromatography on silica gel with petrol.-EtOAc (85:15 to 6:4) as eluent gave **27** as a yellow solid (1.16 g, 2.16 mmol, **79%**). **M.p.** 78-80°C; $[\alpha]_D$ +32.7 (*c* 0.04 in $CHCl_3$) **^{1}H NMR (400 MHz, $CDCl_3$):** δ = 9.97 (s, 1H, H_{12}), 8.11 (d, 1H, *J* = 2.0 Hz, H_7), 7.96 (d, 1H, *J* = 2.0 Hz, H_8), 5.96-5.86 (m, 1H, H_{10}), 5.48 (dd, 1H, *J* = 10.4 Hz, *J* = 7.6 Hz, H_2), 5.37 (d, 1H, *J* = 2.8 Hz, H_4), 5.22-5.14 (m, 2H, H_{11}), 5.05 (dd, 1H, *J* = 10.4 Hz, *J* = 3.2, H_3), 4.95 (d, 1H, *J* = 8.0 Hz, H_1), 4.02 (d, 2H, *J* = 6.8 Hz, H_6), 3.81 (dt, 1H, *J* = 6.8 Hz, *J* = 0.8 Hz, H_5), 3.58 (dd, 2H, *J* = 6.4 Hz, *J* = 1.2 Hz, H_9), 2.18 (s, 3H, *H*-

Ac), 2.16 (s, 3H, *H*-Ac), 1.99 (s, 3H, *H*-Ac), 1.96 (s, 3H, *H*-Ac); **^{13}C NMR (100 MHz, $CDCl_3$):** δ 189.1, 170.3, 170.2, 170.1, 169.6, 149.6, 145.5, 139.2, 134.7, 134.6, 133.1, 124.1, 118.3, 102.3, 71.5, 70.6, 68.7, 66.6, 60.8, 34.1, 20.9, 20.8, 20.7, 20.6; **LRFAB-MS (3-NOBA matrix):** ***m/z*** 538 $[M+H]^+$, 560 $[M+Na]^+$; **HRFAB-MS (3-NOBA matrix):** ***m/z*** 538.15524 (calcd. for $C_{24}H_{28}NO_{13}$ 538.15607 $[M+H]^+$).

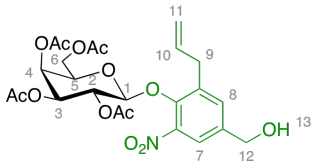

28

To a solution of **27** (700 mg, 1.30 mmol, 1 equiv.) in $CHCl_3$/*i*PrOH (20 mL/14 mL) was added silica (1.0 g). The mixture was cooled 0°C and $NaBH_4$ (594 mg, 15.6 mmol, 12 equiv.) was added portion wise. After stirring for 1 hour at 0°C, the solution was allowed to reach room temperature and filtered over Celite®. Concentration of the filtrate under reduced pressure and purification by flash column chromatography on silica gel with Petrol.-EtOAc (6:4 to 3:7) as eluent gave **28** as a yellow solid (608 mg, 1.13 mmol, **87%**). **M.p.** 110-112°C; $[\alpha]_D$ +39.8 (*c* 0.01 in $CHCl_3$) **^{1}H NMR (400 MHz, $CDCl_3$):** δ = 7.60 (d, 1H, *J* = 2.0 Hz, H_9), 7.40 (d, 1H, *J* = 1.6 Hz, H_{11}), 5.93-5.83 (m, 1H, H_{14}), 5.45 (dd, 1H, *J* = 10.4 Hz, *J* = 8.0 Hz, H_2), 5.35 (d, 1H, *J* = 2.8 Hz, H_4), 5.14 (bs, 1H, H_{15}), 5.11 (dd, 1H, *J* = 7.2 Hz, *J* = 1.2 Hz, H_{15}), 5.02 (dd, 1H, *J* = 10.4 Hz, *J* = 3.6 Hz, H_3), 4.82 (d, 1H, *J* = 8.0 Hz, H_1), 4.69 (bs, 2H, H_{16}), 4.03 (dd, 2H, *J* = 6.8 Hz, *J* = 3.6 Hz, H_6), 3.77 (t, 1H, *J* = 6.4 Hz, H_5), 3.50 (t, 2H, *J* = 4.8 Hz, H_{13}), 2.37 (bs, 1H, H_{13}), 2.18 (s, 3H, *H*-Ac), 2.15 (s, 3H, *H*-Ac), 1.98 (s, 3H, *H*-Ac), 1.96 (s, 3H, *H*-Ac); **^{13}C NMR (100 MHz, $CDCl_3$):** δ 170.5, 170.4, 170.2, 169.7, 145.3, 144.4, 139.0, 137.5, 135.6, 132.2, 121.0, 117.4, 102.7, 71.2, 70.7, 68.7, 66.7, 63.5, 60.8, 34.1, 21.1, 20.9, 20.7, 20.6; **LRFAB-MS (3-NOBA matrix):** ***m/z*** 538 $[M+H]^+$, 562 $[M+Na]^+$; **HRFAB-MS (3-NOBA matrix):** ***m/z*** 562.15284 (calcd. for $C_{24}H_{29}NO_{13}Na$ 562.15366 $[M+Na]^+$).

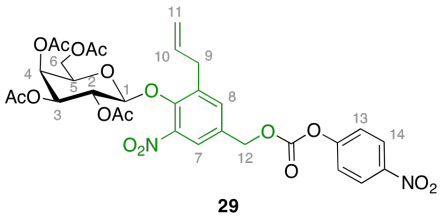

29

To a solution of **28** (433 mg, 0.80 mmol, 1 equiv.) in CH_2Cl_2 (15 mL) was added *p*-nitrophenyl chloroformiate (356 mg, 1.76 mmol, 2.2 equiv.) and pyridine (160 µL, 2.0 mmol 2.5 equiv.) and the reaction mixture was stirred for 24 hours at room temperature. Water was added, the layers were separated and the aqueous layer was extracted with CH_2Cl_2 (3 × 15 mL). The combined organic fractions were washed with H_2O (50mL), dried ($MgSO_4$) and concentrated under reduced pressure. Purification by flash column chromatography on silica gel with petrol.-EtOAc (6:4) as eluent gave **29** as a white solid (540 mg, 0.77 mmol, **96%**). **M.p.** 66-68°C; **^{1}H NMR (400 MHz, $CDCl_3$):** δ = 8.29 (d, 2H, *J* = 9.2 Hz, H_{14}), 7.71 (d, 1H, *J* = 2.0 Hz, H_7), 7.50 (d, 1H, *J* = 2.0 Hz, H_8), 7.39 (d, 2H, *J* = 9.2 Hz, H_{13}), 5.96-5.85 (m, 1H, H_{10}), 5.48 (dd, 1H, *J* = 10.8 Hz, *J* = 8.0 Hz, H_2), 5.38 (d, 1H, *J* = 2.4 Hz, H_4), 5.27 (bs, 2H, H_{12}), 5.20-5.14 (m, 2H, H_{11}), 5.05 (dd, 1H, *J* = 10.8 Hz, *J* = 3.6 Hz, H_3), 4.88 (d, 1H, *J* = 8.0 Hz, H_1), 4.06 (t, 2H, *J* = 6.8 Hz, H_6), 3.80 (t, 1H, *J* = 7.6 Hz, H_5), 3.56 (t, 2H, *J* = 6.0 Hz, H_9), 2.20 (s, 3H, *H*-Ac), 2.17 (s, 3H, *H*-Ac), 2.01 (s, 3H, *H*-Ac), 1.97 (s, 3H, *H*-Ac); **^{13}C NMR (100 MHz, $CDCl_3$):** δ = 170.4, 170.3, 170.2, 169.7, 155.4, 152.4, 145.7, 145.4, 138.5, 135.3, 134.1, 132.1, 125.5, 122.9, 121.8, 118.0, 102.7, 71.3, 70.7, 69.1, 68.7, 66.7, 60.8, 34.1, 20.9, 20.8, 20.7, 20.6; **LRFAB-MS (3-NOBA matrix):** ***m/z*** 705 $[M+H]^+$, 727 $[M+Na]^+$.

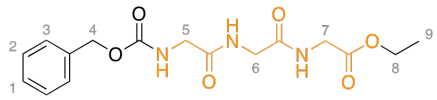

31

To a solution of Cbz-glycine (3.62 g, 17.3 mmol, 1.0 equiv.), EDCI.HCl (3.31 g, 17.3 mmol, 1.0 equiv.) and DMAP (2.11 g, 17.3 mmol, 1.0 equiv.) in CH_2Cl_2 (180 mL) at room temperature, was added glycylglycine ethylester hydrochloride (3.74 g, 19.0 mmol, 1.1 equiv.) and the reaction mixture was stirred overnight. An aqueous solution of HCl (1M) (100 mL) was added, the layers were separated and the aqueous layer was extracted with CH_3Cl/iPrOH (3:1) (3 × 50 mL). The combined organic fractions were dried ($MgSO_4$) and concentrated under reduced pressure. To

the crude solid was added Et_2O (50 mL). The resulting white suspension was sonicated for 5 minutes and filtered by gravity to give **31** as a white solid (5.42 g, 15.4 mmol, 90%). **M.p.** 133-135°C, **^{1}H-NMR (400 MHz, $CDCl_3/CD_3OD$ (1:1), 298 K):** δ = 7.38-7.20 (m, 5H, H_1, H_2 and H_3), 5.06 (s, 2H, H_4), 4.15 (q, J = 7.1 Hz, 2H, H_8), 3.99-3.74 (m, 6H, H_5, H_6 and H_7), 3.30 (t, J = 7.1 Hz, 3H, H_8). **^{13}C-NMR (100 MHz, $CDCl_3/CD_3OD$ (3:1), 298 K):** δ = 170.8, 170.3, 170.2, 136.2, 128.6, 128.3, 128.1, 107.0, 67.3, 61.7, 44.3, 42.4, 41.1, 14.0; **LRESI-MS:** *m/z* = 374 $[M+Na]^+$; **HRESI-MS:** *m/z* = 374.1321 $[M+Na]^+$ (calc. for $C_{16}H_{21}O_6N_3Na_1$ 374.1323 $[M+Na]^+$).

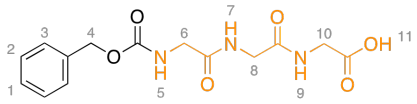

32

To a solution of **31** (2.24 g, 6.37 mmol, 1.0 equiv.) in a 2:3:3 mixture H_2O/EtOH/THF (320 mL) at 0ºC was added crushed NaOH (395 mg, 9.55 mmol, 1.5 equiv.) in one portion and the reaction mixture was stirred at that temperature for 20 min. An aqueous solution (1M) of HCl (40 mL) was added and solvents were evaporated under reduced pressure. To the resulting solid was added H_2O (30 mL), the suspension was sonicated for 5 minutes, filtered under suction and washed with H_2O (50 mL). The solid was re-suspended in a 1:6 mixture of MeOH/Et_2O (50mL), sonicated for 5 minutes, filtered by gravity and washed with Et_2O (20 mL) to afford **32** as a white solid (1.70 g, 5.25 mmol, 82%). **M.p.** 182-184°C; **^{1}H-NMR (400 MHz, DMSO *d_6*, 298 K):** δ = 12.58 (s, 1H, H_{11}), 8.16 (dt, J = 5.6 Hz and J = 5.6 Hz, 2H, H_5 and H_4), 7.49 (t, J = 6.0 Hz, 1H, H_9), 7.14-7.25 (m, 5H, H_1, H_2 and H_3), 5.03 (s, 2H, H_4), 3.75 (dd, J = 5.5 Hz and J = 5.5 Hz, 4H, H_6 and H_8), 3.67 (d, J = 6.0 Hz, 2H, H_{10}); **^{13}C-NMR (100 MHz, DMSO *d_6*, 298 K):** δ = 171.0, 169.3, 169.0, 156.4, 136.9, 128.2, 127.7, 127.6, 65.4, 43.4, 41.6, 40.4; **LRESI-MS:** *m/z* = 346 $[M+Na]^+$; **HRESI-MS:** *m/z* = 324.1196 $[M+H]^+$ (calc. for $C_{14}H_{18}O_6N_3$ 324.1190 $[M+H]^+$).

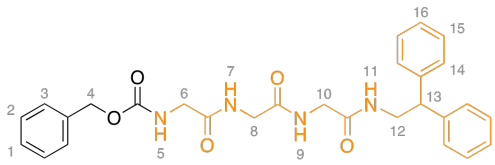

33

To a solution of **32** (1.52 g, 4.7 mmol, 1.0 equiv.), EDCI.HCl (991 mg, 5.17 mmol, 1.1 equiv.) and DMAP (631 mg, 5.17 mmol, 1.1 equiv.) in CH_2Cl_2 (100 mL) at room temperature, was added 2,2-diphenylethanamine (878 mg, 4.4 mmol, 0.95 equiv.) and the reaction mixture was stirred overnight. An aqueous solution (1M) of HCl (50 mL) was added, the layers were separated and the aqueous layer was extracted with CH_2Cl_2 (3 × 50 mL). The combined organic fractions were washed with H_2O (40 mL), dried ($MgSO_4$) and concentrated under reduced pressure to afford **33** as a white solid (1.87 g, 3.72 mmol, 80%). **M.p.** 210-212°C; **^{1}H-NMR (400 MHz, DMSO *d*$_6$, 298 K):** δ = 8.13, 8.05, 7.49 (3t, *J* = 5.6 Hz, *J* = 5.8 Hz and *J* = 6.0 Hz, 3H, H_5, H_7 and H_9), 7.86 (t, *J* = 5.5 Hz, 1H, H_{11}), 7.38-7.09 (m, 15H, H_1, H_2, H_3, H_{14}, H_{15} and H_{16}), 5.03 (s, 2H, H_4), 4.18 (t, *J* = 7.7 Hz, 1H, H_{13}), 3.75-3.67 (m, 4H, H_6, H_{11}), 3.66, 3.58 (2d, *J* = 6.1 Hz and *J* = 5.7 Hz, 4H, H_8 and H_{10}); **^{13}C-NMR (100 MHz, DMSO *d*$_6$, 298 K):** δ = 169.4, 168.9, 168.6, 156.4, 142.7, 136.9, 128.3, 128.2, 127.8, 127.7, 127.6, 126.3, 65.4, 49.9, 43.4, 43.0, 41.9, 41.7; **LRESI-MS:** *m/z* = 525 $[M+Na]^+$; **HRESI-MS:** *m/z* = 503.2286 $[M+H]^+$ (calc. for $C_{28}H_{30}O_5N_4$ 503.2289 $[M+H]^+$).

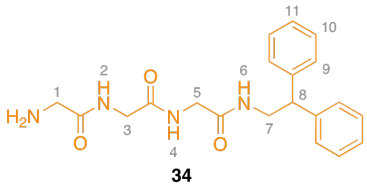

34

A solution of **33** (2.65 g, 5.27 mmol, 1.0 equiv.) in a 3:4:13 mixture H_2O/MeOH/THF (500 mL) was heated up to 50ºC until **33** had fully dissolved (5 min). The solution was then allowed to cool to room temperature and palladium (10%) on carbon (561 mg) was added in one portion. The reaction vessel was purged with H_2 by means of three vacuum/H_2 cycles and the mixture stirred at room temperature for 15 hours. The solid was filtered off with Celite®, MeOH and THF were evaporated under reduced pressure and the remaining aqueous layer was extracted with CH_3Cl/iPrOH (3:1) (3 × 50 mL). The combined organic fractions were dried ($MgSO_4$) and concentrated under reduced pressure. The resulting yellow

oil was re-dissolved in CH_2Cl_2 (10 mL) and Et_2O (50 mL) was added. The resulting white precipitate was sonicated for 5 minutes and filtered by gravity to afford **34** as a white solid (1.30 g, 3.52 mmol, 67%). **M.p.** 50-52°C, **^{1}H-NMR (400 MHz, $CDCl_3$, 298 K):** δ = 8.07-7.81 (m, 1H, H_6), 7.42-7.25, 6.75-6.58 (2m, 2H, H_2 and H_4), 7.25-6.95 (m, 10H, H_9, H_{10} and H_{11}), 4.10 (t, J = 7.8 Hz, 1H, H_8), 3.75-3.67 (m, 4H, H_6, H_{11}), 3.75, 3.64, 3.28 (3s, 4H, H_3, H_5 and H_7); **^{13}C-NMR (100 MHz, $CDCl_3$, 298 K):** δ = 169.7 (× 2), 169.0, 141.7, 128.6, 128.0, 126.7, 50.2, 43.8 (× 2), 42.8, 42.6; LRESI-MS: *m/z* = 391 $[M+Na]^+$; **HRESI-MS:** *m/z* = 369.1924 $[M+H]^+$ (calc. for $C_{20}H_{25}O_3N_4$ 369.1921 $[M+H]^+$).

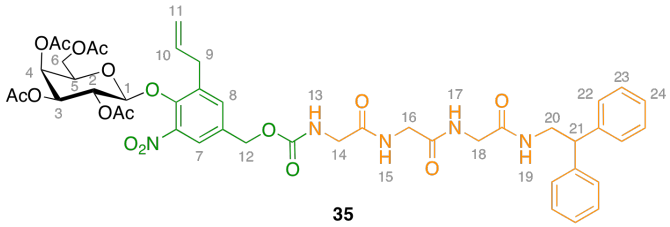

35

To a solution of **29** (529 mg, 0.75 mmol, 1 equiv.) in CH_3CN (35 mL) was added peptide **34** (332 mg, 0.90 mmol, 1.2 equiv.) and Et_3N (260 µL, 1.87 mmol, 2.5 equiv.) and the reaction mixture was stirred for 24 hours. Water was added, the layers were separated and the aqueous layer was extracted with EtOAc (3 × 40 mL). The combined organic fractions were washed with H_2O (50mL), dried ($MgSO_4$) and concentrated under reduced pressure. Purification by flash column chromatography on silica gel with petrol.-EtOAc (4:6 to 2:8) then CH_2Cl_2-MeOH (9:1) as eluent gave **35** as a light brown solid (599 mg, 0.64 mmol, **85%**). **M.p.** 126-128°C; **^{1}H NMR (400 MHz, $CDCl_3$):** δ = 7.57 (d, 1H, J = 2.0 Hz, H_7), 7.39 (m, 2H, H_{15} and H_{17}), 7.37 (d, 1H, J = 2.0 Hz, H_8), 7.27-7.16 (m, 10H, H_{22}, H_{23} and H_{24}), 6.65 (t, 1H, J = 5.2 Hz, H_{19}), 6.08 (t, 1H, J = 4.8 Hz, H_{13}), 5.93-5.82 (m, 1H, H_{10}), 5.46 (dd, 1H, J = 10.8 Hz, J = 8.0 Hz, H_2), 5.37 (d, 1H, J = 2.8 Hz, H_4), 5.15 (d, 1H, J = 1.2 Hz, H_{11}), 5.12 (dd, 1H, J = 9.2 Hz, J = 1.2 Hz, H_{11}), 5.06 (dd, 1H, J = 10.4 Hz, J = 3.6 Hz, H_3), 5.00 (s, 2H, H_{12}), 4.85 (d, 1H, J = 8.0 Hz, H_1), 4.17 (t, 1H, J = 8.0 Hz, H_{21}), 4.03 (d, 2H, J = 6.4 Hz, H_6), 3.91-3.76 (m, 9H, H_5, H_{14}, H_{16}, H_{18} and H_{20}), 3.50 (m, 2H, H_9), 2.19 (s, 3H, *H*-Ac), 2.15 (s, 3H, *H*-Ac), 2.00 (s, 3H, *H*-Ac), 1.95 (s, 3H, *H*-Ac); **^{13}C NMR (100 MHz, $CDCl_3$):** δ = 170.5, 170.4, 170.2, 169.8, 169.7, 169.3, 168.9, 156.4, 145.4, 145.0, 141.9, 137.9, 135.4, 134.4, 133.5, 128.8, 128.1, 126.9, 122.2, 117.7, 102.7, 71.1, 70.7, 68.8, 66.7, 65.3, 60.7, 50.5, 44.4, 44.0, 43.1, 42.9, 34.0,

29.8, 20.9, 20.8, 20.7, 20.6; **LRESI-MS:** ***m/z*** 957 $[M+Na]^+$; **LRFAB-MS (3-NOBA matrix):** ***m/z*** 935 $[M+H]^+$; **HRFAB-MS (3-NOBA matrix):** ***m/z*** 934.33837 (calcd. for $C_{45}H_{52}N_5O_{17}$ 934.33585 $[M+H]^+$).

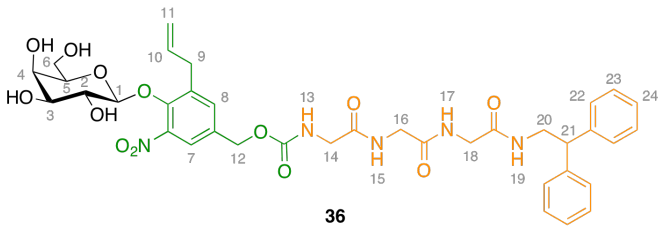

36

Using general method **C**, thread **35** (100 mg, 0.11 mmol, 1 equiv.) and MeONa (58 mg, 1.1 mmol 10 equiv.) at 0°C in MeOH (5 mL) gave crude **36** as a brown solid. Purification by flash column chromatography on silica gel with CH_2Cl_2-MeOH (95:5 to 8:2) as eluent gave **36** as a light brown solid (57 mg, 0.07 mmol, **64%**). For enzymatic trials, a fraction was re-purified by preparative RP-HPLC using a linear gradient (35 to 55 % in 20 min) of MeCN in H_2O at a flow rate of 10 mL/min to give **36** as a white solid. Purity (HPLC): >97%; **M.p.** 145-147°C; **^{1}H NMR (400 MHz, CD_3OD):** δ =7.57 (d, 1H, *J* = 2.0 Hz, H_7), 7.45 (d, 1H, *J* = 2.0 Hz, H_8), 7.24-7.19 (m, 8H, H_{22} and H_{23}), 7.14-7.10 (m, 2H, H_{24}), 5.99-5.89 (m, 1H, H_{10}), 5.11-5.04 (m, 4H, H_{11} and H_{12}), 4.47 (d, 1H, *J* = 8.0 Hz, H_1), 4.24 (t, 1H, *J* = 8.0 Hz, H_{21}), 3.80-3.73 (m, 8H, H_{14}, H_{16}, H_{18} and H_{20}), 3.70 (m, 2H, H_4, and H_5), 3.66-3.54 (m, 4H, H_6 and H_9), 3.44 (dd, 1H, *J* = 10.0 Hz, *J* = 3.6 Hz, H_3); **^{13}C NMR (100 MHz, CD_3OD):** δ = 173.1, 172.1, 171.5, 159.0, 147.9, 147.0, 143.8, 138.5, 137.5, 135.5, 134.7, 129.6, 129.2, 127.7, 122.8, 117.4, 107.1, 77.1, 74.7, 72.5, 69.7, 66.5, 61.6, 51.6, 49.9, 45.1, 43.8, 43.3, 34.5; **LRES$^+$-MS:** ***m/z*** 766 $[M+H]^+$, 788-789-790 $[M+Na]^+$; **LRFAB-MS (3-NOBA matrix):** ***m/z*** 766 $[M+H]^+$; **HRFAB-MS (3-NOBA matrix):** ***m/z*** 766.29279 (calcd. for $C_{37}H_{44}N_5O_{13}$ 766.29356 $[M+H]^+$).

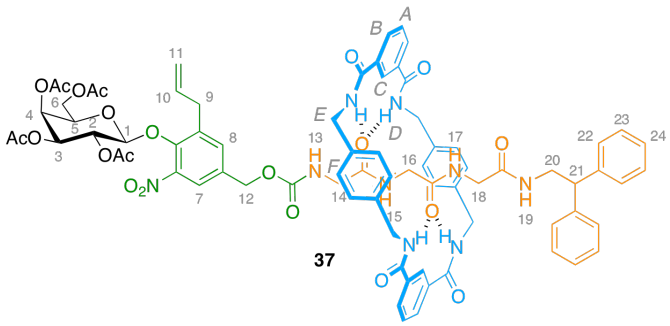

37

Using general method **A**, thread **35** (200 mg, 0.21 mmol, 1 equiv.), *p*-xylylenediamine (466 mg, 3.36 mmol ,16 equiv.), isophthaloyl dichloride (696 mg, 3.36 mmol, 16 equiv.) and Et_3N (1.0 mL, 7.35 mmol, 35 equiv.) at room temperature for 3 hours gave crude **37** as an orange solid. Purification by flash column chromatography on silica gel with $CHCl_3$-MeOH (99:1 to 85:15) as eluent gave a mixture of thread **35** and rotaxane **37**. This mixture was resolved by size exclusion chromatography using $CHCl_3$/MeOH (50/50: v/v) as eluent to give rotaxane **37** as a light brown solid (161 mg, 0.11 mmol, **51%**). **M.p.** 160-162°C; $[\alpha]_D$ +7.8 (*c* 0.009 in $CHCl_3$) **^{1}H NMR (400 MHz, $CDCl_3$):** δ 8.19 (s, 2H, H_C), 8.00 (d, 4H, *J* = 7.2 Hz, H_B), 7.81 (bs, 4H, H_D), 7.47 (t, 2H, *J* = 7.6 Hz, H_A), 7.35 (s, 1H, H_7), 7.23 (s, 1H, H_8), 7.21-7.09 (m, 18H, H_{22}, H_{23}, H_{24} and H_F), 6.98 (bs, 3H, H_{15}, H_{17} and H_{19}), 5.89-5.79 (m, 1H, H_{10}), 5.73 (bs, 1H, H_{13}), 5.46 (t, 1H, *J* = 8.8 Hz, H_2), 5.37 (bs, 1H, H_4), 5.14-5.05 (m, 3H, H_3 and H_{11}), 4.84 (d, 1H, *J* = 7.6 Hz, H_1), 4.74 (bs, 2H, H_{12}), 4.48-4.39 (m, 8H, H_E), 4.05 (t, 1H, *J* = 8.0 Hz, H_{21}), 4.02 (d, 2H, *J* = 6.8 Hz, H_6), 3.80 (t, 1H, *J* = 6.0 Hz, H_5), 3.70 (bs, 2H, H_{20}), 3.46-3.42 (m, 4H, H_9 and H_{14}), 3.30 (bs, 2H, H_{18}), 2.93 (bs, 2H, H_{16}), 2.17 (s, 3H, *H*-Ac), 2.16 (s, 3H, *H*-Ac), 2.01 (s, 3H, *H*-Ac), 1.94 (s, 3H, *H*-Ac); **^{13}C NMR (100 MHz, $CDCl_3$):** δ 170.5, 170.3, 170.2, 170.1, 169.7, 169.2, 168.2, 167.2, 156.3, 145.3, 145.0, 141.7, 137.7, 137.4, 135.3, 134.3, 133.9, 133.7, 131.0, 129.1, 129.0, 128.8, 128.0, 127.0, 125.4, 122.2, 117.7, 102.6, 71.1, 70.7, 68.8, 66.7, 65.3, 60.7, 50.5, 44.5, 44.2, 42.7, 42.1, 33.9, 20.9, 20.8, 20.7, 20.6; **LRFAB-MS (3-NOBA matrix):** ***m/z*** 1467 $[M+H]^+$; **HRFAB-MS (3-NOBA matrix):** ***m/z*** 1466.54845 (calcd. for $C_{77}H_{80}N_9O_{21}$ 1466.54688 $[M+H]^+$).

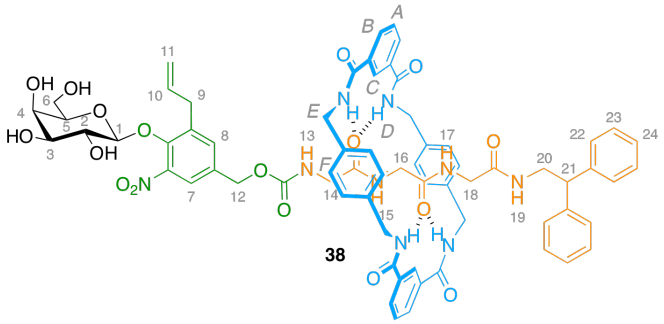

38

Using general method **C**, rotaxane **37** (98 mg, 0.067 mmol, 1 equiv.) and MeONa (36 mg, 0.67 mmol 10 equiv.) at 0°C in MeOH (10 mL) gave crude **38** as a brown solid. Purification by flash column chromatography on silica gel with CH_2Cl_2-MeOH (98:2 to 9:1) as eluent gave **38** as a light brown solid (75 mg, 0.058 mmol, **87%**). **M.p.** 178-180°C; **^{1}H NMR (400 MHz, CD_3OD):** δ = 8.34 (bs, 2H, H_C), 8.05-8.03 (m, 4H, H_B), 7.59 (t, 2H, *J* = 7.6 Hz, H_A), 7.23-7.01 (m, 18H, H_{22}, H_{23}, H_{24} and H_F), 5.97-5.87 (m, 1H, H_{10}), 5.09 (dd, 1H, *J* = 8.8 Hz, *J* = 1.6 Hz, H_{11}), 5.05 (bs, 1H, H_{11}), 4.57 (bs, 2H, H_{12}), 4.48-4.39 (m, 9H, H_1 and H_E), 3.93 (t, 1H, *J* = 8.0 Hz, H_{21}), 3.82 (t, 1H, *J* = 3.2 Hz), 3.76 (dd, 1H, *J* = 9.6 Hz, *J* = 7.6 Hz,), 3.65 (dd, 1H, *J* = 11.2 Hz, *J* = 6.8 Hz), 3.57-3.44 (m, 10H, H_{14}, H_{16}, H_{18} and H_{20}); **^{13}C NMR (100 MHz, CD_3OD):** δ 172.4, 171.2, 170.5, 169.0, 158.1, 147.7, 147.0, 143.6, 138.8, 138.3, 137.5, 135.7, 134.9, 134.7, 131.7, 130.1, 130.0, 129.9, 129.8, 129.6, 129.4, 129.0, 127.8, 127.7, 122.8, 117.4, 107.1, 77.1, 74.7, 72.5, 69.7, 66.2, 61.7, 51.7, 49.9, 45.2, 45.0, 44.9, 43.2, 42.6, 34.4; **LRFAB-MS (3-NOBA matrix):** ***m/z*** 1299 $[M+H]^+$; **HRFAB-MS (3-NOBA matrix):** ***m/z*** 1299.51035 (calcd. for $C_{69}H_{73}N_9O_{17}$ calcd. 1299.51244 $[M+H]^+$).

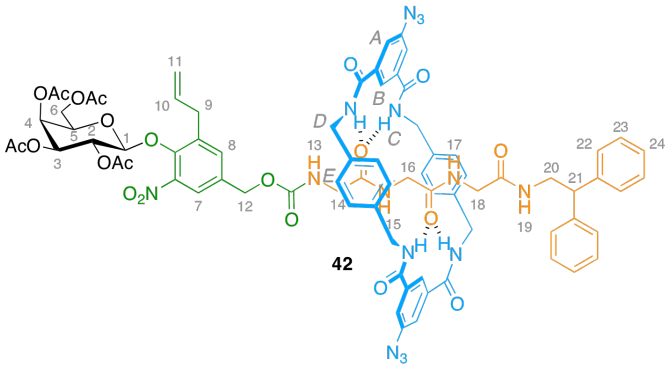

42

Using general method **A**, thread **35** (400 mg, 0.43 mmol, 1 equiv.), *p*-xylylenediamine (933 mg, 6.88 mmol, 16 equiv.), 5-azidoisophthaloyl dichloride (1.67 g, 6.88 mmol, 16 equiv.) and Et_3N (2.1 mL, 15.05 mmol, 35 equiv.) in $CHCl_3$

(200 mL) at room temperature for 3 hours gave crude **42** as an orange solid. Purification by flash column chromatography on silica gel with $CHCl_3$-acetone (9:1 to 4:6) as eluent gave a mixture rotaxane **42** as a light yellow solid (421 mg, 0.27 mmol, **63%**). **M.p.** dec.; **^{1}H NMR (400 MHz, $CDCl_3$):** δ = 7.88 (bs, 2H, H_B), 7.62 (bs, 4H, H_C), 7.54 (bs, 4H, H_A), 7.34 (s, 1H, H_7), 7.18-7.17 (m, 1H, H_{15}), 7.14 (d, 4H, *J* = 7.6 Hz, H_E), 7.10 (s, 1H, H_8), 7.07 (bs, 10H, H_{22}, H_{23} and H_{24}), 7.01 (d, 4H, *J* = 7.2 Hz, H_E), 6.86 (bs, 2H, H_{17} and H_{19}), 5.83-5.73 (m, 1H, H_{10}), 5.63 (bs, 1H, H_{13}), 5.39 (dd, 1H, *J* = 10.4 Hz, *J* = 8.0 Hz, H_2), 5.30 (d, 1H, *J* = 3.6 Hz, H_4), 5.08-4.97 (m, 3H, H_3 and H_{11}), 4.77-4.76 (m, 3H, H_1 and H_{12}), 4.50-4.46 (m, 4H, H_D), 4.31-4.27 (m, 4H, H_D), 4.00-3.91 (m, 3H, H_6 and H_{21}), 3.74 (t, 1H, *J* = 7.2 Hz, H_5), 3.66 (bs, 2H, H_{20}), 3.45 (bs, 2H, H_{14}), 3.41 (d, 2H, *J* = 6.4 Hz, H_9), 3.25 (bs, 2H, H_{16} or H_{18}), 2.97 (bs, 2H, H_{16} or H_{18}), 2.10 (s, 3H, *H*-Ac), 2.08 (s, 3H, *H*-Ac), 1.93 (s, 3H, *H*-Ac), 1.88 (s, 3H, *H*-Ac); **^{13}C NMR (100 MHz, $CDCl_3$):** δ = 170.6, 170.4, 170.2, 169.7, 169.4, 168.1, 166.0, 156.5, 145.3, 145.1, 141.6, 141.5, 137.8, 137.2, 135.7, 135.3, 133.8, 133.5, 129.3, 128.9, 127.9, 127.2, 122.1, 121.6, 121.0, 117.8, 102.7, 71.1, 70.7, 68.7, 66.7, 65.4, 60.7, 53.9, 50.6, 44.5, 44.4, 42.9, 42.4, 34.0, 31.9, 29.4, 21.0, 20.8, 20.7 (x2); **LRESI-MS:** ***m/z*** 1550.44 $[M+H]^+$; **LRFAB-MS (3-NOBA matrix):** ***m/z*** 1550.5 $[M+H]^+$; **HRFAB-MS (3-NOBA matrix)** *submitted*

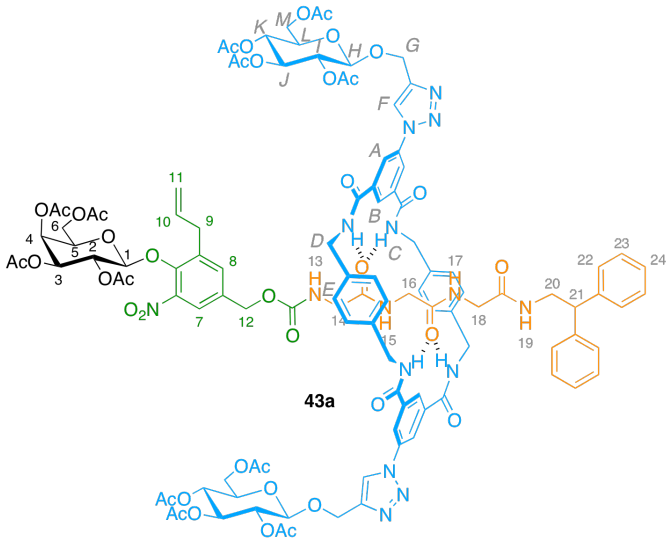

Using general method **B**, rotaxane **42** (61 mg, 39.4 μmol, 1.0 equiv.), alkyne **45** (30 mg, 78.8 μmol, 2.0 equiv.), $[Cu(CH_3CN)_4](PF_6)$ (7 mg, 19.7 μmol, 0.5 equiv.) and NEt_3 (12 μL, 78 μmol, 2.0 equiv.) in CH_2Cl_2 (7 mL) at room temperature overnight gave crude **43a** as an yellow solid. Purification by flash column chromatography on

silica gel with $CHCl_3$-acetone (7:3 to 45:55) as eluent gave **43a** as a light yellow solid (31 mg, 13.4 μmol, **34%**). **M.p.** 166-168°C; **^{1}H NMR (400 MHz, $CDCl_3$):** δ = 8.27-8.23 (m, 4H, H_A and H_F), 8.20 (bs, 2H, H_B), 8.09 (bs, 2H, H_C), 8.01 (bs, 4H), 7.35 (s, 1H, H_7), 7.17 (s, 1H, H_8), 7.10-7.08 (m, 8H, H_E), 7.04-6.99 (m, 10H, H_{22}, H_{23} and H_{24}), 6.93- 6.87 (m, 3H, H_{15}, H_{17} and H_{19}), 5.79-5.69 (m, 2H, H_{10} and H_{13}), 5.36 (dd, 1H, J = 10.4 Hz, J = 8.0 Hz, H_2), 5.31 (d, 1H, J = 3.2 Hz, H_4), 5.20-5.16 (m, 2H, H_J), 5.08-4.99 (m, 7H, H_3, H_{11}, H_I and H_K), 4-99-4.80 (m, 4H, H_G and H_H), 4.80-4.69 (m, 3H, H_{12} and H_1), 4.47-4.44 (m, 4H, H_D), 4.34-4.31 (m, 4H, H_D), 4.22-4.11 (m, 4H, H_M), 4.00-3.90 (m, 3H, H_{21} and H_6), 3.79-3.71 (m, 4H, H_5 and H_L), 3.62 (bs, 2H, H_{14}), 3.51 (bs, 2H, H_{16}), 3.36 (d, 2H, J = 6.8 Hz, H_9), 3.24 (bs, 2H, H_{18}), 2.82 (bs, 2H, H_{20}), 2.11 (s, 3H, *H*-Ac), 2.07 (s, 3H, *H*-Ac), 2.01 (s, 6H, *H*-Ac), 1.97 (s, 6H, *H*-Ac), 1.95 (s, 6H, *H*-Ac), 1.94 (s, 6H, *H*-Ac), 1.93 (s, 3H, *H*-Ac), 1.88 (s, 3H, *H*-Ac); **^{13}C NMR (100 MHz, $CDCl_3$):** δ = 171.1, 170.7, 170.4, 170.2, 170.0, 169.7, 169.6, 169.2, 165.7, 145.5, 145.3, 145.0, 141.7, 137.8, 137.3, 137.2, 136.3, 136.2, 135.3, 133.4, 129.2 (x2), 128.8, 127.9, 127.0, 122.1, 121.9, 121.6, 117.8, 102.6, 100.4 (x2), 72.8, 72.1, 71.3, 71.1, 70.7, 68.8, 68.4, 66.7, 65.3, 63.0, 62.0, 60.7, 44.7, 44.2, 33.9, 29.8, 21.0 (x3), 20.9 (x2), 20.8 (x 6), 20.7; **LRFAB-MS (3-NOBA matrix):** ***m/z*** 2322 $[M+H]^+$; **HRFAB-MS (3-NOBA matrix):** ***m/z*** 2321.80494 (calcd. for $C_{110}{}^{13}CH_{122}N_{15}O_{41}$ calcd. 2321.79562 $[M+H]^+$).

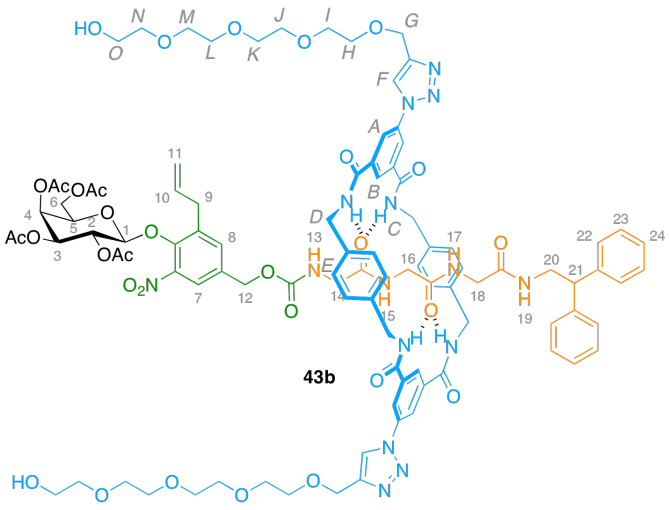

Using general method **B**, rotaxane **42** (100 mg, 64.6 µmol, 1.0 equiv.), alkyne **46** (30 mg, 129.2 µmol, 2.0 equiv.), $[Cu(CH_3CN)_4](PF_6)$ (12 mg, 32.3 µmol, 0.5 equiv.) and NEt_3 (20 µL, 142.1 µmol, 2.0 equiv.) in CH_2Cl_2 (10 mL) at room temperature overnight gave crude **43b** as yellow solid. Purification by flash column

chromatography on silica gel with $CHCl_3$-acetone (7:3 to 45:55) as eluent gave **43b** as a light yellow waxy solid (31 mg, 13.4 μmol, **24%**). **^{1}H NMR (400 MHz, $CDCl_3$):** δ = 8.31 (bs, 4H, H_A and H_F), 8.22 (bs, 2H, H_B), 8.18 (bs, 2H, H_C), 7.35 (s, 1H, H_7), 7.18 (s, 1H, H_8), 7.09-6.99 (m, 21H, H_E, H_{15}, H_{17}, H_{19}, H_{22}, H_{23} and H_{24}), 5.96 (bs, 1H, H_{13}), 5.79-5.69 (m, 1H, H_{10}), 5.36 (dd, 1H, *J* = 10.4 Hz, *J* = 8.0 Hz, H_2), 5.30 (d, 1H, *J* = 3.2 Hz, H_2), 5.03-4.98 (m, 3H, H_3 and H_{11}), 4.77-4.74 (m, 3H, H_1 and H_{12}), 4.68 (bs, 4H, H_G), 4.39-4.35 (m, 8H, H_D), 3.97-3.94 (m, 3H, H_6 and H_{21}), 3.77 (t, 1H, *J* = 6.8 Hz, H_5), 3.69-3.47 (m, 34H, H_H, H_I, H_J, H_K, H_L, H_M, H_N, H_O, and H_{14}), 3.37-3.35 (m, 2H, H_9), 2.96-2.79 (m, 6H, H_{16}, H_{18} and H_{20}), 2.11 (s, 3H, *H*-Ac), 2.06 (s, 3H, *H*-Ac), 1.93 (s, 3H, *H*-Ac), 1.87 (s, 3H, *H*-Ac); **^{13}C NMR (100 MHz, $CDCl_3$):** δ = 170.6, 170.4, 170.2, 170.1, 170.0, 169.7, 169.2, 168.6, 166.0 (x2), 156.3, 146.2, 145.3, 145.0, 141.9, 137.7, 137.3, 137.2, 136.3, 136.2, 135.4, 134.2, 133.4, 129.1, 128.7, 128.0, 126.9, 126.2, 122.0, 121.4, 117.7, 102.6, 72.7, 71.1, 70.7, 70.5 (x2), 70.2, 70.1, 68.8, 66.7, 65.2, 64.6, 61.5, 60.7, 50.5, 44.7, 44.2, 42.4, 41.8, 34.0, 29.8, 20.9, 20.8, 20.7 (x2); **LRFAB-MS (3-NOBA matrix):** ***m/z*** 2014 $[M+H]^+$ 2036 $[M+Na]^+$; **HRFAB-MS (3-NOBA matrix):** ***m/z*** 2013.81525 (calcd. for $C_{98}H_{118}{}^{13}CN_{15}O_{31}$ 2013.81517 $[M+H]^+$).

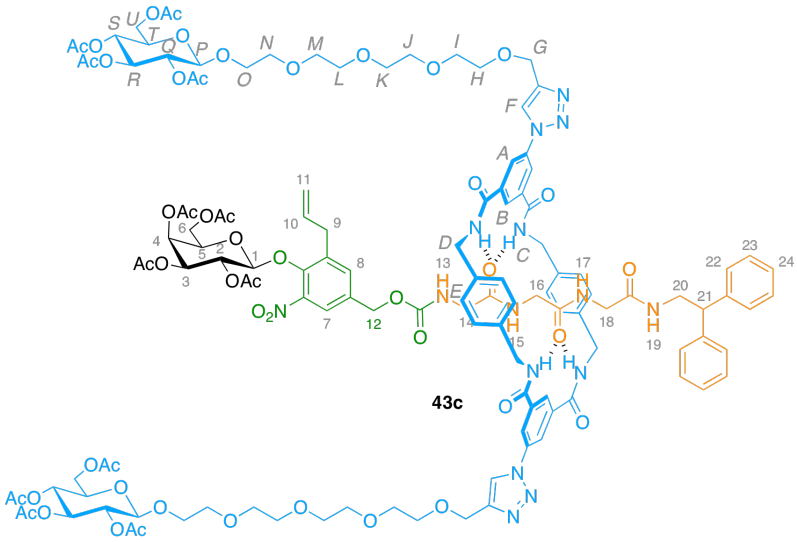

Using general method **B**, rotaxane **42** (70 mg, 45.2 μmol, 1.0 equiv.), alkyne **47** (51 mg, 90.4 μmol, 2.0 equiv.), $[Cu(CH_3CN)_4](PF_6)$ (8 mg, 11.3 μmol, 0.5 equiv.) and NEt_3 (14 μL, 90.4 μmol, 2.0 equiv.) in CH_2Cl_2 (7 mL) at room temperature overnight gave crude **43c** a yellow solid. Purification by preparative TLC on silica eluted 4 times with $CHCl_3$/acetone (1:1) as eluent gave **43c** as a white solid (84 mg, 31.6 μmol, **70%**). **M.p.** 133-135°C; $[\alpha]_D$ +51.3 (*c* 0.008 in $CHCl_3$) **^{1}H NMR (400 MHz,**

$CDCl_3$): δ 8.38 (m, 2H, H_B), 8.24 (bs, 2H, H_F), 8.19 (bs, 6H, H_A and H_C), 7.40 (s, 1H, H_7), 7.22 (s, 1H, H_8), 7.18-7.06 (m, 20H, H_E, H_{15}, H_{17}, H_{22}, H_{23} and H_{24}), 6.95 (bs, 2H, H_{19}), 5.85-5.75 (m, 2H, H_{10} and H_{13}), 5.43 (dd, 1H, J = 10.4 Hz, J = 8.0 Hz, H_2), 5.37 (d, 1H, J = 3.6 Hz, H_4), 5.20 (t, 2H, J = 9.6 Hz, H_R), 5.10-5.04 (m, 5H, H_3, H_{11} and H_S), 5.97 (dd, 2H, J = 9.6 Hz, J = 8.0 Hz, H_Q), 4.82 (m, 2H, H_1 and H_{12}), 4.76 (s, 4H, H_G), 4.58 (d, 2H, J = 8.0 Hz, H_P), 4.55-4.43 (m, 8H, H_D), 4.24 (dd, 2H, J = 12.0 Hz, J = 4.4 Hz, H_U), 4.11 (dd, 3H, J = 12.0 Hz, J = 2.0 Hz, $H_{U'}$), 4.07-3.98 (m, 4H, H_6 and H_{21}), 3.93 (dt, 2H, J = 4.0 Hz, J = 4.4 Hz, H_T), 3.85 (t, 1H, J = 6.8 Hz, H_5), 3.77-3.56 (m, 36H, H_H, H_I, H_J, H_K, H_L, H_M, H_N, H_O, H_{14} and H_{16}), 3.42 (d, 2H, J = 6.4 Hz, H_9), 3.30-3.22 (m, 2H, H_{18}), 2.84 (bs, 2H, H_{20}), 2.17-1.95 (s, 36H, *H*-Ac); **^{13}C NMR (100 MHz, $CDCl_3$):** δ 170.9, 170.4 (x2), 170.2, 169.7, 169.6, 165.8, 146.5, 145.0, 141.8, 137.7, 137.4, 137.3, 136.4, 136.3, 135.3, 134.1, 133.3, 129.9, 129.1, 128.8, 128.0, 126.9, 126.1, 121.9 (x2), 121.2, 117.7, 102.6, 101.0 (x2), 72.9, 71.9, 71.4, 71.0, 70.7, 70.6, 70.3, 70.1, 69.3, 68.8, 68.5, 66.8, 65.2, 64.6, 62.1, 60.7, 50.5, 44.7, 44.3, 44.1, 42.4, 42.3, 41.8, 33.9, 29.8, 29.4, 21.0, 20.9 (x2), 20.8, 20.7; **LRFAB-MS (3-NOBA matrix):** ***m/z*** 2675 $[M+H]^+$, 2698.9 $[M+Na]^+$; **HRFAB-MS (3-NOBA matrix):** ***m/z*** 2695.98021 (calcd. for $C_{126}{}^{13}CH_{153}N_{15}O_{49}Na$ calcd. 2695.98728 $[M+Na]^+$).

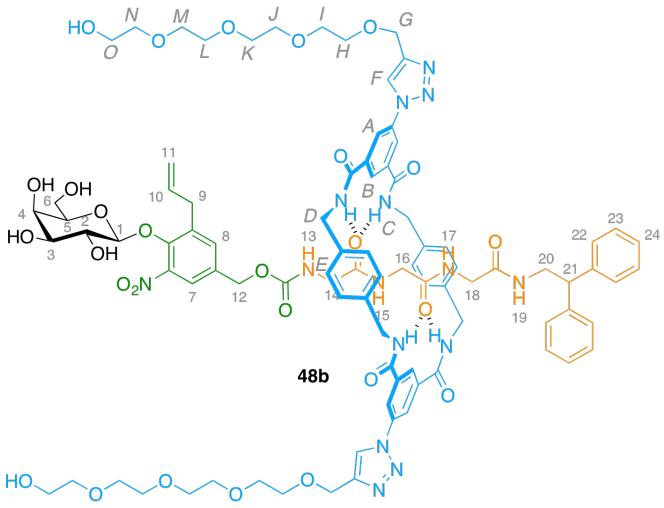

Using general method **C**, rotaxane **43b** (27 mg, 13.4 µmol, 1 equiv.) and MeONa (7 mg, 0.134 mmol 10 equiv.) at 0°C in MeOH (4 mL) gave crude **48b** as a brown solid. Purification by preparative RP-HPLC using a linear gradient (37 to 55 % in 20 min) of MeCN in H_2O at a flow rate of 10 mL/min to give rotaxane **48b** as a light

yellow solid. Purity (HPLC): >94%. **M.p.** 102-104°C; **^{1}H NMR (400 MHz, CD_3OD):** δ 8.57 (s, 2H, H_B), 8.36 (s, 4H, H_A), 8.29 (s, 2H, H_F), 7.14 (s, 8H, H_E), 7.12-6.89 (m 12H, H_7, H_8 H_{22}, H_{23} and H_{24}) , 5.78-5.68 (m, 1H, H_{10}), 4.95-4.90 (m, 2H, H_{11}), 4.65 (s. 4H, H_G), 4.45-4.34 (m, 10H, H_{12} and H_D), 4.21 (d, 1H, J = 7.7 Hz, H_1), 3.88 (t, 1H, J = 7.7 Hz, H_{21}), 3.69-3.10 (m, 48H, H_2, H_3, H_4, H_5, H_6, H_9, H_{14}, H_{16}, H_{18}, H_{20} H_H, H_I, H_J, H_K, H_L H_M, H_N and H_O); **^{13}C NMR (100 MHz, CD_3OD):** δ 171.2, 167.5, 167.4, 158.1, 147.4, 143.6, 138.7 (x2), 137.4, 134.4, 130.0, 129.6, 129.0, 127.8, 127.7, 127.3, 123.5, 123.1, 123.0, 122.6, 117.4, 106.9, 77.1, 74.6, 73.6, 72.4, 71.6, 71.5, 71.4, 71.0, 69.7, 66.1, 65.0, 62.2, 61.8, 51.7, 45.2, 45.0, 43.1, 42.8, 34.3, 30.8; **LRFAB-MS (3-NOBA matrix):** ***m/z*** **HRFAB-MS (3-NOBA matrix):** *submitted*

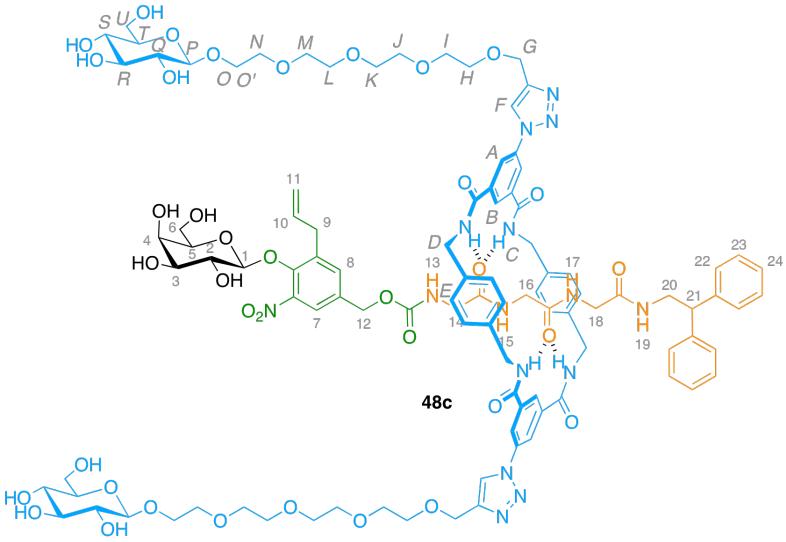

Using general method **C**, rotaxane **43c** (24 mg, 9.0 umol, 1 equiv.) and MeONa (16 mg, 0.270 mmol 30 equiv.) at 0°C in MeOH (3 mL) gave crude **48c** as a brownish solid. Purification by preparative RP-HPLC using a linear gradient (33 to 45 % in 15 min) of MeCN in H_2O at a flow rate of 10 mL/min to give rotaxane **48c** as a pink solid. Purity (HPLC): >94%. **M.p.** 130°C (dec.); **^{1}H-NMR (400 MHz, CD_3OD, 300 K):** δ = 8.69 (s, 2H, H_B), 8.47 (s, 4H, H_A), 8.39 (s, 2H, H_F), 7.41-6.92 (m, 20H, H_7, H_8, H_{22}, H_{23}, H_{24}, H_E), 5.92-5.77 (m, 8H, H_{10}), 5.07-4.98 (m, 2H, H_{11}), 4.78 (s, 4H, H_G), 4.56-4.38 (m, 8H, H_D), 4.32 (d, J = 7.7 Hz, 2H, H_1), 4.29 (d, J = 7.8 Hz, 2H, H_P), 4.04-3.93 (m, 3H, H_O and H_{21}), 3.90-3.10 (m, 52H, H_H, H_I, H_J, H_K, H_L, H_M, H_N, $H_{O'}$, H_U, H_2, H_3, H_4, H_5, H_6, H_9, H_{12}, H_{14}, H_{16}, H_{18} and H_{20}); **^{13}C-NMR (100 MHz, CD_3OD, 300 K):** δ = 172.5, 171.2, 170.6, 167.5, 167.4, 158.1, 147.4, 146.8, 143.6, 138.8, 138.7, 138.2, 137.4, 134.7, 134.5, 130.0 (× 2), 129.6, 129.5, 129.0 (× 2),

127.9, 127.7, 123.6, 123.2, 123.1, 122.6, 117.4, 106.9, 104.4, 78.0, 77.9, 77.1, 75.1, 74.6, 72.4, 71.7, 71.6, 71.6, 71.5, 71.4, 71.0, 69.7, 69.6, 66.1, 65.0, 62.8, 61.8, 51.7, 45.2, 45.0, 43.1, 42.8, 34.3; **LRESI-MS:** *m/z* = 1085.4 (100%) $[M+2H]^{2+}$; isotopic pattern matches that calculated for $C_{103}H_{131}Cl_6N_{15}O_{37}$.

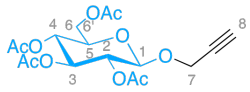

45

To a solution of peracetylated β-D-glucose (1.21 g, 3.1 mmol, 1.0 equiv.) and propargyl alcohol (0.27 mL, 4.65 mmol, 1.5 equiv.) in anhydrous CH_2Cl_2 (8 mL) under N_2 at 0ºC, was added $BF_3.Et_2O$ (2 mL, 15.5 mmol, 5 equiv.) drop wise. The reaction mixture was allowed to warm up to room temperature and stirred overnight. An aqueous saturated solution of $NaHCO_3$ (30 mL) was added, the layers were separated and the aqueous layer was extracted with CH_2Cl_2 (3 × 25 mL). The combined organic fractions were dried (Na_2SO_4) and concentrated under reduced pressure. The resulting brown residue was purified by flash column chromatography on Silica gel with CH_2Cl_2-acetone (98:2) as eluent to give pure **45** as a white solid (940 mg, 2.43 mmol, 79%). **M.p.** 100-102°C; $[\alpha]_D$ +59.2 (*c* 0.1 in $CHCl_3$) **^{1}H-NMR (400 MHz, $CDCl_3$, 298 K):** δ = 5.22 (t, *J* = 9.5 Hz, 1H, H_3), 5.08 (t, *J* = 9.5 Hz, 1H, H_4), 4.99 (t, *J* = 9.5 Hz, 1H, H_2), 4.76 (d, *J* = 7.9 Hz, 1H, H_1), 4.35 (d, *J* = 2.3 Hz, 2H, H_7), 4.26 (dd, *J* = 4.6 Hz and *J* = 12.3 Hz, 1H, H_6), 4.13 (dd, *J* = 2.2 Hz and *J* = 12.3 Hz, 1H, $H_{6'}$), 3.71 (ddd, *J* = 2.4 Hz, *J* = 4.5 Hz and *J* = 10.0 Hz, 1H, H_5), 2.46 (t, *J* = 2.4 Hz, 1H, H_8), 2.07, 2.04, 2.10, 1.99 (4s, 12H, O*Ac*); **^{13}C-NMR (100 MHz, $CDCl_3$, 298 K):** δ = 170.6, 170.2, 169.3, 169.2, 98.0, 78.0, 75.4, 72.6, 71.8, 70.8, 68.2, 61.6, 55.8, 20.7, 20.6, 20.5, 20.4; **LRESI-MS:** *m/z* = 409 $[M+Na]^+$; **HRESI-MS:** *m/z* = 404.1552 $[M+NH_4]^+$ (calc. for $C_{17}H_{26}O_{10}N$ 404.1551 $[M+H]^+$).

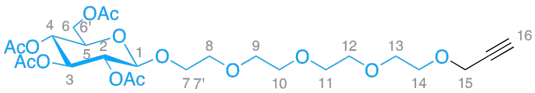

47

To a solution of peracetylated β-D-glucose (317 mg, 0.81 mmol, 1.0 equiv.) and **46** (283 mg, 1.22 mmol, 1.5 equiv.) in anhydrous CH_2Cl_2 (2 mL) under N_2 at 0ºC, was added $BF_3.Et_2O$ (0.52 mL, 0.40 mmol, 5 equiv.) drop wise. The reaction mixture was allowed to warm up to room temperature and stirred overnight. An aqueous saturated

solution of $NaHCO_3$ (10 mL) was added, the layers were separated and the aqueous layer was extracted with CH_2Cl_2 (3×15 mL). The combined organic fractions were dried (Na_2SO_4) and concentrated under reduced pressure. The resulting brown residue was purified by flash column chromatography on silica gel with CH_2Cl_2-acetone (93:7) as eluent to give pure **47** as a colourless oil (378 mg, 0.67 mmol, 83%). **^{1}H-NMR (400 MHz, $CDCl_3$, 298 K):** δ = 5.13 (t, J = 9.5 Hz, 1H, H_3), 5.01 (t, J = 9.6 Hz, 1H, H_4), 4.91 (dd, J = 8.0 Hz and J = 9.5 Hz, 1H, H_2), 4.55 (d, J = 8.0 Hz, 1H, H_1), 4.19 (dd, J = 4.7 Hz and J = 12.3 Hz, 1H, H_6), 4.14 (d, J = 2.4 Hz, 2H, H_{15}), 4.06 (dd, J = 2.3 Hz and J = 12.3 Hz, 1H, $H_{6'}$), 3.87 (dt, J = 4.0 Hz and J = 11.0 Hz, 1H, H_7), 3.71-3.52 (m, 16H, H_5, $H_{7'}$, H_8, H_9, H_{10}, H_{11}, H_{12}, H_{13}, and H_{14}), 2.40 (t, J = 2.3 Hz, 1H, H_{16}), 2.01, 1.97, 1.95, 1.93 (4s, 12H, O*Ac*); **^{13}C-NMR (100 MHz, $CDCl_3$, 298 K):** δ = 170.4, 170.0, 169.2, 169.1, 100.6, 79.5, 74.4, 72.6, 71.5, 71.0, 70.5, 70.4 (× 2), 70.3, 70.1, 70.0, 68.8 (× 2), 68.2, 61.7, 58.1, 20.6, 20.5, 20.4, 20.3; **LRESI-MS:** *m/z* = 585 $[M+Na]^+$; **HRESI-MS:** *m/z* = 580.2600 $[M+NH_4]^+$ (calc. for $C_{25}H_{42}O_{14}N$ 580.2600 $[M+ NH_4]^+$).

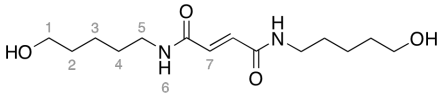

22

To a solution of 5-Amino-pentan-1-ol (3.0 g, 29.10 mmol, 1.0 equiv.) in dry DMF (40 mL) at 0 ^oC was added a solution of fumaroyl dichloride (0.90 g, 5.81 mmol, 2.0 equiv.) in DMF (15 mL) over a period of 2 hours using motor-driven syringe pumps. The reaction mixture was stirred for a further 2 hours, concentrated under reduced pressure. The residue was re-dissolved in CH_2Cl_2 (300 mL) and a solution of HCl (3M) in diethyl ether was added until all of the unreacted 5-Amino-pentan-1-ol had precipitated. The solid was filtered through a plug of Celite®, the plug was washed with warm DMF (2 × 15 mL) and solvents were removed under reduced pressure to afford **22** as a light yellow solid. (1.16 g, 4.05 mmol, 70%). **M.p.** = 219-222^{o}C; **^{1}H-NMR (400 MHz, DMSO *d6*, 300 K):** δ = 8.36 (t, 2H, J = 5.6 Hz, H_6), 6.80 (s, 2H, H_7), 3.36 (t, 4H, J = 6.4 Hz, H_1), 3.12 (q, 4H, J = 6.0 Hz, H_5), 1.47-1.34 (m, 8H, H_2 and H_4), 1.32-1.21 (m, 4H, H_3); **^{13}C-NMR (100 MHz, DMSO *d6*, 300 K):** δ = 163.6, 132,6, 60.6, 32.2, 28.8, 28.6, 23.0; **FAB-MS:** *m/z* = 286 $[M]^+$. **HRESI-MS:** *m/z* = 287.1967 $[M+H]^+$ (calcd for $C_{14}H_{27}N_2O_4$ 287.1965 $[M+H]^+$).

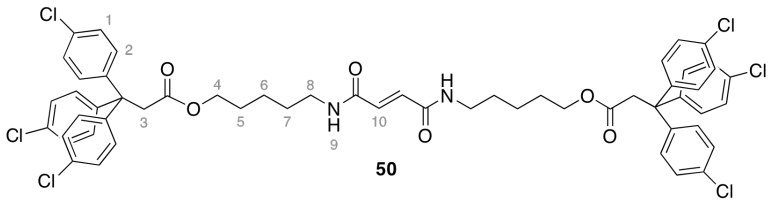

50

To a solution of 3,3,3-Tris-(4-chloro-phenyl)-propionic acid **49** (1.53 g, 3.77 mmol, 2.0 equiv.), EDCI.HCl (984 mg, 5.13 mmol) and DMAP (625 mg, 5.12 mmol) in CH_2Cl_2 (30 mL) at room temperature, was added **22** (490 mg, 1.71 mmol) and the reaction mixture was stirred overnight. CH_2Cl_2 (250 mL) and an aqueous solution of HCl (1M) (50 mL) were added, the layers were separated and the aqueous layer was extracted with CH_2Cl_2 (2 × 25 mL). The combined organic fractions were washed with an aqueous saturated solution of $NaHCO_3$, dried ($MgSO_4$) and concentrated under reduced pressure. Purification by flash column chromatography on silica gel with CH_2Cl_2-MeOH (98:2) as eluent gave **50** as a white solid. (1.50 g, 1.41 mmol 84%). **M.p.** 132-136 °C; **^{1}H-NMR (400 MHz, $CDCl_3/CD_3OD$, 9:1):** δ = 8.01 (t, 2H, *J* = 5.6 Hz, H_9), 7.23-7.16 (m, 12H, H_1), 7.12-7.04 (m, 12H, H_2), 6.71 (s, 2H, H_{10}), 3.75 (t, 4H, *J* = 6.5 Hz, H_4), 3.59 (s, 4H, H_3), 3.23-3.17 (m, 4H, H_8), 1.51-1.26 (m, 8H, H_5 and H_7), 1.19-1.05 (m, 4H, H_6); **^{13}C-NMR (400 MHz, $CDCl_3/CD_3OD$, 9:1):** δ = 170.4, 164.2, 144.2, 133.0, 132.6, 130.3, 128.2, 64.3, 54.6, 46.0, 39.6, 29.0, 28.0, 23.2; **FAB-MS:** *m/z* = 1061 $[M+H]^+$; **HRFAB-MS (glycerol matrix):** *m/z* = 1061.20286 $[M+H]^+$ (calcd for $C_{56}{}^{13}CH_{52}D^{35}Cl_6N_2O_6$ 1061.20053 $[M+H]^+$).

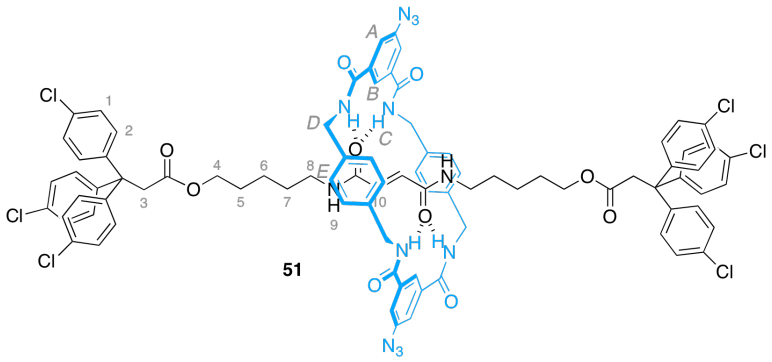

51

To a vigourously stirred solution of thread **50** (525 mg, 4.94 mmol, 1 equiv.) and NEt_3 (2 mL, 14.8 mmol, 30 equiv.) in 1 L of dry $CHCl_3$ under nitrogen, was simultaneously added a solution of *p*-xylylenediamine (1.00 g, 7.40 mmol, 15 equiv.) in $CHCl_3$ (50 mL) and a solution of isophthaloyl dichloride (1.81 g, 7.40 mmol, 15 equiv.) in $CHCl_3$ (50 mL) over a period of 3 hours using motor-driven syringe

pumps. The reaction mixture was stirred for a further 2 hours, filtered over a celite® pad and the filtrate was concentrated under reduced pressure. The resulting orange solid was purified by flash column chromatography on silica gel with acetone-CH_2Cl_2 (10:90) as eluent to give rotaxane **51** as a light orange solid (690 mg, 4.12 mmol, 83%). **M.p.** 175°C (dec.); **^{1}H-NMR (400 MHz, $CDCl_3$, 298 K):** δ = 8.03 (m, 2H, H_C), 7.81-7.67 (m, 6H, H_D and H_{10}), 7.66 (s, 4H, H_B), 7.21-7.12 (m, 20H, H_F, H_1), 7.09-7.01 (m, 12H, H_2), 5.74 (s, 2H, H_{10}), 4.45 (bs, 8H, H_E), 3.72 (t, J = 6.5 Hz, 4H, H_4), 3.14 (m, 2H, H_8), 1.45 (bquint, J = 7.2 Hz, 4H, H_5), 1.37-1.21 (m, 4H, H_7), 1.17-1.05 (m, 4H, H_6); **^{13}C-NMR (100 MHz, $CDCl_3$, 298 K):** δ = 170.3, 165.9, 165.4, 143.8, 141.6, 136.6, 135.3, 132.3, 130.0, 129.5, 128.7, 127.9, 121.4, 120.8, 64.0, 54.4, 45.7, 43.8, 39.5, 28.4, 27.7, 23.0; **LRESI-MS:** *m/z* = 1697.4 $[M+Na]^+$; **HRESI-MS :** *m/z* = 1694.4408 (100%) $[M+NH_4]^+$, isotopic pattern matches that calculated for $C_{88}H_{82}Cl_6N_{13}O_{10}$.

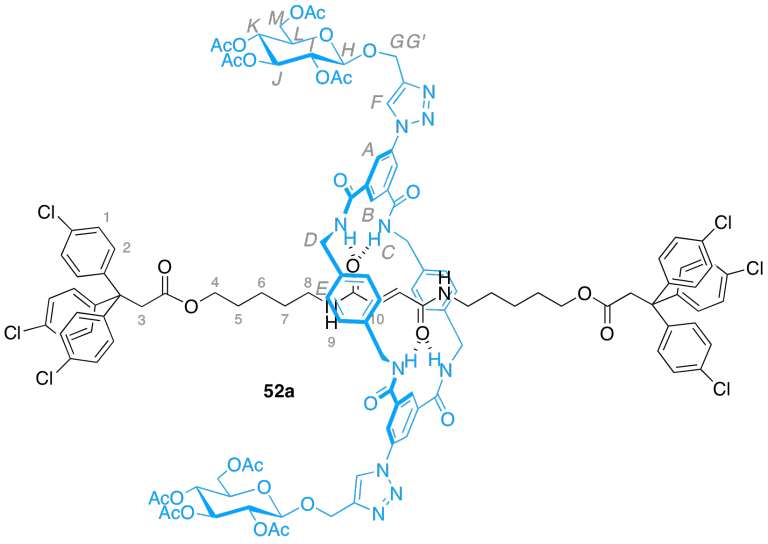

Using general method **B**, rotaxane **51** (59 mg, 0.035 mmol, 1.0 equiv.), alkyne **45** (27 mg, 0.070 mmol, 2.0 equiv.), $[Cu(CH_3CN)_4](PF_6)$ (6.6 mg, 0.017 mmol, 0.5 eq) and NEt_3 (11 µL, 0.077 mmol, 2.2 equiv.) in CH_2Cl_2 (5 mL) at room temperature overnight gave pure **52a** as a light yellow solid (80 mg, 0.032 mmol, 81%). **M.p.** 120-124 °C; $[\alpha]_D$ +78.2 (*c* 0.05 in $CHCl_3$) **^{1}H-NMR (400 MHz, $CDCl_3$):** δ = 8.50-8.19 (m, 8H, H_A, H_B and H_F), 8.19-7.95 (m, 2H, H_9), 7.95-7.58 (m, 4H, H_C), 7.24-6.87 (m, 32H, H_1, H_2 and H_E), 5.84 (s, 2H, H_{10}), 5.23 (t, 2H, J = 9.4 Hz, H_J), 5.17-4.99 (m, 6H, H_G, H_I and H_K), 4.93 (d, 2H, J = 12.5 Hz, H_H), 4.79, 4.77 (2s, 2H, $H_{G'}$) 4.51-402 (m, 12H, H_D and H_M), 3.69 (bt, 4H, J = 6.3 Hz, H_4), 3.57-3.43 (m, 4H, H_3),

3.26-3.05 (m, 4H, H_8), 2.07, 2.03, 1.99, 1.97 (4s, 24H, O*Ac*), 1.55-1.18 (m, 8H, H_5 and H_7), 1.18-1.02 (m, 4H, H_6); **^{13}C-NMR (100 MHz, $CDCl_3$, 300 K):** 170.7, 170.2, 169.5, 169.4, 165.7, 145.1, 144.0, 137.4, 136.6, 135.5, 132.4, 130.2, 129.1, 128.1, 122.2, 99.4, 98.0, 72.7, 71.8, 71.1, 70.8, 69.7, 68.3, 68.2, 64.1, 62.2, 61.9, 55.9, 54.5, 45.8, 39.7, 28.7, 27.8, 23.1, 20.8, 20.7, 20.6, 20.5; **LRMALDI-MS:** *m/z* = 2471.5 (100%) $[M+Na]^+$, isotopic pattern matches that calculated for $C_{122}H_{122}Cl_6N_{12}O_{30}Na$.

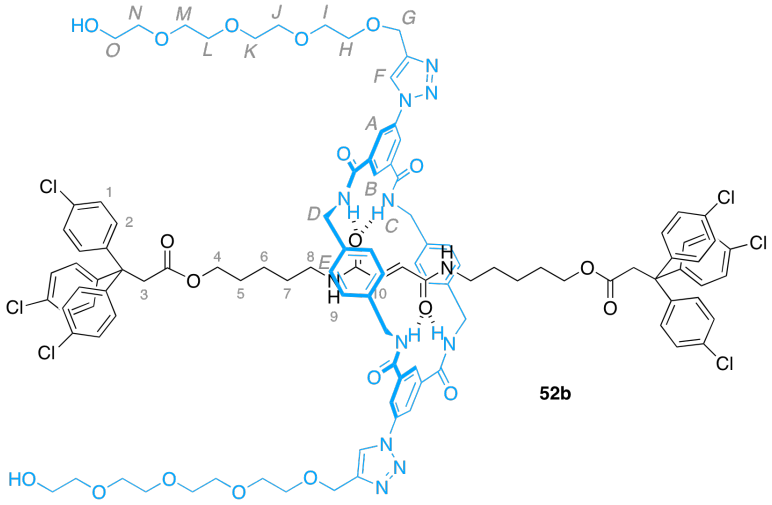

Using general method **B**, rotaxane **51** (97 mg, 0.058 mmol, 1.0 equiv.), alkyne **46** (27 mg, 0.116 mmol, 2.0 equiv.), $[Cu(CH_3CN)_4](PF_6)$ (11 mg, 0.029 mmol, 0.5 eq) and NEt_3 (16 μL, 0.127 mmol, 2.2 equiv.) in CH_2Cl_2 (15 mL) at room temperature overnight gave pure **52b** as a light yellow solid (115 mg, 0.054 mmol, 93%). **M.p.** 100-102°C; **^{1}H-NMR (400 MHz, $CDCl_3$, 300 K):** 8.50-8.23 (m, 8H, H_A, H_B and H_F), 8.23-8.07 (m, 2H, H_9), 7.95-7.74 (m, 4H, H_C), 7.21-6.92 (m, 32H, H_1, H_2 and H_E), 5.86 (s, 2H, H_{10}), 4.80 (s, 4H, H_G), 4.46-409 (m, 8H, H_D), 3.84-3.43 (m, 40H, H_3, H_4, H_H, H_I, H_J, H_K, H_L H_M, H_N and H_O), 3.21-3.03 (m, 4H, H_8), 1.53-1.19 (m, 8H, H_5 and H_7), 1.18-1.00 (m, 4H, H_6); **^{13}C-NMR (100 MHz, $CDCl_3$, 300 K):** 170.2, 165.6, 165.0, 146.1, 144.0, 137.4, 136.6, 135.5, 132.4, 130.2, 129.1 (× 2), 129.0, 128.1, 124.5, 122.2, 121.8, 72.5, 70.5, 70.4, 70.3, 70.0, 69.9, 64.5, 64.1, 61.4, 54.5, 45.8, 44.1, 39.7, 29.6, 27.9, 23.2; **LRMALDI-MS:** *m/z* = 2163.6 (100%) $[M+Na]^+$, isotopic pattern matches that calculated for $C_{110}H_{118}Cl_6N_{12}O_{20}Na$.

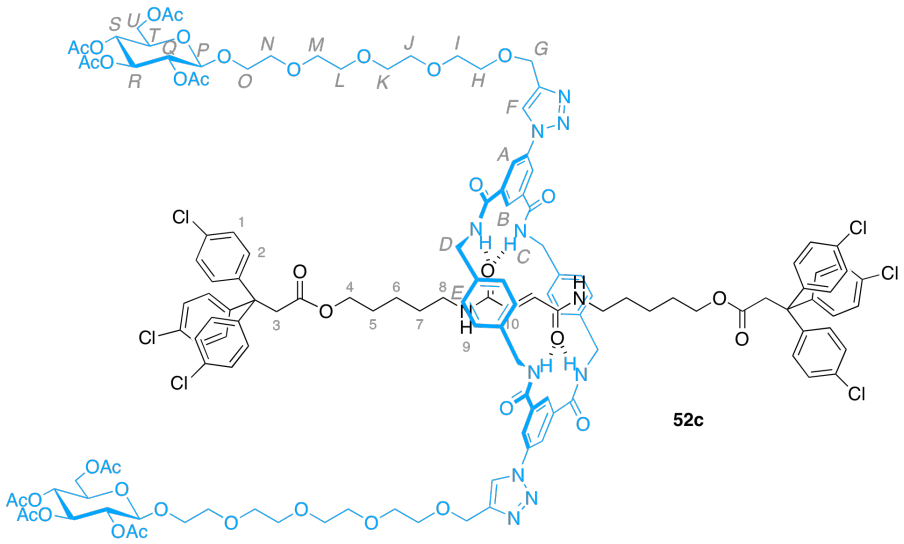

52c

Using general method **B**, rotaxane **51** (250 mg, 0.149 mmol, 1.0 equiv.), alkyne **47** (168 mg, 0.298 mmol, 2.0 equiv.), $[Cu(CH_3CN)_4](PF_6)$ (28 mg, 0.074 mmol, 0.5 eq) and NEt_3 (455 µL, 0.077 mmol, 2.2 equiv.) in CH_2Cl_2 (15 mL) at room temperature overnight gave pure **52c** as a light yellow solid (296 mg, 0.105 mmol, 78%). **M.p.** 95-98°C; $[\alpha]_D$ +9.8 (*c* 0.008 in $CHCl_3$) **^{1}H-NMR (400 MHz, $CDCl_3$):** 8.41 (s, 2H, H_B), 8.36 (s, 4H, H_A), 8.26 (s, 2H, H_F), 7.98-7.77 (m, 4H, H_C), 7.74-7.56 (m, 2H, H_9), 7.22-7.12 (m, 12H, H_1), 7.12-6.97 (m, 20H, H_2 and H_E), 5.75 (s, 2H, H_{10}) 5.21 (t, 2H, J = 9.5 Hz, H_R), 5.08 (t, 2H, J = 9.6 Hz, H_S), 4.98 (t, 2H, J = 8.8 Hz, H_Q), 4.80 (s, 4H, H_G), 4.60 (d, 2H, J = 7.9 Hz, H_P), 4.47-4.30 (m, 8H, H_D), 4.25 (dd, 2H, J = 4.4 Hz and J = 12.2 Hz, H_U), 4.13 (d, 2H, J = 11.5Hz, $H_{U'}$), 3.93 (dt, 2H, J = 4.3Hz and J = 11.1 Hz, H_H), 3.81-3.45 (m, 40H, H_3, H_4, $H_{H'}$, H_I, H_J, H_K, H_L H_M, H_N and H_O), 3.20-297 (m, 4H, H_8), 2.07, 2.04, 2.01, 1.99 (4s, 24H, O*Ac*), 1.51-1.17 (m, 8H, H_5 and H_7), 1.17-1.00 (m, 4H, H_6); **^{13}C-NMR (100 MHz, $CDCl_3$, 300 K):** 170.7, 170.2, 169.4, 165.6, 165.5, 165.1, 144.0, 132.5, 130.2, 128.9, 128.1, 122.3, 100.8, 72.8, 71.7, 71.2, 70.6, 70.5, 70.5, 70.2, 70.0, 69.0, 68.3, 64.5, 64.1, 61.9, 55.4, 54.5, 45.9, 44.2, 44.2, 39.6, 29.6, 28.7, 27.8, 20.7, 20.6, 20.6, 20.5; **LRMALDI-MS:** *m/z* = 2823.8 $[M+Na]^+$, isotopic pattern matches that calculated for $C_{138}H_{154}Cl_6N_{12}O_{38}Na$.

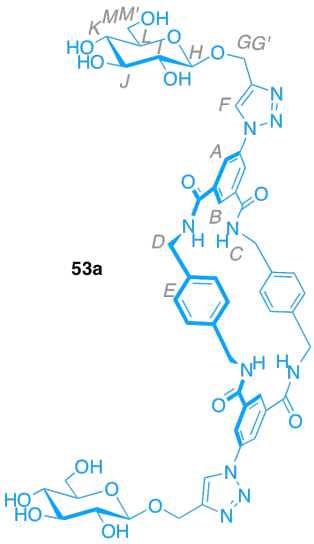

53a

Rotaxane **52a** (195 mg, 0.092 mmol) was stirred for 24 hours at room temperature in a solution of NaOH (10M) in THF/H2O/EtOH (1:1:1) (10 mL). The resulting suspension was filtered by suction and the solid rinsed with water (75 mL), followed by MeOH (15 mL) and DCM (15 mL) to give macrocycle **53a** as colourless solid (54 mg, 0.051 mmol, 55%). **M.p.** 250°C (dec.), **^{1}H-NMR (400 MHz, DMSO *d6*, 300 K):** δ = 9.35-9.14 (m, 4H, H_C), 8.97 (s, 2H, H_B), 8.45 (s, 4H, H_A), 8.20 (s, 2H, H_F), 7.27 (s, 8H, H_E), 5.24-4.88 (m, 6H, -OH), 4.97 (d, J = 12.5 Hz, 2H, H_G), 4.76 (d, J = 12.5 Hz, 2H, $H_{G'}$), 4.64 (bs, 2H, -OH), 4.44 (bs, 8H, H_D), 4.34 (d, J = 12.5 Hz, 2H, H_H), 3.72 (d, J = 11.5 Hz, 2H, H_M), 3.54-3.41 (m, 2H, $H_{M'}$), 3.24-2.96 (m, 8H, H_I, H_J, H_K and H_L); **^{13}C-NMR (100 MHz, DMSO *d6*, 300 K):** δ = 164.6, 145.4, 137.9, 136.6, 136.4, 127.9, 125.7, 122.7, 121.0, 102.2, 76.9, 76.5, 73.3, 70.0, 61.4, 61.1, 42.7; **LRESI-MS:** *m/z* = 1051 $[M+H]^+$; **HRESI-MS:** *m/z* = 1051.3797 $[M+H]^+$ (calc. for $C_{50}H_{55}N_{10}O_{16}$ $[M+H]^+$ 1051.3792); isotopic pattern matches that calculated for $C_{50}H_{55}N_{10}O_{16}$.

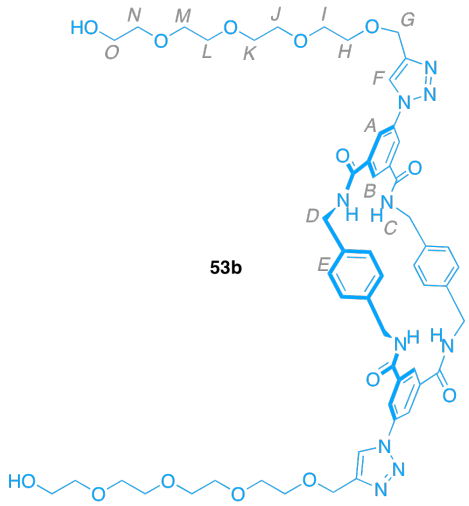

53b

Rotaxane **52b** (40 mg, 0.018 mmol) was stirred for 4 days at room temperature in a solution of NaOH (1M) in THF/H2O/EtOH (3:2:5) (10 mL). An aqueous solution of HCl (1M) was added drop wise until pH equalled 7. The whole solution was loaded on a preparative Silica TLC plate that was eluted with CH_2Cl_2/MeOH (15:85) to give macrocycle **53b** as white waxy solid (18 mg, 0.016 mmol, 90%). **^{1}H-NMR (400 MHz, $CD_3OD/CDCl_3$ (1:1), 300 K):** δ = 8.42, 8.41 (2s, 4H, H_A), 8.35 (bs, 2H, H_B), 8.11 (t, 2H, J = 1.4 Hz, H_F), 7.28 (s, 8H, H_E), 4.70 (s, 2H, H_G), 4.53 (s, 8H, H_D), 3.72-3.49 (m, 32H, H_H, H_I, H_J, H_K, H_L H_M, H_N and H_O). **^{13}C-NMR (100 MHz, $CD_3OD/CDCl_3$ (1:1), 300 K):** δ = 166.4, 137.8, 137.7, 136.9, 128.9, 125.3, 122.7, 122.1, 72.8, 70.8, 70.7, 70.6, 70.5, 70.3, 70.1, 64.4, 61.4, 44.3 (× 2); **LRESI-MS:** *m/z* = 1101 $[M+Na]^+$; **HRESI-MS:** *m/z* = 1101.4651 $[M+Na]^+$ (calc. for $C_{54}H_{66}N_{10}O_{14}Na$ $[M+Na]^+$ 1101.4652); isotopic pattern matches that calculated for $C_{54}H_{66}N_{10}O_{14}Na$.

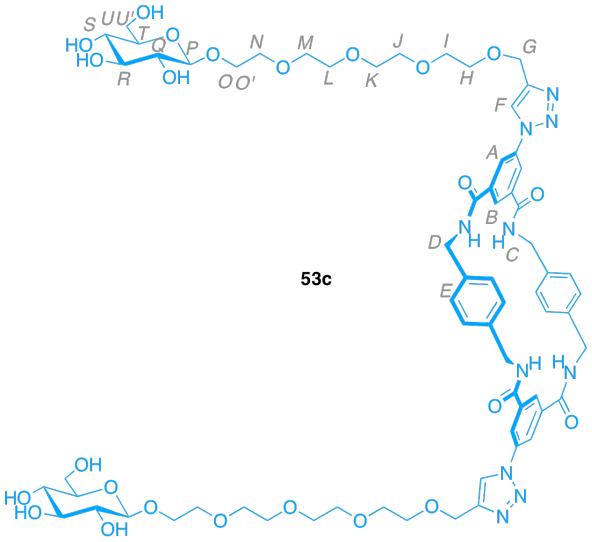

53c

Rotaxane **53c** (122 mg, 0.050 mmol) was stirred for 48 hours at room temperature in a solution of NaOH (10M) in THF/H2O/EtOH (1:1:1) (10 mL). An aqueous solution of HCl (1M) was added drop wise until pH equaled 7. Solvents were removed under vacuum. The resulting solid was re-dissolved in a 1:1 mixture of MeCN/H_2O (10 mL), filtered by gravity and the filtrate was used for purification by preparative RP-HPLC using a linear gradient of MeCN (25 to 40 % in 20 min) in H_2O to give macrocycle **53c** as a white solid (18 mg, 0.012 mmol, 25%). **M.p.** 205-207°C; **^{1}H-NMR (400 MHz, $CD_3OD/CDCl_3$ (1:1), 300 K):** δ = 8.41, 8.40 (2s, 6H, H_A and H_B), 8.09 (s, 2H, H_F), 7.23 (s, 8H, H_E), 4.70 (s, 4H, H_G), 4.55-4.42 (m, 8H, H_D), 4.16 (d, J = 7.8 Hz, 2H, H_P), 3.95-3.83 (m, 2H, H_O), 3.74 (dd, J = 2.7 Hz and J = 12.1 Hz, 2H, H_U) 3.73-3.49 (m, 32H, H_H, H_I, H_J, H_K, H_L, H_M, H_N, $H_{O'}$ and $H_{U'}$) 3.26-3.00 (m, 8H, H_Q, H_R, H_S and H_T); **^{13}C-NMR (100 MHz, $CD_3OD/CDCl_3$ (1:1), 300 K):** δ = 166.5, 146.3, 137.8, 137.7, 136.8, 128.9, 125.4, 122.7, 122.2, 103.1, 76.6, 76.5, 73.8, 70.8 (× 2), 70.7, 70.6, 70.5, 70.4, 70.3, 70.0, 68.7, 64.4, 61.9, 44.3; **LRESI-MS:** *m/z* = 1425 $[M+H]^+$; **HRESI-MS:** *m/z* = 1425.5709 $[M+Na]^+$ (calc. for $C_{66}H_{86}N_{10}O_{24}Na$ $[M+Na]^+$ 1425.5709); isotopic pattern matches that calculated for $C_{66}H_{86}N_{10}O_{24}Na$.

6.5 References and notes

[1] T. M. Allen, *Nat. Rev. Cancer,* **2002**, *2*, 750-763.

[2] F. Kratz, I. A. M. ller, C. Ryppa, A. Warnecke, *ChemMedChem,* **2008**, *3*, 20-53.

[3] H.-C. Wu, D.-K. Chang, C.-T. Huang, *J. Cancer Mol.,* **2006**, *2*, 57-66.

[4] S. Miyamoto, T. Fukami, H. Yagi, M. Kuroki, F. Yotsumoto, *Anticancer Res.,* **2009**, *29*, 823-830.

[5] C. P. Leamon, J. A. Reddy, *Adv. Drug Delivery Rev.,* **2004**, *56*, 1127-1141; P. S. Low, A. C. Antony, *Adv. Drug Delivery Rev.,* **2004**, *56*, 1055-1058; Y. Lu, E. Sega, C. P. Leamon, P. S. Low, *Adv. Drug Delivery Rev.,* **2004**, *56*, 1161-1176; S. Sabharanjak, S. Mayor, *Adv. Drug Delivery Rev.,* **2004**, *56*, 1099-1109.

[6] R. A. Medina, G. I. Owen, *Biol. Res.,* **2002**, *35*, 9-26; S. Ito, T. Fukusato, T. Nemoto, H. Sekihara, Y. Seyama, S. Kubota, *J. Natl. Cancer Inst.,* **2002**, *94*, 1080-1091.

[7] A. Danguy, I. Camby, R. Kiss, *Biochim. Biophys. Acta,* **2002**, *1572*, 285-293.

[8] I. Geffen, M. Spiess, F. Martin, M. Michael, *International Review of Cytology*, Academic Press: **1993**; Vol. 137, Part 2, p 181-219; P. H. Weigel, J. H. N. Yik, *Biochim. Biophys. Acta,* **2002**, *1572*, 341-363.

[9] N. Yui, T. Ooya, *J. Artif. Organs,* **2004**, *7*, 62-8.

[10] N. Yui, T. Ooya, T. Kawashima, Y. Saito, I. Tamai, Y. Sai, A. Tsuji, *Bioconjugate Chem.,* **2002**, *13*, 582-587.

[11] N. Yui, T. Ooya, *Mater. Sci. Forum,* **2003**, *426-432*, 3243-3248; T. Ooya, M. Eguchi, N. Yui, *J. Am. Chem. Soc.,* **2003**, *125*, 13016-13017.

[12] M. Rooseboom, J. N. M. Commandeur, N. P. E. Vermeulen, *Pharmacol. Rev.,* **2004**, *56*, 53-102.

[13] H. B. Bosmann, T. C. Hall, *Proc. Natl. Acad. Sci. U. S. A.,* **1974**, *71*, 1833-1837; H. Blüthmann, E. Vogt, P. Hösli, L. C. Stevens, K. Illmensee, *Differentiation,* **1983**, *24*, 65-73; S. Balasubramanian, B. Nagarajan, S. Govindasamy, *Cancer Lett.,* **1996**, *101*, 9-14; V. Paradis, N. Youssef, D. Dargère, N. Bâ, F. Bonvoust, J. Deschatrette, P. Bedossa, *Hum. Pathol.,* **2001**, *32*, 327-332; N. G. Beratis, A. Kaperonis, M. I. Eliopoulou, G. Kourounis, V. A. Tzingounis, *J. Cancer. Res. Oncol.,* **2005**, *131*, 371-376; A. Altorjay, B. Paal, N. Sohar, J. Kiss, I. Szanto, I. Sohar, *World J. Gastroenterol.,* **2005**, *11*, 5751-5756; Bo Yun Lee, Jung A. Han, Jun Sub Im, Amelia Morrone, Kimberly Johung, Edward C. Goodwin, Wim J. Kleijer, Daniel DiMaio, Eun Seong Hwang, *Aging Cell,* **2006**, *5*, 187-195; Ahmed Kamal,

Venkatesh Tekumalla, Anita Krishnan, Manika Pal-Bhadra, Utpal Bhadra, *ChemMedChem,* **2008**, *3*, 794-802.

[14] C. W. Tornoe, C. Christensen, M. Meldal, *J. Org. Chem,* **2002**, *67*, 3057-3064.

[15] V. V. Rostovtsev, L. G. Green, V. V. Fokin, K. B. Sharpless, *Angew. Chem., Int. Ed. Engl.,* **2002**, *41*, 2596-2599.

[16] W. Peng, V. V. Fokin, *Aldrichimica Acta,* **2007**, *40*, 7-17; M. Meldal, C. W. Tornoe, *Chem. Rev.,* **2008**, *108*, 2952-3015.

[17] D. Gonzalez Cabrera, B. D. Koivisto, D. A. Leigh, *Chem. Commun.,* **2007**, 4218-4220.

[18] J. Pohl, B. Bertram, P. Hilgard, M. Nowrousian, J. Stüben, M. Wießler, *Cancer Chemother. Pharmacol.,* **1995**, *35*, 364-370.

[19] G. Di Stefano, F. Kratz, M. Lanza, L. Fiume, *Dig. Liver Dis.,* **2003**, *35*, 428-433; G. Di Stefano, M. Derenzini, F. Kratz, M. Lanza, L. Fiume, *Liver Int.,* **2004**, *24*, 246-252.

[20] P. J. Julyan, L. W. Seymour, D. R. Ferry, S. Daryani, C. M. Boivin, J. Doran, M. David, D. Anderson, C. Christodoulou, A. M. Young, S. Hesslewood, D. J. Kerr, *J. Controlled Release,* **1999**, *57*, 281-290.

[21] For a detailed synthesis of **8** see: S. Papot, D. Combaud, J.-P. Gesson, *Bioorg. Med. Chem. Lett.*, **1998**, 8, 2545-2548.

[22] N. Sewald, H.-D. Jakubke, *Peptides: Chemistry and Biology*; Wiley-VCH: Weinheim, 2002.

[23] Light triggered-decomposition of aliphatic nitro groups has been reported on some substrates, see: V. I. Slovetskii, S. A. Shevelev, A. A. Fainzil'berg, S. S. Novikov, *Russ. Chem. Bull.*, **1962**, 11, 335-335.

[24] J.-C. Florent, X. Dong, G. Gaudel, S. Mitaku, C. Monneret, J.-P. Gesson, J.-C. Jacquesy, M. Mondon, B. Renoux, S. Andrianomenjanahary, S. Michel, M. Koch, F. Tillequin, M. Gerken, J. Czech, R. Straub, K. Bosslet, *J. Med. Chem.,* **1998**, *41*, 3572-3581.

[25] Direct infusion mass spectrometry and LCMS on a commercial sample of the structurally very similar nitrophenol **24**, did not give the expected ion peak in positive ionization mode under the same conditions as that used to identify **14**. Negative ionization gave only a slight improvement with a weak peak at [M-H]. These test experiment suggest that an alternative technique to electrospray ionization should be considered.

[26] E. E. Weinert, R. Dondi, S. Colloredo-Melz, K. N. Frankenfield, C. H. Mitchell, M. Freccero, S. E. Rokita, *J. Am. Chem. Soc.,* **2006**, *128*, 11940-11947.

[27] Quinone methides are in fact well known to be attacked by nucleophilic residues in certain types of enzymes. See: S. E. Rokita, *Quinone Methides*; John Wiley & Sons, Inc., New York, 2009.

[28] Spacer elimination adduct **41** has been synthesized from precursor **26**, by $NaBH_4$ reduction of the aldehyde group. Its synthesis and characterization are described in the experimental section.

[29] This assumption is based on the comparison of the relative area of both peaks. However, quantifying the amount of **39** in solution would require comparison with a pure sample of **39**. Assuming that the size of the peaks can be extrapolated to a rough relative concentration of compounds, in this particular case, did not seem irrational to us. Indeed, UV-absorbance at 220 nm (the wavelength where the chromatogram is recorded) is expected to be rather similar for **39** and starting propeptide **36** since both molecules only differ from the presence of the galactose unit, which absorption at that wavelength is negligible. Additionally, since the phenol of **39** is protonated (pH is maintained at 2 in the HPLC conditions), the absorption pattern of **39** is expected to be similar to that of a substituted nitrophenol unit (e.g. **36**) rather than that of a phenolate ion.

[30] H. C. Kolb, M. G. Finn, K. B. Sharpless, *Angew. Chem. Int. Ed. Engl.,* **2001**, *40*, 2004-2021.

[31] C. Bouillon, A. Meyer, S. Vidal, A. Jochum, Y. Chevolot, J.-P. Cloarec, J.-P. Praly, J.-J. Vasseur, F. Morvan, *J. Org. Chem.,* **2006**, *71*, 4700-4702.

[32] X.-L. Sun, C. L. Stabler, C. S. Cazalis, E. L. Chaikof, *Bioconjugate Chem.,* **2006**, *17*, 52-57.

[33] V. Aucagne, J. Berna, J. D. Crowley, S. M. Goldup, K. D. Haenni, D. A. Leigh, P. J. Lusby, V. E. Ronaldson, A. M. Z. Slawin, A. Viterisi, D. B. Walker, *J. Am. Chem. Soc.,* **2007**, *129*, 11950-11963.

[34] tris-(benzyltriazolylmethyl)amine (TBTA), as shown to be a powerful stabilizing ligand for copper(I). It protects copper from being oxidized or disproportionated, therefore enhancing its catalytic activity. TBTA is now widely used as an additive in CuAAC reaction to increase their rate and avoid side reactions promoted by copper (II).

[35] T. R. Chan, R. Hilgraf, K. B. Sharpless, V. V. Fokin, *Org. Lett.,* **2004**, *6*, 2853-2855.

[36] The tetraamide motif of the macrocycle has already shown to induce cytotoxicity, see [N. Ono, *Antitumor agents containing an amide[2]catenane*, JP. Patent, 2005247790, 15 sep. 2005]. The concomitant release of the macrocycle could potentially be an advantage for anti-cancer therapy, without the need for further functionalization of the macrocycle with bioactive compounds.

[37] A. G. Johnston, D. A. Leigh, L. Nezhat, J. P. Smart, M. D. Deegan, *Angew. Chem. Int. Ed. Engl.,* **1995**, *34*, 1212-16; A. G. Johnston, D. A. Leigh, R. J. Pritchard, M. D. Deegan, *Angew. Chem. Int. Ed.,* **1995**, *34*, 1209-12.

[38] A. G. Johnston, D. A. Leigh, A. Murphy, J. P. Smart, M. D. Deegan, *J. Am. Chem. Soc.,* **1996**, *118*, 10662-10663.

[39] A. G. Johnston, D. A. Leigh, A. Murphy, J. P. Smart, *Bull. Soc. Chim. Belg* . **1996**, *105*, 721-727.

[40] A. Gopin, N. Pessah, M. Shamis, C. Rader, D. Shabat, *Angew. Chem., Int. Ed.,* **2003**, *42*, 327-332.

J|A|C|S
ARTICLES
Published on Web 09/11/2007

Catalytic "Active-Metal" Template Synthesis of [2]Rotaxanes, [3]Rotaxanes, and Molecular Shuttles, and Some Observations on the Mechanism of the Cu(I)-Catalyzed Azide−Alkyne 1,3-Cycloaddition

Vincent Aucagne,† José Berná,† James D. Crowley,† Stephen M. Goldup,† Kevin D. Hänni,† David A. Leigh,*,† Paul J. Lusby,† Vicki E. Ronaldson,† Alexandra M. Z. Slawin,‡ Aurélien Viterisi,† and D. Barney Walker†

Contribution from the Schools of Chemistry, University of Edinburgh, The King's Buildings, West Mains Road, Edinburgh EH9 3JJ, and University of St. Andrews, Purdie Building, St. Andrews, Fife KY16 9ST, United Kingdom

Received May 17, 2007; E-mail: David.Leigh@ed.ac.uk

Abstract: A synthetic approach to rotaxane architectures is described in which metal atoms catalyze covalent bond formation while simultaneously acting as the template for the assembly of the mechanically interlocked structure. This "active-metal" template strategy is exemplified using the Huisgen−Meldal−Fokin Cu(I)-catalyzed 1,3-cycloaddition of azides with terminal alkynes (the CuAAC "click" reaction). Coordination of Cu(I) to an endotopic pyridine-containing macrocycle allows the alkyne and azide to bind to metal atoms in such a way that the metal-mediated bond-forming reaction takes place through the cavity of the macrocycle—or macrocycles—forming a rotaxane. A variety of mono- and bidentate macrocyclic ligands are demonstrated to form [2]rotaxanes in this way, and by adding pyridine, the metal can turn over during the reaction, giving a catalytic active-metal template assembly process. Both the stoichiometric and catalytic versions of the reaction were also used to synthesize more complex two-station molecular shuttles. The dynamics of the translocation of the macrocycle by ligand exchange in these two-station shuttles could be controlled by coordination to different metal ions (rapid shuttling is observed with Cu(I), slow shuttling with Pd(II)). Under active-metal template reaction conditions that feature a high macrocycle:copper ratio, [3]-rotaxanes (two macrocycles on a thread containing a single triazole ring) are also produced during the reaction. The latter observation shows that under these conditions the mechanism of the Cu(I)-catalyzed terminal alkyne−azide cycloaddition involves a reactive intermediate that features at least two metal ions.

Introduction

Most noncovalent bond directed approaches[1] to rotaxanes developed to date require at least stoichiometric quantities of a template which often involves pre-established strongly binding recognition motifs that "live on"[2] in the mechanically interlocked molecule that is formed. Besides holding the reactive fragments in an orientation that directs interlocking, the template is generally otherwise passive during the reaction. Building on the principles of transition-metal catalysis, we recently[3] began to explore a strategy in which template ions could also play an active role in promoting the crucial final covalent bond forming reaction that captures the interlocked structure (i.e., the metal has a dual function, acting as a template for entwining the precursors *and* catalyzing covalent bond formation between the reactants). This "active-metal"[4] template process is shown schematically in Figure 1 in both stoichiometric (1 equiv of

† University of Edinburgh.
‡ University of St. Andrews.

(1) For reviews which highlight various aspects of template strategies to rotaxanes, see: (a) Amabilino, D. B.; Stoddart, J. F. *Chem. Rev.* **1995**, *95*, 2725−2828. (b) *Molecular Catenanes, Rotaxanes and Knots: A Journey Through the World of Molecular Topology*; Sauvage, J.-P., Dietrich-Buchecker, C., Eds.; Wiley-VCH: Weinheim, Germany, 1999. (c) Breault, G. A.; Hunter, C. A.; Mayers, P. C. *Tetrahedron* **1999**, *55*, 5265−5293. (d) *Templated Organic Synthesis*; Diederich, F., Stang, P. J., Eds.; Wiley-VCH: Weinheim, Germany, 2000. (e) Hubin, T. J.; Busch, D. H. *Coord. Chem. Rev.* **2000**, *200*, 5−52. (f) Raehm, L.; Hamilton, D. G.; Sanders, J. K. M. *Synlett* **2002**, 1743−1761. (g) Kim, K. *Chem. Soc. Rev.* **2002**, *31*, 96−107. (h) Aricó, F.; Badjić, J. D.; Cantrill, S. J.; Flood, A. H.; Leung, K. C.-F.; Liu, Y.; Stoddart, J. F. *Top. Curr. Chem.* **2005**, *249*, 203−259. (i) Dietrich-Buchecker, C.; Colasson, B. X.; Sauvage, J.-P. *Top. Curr. Chem.* **2005**, *249*, 261−283. (j) Kay, E. R.; Leigh, D. A. *Top. Curr. Chem.* **2005**, *262*, 133−177. (k) Loeb, S. J. *Chem. Commun.* **2005**, 1511−1518. (l) Bogdan, A.; Rudzevich, Y.; Vysotsky, M. O.; Böhmer, V. *Chem. Commun.* **2006**, 2941−2952. (m) Nitschke, J. R. *Acc. Chem. Res.* **2007**, *40*, 103−112. (n) Vickers, M. S.; Beer, P. D. *Chem. Soc. Rev.* **2007**, *36*, 211−225. (o) Loeb, S. J. *Chem. Soc. Rev.* **2007**, *36*, 226−235. For reviews on polyrotaxanes, see: (p) Harada, A. *Acta Polym.* **1998**, *49*, 3−17. (q) Takata, T.; Kihara, N.; Furusho, Y. *Adv. Polym. Sci.* **2004**, *171*, 1−75. (r) Huang, F.; Gibson, H. W. *Prog. Polym. Sci.* **2005**, *30*, 982−1018. (s) Wenz, G.; Han, B.-H.; Müller, A. *Chem. Rev.* **2006**, *106*, 782−817.

(2) (a) Philp, D.; Stoddart, J. F. *Angew. Chem., Int. Ed. Engl.* **1996**, *35*, 1154−1196. For a discussion of how and why this feature can be usefully exploited in the field of molecular machinery, see: (b) Kay, E. R.; Leigh, D. A.; Zerbetto, F. *Angew. Chem., Int. Ed.* **2007**, *46*, 72−191.

(3) Aucagne, V.; Hänni, K. D.; Leigh, D. A.; Lusby, P. J.; Walker, D. B. *J. Am. Chem. Soc.* **2006**, *128*, 2186−2187.

(4) We use "active template" as a general term to describe a reaction in which a moiety both catalyzes covalent bond formation and acts as a template for the assembly of a particular structure. The term "active-metal template" describes a subset of active-template reactions in which the "active" moiety is a metal. A "catalytic active-metal template" reaction is one in which the metal catalyst turns over; a "stoichiometric active-metal template" reaction is one in which it does not.

10.1021/ja073513f CCC: $37.00

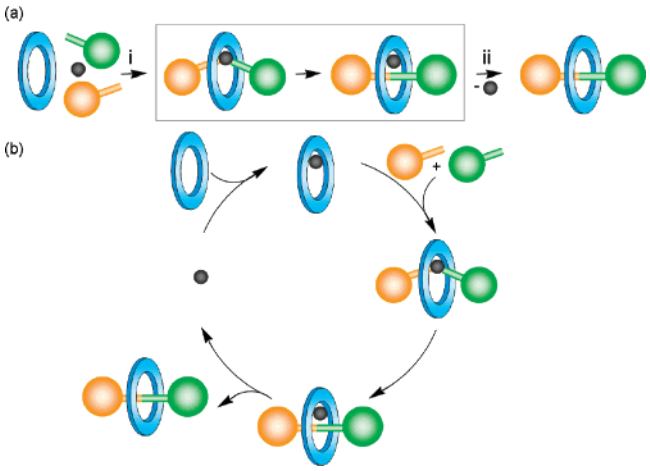

Figure 1. "Active-template" strategy to rotaxane architectures. The formation of a covalent bond between the green and orange "stoppered" units to generate the thread is promoted by the catalyst (shown in gray) and directed through the cavity of the macrocycle (shown in blue) by the catalyst's coordination requirements. (a) Stoichiometric active-metal template synthesis of a [2]rotaxane: (i) template assembly and covalent bond forming catalysis, (ii) subsequent demetalation. (b) Catalytic active-metal template synthesis of a [2]rotaxane.

the active template is required) and catalytic (the active template turns over during the reaction) forms. There are several potentially attractive features of such a synthetic approach to mechanically interlocked architectures, including (i) the inherent efficiency of a reaction in which the macrocycle−metal complex performs multiple functions, (ii) the lack of a requirement for permanent recognition elements in each component of the interlocked product, which increases the structural diversity possible in catenanes and rotaxanes and enables their formation to be "traceless", (iii) in some cases only substoichiometric quantities of the active template may be required (i.e., the catalytic active-metal template variant, Figure 1b), (iv) the strategy could prove applicable to many different types of well-known transition-metal-catalyzed (and even organocatalytic) reactions, (v) reactions that *only* proceed through a threaded intermediate would allow access to several currently inaccessible mechanically linked macromolecular architectures, and, finally, (vi) the coordination requirements during key stages of the catalytic cycle of active-template reactions could provide insight into the mechanisms of the catalyzed reactions.

Since the preliminary report[3] appeared on the realization of this strategy for rotaxane formation utilizing the Cu(I)-catalyzed[5−7] 1,3-cycloaddition[8] of organic azides and terminal alkynes (the CuAAC "click"[9,10] reaction), we have been delighted to see the concept be quickly adopted[11] to make rotaxanes[12] with other Cu(I)-catalyzed reactions, including alkyne-homocoupling and C−S bond forming reactions.[13,14] Here we expand on our investigation of the original system, showing that the active-metal template rotaxane-forming CuAAC reaction works well for both mono- and bidentate pyridine-containing macrocyclic ligands and can also be used to synthesize more complex two-station degenerate molecular shuttles whose interstation shuttling can be controlled by coordination to different metal ions. Furthermore, using a high macrocycle:copper ratio, [3]rotaxanes with two macrocycles on a single thread are somewhat unexpectedly produced during the active-metal template reaction. Together with some simple kinetic studies carried out under various rotaxane- and thread-forming reaction conditions, these experimental results provide some insight into the mechanism of the CuAAC reaction.

(5) (a) Tornøe, C. W.; Christensen, C.; Meldal, M. *J. Org. Chem.* **2002**, *67*, 3057−3064. (b) Rostovtsev, V. V.; Green, L. G.; Fokin, V. V.; Sharpless, K. B. *Angew. Chem., Int. Ed.* **2002**, *41*, 2596−2599.

(6) For some interesting examples of the CuAAC reaction, see: (a) Lee, L. V.; Mitchell, M. L.; Huang, S.-J.; Fokin, V. V.; Sharpless, K. B.; Wong, C.-H. *J. Am. Chem. Soc.* **2003**, *125*, 9588−9589. (b) Wang, Q.; Chan, T. R.; Hilgraf, R.; Fokin, V. V.; Sharpless, K. B.; Finn, M. G. *J. Am. Chem. Soc.* **2003**, *125*, 3192−3193. (c) Horne, W. S.; Yadav, M. K.; Stout, C. D.; Ghadiri, M. R. *J. Am. Chem. Soc.* **2004**, *126*, 15366−15367. (d) Diaz, D. D.; Punna, S.; Holzer, P.; McPherson, A. K.; Sharpless, K. B.; Fokin, V. V.; Finn, M. G. *J. Polym. Sci., Part A: Polym. Chem.* **2004**, *42*, 4392−4403. (e) Manetsch, R.; Krasiński, A.; Radić, Z.; Raushel, J.; Taylor, P.; Sharpless, K. B.; Kolb, H. C. *J. Am. Chem. Soc.* **2004**, *126*, 12809−12818. (f) Helms, B.; Mynar, J. L.; Hawker, C. J.; Frechet, J. M. J. *J. Am. Chem. Soc.* **2004**, *126*, 15020−15021. (g) Steffensen, M. B.; Simanek, E. E. *Angew. Chem., Int. Ed.* **2004**, *43*, 5178−5180. (h) Collman, J. P.; Devaraj, N. K.; Chidsey, C. E. D. *Langmuir* **2004**, *20*, 1051−1053. (i) Jang, H.; Fafarman, A.; Holub, J. M.; Kirshenbaum, K. *Org. Lett.* **2005**, *7*, 1951−1954; (j) Krasiński, A.; Radić, Z.; Manetsch, R.; Raushel, J.; Taylor, P.; Sharpless, K. B.; Kolb, H. C. *J. Am. Chem. Soc.* **2005**, *127*, 6686−6692. (k) Wu, P.; Malkoch, M.; Hunt, J. N.; Vestberg, R.; Kaltgrad, E.; Finn, M. G.; Fokin, V. V.; Sharpless, K. B.; Hawker, C. J. *Chem. Commun.* **2005**, 5775−5777. (l) Mocharla, V. P.; Colasson, B.; Lee, L. V.; Roeper, S.; Sharpless, K. B.; Wong, C.-H.; Kolb, H. C. *Angew. Chem., Int. Ed.* **2005**, *44*, 116−120. (m) Srinivasachari, S.; Liu, Y.; Zhang, G.; Prevette, L.; Reineke, T. M. *J. Am. Chem. Soc.* **2006**, *128*, 8176−8184. (n) Slater, M.; Snauko, M.; Svec, F.; Frechet, J. M. J. *Anal. Chem.* **2006**, *78*, 4969−4975. (o) Ladmiral, V.; Mantovani, G.; Clarkson, G. J.; Cauet, S.; Irwin, J. L.; Haddleton, D. M. *J. Am. Chem. Soc.* **2006**, *128*, 4823−4830. (p) White, M. A.; Johnson, J. A.; Koberstein, J. T.; Turro, N. J. *J. Am. Chem. Soc.* **2006**, *128*, 11356−11357. (q) Collman, J. P.; Devaraj, N. K.; Eberspacher, T. P. A.; Chidsey, C. E. D. *Langmuir* **2006**, *22*, 2457−2464. (r) Devaraj, N. K.; Dinolfo, P. H.; Chidsey, C. E. D.; Collman, J. P. *J. Am. Chem. Soc.* **2006**, *128*, 1794−1795. (s) Detz, R. J.; Arevalo Heras, S.; de Gelder, R.; van Leeuwen, P. W. N. M.; Hiemstra, H.; Reek, J. N. H.; van Maarseveen, J. H. *Org. Lett.* **2006**, *8*, 3227−3230. (t) Aucagne, V.; Leigh, D. A. *Org. Lett.* **2006**, *8*, 4505−4507. (u) Viguier, R. F. H.; Hulme, A. N. *J. Am. Chem. Soc.* **2006**, *128*, 11370−11371.

(7) For reviews of the CuAAC reaction, see: (a) Bock, V. D.; Hiemstra, H.; van Maarseveen, J. H. *Eur. J. Org. Chem.* **2005**, 51−68. (b) Wang, Q.; Chittaboina, S.; Barnhill, H. N. *Lett. Org. Chem.* **2005**, *2*, 293−301. (c) Wu, P.; Fokin, V. V. *Aldrichimica Acta* **2007**, *40*, 7−17.

(8) (a) *1,3-Dipolar Cycloadditions Chemistry*; Huisgen, R., Ed.; Wiley: New York, 1984; Vol. 1, pp 1−176. (b) Huisgen, R. *Pure Appl. Chem.* **1989**, *61*, 613−628.

(9) For reviews and discussion of the "click chemistry" concept, see: (a) Kolb, H. C.; Finn, M. G.; Sharpless, K. B. *Angew. Chem., Int. Ed.* **2001**, *40*, 2004−2021. (b) Kolb, H. C.; Sharpless, K. B. *Drug Discovery Today* **2003**, *8*, 1128−1137. (c) Ball, P. *Chem. World* **2007**, *4* (4), 46−51.

(10) A listing of examples of the use of "click" reactions is available at http://www.scripps.edu/chem/sharpless/click.html.

(11) Indeed, it was predicted[3] that, "Chelation to catalytic centers could lead to rotaxane- and catenane-forming protocols based on other metal-mediated reactions, including cross-couplings, condensations, and other cycloaddition reactions". For a recent example involving Pd(II)-catalyzed alkyne homo-couplings, see: Berná, J.; Crowley, J. D.; Goldup, S. M.; Hänni, K. D.; Lee, A.-L.; Leigh, D. A. *Angew. Chem., Int. Ed.* **2007**, *46*, 5709−5713.

(12) For the synthesis of rotaxanes and catenanes using the CuAAC reaction in "passive" template stoppering or macrocyclization protocols, see: (a) Mobian, P.; Collin, J.-P.; Sauvage, J.-P. *Tetrahedron Lett.* **2006**, *47*, 4907−4909. (b) Dichtel, W. R.; Miljanić, O. Š.; Spruell, J. M.; Heath, J. R.; Stoddart, J. F. *J. Am. Chem. Soc.* **2006**, *128*, 10388−10390. (c) Miljanić, O. Š.; Dichtel, W. R.; Mortezaei, S.; Stoddart, J. F. *Org. Lett.* **2006**, *8*, 4835−4838. (d) Aprahamian, I.; Dichtel, W. R.; Ikeda, T.; Heath, J. R.; Stoddart, J. F. *Org. Lett.* **2007**, *9*, 1287−1290; (e) Braunschweig, A. B.; Dichtel, W. R.; Miljanić, O. Š.; Olson, M. A.; Spruell, J. M.; Khan, S. I.; Heath, J. R.; Stoddart, J. F. *Chem. Asian J.* **2007**, *2*, 634−647.

(13) Saito, S.; Takahashi, E.; Nakazono, K. *Org. Lett.* **2006**, *8*, 5133−5136.

(14) Saito et al. imply[13] that the concept of binding of a substrate in a cavity while simultaneously activating it to catalysis is an extension of Vögtle's anion template route to rotaxanes [(a) Seel, C.; Vögtle, F. *Chem.—Eur. J.* **2000**, *6*, 21−24]. Actually the two strategies are rather fundamentally different. In the Vögtle reaction the macrocycle does not increase the reactivity of any of the building blocks for the rotaxane. In fact, the hydrogen bonding of the macrocycle to the phenoxide anion, combined with the steric hinderance conferred by the presence of the macrocycle, greatly *decreases* its reactivity. The only reason that rotaxane is formed in the Vögtle system is that the more reactive unthreaded phenoxide anion is completely insoluble under the reaction conditions. The active-template strategy described in ref 3 and elaborated upon in this paper has much more in common with Sauvage's original (passive) metal template ideas combined with Mock's [(b) Mock, W. L.; Irra, T. A.; Wepsiec, J. P.; Adhya, M. *J. Org. Chem.* **1989**, *54*, 5302−5308] and later Steinke's [(c) Tuncel, D.; Steinke, J. H. G. *Chem. Commun.* **1999**, 1509−1510. (d) Tuncel, D.; Steinke, J. H. G. *Chem. Commun.* **2002**, 496−497. (e) Tuncel, D.; Steinke, J. H. G. *Macromolecules* **2004**, *37*, 288−302] use of curcubituril to accelerate a reaction within a macrocycle cavity to form rotaxanes.

Cu(I)-Catalyzed Terminal Alkyne−Azide Cycloaddition (CuAAC Reaction)

Recently, there has been a tremendous surge of interest in so-called click[9,10] methodologies for functional molecule synthesis, the most popular of which is the Huisgen−Meldal−Fokin[15] Cu(I)-catalyzed 1,3-cycloaddition of organic azides with terminal alkynes (the CuAAC reaction).[5−7] The most common catalyst systems for this reaction employ water or alcohol solvents and use a Cu(II) salt in the presence of a reducing agent (often sodium ascorbate) to generate the required Cu(I) catalyst in situ.[5b,7a] Metallic copper[5b,7a] or copper clusters[16] have also been employed as precatalysts, and in some cases Cu(I) salts can be used directly. However, in apolar solvents Cu(I) salts usually require the presence of nitrogen[5b,7a,17] or phosphorus[18] ligands, or acetonitrile as a cosolvent, to stabilize the Cu(I) oxidation state, and undesired alkyne−alkyne homocoupling products are often observed under such reaction conditions.[5b,7a]

The basic mechanism of the CuAAC reaction is believed to be that shown in Scheme 1. A [2+3] cycloaddition—the mechanism of the thermal (i.e., uncatalyzed) Huisgen reaction[8]—is ruled out[19] for the Cu(I)-catalyzed reaction on the basis of DFT calculations which show that reaction via a (formally Cu(III)) metallacycle is a more favorable pathway by up to 11.7 kcal mol^{-1} (Scheme 1).[5b,20,21] The same calculations suggest that the rate-determining step is the formation of the Cu metallacycle from a reactive intermediate involving copper-coordinated alkyne and, presumably, azide (organoazido−metal complexes are likely intermediates in many transition-metal-mediated reactions of azides, and Cu(I)−N_3R complexes have been characterized by X-ray crystallography[22]). However, the exact nature of this reactive intermediate is unclear (Scheme 1, types A−C).

In the absence of competing ligands,[23] copper(I) acetylides exist as complex multi metal atom aggregates,[24] and kinetic studies[17a,25] by Fokin and Finn on the generic ligand-free[23] Cu(I)-catalyzed alkyne−azide reaction show that in DMSO−water mixtures the reaction mechanism is second-order with respect to copper. The same studies found first-order kinetics with respect to the azide and alkyne (actually slightly higher than first-order with respect to the alkyne).[25] However, relatively little is known about the ligand-promoted Cu(I)-catalyzed cycloaddition in organic solvents. Recent experiments by Straub,[26] in which mononuclear copper(I) acetylides ligated to a sterically demanding *N*-heterocyclic carbene react efficiently with bulky organoazides at room temperature, support the notion that a single copper atom mechanism (A(i), Scheme 1) is viable for the reaction, at least when the copper is bound to bulky ligands. Recent DFT calculations[7c,21] suggest that π-activation of the copper acetylide unit by coordination of a second copper atom (e.g., A(ii) or, more likely under ligand-free conditions or with small monodentate ligands, bridged[27] intermediates such as B(i) or B(ii), Scheme 1) greatly enhances the reactivity of the copper σ-acetylide, accelerating formation of the metallacycle. Alternatively, a pathway[25] in which the reacting azide and alkyne are coordinated to different copper(I) atoms (intermediate C(i) or C(ii)) would also be consistent with the second-order kinetics observed in DMSO−water. It may well be that several of these types of intermediates[28] can provide viable pathways for the CuAAC reaction, with the different characteristics of the intermediates being relatively favored or inhibited by factors such as the solvent, bulk and coordination number of an added ligand, the strength of ligand−copper binding, and the amount of ligand-free Cu(I) present in solution. Given the tendency of copper(I) acetylides to aggregate, however, doubly bridged intermediates such as B or C should be abundant species under most conditions. Accordingly, if coordination of the azide to the same copper atom significantly increases the reactivity of the σ-acetylide, type B(ii) intermediates are probably involved in the dominant pathways in most reported CuAAC reactions.

Despite the uncertainty over the precise nature of the reactive intermediate, since tertiary amines and pyridines facilitate[5b,17] the reaction in organic solvents, we reasoned that a macrocycle, **1**, bearing an endotopic ligating nitrogen atom might be able to direct the CuAAC reaction of a "stoppered" alkyne, **2**, and a "stoppered" azide, **3**, through the macrocycle cavity to give a [2]rotaxane, **4**, in an active-metal template synthesis (Scheme 2).

Active-Metal Template CuAAC Rotaxane Synthesis

A 2,6-bis[(alkyloxy)methyl]pyridine macrocycle (**1a**), previously used[29] as both a mono- and bidentate ligand for various transition metals in classical "passive" template rotaxane and catenane syntheses, seemed a suitable candidate for initial investigations. Pleasingly, stirring of an equimolar mixture of

(15) The Cu(I)-catalyzed terminal alkyne−azide cycloaddition is often referred to as the "Sharpless copper click reaction" or the "Sharpless−Huisgen alkyne−azide cycloaddition". However, Sharpless gives Fokin the credit for the idea and recognition of the copper catalysis of this reaction at Scripps [Rouhi, A. M. *Chem. Eng. News* **2004**, *82* (7), 63−65]. The initial work at Scripps was carried out shortly after, and without knowledge of, the first paper (ref 5a) describing the Cu(I)-catalyzed alkyne−azide cycloaddition (on solid-supported resins) had been submitted by Meldal and co-workers.

(16) Pachon, L. D.; van Maarseveen, J. H.; Rothenberg, G. *Adv. Synth. Catal.* **2005**, *347*, 811−815.

(17) (a) Chan, T. R.; Hilgraf, R.; Sharpless, K. B.; Fokin, V. V. *Org. Lett.* **2004**, *6*, 2853−2855. (b) Lewis, W. G.; Magallon, F. G.; Fokin, V. V.; Finn, M. G. *J. Am. Chem. Soc.* **2004**, *126*, 9152−9153.

(18) Perez-Balderas, F.; Ortega-Munoz, M.; Morales-Sanfrutos, J.; Hernandez-Mateo, F.; Calvo-Flores, F. G.; Calvo-Asin, J. A.; Isac-Garcia, J.; Santoyo-Gonzalez, F. *Org. Lett.* **2003**, *5*, 1951−1954.

(19) If the [2+3] cycloaddition were the preferred mechanism of the Cu-catalyzed reaction, the structures A−C shown in Scheme 1 would still be relevant as reactive intermediates.

(20) Himo, F.; Lovell, T.; Hilgraf, R.; Rostovtsev, V. V.; Noodleman, L.; Sharpless, K. B.; Fokin, V. V. *J. Am. Chem. Soc.* **2005**, *127*, 210−216.

(21) Ahlquist, M.; Fokin, V. V. *Organometallics*, in press, cited in ref 7c.

(22) Dias, H. V. R.; Polach, S. A.; Goh, S.-K.; Archibong, E. F.; Marynick, D. S. *Inorg. Chem.* **2000**, *39*, 3894−3901.

(23) In this paper we use the phrases "ligandless" and "ligand-free" to describe copper that is not bound to the macrocyclic pyridine ligands added to the CuAAC reactions to generate the active-template synthesis. As discussed in the text and ref 28, any Cu(I) that is not coordinated to pyridine units will be complexed by molecules of acetonitrile, azide, alkyne, water, or other donor atoms present.

(24) Mykhalichko, B. M.; Temkin, O. N.; Mys'kiv, M. G. *Russ. Chem. Rev.* **2000**, *69*, 957−984.

(25) Rodionov, V. O.; Fokin, V. V.; Finn, M. G. *Angew. Chem., Int. Ed.* **2005**, *44*, 2210−2215.

(26) Nolte, C.; Mayer, P.; Straub, B. F. *Angew. Chem., Int. Ed.* **2007**, *46*, 2101−2103.

(27) (a) Bohlmann, F.; Schönowsky, H.; Inhoffen, E.; Grau, G. *Chem. Ber.* **1964**, *97*, 794−800. (b) Siemsen, P.; Livingston, R. C.; Diederich, F. *Angew. Chem., Int. Ed.* **2000**, *39*, 2632−2657.

(28) Note: Copper(I) acetylides are generally complex extended multiatom aggregates, at least in the solid state and in the absence of good nitrogen ligands (see ref 24). The types of reactive intermediates shown in Scheme 1 are not meant to be precise or definitive structures—indeed, some of them (e.g., A(ii) and B(ii)) are very closely related—but rather are meant to illustrate different (possible) features of the putative reactive intermediate: How many copper atoms are needed to play significant structural or electronic roles during the catalysis? Is the copper σ-acetylide π-activated by an additional Cu atom? If the intermediate has two or more copper atoms, is it doubly bridged—as envisaged for a Glaser coupling, which can be ruled out with bidentate ligands for Cu if azide is also coordinated—or singly bridged? Are the reacting azide and alkyne attached to the same or different Cu atoms?

Scheme 1. Proposed Mechanism of the Huisgen−Meldal−Fokin Cu(I)-Catalyzed Alkyne−Azide Cycloaddition (CuAAC) Reaction[48]

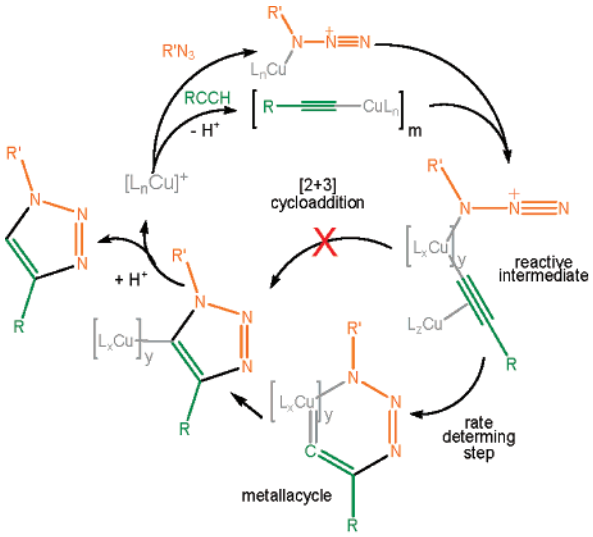

Possible types of reactive intermediate

Type A
(i) one copper atom or (ii) one copper atom + π-activation of Cu-acetylide by a second copper atom

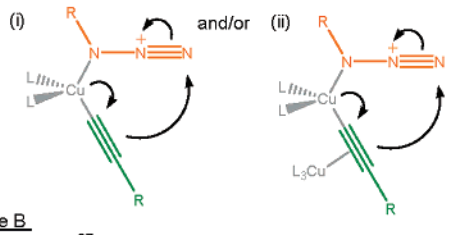

Type B
(i) Glaser-like[27] *bis*-alkyne bridged intermediate, or more generally since kinetic studies do not implicate two alkynes in the reaction, (ii) two μ-coordinated copper atoms featuring a π-activated Cu-acetylide. These structures differ from A(ii) only by the two copper atoms being doubly bridged. Doubly-bridged intermediates are not possible with bidentate ligands for copper (assuming RN_3 coordinates to Cu).

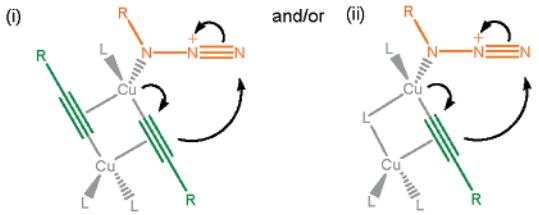

Type C
The azide and alkyne groups that react are on different copper atoms - (i) non-π-activated alkyne, (ii) π-activated alkyne. These differ from B only in the location of the alkyne which reacts with the azide. Doubly-bridged intermediates are not possible with bidentate ligands for copper (assuming RN_3 coordinates to Cu).

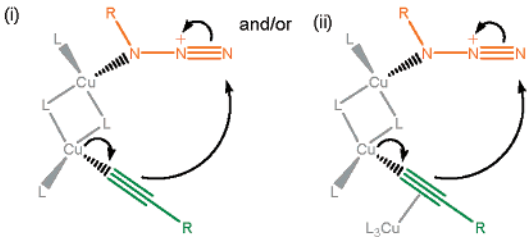

the pyridine macrocycle **1a**, alkyne **2**, azide **3**, and [Cu(CH_3-$CN)_4$](PF_6) in CH_2Cl_2 for 24 h afforded—after demetalation with KCN—a mixture of [2]rotaxane **4a** (57%) and the noninterlocked triazole thread **5** (41%), together with some of the unconsumed starting macrocycle (Scheme 2 and Table 1, entry 1).[3] By varying the reaction conditions and reactant stoichiometry (Table 1), yields of up to 94% of [2]rotaxane with respect to the amount of macrocycle used were achieved (5 equiv of **2** and **3**; Table 1, entry 2) for this stoichiometric active-metal template reaction (Figure 1a). The use of substoichiometric amounts of copper was investigated to determine whether the metal would turn over as both a template and a cycloaddition catalyst (i.e., a

Scheme 2. Active-Metal Template CuAAC Synthesis of [2]Rotaxanes **4a**−**o** from Alkyne **2**, Azide **3**, and Macrocycles **1a**−**o**[a]

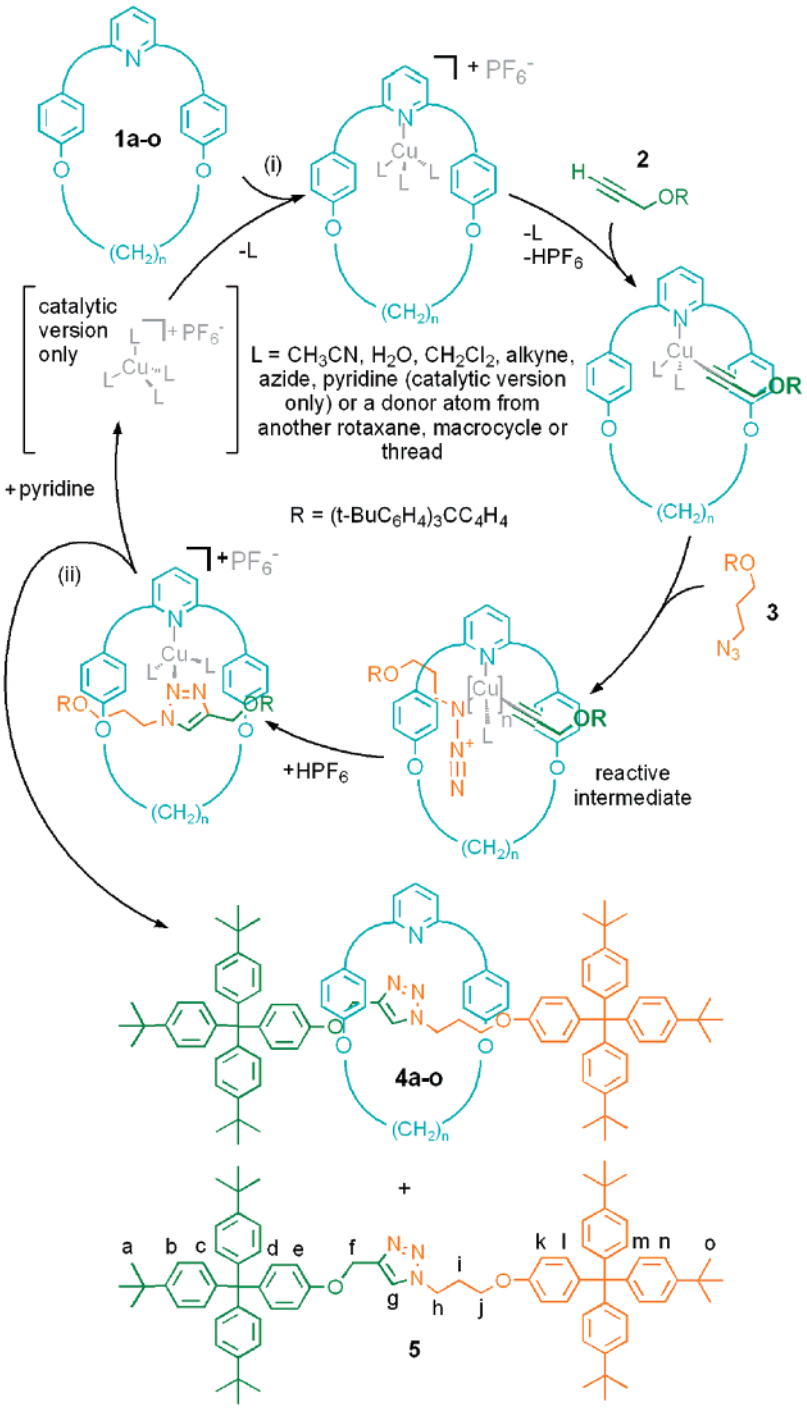

[a] Reagents and conditions: (i) **1a**−**o** (0.01 M), Cu(I) salt (generally $[Cu(CH_3CN)_4](PF_6)$; see the text), poorly coordinating solvent (generally CH_2Cl_2; see the text), and, in the catalytic version of the active-metal template reaction (Figure 1b), 3 equiv of pyridine; (ii) KCN, CH_2Cl_2/CH_3OH.[3] For the effect of the reaction conditions and reagent stoichiometry on the yields of **4a** and **5**, see Table 1. For the relative yields of **4a**−**o** using a standardized set of reaction conditions see Figure 4
.

catalytic active-metal template synthesis, Figure 1b). When using 20 mol % (with respect to **1a**) $[Cu(CH_3CN)_4](PF_6)$ at room temperature, the reaction appeared to stop after an amount of [2]rotaxane equivalent to the amount of copper present had been formed, suggesting that the multidentate rotaxane sequesters the transition metal during the reaction, inhibiting further catalytic activity. Addition of pyridine as a competing ligand enabled the catalyst to turn over, producing a substoichiometric reaction, but the reaction was extremely slow at 25 °C (Table 1, entry 3). Elevating the temperature (70 °C, $ClCH_2CH_2Cl$) gave an

(29) (a) Fuller, A.-M.; Leigh, D. A.; Lusby, P. J.; Oswald, I. D. H.; Parsons, S.; Walker, D. B. *Angew. Chem., Int. Ed.* **2004**, *43*, 3914−3918. (b) Fuller, A.-M. L.; Leigh, D. A.; Lusby, P. J.; Slawin, A. M. Z.; Walker, D. B. *J. Am. Chem. Soc.* **2005**, *127*, 12612−12619. (c) Leigh, D. A.; Lusby, P. J.; Slawin, A. M. Z.; Walker, D. B. *Chem. Commun.* **2005**, 4919−4921. (d) Leigh, D. A.; Lusby, P. J.; Slawin, A. M. Z.; Walker, D. B. *Angew. Chem., Int. Ed.* **2005**, *44*, 4557−4564. (e) Fuller, A.-M. L.; Leigh, D. A.; Lusby, P. J. *Angew. Chem., Int. Ed.* **2007**, *46*, 5015−5019.

Table 1. Effect of Reaction Conditions and Reagent Stoichiometry on the Active-Metal Template CuAAC Synthesis of [2]Rotaxane **4a** (Scheme 2)[3]

entry	amt of **2** and **3** (equiv)	amt of $[Cu(CH_3CN)_4](PF_6)$ (equiv)	solvent	*T* (°C)	conversion to triazole **2** + **3** →**4a** + **5** (%)	yield of rotaxane **1a** →**4a** (%)
1[a]	1	1	CH_2Cl_2	25[d]	>95	57
2[a]	5	1	CH_2Cl_2	25[d]	92	94
3[b]	5	0.2	CH_2Cl_2	25[d]	44	59
4[b]	5	0.2	$ClCH_2CH_2Cl$	25 → 70[e]	94	82
5[c]	1	0	$ClCH_2CH_2Cl$	25 → 70[f]	<5	0

[a] All reactions were carried out at 0.01 M concentration with respect to **1a** using the procedure shown in Scheme 2. [b] 3 equiv of pyridine. [c] Control experiment with no $[Cu(CH_3CN)_4](PF_6)$ present to demonstrate that the thermal reaction does not occur at these temperatures. [d] 24 h. [e] 12 h and then 24 h. [f] 12 h and then 72 h.

improved yield (82%) of rotaxane **4a** in a reasonable time period (36 h) using only 4 mol % Cu(I) with respect to both **2** and **3** (Table 1, entry 4).

Effect of the Nature of the Cu(I) Source

A number of different Cu(I) salts were screened for the reaction shown in Scheme 2 using the conditions shown in Table 1, entry 1, but replacing the $[Cu(CH_3CN)_4](PF_6)$ salt with other Cu(I) complexes. The use of CuOTf·benzene gave a 78% conversion of **2** and **3** into triazole products after 24 h but only a 46% yield of [2]rotaxane **4a**. By letting the reaction continue for a further 2 days (72 h in total), complete conversion of the starting azide and alkyne to triazole products was achieved (48% rotaxane). Substituting CuI for $[Cu(CH_3CN)_4](PF_6)$ led to very little reaction during the first 24 h (8% conversion to triazole), presumably due to the low solubility of CuI in CH_2Cl_2, but interestingly, what little alkyne and azide had reacted formed rotaxane with high selectivity (7:1 rotaxane:thread). The reaction proceeded slowly to completion (>98% conversion) over three weeks. However, at the end point of the reaction the product ratio (56:44 rotaxane:thread) was no different from that of the analogous $[Cu(CH_3CN)_4](PF_6)$-mediated experiment.

We also synthesized and isolated various discrete Cu(I)−**1a** complexes and tested their efficacy in the active-metal template reaction. The macrocycle **1a** and the different Cu(I) salts were mixed in CH_3CN solution and the resulting Cu(I)−**1a** complexes obtained through precipitation by vapor diffusion with diethyl ether. The preformed Cu(I)−**1a** complexes were submitted to the standard rotaxane-forming reaction conditions (Table 1, entry 1). The preformed $[Cu(CH_3CN)_4](PF_6)$−**1a** complex gave 76% conversion to triazole and a 53% yield of [2]rotaxane; the preformed CuOTf−**1a** complex gave 53% conversion to triazole but only a 5% yield of [2]rotaxane; the preformed CuI−**1a** complex gave results identical to those of the CuI−**1a** complex formed in situ (i.e., >98% triazole conversion over 3 weeks, 56% rotaxane).

Although there is some variation in the efficacy of the various Cu(I) salts on the rotaxane-forming reaction and some unexplained variation in the rotaxane:thread ratio during the course of the reaction with some sources of Cu(I), simple addition of $[Cu(CH_3CN)_4](PF_6)$ is the most convenient way of maximizing the CuAAC yield of rotaxane.[30]

(30) We also examined the effect of different alkyne substrates on the rotaxane formation. The alkynes (see the Supporting Information) were submitted to the standard click reaction conditions (Scheme 2). Using a longer, more flexible, alkylalkyne or an arylalkyne in the place of **2** led to similar yields of the corresponding [2]rotaxanes (and similar overall conversions of the substrates into triazole products), indicating the active-metal template rotaxane-forming reaction is rather insensitive to substrate modifications.

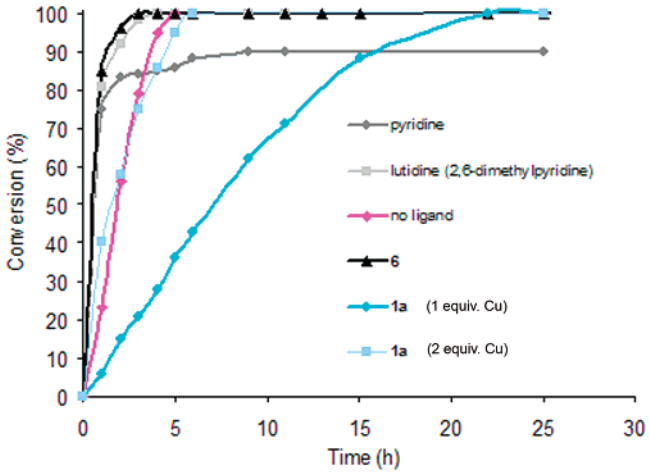

Figure 2. Conversion to triazole (i.e., thread + rotaxane if applicable) vs time for different pyridine-based ligands for the CuAAC reaction. Conditions: (i) ligand (1 equiv), alkyne **2** (1 equiv), azide **3** (1 equiv), $[Cu(CH_3CN)_4](PF_6)$ (1 equiv, 1 or 2 equiv with **1a**), CD_2Cl_2, rt, 0.01 M. The conversion of **2** and **3** into the triazole products (thread **5**, + rotaxane **4a** where relevant) was monitored by ^1H NMR.

Kinetic Studies

Some simple kinetic measurements were made to determine whether, under these reaction conditions, the Cu(I)-catalyzed alkyne−azide cycloaddition is actually accelerated by pyridine-based ligands. The rate of formation of triazole products (i.e., thread, plus rotaxane where relevant) was compared for the ligand-free[23] reaction and reactions containing pyridine, 2,6-dimethylpyridine (lutidine), 2,6-bis[(alkyloxy)methyl]pyridine macrocycle **1a**, and **6**, a close but acyclic analogue of **1a**.

The results (Figure 2) show that both lutidine and **6**, the acyclic analogue of **1a**, significantly accelerate the CuAAC reaction rate (essentially complete conversion to triazole after 3 h) compared to that of the Cu(I)-catalyzed reaction when no pyridine-based ligand is added (complete conversion after 6 h). The presence of pyridine also initially accelerates the reaction, but the conversion tails off after 2 h, suggesting that using unsubstituted pyridine as a ligand facilitates the oxidation of Cu(I) to noncatalytic Cu(II) under the reaction conditions. The role of the pyridine ligands in the rate acceleration is probably to break up extended copper(I) acetylide aggregates to form smaller reactive intermediates of the types shown in Scheme 1, although we cannot rule out an electronic effect of the ligand on the metal as well.

Interestingly, the Cu(I)-catalyzed formation of triazole products (both rotaxane and thread) in the presence of macrocycle **1a** (with 1 equiv of Cu)—which also presumably breaks up the

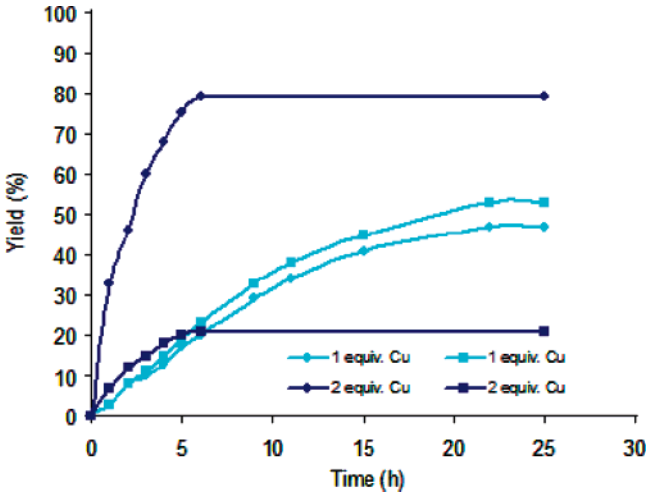

Figure 3. Formation of triazole products (rotaxane **4a,** ■; thread **5**, ●) vs time for the CuAAC reaction in the presence of macrocycle **1a**. Conditions: (i) **1a** (1 equiv), **2** (1 equiv), **3** (1 equiv), $[Cu(CH_3CN)_4](PF_6)$ (1 or 2 equiv), CD_2Cl_2, rt, 0.01 M. The conversion of **2** and **3** into thread **5** and rotaxane **4a** was monitored by ^1H NMR.

copper acetylide aggregates—is actually *slower* (24 h compared to 6 h) than the ligand-free Cu(I)-catalyzed reaction. While it might seem surprising that the active-metal template reaction is slower than the ligand-free reaction given that excellent yields of rotaxane are obtained under both stoichiometric and catalytic active-metal template conditions (Table 1), the rationale for this is quite straightforward. First, the alkyne−azide cycloaddition with the macrocyclic ligand must take place *through* the macrocycle cavity, a sterically restricted environment compared to the ligandless Cu(I)-catalyzed reaction, effecting the solvation of the reactive species as well as hindering any motion required to achieve bond formation or changes of geometry at the copper center. Second, the macrocyclic ligand might disfavor certain types of reactive intermediates (e.g., B) on steric grounds, so the reaction may proceed through another type of slower reacting, but still viable, intermediate (e.g., A or C rather than B). The reason that the ligandless formation of the triazole thread does not dominate given the slow rate of rotaxane formation is that the macrocycle is an excellent ligand for the Cu(I) and sequesters it, preventing the inherently faster ligand-free reaction (probably via B(ii)) from occurring. Accordingly, addition of a second equivalent of Cu(I) to the reaction containing **1a** should accelerate the rate of triazole formation to close to the ligand-free rate. Indeed, this was found to be the case (Figures 2 and 3). However, while one might expect this increase to be totally due to thread formation, analysis shows that the rate of *rotaxane* formation is also increased by adding an extra equivalent of Cu(I) to this reaction (Figure 3). In fact, the final yield of [2]-rotaxane only falls from 57% to 22% even though the triazole-forming reaction is complete in 6 h instead of 24 h. The acceleration of the rotaxane-forming reaction by excess Cu(I) strongly suggests that π-activation of the copper acetylide unit (see Scheme 1) is the dominant process in the CuAAC reaction mechanism of **1a**.

Effect of the Macrocycle Structure on [2]Rotaxane Formation

To further investigate both the scope and the mechanism of the active-template rotaxane-forming reaction shown in Scheme 2, we varied the structure of the pyridine-based macrocycle. The macrocycles used in the study are shown in Figure 4, and their syntheses are detailed in the Supporting Information. To compare the relative yields of rotaxane and thread within the ligand series, the macrocyclic ligands were screened using a standard, rather than optimized,[31] set of stoichiometric active-metal template reaction conditions in which the original macrocycle **1a** generates appreciable quantities of both rotaxane and thread. The conditions used were 1 equiv of macrocycles **1a**−**o**, 1 equiv of alkyne **2**, 1 equiv of azide **3**, and 1 equiv of $[Cu(CH_3CN)_4](PF_6)$ at a concentration of 0.01 M in CH_2Cl_2 at room temperature for 24 h. In most cases the starting alkyne **2** and azide **3** were completely consumed during the course of the reaction. After 24 h (72 h for **1n** and **1o**) each reaction was treated with KCN to remove the Cu(I), analyzed by ^1H NMR to determine the yield (shown in Figure 4) under the standard set of conditions, and then purified to give authentic samples of each [2]rotaxane. The yield (the percentage shown in red in Figure 4) of each rotaxane is the conversion of the macrocycles **1a**−**o** to the corresponding [2]rotaxanes **4a**−**o**. The conversion to triazole (the percentage shown in parentheses in Figure 4) is the overall conversion of the alkyne **2** and azide **3** into both thread **5** and rotaxanes **4a**−**o**.

Mono- and Tridentate Macrocycles. In addition to the strongly coordinating pyridine nitrogen, macrocycle **1a** has two ether oxygen atoms that could potentially be involved in (albeit weak) coordination to the metal atom during the active-template reaction, making **1a** a monodentate or possibly weakly bidentate or very weakly tridentate ligand.[32] Not only is macrocycle **1b** missing the ether oxygen atoms, but the pyridine nitrogen atom lone pair is tied up in strong intramolecular bifurcated hydrogen bonds to the adjacent amide groups,[33] so it was rather surprising to find that [2]rotaxane **4b** was successfully produced in the active-metal template reaction, albeit in only 6% yield. Coordination of **1b** to the copper occurs at the expense of the intramolecular hydrogen bonds[34,35] so that **1b** is able to act as an effective monodentate ligand. In contrast, the use of **1c**—a tridentate macrocyclic ligand with three hard donor atoms—gave a similar overall conversion to triazole but with no rotaxane

(31) The standard reaction conditions use 1 equiv of each reagent and low temperatures to minimize the background uncatalyzed thermal cycloaddition. These conditions were chosen to allow the relative efficacy of the different macrocycles in promoting rotaxane formation to be assessed. No attempt was made to optimize the reaction conditions to improve the rotaxane yields reported in Figure 4. For macrocycles **1a**, **1i**, **1j**, **1f**, **1l**, **1m**, and **1n**—all of which produce significant rotaxane and are not degraded under the reaction conditions—virtually all the macrocyclic ligand can be converted to rotaxane by using extended reaction times and an excess of the azide and alkyne building blocks.

(32) For an X-ray structure of **1a** as a monodentate ligand in a rotaxane (Pd(II) as the metal atom) see ref 29b; for X-ray structures of a related pyridine diether ligand acting as a bidentate ligand in a rotaxane (Cu(II) or Ni(II) as the metal atom) see ref 29d.

(33) (a) Hunter, C. A.; Purvis, D. H. *Angew. Chem., Int. Ed. Engl.* **1992**, *31*, 792−795. (b) Johnston, A. G.; Leigh, D. A.; Nezhat, L.; Smart, J. P.; Deegan, M. D. *Angew. Chem., Int. Ed. Engl.* **1995**, *34*, 1212−1216. (c) Leigh, D. A.; Moody, K.; Smart, J. P.; Watson, K. J.; Slawin, A. M. Z. *Angew. Chem., Int. Ed. Engl.* **1996**, *35*, 306−310. (d) Leigh, D. A.; Murphy, A.; Smart, J. P.; Slawin, A. M. Z. *Angew. Chem., Int. Ed. Engl.* **1997**, *36*, 728−732. (e) Leigh, D. A.; Murphy, A.; Smart, J. P.; Deleuze, M. S.; Zerbetto, F. *J. Am. Chem. Soc.* **1998**, *120*, 6458−6467. (f) Deleuze, M. S.; Leigh, D. A.; Zerbetto, F. *J. Am. Chem. Soc.* **1999**, *121*, 2364−2379. (g) Clegg, W.; Gimenez-Saiz, C.; Leigh, D. A.; Murphy, A.; Slawin, A. M. Z.; Teat, S. J. *J. Am. Chem. Soc.* **1999**, *121*, 4124−4129. (h) Biscarini, F.; Cavallini, M.; Leigh, D. A.; León, S.; Teat, S. J.; Wong, J. K. Y.; Zerbetto, F. *J. Am. Chem. Soc.* **2002**, *124*, 225−233. (i) Bottari, G.; Dehez, F.; Leigh, D. A.; Nash, P. J.; Pérez, E. M.; Wong, J. K. Y.; Zerbetto, F. *Angew. Chem., Int. Ed.* **2003**, *42*, 5886−5889. (j) Leigh, D. A.; Venturini, A.; Wilson, A. J.; Wong, J. K. Y.; Zerbetto, F. *Chem.—Eur. J.* **2004**, *10*, 4960−4969.

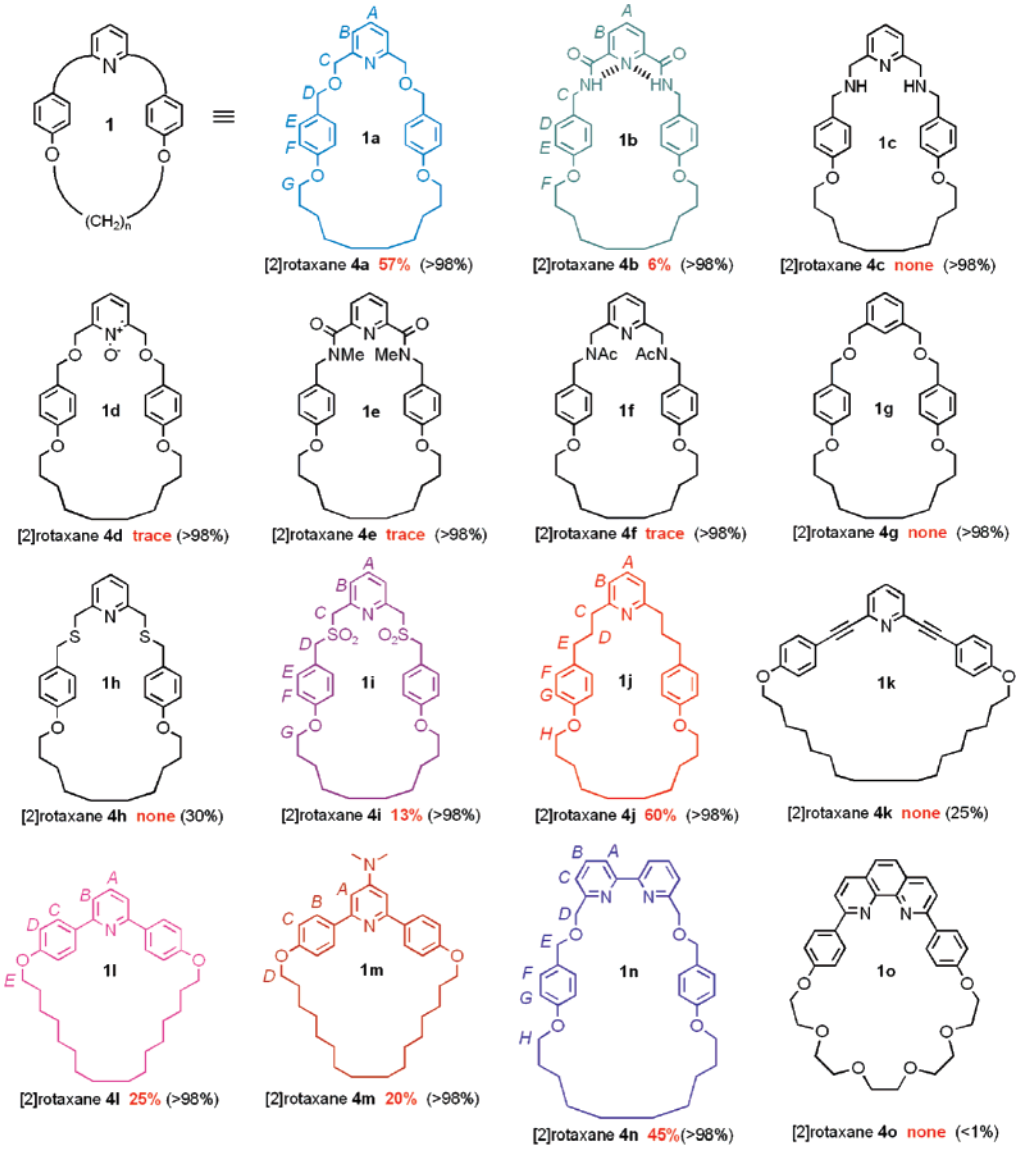

Figure 4. Influence of the macrocycle structure on the active-metal template CuAAC rotaxane-forming reaction in Scheme 2 under a standardized set of reaction conditions. Conditions for Scheme 2: (i) **1a**−**o**, **2**, **3**, $[Cu(CH_3CN)_4](PF_6)$, CH_2Cl_2, rt, 24 h (72 h for **4n** and **4o**), 0.01 M concentration with respect to each of **1a**−**o**, alkyne **2**, azide **3**, and $[Cu(CH_3CN)_4](PF_6)$; the reactions were not run under an inert atmosphere, nor using distilled or dried solvents; (ii) KCN, CH_2Cl_2/CH_3OH. The conversion of each macrocycle to [2]rotaxane is given as a percentage yield in red, and the overall conversion of **2** and **3** into triazole products (rotaxanes **4a**−**o** and thread **5**) is shown for each macrocycle in parentheses. The designation "trace" means that the rotaxane was observed by ESI-MS but could not be detected by ^{1}H NMR. The colors and lettering correspond to the signals and assignments of the ^{1}H NMR spectra shown in Figure 5.

formed. Upon addition of **1c** to the copper catalyst and other reagents the solution changed color immediately from colorless to blue-green. This suggests that most of the Cu(I) is rapidly oxidized to Cu(II) upon coordination to **1c**.[36] The resulting Cu(II)−**1c** complex is not catalytically active for the alkyne−azide cycloaddition, and any tridentate Cu(I)−**1c** complex lacks the free coordination sites necessary to bind azide and alkyne in the same aggregate.[37] However, enough of the copper in the reaction is not tied up as the **1c** complex for the ligandless thread-forming triazole reaction to proceed to completion within 24 h.

Macrocycle **1d** has a structure similar to that of **1a** except that the pyridine nitrogen is oxidized. The result, >98% conversion to triazole but only a trace of rotaxane when using **1d** as the macrocycle in the active-template reaction, shows that the *N*-oxygen atom greatly affects the ligand's ability to coordinate to Cu(I). Macrocycle **1e** also has a constitution

(34) Hydrogen bond energies are usually in the range of 1−10 kcal/mol, whereas coordinate bonds have energies of 20−80 kcal/mol;[35] thus, the stabilization of the copper(I) ion upon coordination should compensate for the loss of the two hydrogen bond interactions. In fact, all of the pyridine-containing macrocycles studied exhibit complexation-induced shifts in the ^{1}H NMR spectra ($CDCl_3$) upon addition of $[Cu(CH_3CN)_4](PF_6)$, indicating that copper(I) ions interact with the macrocycles in every case.

(35) Goshe, A. J.; Crowley, J. D.; Bosnich, B. *Helv. Chim. Acta* **2001**, *84*, 2971−2985.

(36) This oxidation of Cu(I) to Cu(II) in the presence of **1c** occurs even when great care is taken to exclude both moisture and oxygen from the reaction mixture. It appears that the macrocycle itself is the oxidant. However, there is some remaining $[Cu(CH_3CN)_4](PF_6)$ which catalyzes the formation of the thread **5**.

(37) The multidentate ligand tris[(1-benzyl-1*H*-1,2,3-triazol-4-yl)methyl]amine (TBTA) is a highly effective copper ligand for the CuAAC reaction [see refs 6b and 17a,b and Gupta, S. S.; Kuzelka, J.; Singh, P.; Lewis, W. G.; Manchester, M.; Finn, M. G. *Bioconjugate Chem.* **2005**, *16*, 1572−1579]. However, the individual triazole-functionalized "arms" of TBTA are weakly coordinating ligands, so TBTA probably functions by the alkyne and azide displacing two of the triazole groups to form the reactive intermediate.

similar to that of **1b**, but the secondary amides are methylated, eliminating their ability to form hydrogen bonds. AM1 calculations[38,39] using Spartan (see the Supporting Information) show that the methyl groups distort and partially fill the macrocycle cavity. The result is that, like that of **1d**, little of the CuAAC reaction is directed through the macrocycle cavity to form rotaxane. The same effect is seen for macrocycle **1f**, the bis-*N*-acetylated analogue of **1c**.

Removing the pyridine nitrogen atom, macrocycle **1g**, completely switches off rotaxane formation, confirming the need for a ligating donor atom. Replacing the benzylic oxygens of **1a** by more strongly coordinating sulfur atoms produces another tridentate macrocycle, **1h**. As with **1c**, no rotaxane is formed—consistent with the premise that tridentate ligand complexes of Cu(I) lack the vacant coordination sites necessary to bind both azide and alkyne[37]—and the yield of triazole is also only 30%, indicating that **1h** is particularly effective in sequestering the copper. Oxidation of the sulfide groups to sulfones, macrocycle **1i**, restores the ability of the macrocycle to bind to the Cu(I) as a monodentate ligand, and despite the increased bulk around the coordinated metal ion, a significant amount (13%) of [2]-rotaxane **4i** is formed by the stoichiometric active-metal template reaction. In fact, substitution of the benzylic ether oxygen atoms by methylene groups confirms that only a monodentate macrocycle with a single strongly coordinating donor atom is required for an efficient active-template rotaxane-forming reaction; macrocycle **1j** generates just as much [2]rotaxane as the parent macrocycle **1a**. Modeling suggests that the cavity of macrocycle **1j** is rather more flexible than that of **1a**, yet this is not detrimental for rotaxane formation.

To test whether other macrocycle geometries would be tolerated by the active-template reaction, we prepared **1k** and **1l** in which the substituted benzylic units were replaced by arylalkynyl and aryl groups, respectively. The 2,6-bisalkynylpyridine unit proved to be unstable[40,41] under the reaction conditions, suppressing the overall yield of the CuAAC reaction, with no rotaxane being produced. However, the active-metal template CuAAC reaction proceeded smoothly with **1l**, albeit generating rather less rotaxane (25%) than the most effective examples of other macrocycle geometries (**1a** and **1j**). AM1 calculations[38] using Spartan (see the Supporting Information) indicate that **1l** has a well-defined persistent cavity suitable for the threading of a molecular chain. However, the phenyl groups flanking the pyridine sterically encumber the nitrogen donor atom of the macrocycle, and a combination of steric and electronic factors probably reduces the binding strength of this macrocycle for Cu(I) ions. The weaker binding leads to more ligandless[23] Cu(I) in solution, resulting in higher conversion of the substrates into the noninterlocked thread **5** and the relatively modest yield of [2]rotaxane **4l**. Increasing the steric bulk at the 4-position of the pyridine group while simultaneously increasing the electron-donating ability of the heterocyclic nitrogen atom, macrocycle **1m**, had little effect on the rotaxane yield.

Bidentate Macrocycles. Having established that monodentate ligands of several different macrocycle geometries and donor atom orientations (**1a**, **1j**, **1l**, **1m**) efficiently promote active-template rotaxane formation, whereas strongly tridentate macrocycles (**1c** and **1h**) do not, we investigated the efficacy of bidentate macrocycles **1n** and **1o**.[17,42] The bipyridyl macrocycle **1n** directs the CuAAC reaction through its cavity to form rotaxane almost as efficiently as the best monodentate macrocycles (45% for **1n** → **4n** compared to 57% for **1a** → **4a** and 60% for **1j** → **4j**). However, it severely inhibits the rate of the Cu(I)-catalyzed reaction, and it took 3 days for the active-metal template reaction **1n** → **4n** to go to completion, compared to 24 h for **1a** → **4a** and 6 h for the ligand-free Cu(I)-catalyzed control reaction (Figure 3). The inhibition of the Cu(I)-catalyzed cycloaddition is even more dramatic with the other bidentate ligand investigated, the 2,9-diphenylphenanthroline macrocycle **1o** used extensively to assemble rotaxanes and catenanes by the Sauvage group.[1b,i] Macrocycle **1o** completely inhibits the CuAAC reaction. Even after 3 days under the standard stoichiometric active-metal reaction conditions in the presence of **1o**, no triazole products were observed. This latter result is particularly interesting given that phenanthroline ligands have previously been reported[17] to promote the CuAAC reaction. The lack of reactivity is presumably a result of the steric bulk about the Cu(I) center in the complex preventing the complex from undergoing the various structural variations required for reaction to take place (e.g., tolerating the change in geometry from Cu(I) to the formal Cu(III) species, Scheme 1), together with the macrocycle being very effective in sequestering the Cu(I) in this unreactive form. A related Cu(I)—macrocycle complex has recently been reported to promote the formation of [2]rotaxanes via a Glaser alkyne homocoupling.[13] However, in that case, intermediates of type B (Scheme 1) are possible with a bidentate ligand for copper because no azide need be coordinated to the metal atom.

^{1}H NMR Spectra of the Metal-Free [2]Rotaxanes

The ^{1}H NMR spectra (400 MHz, 300 K, $CDCl_3$) for each of the rotaxanes formed in >5% yield are shown in Figure 5. The ^{1}H NMR spectra of the rotaxanes (Figure 5b—g) all show upfield shifts of several signals with respect to the signals of the noninterlocked components (thread **5**, Figure 5a, and the macrocycles **1a**, **1b**, **1i**, **1j**, **1m**, and **1n**; see the Supporting Information). Such shielding is typical of interlocked structures in which the aromatic rings of one component are positioned face on to with another component and is observed for all the nonstopper resonances of the axle (H_{f-j}), indicating that the macrocycle accesses the full length of the thread. This is as expected; there should be no strong intercomponent noncovalent interactions between the thread and the macrocycle in the metal-free rotaxanes. The one exception is the amide-containing rotaxane **4b** (Figure 5c), which exhibits a significant downfield shift of the amide resonance with respect to that of the free macrocycle (see Supporting Information). This can be attributed to hydrogen bonding between the amides of the macrocycle and

(38) Minimum energy conformations were calculated for each of the metal-free macrocycles using the Spartan molecular modeling program (Semi-Empirical, AM1). The results are provided in the Supporting Information.
(39) In the case of **1e** no hydrogen bonds are present, thus allowing the Cu(I) ion better access to the macrocycle's pyridine nitrogen atom. However, in each of macrocycles **1e** and **1f** the nitrogen atom of the pyridine is more hindered, which may reduce the binding ability of the ligand.
(40) Internal alkynes have been found to react under CuAAC conditions; see: Díez-González, S.; Correa, A.; Cavallo, L.; Nolan, S. P. *Chem.—Eur. J.* **2006**, *12*, 7558—7564.
(41) Macrocycle **1k** is also photosensitive and decomposes slowly in ambient light.
(42) Bidentate bipyridine and phenanthroline ligands have been shown to significantly enhance the kinetics of the CuAAC reaction; see ref 17b.

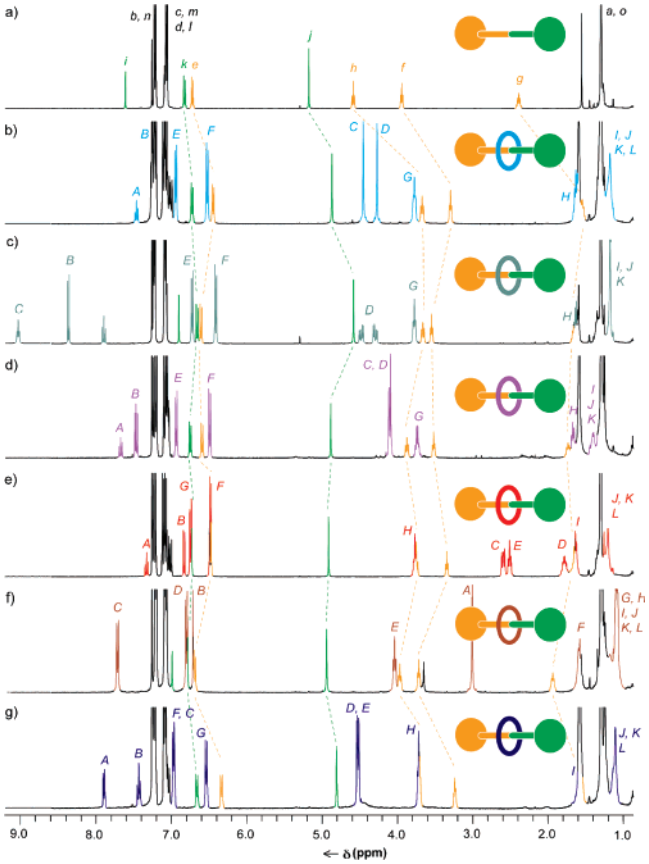

Figure 5. ^{1}H NMR spectra (400 MHz, $CDCl_3$, 300 K) of (a) triazole thread **5**, (b) [2]rotaxane **4a**, (c) [2]rotaxane **4b**, (d) [2]rotaxane **4i**, (e) [2]rotaxane **4j**, (f) [2]rotaxane **4m**, and (g) [2]rotaxane **4n**. The assignments correspond to the lettering shown in Scheme 2 and Figure 4.

the triazole unit of the thread in an interaction similar to that previously observed between interlocked amide and pyridine components in rotaxanes and catenanes.[1j,29]

Active-Metal Template CuAAC Reaction at High Macrocycle:Cu(I) Ratios: Unexpected Formation of [3]Rotaxanes

The picture of the active-metal template CuAAC reaction that we can build up that is consistent with the experimental observations so far is that the ligand-free $[Cu(CH_3CN)_4](PF_6)$ salt and macrocycles **1a**−**o** are in equilibrium with the corresponding copper(I)−macrocycle complex in which, in most cases, the metal atom directs the cycloaddition of the azide and alkyne through the macrocycle cavity. Although the ligand-free reaction is inherently faster than the active-metal template one, the coordinating ability of the macrocycle means that the rotaxane-forming reaction can become competitive with, or even dominate, the thread-forming reaction. In general, a stronger binding macrocyclic ligand (e.g., **1a** compared to **1b**) should move this equilibrium in favor of rotaxane formation. However, some changes in coordination geometry about the metal are required for the CuAAC mechanism to operate (Scheme 1), so the most strongly binding macrocycle (**1o**), which apparently does not tolerate such changes, actually inhibits the rotaxane-forming reaction. In view of this, we decided to investigate other conditions in which rotaxane formation might be increased at the expense of the thread.

In an attempt to minimize the amount of ligandless Cu(I) present in the reaction, we carried out the active-metal template CuAAC protocol under the standard set of conditions (1 equiv of **2**, 1 equiv of **3**, 1 equiv of $[Cu(CH_3CN)_4](PF_6)$, CH_2Cl_2, rt) used previously but in the presence of 10 equiv of macrocycle (Scheme 3). Our initial experiments[43] were carried out with monodentate macrocycle **1l**, and we were immediately intrigued to find that the reaction was much slower with 10 equiv of the macrocycle than it had been with 1 equiv, the higher macrocycle:Cu(I) reaction taking more than one week to go to completion. Upon reaching this end point, the mixture of triazole products was found to consist of 30% thread **5**, 37% [2]rotaxane **4l**, and, to our surprise, 33% [3]rotaxane **7l** (yields quoted with respect to the alkyne and azide reactants). A reaction using macrocycle **1a** under the same experimental conditions (1 equiv of **2**, 1 equiv of **3**, 1 equiv of $[Cu(CH_3CN)_4](PF_6)$, and 10 equiv of **1a**, CH_2Cl_2, rt) was again slower than the same reaction with 1 equiv of macrocycle (3 days to reach completion compared to 24 h), generating a product mixture of 5% thread **5**, 90% [2]rotaxane **4a**, and 5% [3]rotaxane **7a** (yields quoted with respect to the alkyne and azide reactants). A similar but less dramatic trend was seen with bidentate macrocycle **1n**; with 10 equiv of **1n** the reaction took 10 days to complete (cf. 3 days with 1 equiv), producing 3% thread **5** and 97% [2]rotaxane **4n** (in this case no [3]rotaxane **7n** could be detected by ^{1}H NMR spectroscopy).

The remarkable features of these high macrocycle:Cu(I) ratio active-metal template reactions are the following:

(i) Exceptional combined rotaxane yields: 95% ([2]rotaxane **4a** + [3]rotaxane **7a**) compared to 57% for **4a** with 1 equiv of **1a**; 70% ([2]rotaxane **4l** + [3]rotaxane **7l**) compared to 25% for **4l** with 1 equiv of **1l**; 97% ([2]rotaxane **4n**) compared to 45% for **4n** with 1 equiv of **1n**.

(ii) Significant slowing of the reaction rates compared to the low macrocycle:Cu(I) ratio reactions. The largest effect on the rate is seen with the weakly copper-binding macrocycle **1l**; the smallest effect on the rate occurs for the strongly copper-binding macrocycle **1n**. Again, this is strongly suggestive experimental evidence that the dominant mechanism of the CuAAC reaction under these conditions involves activation of the copper σ-acetylide unit by a second, preferably ligandless for steric reasons, copper atom (i.e., **I** or **II**, Scheme 3).

(iii) Formation of [3]rotaxane (in 33% yield using macrocycle **1l**)—i.e., *two* macrocycles being threaded during the formation of *one* triazole ring. Molecular models show that this can most reasonably occur through the sort of bridged two copper atom intermediate **III** shown in Scheme 3. Since such a doubly bridged intermediate cannot occur with bidentate ligands (and no [3]rotaxane is observed with **1n**), it seems likely that monodentate pyridine ligand-promoted CuAAC reactions proceed via doubly bridged intermediates such as **I** (Scheme 3), the equivalent of intermediate B(ii) in Scheme 1, whereas bidentate bipyridyl ligand-promoted CuAAC reactions proceed

(43) We chose macrocycle **1l** for this study because it is a rather poor ligand (indeed, we were unable to generate complexes with it using several other metals) due to the steric crowding around the pyridine nitrogen and the π-electron density presented to the low-oxidation-state copper from the adjacent aromatic rings. The rather weak Cu(I) binding affinity—meaning there is more ligandless[23] Cu(I) present in solution than many of the other macrocycles shown in Figure 4—is most likely the reason for the modest yield of rotaxane using 1 equiv of this macrocycle. We reasoned the yield should be improved by increasing the macrocycle:copper ratio.

Scheme 3. Effect of the Macrocycle:Cu(I) Ratio on the Active-Metal Template CuAAC Reaction[a,b]

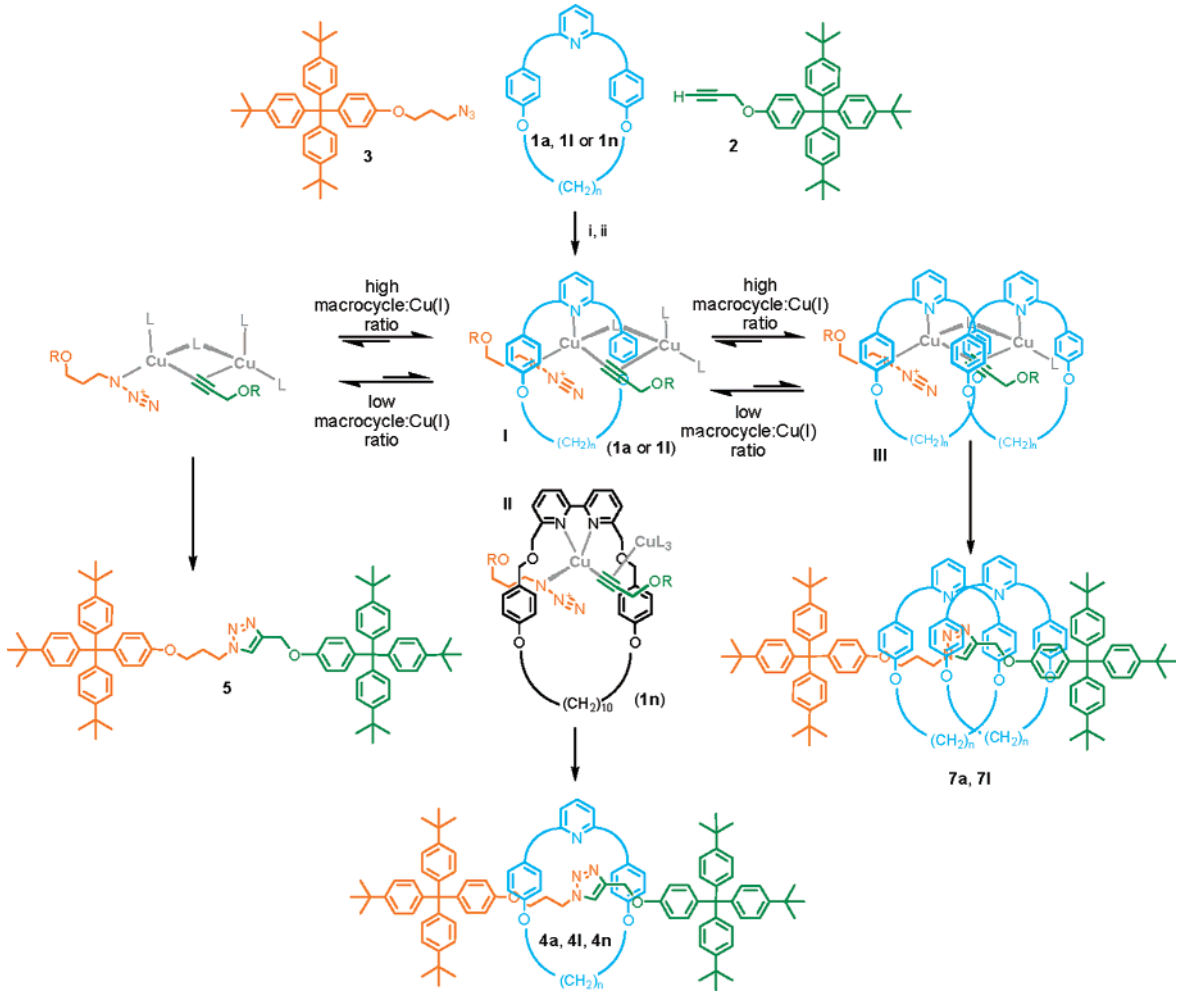

[a] Reagents and conditions: (i) **1a**, **1l**, or **1n** (10 equiv), **2** (1 equiv), **3** (1 equiv), $[Cu(CH_3CN)_4](PF_6)$ (1 equiv), CH_2Cl_2, rt, 24 h (**1a**), 7 days (**1l**), 10 days (**1n**); (ii) KCN, CH_2Cl_2/CH_3OH. Product yields starting from macrocycle **1a**: thread **5** (5%), [2]rotaxane **4a** (90%), [3]rotaxane **7a** (5%). Product yields starting from macrocycle **1a**: thread **5** (5%), [2]rotaxane **4i** (33%), [3]rotaxane **7l** (37%). Product yields starting from macrocycle **1n**: thread **5** (3%), [2]rotaxane **4n** (97%), [3]rotaxane **7n** (0%). [b] In the reactive intermediates shown, the copper azide (orange) reacts with any of the copper alkyne units shown in green. L can be any nonreacting ligand, including other alkyne and azide groups.

via simple π-coordinated complexes such as **II** (Scheme 3), the equivalent of intermediate A(ii) in Scheme 1.

The ^{1}H NMR spectra of [2]rotaxane **4l** and [3]rotaxane **7l** are shown in parts b and c, respectively, of Figure 6. The resonances for the axle (H_{f-j}) of the rotaxanes are shifted upfield compared to the signal for the free noninterlocked thread **5** (Figure 6a). The effect is more pronounced in the [3]rotaxane (Figure 6c) than in the [2]rotaxane (Figure 6b). Due to the asymmetry of the thread, the ^{1}H NMR spectrum of [3]rotaxane **7l** (Figure 6c) displays inequivalent but overlapping peaks for the two macrocycle components, which are double the intensity of the corresponding macrocycle signals in the [2]rotaxane. Single crystals of **7l** suitable for X-ray crystallography were grown by slow cooling of a hot saturated solution of **7l** in acetonitrile. The solid-state structure (Figure 7) confirmed the constitution of **7l** as a [3]rotaxane. Although it may superficially appear that face-to-face π-stacking interactions might aid the relative orientation of the two macrocycles on the thread, in the solid state the aromatic rings of adjacent macrocycles are not coplanar and their separation (>3.8 Å) is somewhat greater than that typically associated with aromatic stacking interactions.

Stoichiometric and Catalytic Active-Metal Template Synthesis of Bistriazole [2]Rotaxanes

To see whether the copper(I) would turn over catalytically during the formation of a single molecule, we investigated systems which require *two* cycloaddition reactions to be catalyzed in the formation of each molecule of [2]rotaxane (Scheme 4). [2]Rotaxanes **10** and **12** were each obtained in good yields (81% and 74%, respectively) using the conditions shown in Scheme 4 (0.5 equiv of Cu(I) for each triazole ring formed in a rotaxane) with either **1a**, **2**, and the diazide **8** or **1a**, **3**, and the dialkyne **9**. Since the rotaxane−Cu(I) complex in **4a** is strong enough to sequester the metal in the absence of pyridine, the lack of formation of more than trace amounts of [3]rotaxane in the reaction mixtures from Scheme 4 suggests that one macrocycle−Cu(I) complex may act processively to catalyze the formation of both triazole rings of an individual rotaxane thread. Such a hypothesis is consistent with the observation[25] by Rodionov et al. (albeit in a ligand-free Cu(I) system) of a strong kinetic enhancement in the second cycloaddition reaction when using diazide reactants. Reducing the amount of the copper salt to 20 mol % with respect to **1a** (10 mol % with respect to each

Scheme 4. Active-Metal Template CuAAC Synthesis of Bistriazole Molecular Shuttles **10** and **12**[a]

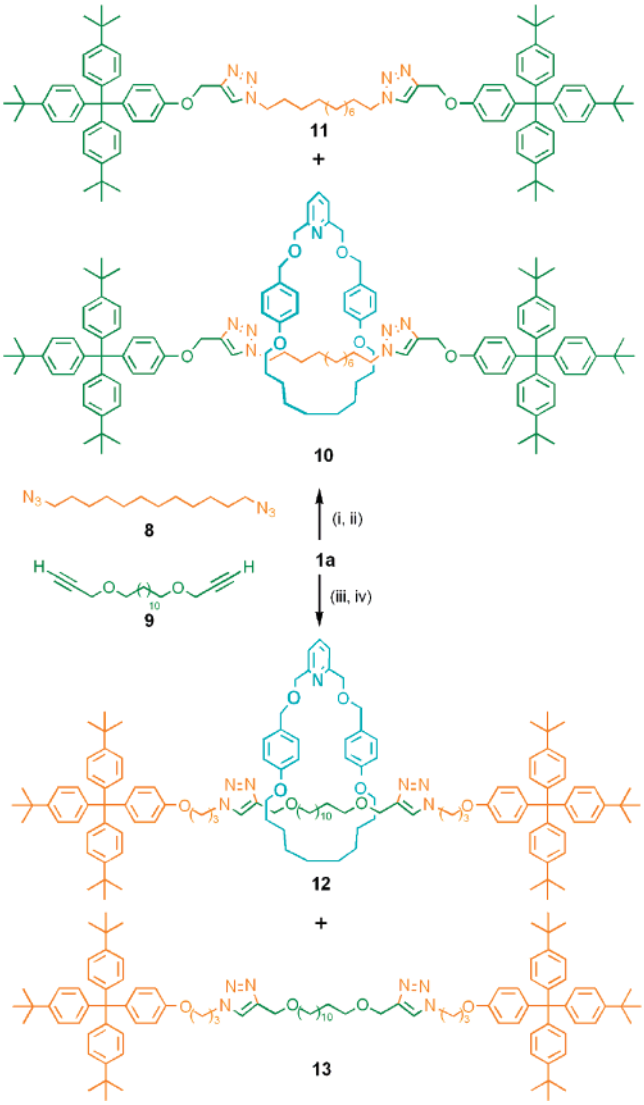

[a] Reagents and conditions: (i) **2**, $[Cu(CH_3CN)_4](PF_6)$, CH_2Cl_2, 25 °C, 72 h; (ii) KCN, CH_2Cl_2/CH_3OH, 81% ([2]rotaxane **10**) over two steps with 0.5 equiv of Cu(I), 63% ([2]rotaxane **10**) over two steps with 0.1 equiv of Cu(I) + 3 equiv of pyridine; (iii) **3**, $[Cu(CH_3CN)_4](PF_6)$, CH_2Cl_2, 25 °C, 72 h; (iv) KCN, CH_2Cl_2/CH_3OH, 74% ([2]rotaxane **12**) over two steps.

rotaxane triazole ring formed) and introducing 3 equiv of pyridine to the reaction of **1a**, **2**, and **8** to allow the processive catalyst to turn over intermolecularly still generated [2]rotaxane **10** in 63% yield (Scheme 4).

Transition-Metal-Mediated Control of the Shuttling Rate in Degenerate Two-Triazole-Station Molecular Shuttles

The shuttling of the ring in the degenerate two-station bistriazole rotaxane **10** in the presence of different diamagnetic transition-metal salts was investigated using ^{1}H NMR spectroscopy. Unlike most previously reported molecular shuttles—where the interactions used to direct the synthesis of the rotaxanes persist in the interlocked structure, resulting in a well-defined coconformation—there are no strong noncovalent interactions between the components of metal-free **10**. Comparison of the ^{1}H NMR spectrum of the free thread **11** (Figure 8a) with that of the rotaxane **10** (Figure 8b) shows uniform shielding of

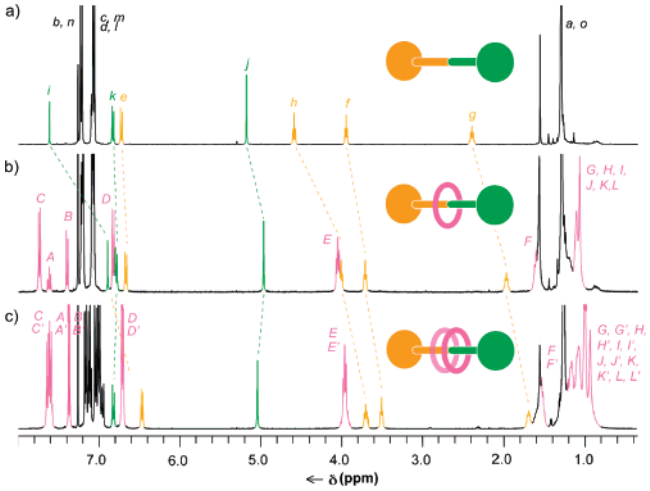

Figure 6. ^{1}H NMR spectra (400 MHz, $CDCl_3$, 300 K) of (a) triazole thread **5**, (b) [2]rotaxane **4l**, and (c) [3]rotaxane **7l**. The assignments correspond to the lettering shown in Scheme 2 and Figure 4.

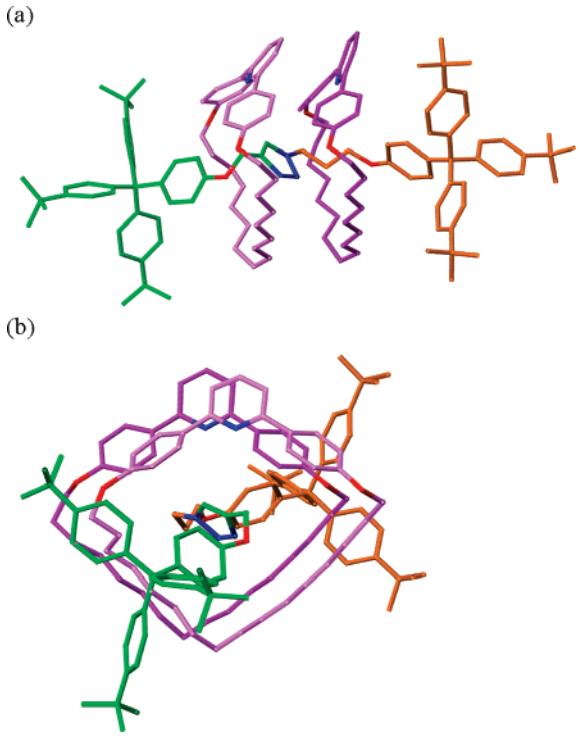

Figure 7. X-ray structure of [3]rotaxane **7l**, from a single crystal obtained from a saturated acetonitrile solution: (a) viewed side-on; (b) viewed along the axis of the thread. For clarity, different shades of purple are used for the carbon atoms of the two rings.

the thread signals (H_d, H_e, H_f, H_g, H_h), indicating that the macrocycle randomly explores the full length of the thread.

Reintroducing copper(I) into the bistriazole rotaxane[44] to form $[Cu\mathbf{10}](PF_6)$ (Scheme 5) gave a complex that exhibited fast shuttling of the macrocycle between the two triazole units in the room temperature ^{1}H NMR spectra in CD_3CN/CD_2Cl_2

(44) For examples of 1,2,3-triazoles as ligands see refs 3, 6s, and 17a,b and (a) Liu, D.; Gao, W.; Dai, Q.; Zhang, X. *Org. Lett.* **2005**, *7*, 4907−4910. (b) Dai, Q.; Gao, W.; Liu, D.; Kapes, L. M.; Zhang, X. *J. Org. Chem.* **2006**, *71*, 3928−3934. (c) Mindt, T. L.; Struthers, H.; Brans, L.; Anguelov, T.; Schweinsberg, C.; Maes, V.; Tourwe, D.; Schibli, R. *J. Am. Chem. Soc.* **2006**, *128*, 15096−15097. (d) Suijkerbuijk, B. M. J. M.; Aerts, B. N. H.; Dijkstra, H. P.; Lutz, M.; Spek, A. L.; van Koten, G.; Klein Gebbink, R. J. M. *Dalton Trans.* **2007**, 1273−1276. (e) Huffman, J. C.; Flood, A. H.; Li, Y. *Chem. Commun.* **2007**, 2692−2694.

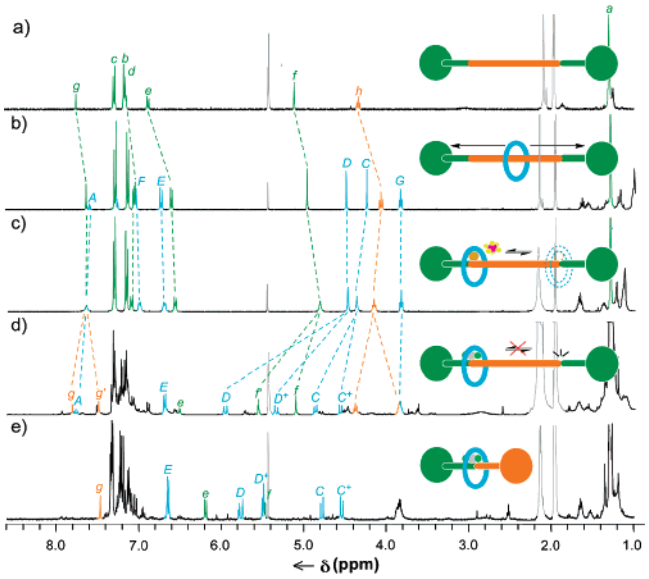

Figure 8. ^{1}H NMR spectra (400 MHz, CD_3CN/CD_2Cl_2 (9/1), 300 K) of (a) bistriazole thread **11**, (b) bistriazole [2]rotaxane **10**, (c) copper−bistriazole [2]rotaxane complex [Cu**10**](PF_6), (d) palladium dichloride−bistriazole [2]rotaxane complex Cl_2Pd**10**, and (e) palladium dichloride−triazole rotaxane complex Cl_2Pd**4a**. The assignments correspond to the lettering shown in Scheme 5.

(Figure 8c).[45] Although fast shuttling between well-defined macrocycle binding sites is very unusual for metal-coordinated molecular shuttles,[46] Cu(I) complexes can exhibit extremely fast exchange rates.[47] In contrast to this dynamic behavior, the ^{1}H NMR spectrum (Figure 8d) of rotaxane **10** following coordination of $PdCl_2$ (Scheme 5, ii) displays two sets of peaks for protons close to the thread triazole rings (e.g., $H_{f/f'}$, $H_{g/g'}$). This observation is indicative of the macrocycle in the Cl_2Pd**10** complex being unable to shuttle between the triazole stations on the NMR time scale. This restriction to shuttling also manifests itself in the geminal splitting of the signals corresponding to H_C and H_D of the macrocycle, which occurs as a consequence of the two "faces" of the ring being in different chemical environments. The chemical shifts of one set of the duplicated signals (e.g., H_f) correspond closely to those of the free thread **11** (Figure 8a). The other set of duplicate signals (e.g., $H_{f'}$) correspond closely to a model single-triazole rotaxane−$PdCl_2$ complex, Cl_2Pd**4a** (Figure 8e, Scheme 5). Heating the sample of Cl_2Pd**10** to 343 K (close to the solvent boiling point of CD_3CN) did not lead to any broadening of the signals in the ^{1}H NMR spectrum, indicating that the macrocycle shuttling is very effectively blocked by coordination to Pd.

The notable features of these degenerate two-station bistriazole rotaxanes are the following:

(i) To our knowledge these are the first examples of molecular shuttles containing two degenerate transition-metal-binding stations.

(ii) The dynamics of the macrocycle exchange between the two well-defined discrete binding sites can be controlled with remarkable ease, simply through the judicious choice of different transition-metal ions.

(iii) An active-metal template strategy is much more amendable to the synthesis of such shuttles than traditional (passive) metal template strategies, because the number of binding sites in the products is not necessarily related to the number of template sites used for the shuttle synthesis.

Scheme 5. Controlling the Dynamics of Bistriazole Molecule Shuttle **10** by Coordination to Cu(I) or Pd(II)[a]

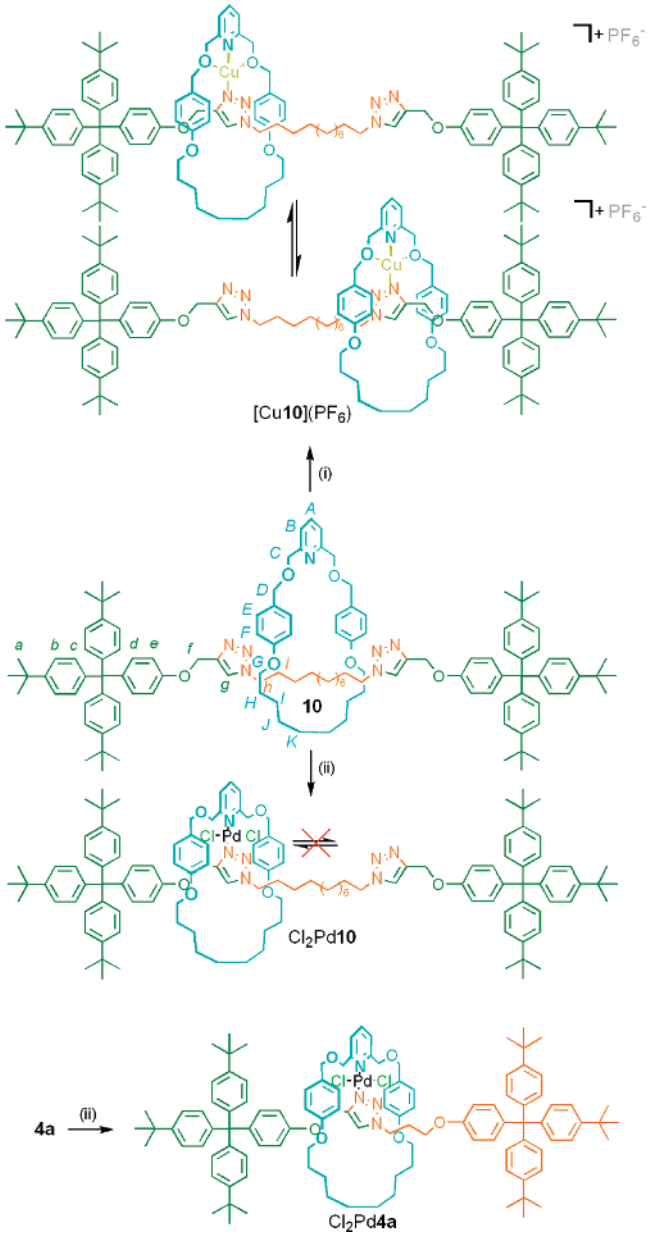

[a] Reagents and conditions: (i) $[Cu(CH_3CN)_4](PF_6)$ (1 equiv), CD_2Cl_2 (90%)/CD_3CN (10%), 25 °C, 5 min, >99%; (ii) $Pd(CH_3CN)_2Cl_2$ (1 equiv), CD_2Cl_2 (90%)/CD_3CN (10%), 25 °C, 5 min, >99%.

Conclusions

The Cu(I)-catalyzed 1,3-cycloaddition of azides with terminal alkynes is a highly effective reaction for the active-metal template synthesis of rotaxanes, as illustrated through both stoichiometric (up to 97% yields) and catalytic (up to 82% yields) versions of the strategy. The reaction tolerates a wide

(45) We were unable to slow the macrocycle shuttling dynamics in [Cu(**10**)](PF_6) sufficiently, nor isolate that motion from other conformational processes at low temperatures, to determine an accurate shuttling rate.
(46) Durola, F.; Sauvage, J.-P. *Angew. Chem., Int. Ed.* **2007**, *46*, 3537−3540.
(47) For an evaluation of ligand exchange rates at Cu(I) centers, see: Riesgo, E.; Hu, Y.-Z.; Bouvier, F.; Thummel, R. P. *Inorg. Chem.* **2001**, *40*, 2541−2546.

variety of both monodentate and bidentate macrocyclic ligands which, although inherently slower in promoting covalent bond formation than the ligand-free[23] Cu(I)-catalyzed reaction, all work by sequestering the majority of the Cu(I) present so that the rotaxane-forming CuAAC reaction becomes competitive with—and under many conditions dominates—the ligand-free CuAAC reaction. The addition of pyridine enables the Cu(I) active-metal template to turn over without significantly compromising the rotaxane yield. Among several potentially attractive features of this type of synthetic strategy is that it offers an unusual experimental probe of the reaction mechanism. The increase in rates of rotaxane formation by excess ligand-free Cu(I) supports the suggestion that in CH_2Cl_2 the copper σ-acetylide is activated by coordination to a second ligandless copper atom, and the sluggish reaction rates and remarkable formation of [3]rotaxanes with monodentate macrocycles at high macrocycle:Cu(I) ratios suggest that, under these conditions, the CuAAC reaction proceeds via a doubly bridged two copper atom intermediate (type B(ii), Scheme 1) when using a monodentate macrocyclic ligand and a simpler π-coordinated two copper atom intermediate (type A(ii), Scheme 1) when using a bidentate macrocyclic ligand.[48]

The experimental results concerning the active-metal template CuAAC synthesis of bistriazole rotaxanes suggest that the macrocycle−Cu(I) complex may act processively to catalyze the formation of more than one triazole ring per thread molecule. The resulting two-triazole-station molecular shuttles have interesting and unusual dynamic properties: coordination of the rotaxane macrocycle to Cu(I) gives a metal-complexed shuttle in which the ring still shuttles rapidly between the two triazole units of the thread, even at low temperatures in noncoordinating solvents. In contrast, complexation of the same two-triazole-station shuttle to $PdCl_2$ gives a rotaxane in which shuttling does not occur even at 343K in the presence of d_3-acetonitrile.

The template-directed assembly of otherwise difficult-to-access molecular architectures and the catalysis of covalent bond formation are two of the most useful tasks that transition metals can perform in organic chemistry. The active-template concept combines these two apparently disparate functions into one, which can produce—as the present work exemplifies—high-yielding, mild and effective synthetic routes to complex molecular structures requiring only catalytic quanitities of metal. The development of other active-template systems is in progress.

Acknowledgment. This work was supported by the European Union Future and Emerging Technology program Hy3M, the Ramsay Memorial Fellowships Trust, the Royal Society of Edinburgh, and the EPSRC. D.A.L. is an EPSRC Senior Research Fellow and holds a Royal Society-Wolfson Research Merit Award, P.J.L. is a Royal Society University Research Fellow, and J.D.C. is a British Ramsay Memorial Fellow. We thank Patrice Staub and Professor J.-P. Sauvage (Strasbourg) for generously providing us with a sample of macrocycle **1o**, termed "m-30" by the Strasbourg group in many papers. We thank Professor B. F. Straub (Munich) for a preprint of ref 26. We thank Professor V. V. Fokin (Scripps) for a preprint of ref 21 and for sharing with us his thoughts on the mechanism of the CuAAC reaction.

Supporting Information Available: Synthetic schemes, experimental procedures, and spectroscopic data for all new compounds. This material is available free of charge via the Internet at http://pubs.acs.org.

JA073513F

(48) Note added in proof: Very recent calculations (Straub, B. F. *Chem. Commun.* published online 12th July 2007 DOI: 10.1039/b706926j) suggest that the metallacycle formed in Scheme 1 consists of a strain-free Cu-C(Cu)=C unit rather than the depicted Cu=C=C unit. The second copper atom in the type B(ii) and A(ii) reactive intermediates shown in Scheme 1 means they are perfectly set up to form such a Cu-C(Cu)=C metallacycle.

Peptide Rotaxanes

DOI: 10.1002/anie.200903215

Rotaxane-Based Propeptides: Protection and Enzymatic Release of a Bioactive Pentapeptide**

Anthony Fernandes, Aurélien Viterisi, Frédéric Coutrot, Stéphanie Potok, David A. Leigh, Vincent Aucagne,* and Sébastien Papot**

Rotaxane and pseudorotaxane architectures are starting to attract interest as a means of molecularly encapsulating substrates for potential biological applications.[1–5] 'Nanovalves' that can store and release cargo molecules have been developed,[1] and the encapsulation of squaraine dyes within rotaxanes has been shown to enhance dye fluorescence and stability as well as imparting different cell-localization propensities on the substrates.[2] A stilbene-based rotaxane has been used to control the reactivity of a dipeptidic thread against protease hydrolysis,[3] and functionalized rotaxanes have also been shown to serve as effective vehicles for the intracellular delivery[4] of fluorescein-derivatized peptides. Polyrotaxanes have been studied for their potential as drug-delivery systems.[5] Herein, we report the synthesis and properties of a rotaxane in which a macrocycle protects an extended pentapeptide thread from degradation by different types of peptidases and the cocktail of enzymes present in human plasma. The glycosidase-catalyzed cleavage of a carbohydrate unit in a 'stopper' of the rotaxane triggers the release of the bioactive parent peptide through a self-immolative mechanism (Scheme 1). The demonstration that a macrocycle is able to protect an oligopeptide of significant length from degradation by peptidases, whilst simultaneously allowing an orthogonal enzyme-activated release mechanism to be built into the structure, is an important step toward the ultimate goal of a 'molecular sheath' peptide delivery system.

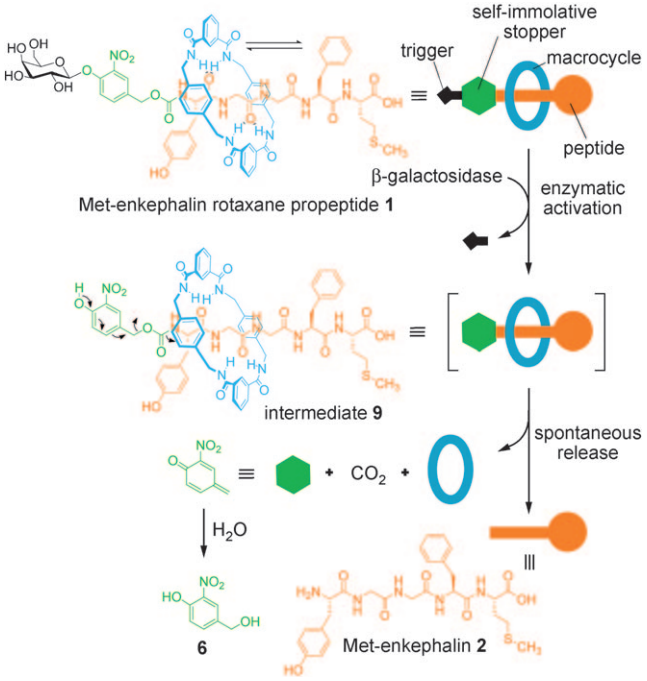

Scheme 1. Enzyme-triggered release of Met-enkephalin **2** from [2]rotaxane propeptide **1**.

Benzylic amide macrocycles can be templated around dipeptides in which glycine is the N-terminal amino acid residue, to form [2]rotaxanes in good yields.[6] Unfortunately, investigation of their efficacy in protecting peptide-based threads from enzymatic degradation (a common drawback to the use of oligopeptides in biological applications[7]) has been hampered because the yield of the rotaxane-forming reaction decreases rapidly with increasing peptide length.[6c,8] We envisaged that a solution might lie in employing a bulky nitrophenol ester[9] as a stopper for an extendable,[10] shorter, and more efficiently constructed, peptide rotaxane. We used this synthetic methodology to target a [2]rotaxane **1** based on Met-enkephalin **2** (H-Tyr-Gly-Gly-Phe-Met-OH), also known as opioid growth factor (OGF). Met-enkephalin **2** is a pentapeptide with a range of bioactivities that include regulation of nociception and also antitumor activity by control of cell growth.[11] Release of the free pentapeptide was designed to occur through cleavage of an enzyme-accessible monosaccharide on one of the stoppers (Scheme 1) using *E. coli* β-galactosidase, an enzyme that has been successfully

[*] Dr. A. Fernandes,[+] A. Viterisi,[+] Dr. F. Coutrot, Dr. S. Potok, Prof. D. A. Leigh
School of Chemistry, University of Edinburgh
The King's Buildings, West Mains Road, Edinburgh EH9 3JJ (UK)
Fax: (+44) 131-650-6453
http://www.catenane.net
E-mail: david.leigh@ed.ac.uk
Dr. V. Aucagne
Centre de Biophysique Moléculaire, UPR 4301 CNRS
Rue Charles Sadron, 45071 Orléans, Cedex 2 (France)
E-mail: aucagne@cnrs-orleans.fr
Dr. A. Fernandes,[+] Dr. S. Papot
Université de Poitiers, UMR 6514 Laboratoire de Synthèse et Réactivité des Substances Naturelles
40 Avenue du Recteur Pineau, 86022 Poitiers (France)
E-mail: sebastien.papot@univ-poitiers.fr
[+] These authors contributed equally to this work.

[**] We thank Prof. Jean-Pierre Gesson (Poitiers) for many useful discussions and the EPSRC National Mass Spectrometry Service Centre (Swansea, UK) for accurate mass data. This work was supported by the Science and Technology Department of the French Embassy in the United Kingdom, the Scottish Executive and the Royal Society of Edinburgh. D.A.L. is an EPSRC Senior Research Fellow and holds a Royal Society-Wolfson Research Merit Award.

Supporting information for this article is available on the WWW under http://dx.doi.org/10.1002/anie.200903215.

targeted[12] to specific cell types in antibody-directed enzyme prodrug therapy (ADEPT[13]) strategies.

Met-enkephalin **2** possesses the glycine residue necessary for rotaxane assembly and a C-terminal amino acid sequence (Phe-Met) that is bulky enough to act as a stopper for a benzylic amide macrocycle. The carbohydrate trigger[14] intended to release the bioactive peptide is covalently attached to the rest of the thread by a nitrobenzyloxycarbonyl linker. Following enzymatic activation with β-galactosidase, self-immolation of the deglycosylated stopper should result in the release of **2** along with the mechanical disassembly of the rotaxane architecture (Scheme 1).

Glycorotaxane[15] **4** was prepared from galactosylated thread **3**, which bears a bulky 2,6-diphenyl-4-nitrophenyl stopper, in 26% yield (Scheme 2, step a). The rotaxane yield is not dissimilar to that found previously[6c] using Phe-Gly threads (32%), despite the presence of both a nitrophenyl and tyrosyl ester in **3** that could potentially react with *p*-xylylenediamine. We were delighted to find that although nucleophile access to the activated ester group was hindered by both the macrocycle (which was tightly locked on the short peptide portion of the thread) and the phenyl groups on the stopper, treatment of **4** with H-Phe-Met-OH in $CHCl_3$ at reflux afforded the elongated [2]rotaxane **5** in 40% yield (Scheme 2, step b), with no evidence of any dethreading of **4** or **5** (59% of **4** was recovered from the reaction). Deprotection of the hydroxy groups (Scheme 2, step c) furnished Met-enkephalin rotaxane propeptide **1**. The corresponding thread **7** was also prepared (see the Supporting Information).

The partial ^{1}H NMR spectra of [2]rotaxane **1** and thread **7** are shown in Figure 1. Apart from the signals that correspond to the carbohydrate protons (shown in black), most of the resonances in the thread are shifted upfield in the rotaxane, thus indicating that the macrocycle is able to (and does) move beyond the original template. Although

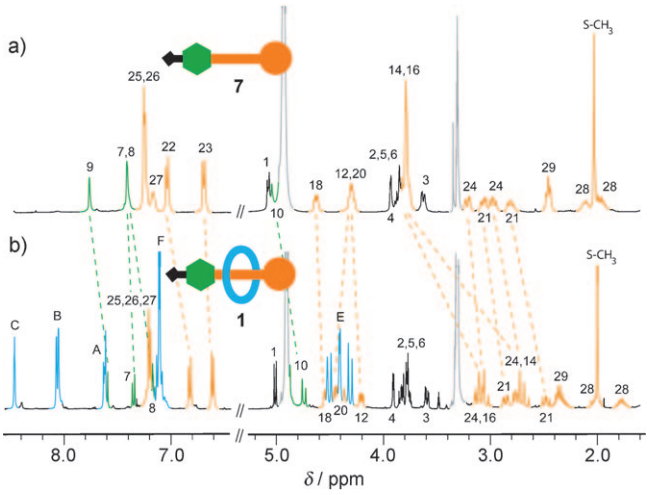

Figure 1. Partial ^{1}H NMR spectra (400 MHz, 298 K, CD_3OD) of a) thread **7** and b) rotaxane propeptide **1**. The assignments and coloring of signals correspond to that shown in Scheme 2. Residual solvent peaks are shown in gray.

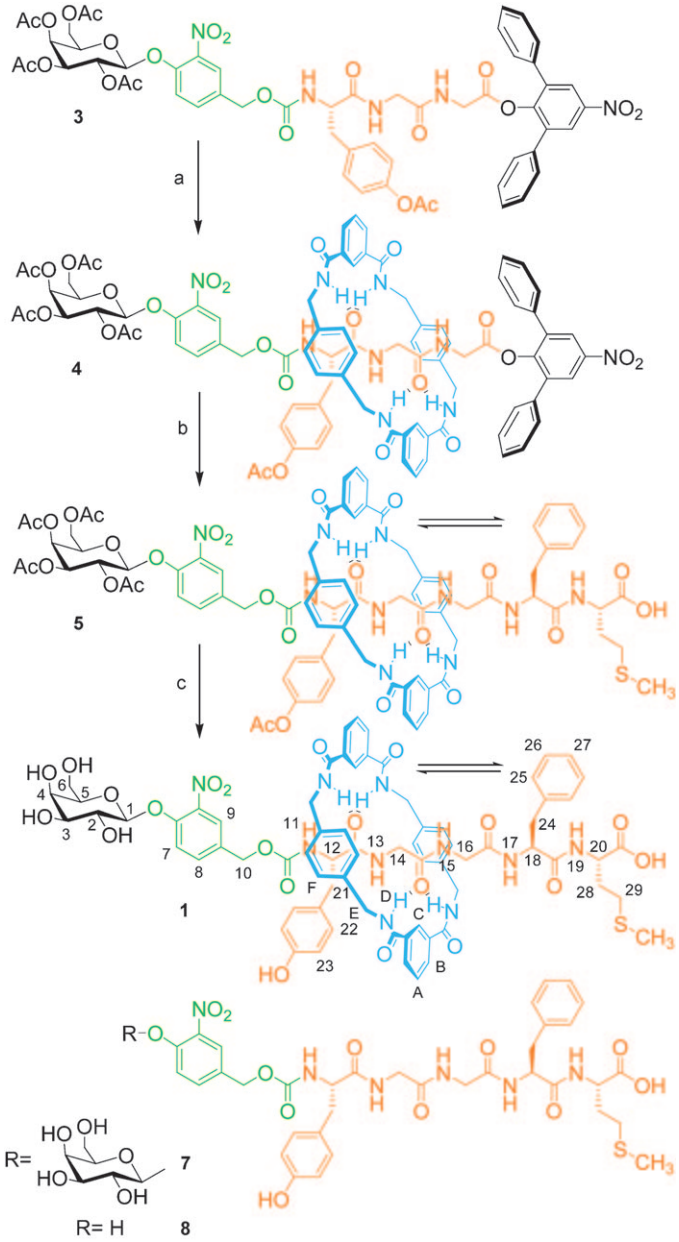

Scheme 2. Synthesis of [2]rotaxane propeptide **1**. a) Isophthaloyl chloride, *p*-xylylenediamine, Et_3N, $CHCl_3$, 26%; b) H-Phe-Met-OH, *N*,*N*-diisopropylethylamine (DIPEA), $CHCl_3$, reflux, 96 h, 40%; c) NaOMe, MeOH, 0 °C, quantitative.

the rotaxane Gly-Gly methylene protons H_{14} and H_{16} are the most shielded, which indicates that the macrocycle spends most of its time in this region, various peptide protons (orange) near the C terminus (e.g., H_{24}) and protons in the nitrobenzyloxycarbonyl spacer (green) near the N terminus are shielded to some extent by the aromatic rings of the macrocycle.[6]

The ability of the benzylic amide macrocycle to access almost the full length of the extended peptide augured well for its ability to protect the thread from degradation. We first confirmed that Met-enkephalin rotaxane **1** was stable in phosphate buffer at 37 °C. After 48 hours, no decomposition

was observed by HPLC. The protease resistance of the rotaxane was then probed by comparing the behavior of Met-enkephalin **2**, rotaxane **1**, and the thread **7** under the action of different types of peptidases, the results of which are shown in Figures 2–4.

Enzymatic digestion of each of the three substrates with aminopeptidase M, an exopeptidase that hydrolyses Met-enkephalin sequentially from the N-terminal amino acid,[16] was monitored by HPLC (Figure 2). While Met-enkephalin

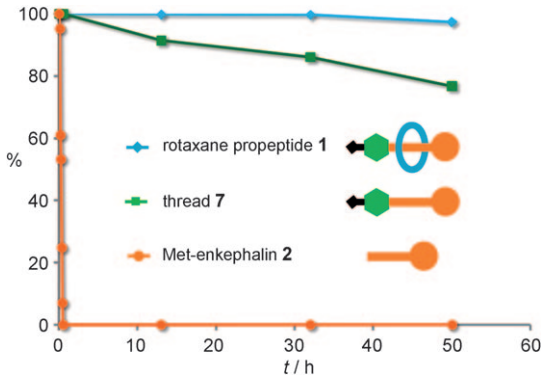

Figure 2. Enzymatic digestion of rotaxane propeptide **1** (blue diamonds), thread **7** (green squares), and Met-enkephalin **2** (orange circles) with porcine kidney aminopeptidase M. Reactions were carried out at 25 °C in 95 % phosphate buffer (0.05 M, pH 7.2), 5 % DMSO, using 0.005 U μmol^{-1} of substrate. 0.0025 U μmol^{-1} of enzyme was added every 12 h.

was rapidly degraded (< 30 minutes) using 0.005 units (U) of enzyme per μmol of substrate, thread **7** and rotaxane **1** proved stable for many hours under identical conditions and more than 70 % of **7** and more than 95 % of **1** were recovered after 2 days. In this case, the stability of both thread and rotaxane presumably arises from the fact that the part of Met-enkephalin that is recognized by the enzyme (the N terminus) is chemically derivatized in both **1** and **7**.

We next explored (Figure 3) the stability of **1**, **2**, and **7** towards angiotensin converting enzyme (ACE), a peptidase that hydrolyses Met-enkephalin between the Gly and Phe residues.[17] HPLC showed that while both pristine Met-enkephalin **2** and the N-functionalized, but non-interlocked, derivative **7** were degraded within hours, rotaxane **1** exhibited exceptional resistance towards the action of ACE (> 90 % remaining after 2 days). The difference in stability between the rotaxane and thread can be attributed solely to the mechanical barrier to the enzyme provided by the macrocycle.

Finally, the stability of each of **1**, **2**, and **7** to the cocktail of peptidases and other enzymes present in human plasma was evaluated (Figure 4). Met-enkephalin **2** was completely consumed in less than 5 minutes in reconstituted human plasma at 37 °C. The non-interlocked thread **7** was degraded with a half-life of approximately 5 hours, whilst 90 % of rotaxane **1** was still present after 5 days incubation in the plasma.

Whilst the resistance to peptidases conferred by the macrocycle on the extended oligopeptide in the rotaxane is

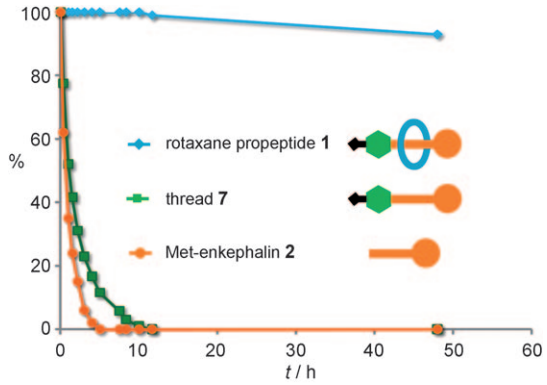

Figure 3. Enzymatic digestion of rotaxane propeptide **1** (blue diamonds), thread **7** (green squares), and Met-enkephalin **2** (orange circles) with rabbit lung angiotensin converting enzyme (ACE). Reactions were carried out at 25 °C in 95 % HEPES (4-(2-hydroxyethyl)-1-piperazineethanesulfonic acid) buffer (0.05 M, pH 8.3), 5 % DMSO, 0.3 M NaCl, using 0.8 U μmol^{-1} of substrate. 0.4 U μmol^{-1} of enzyme was added every 12 h.

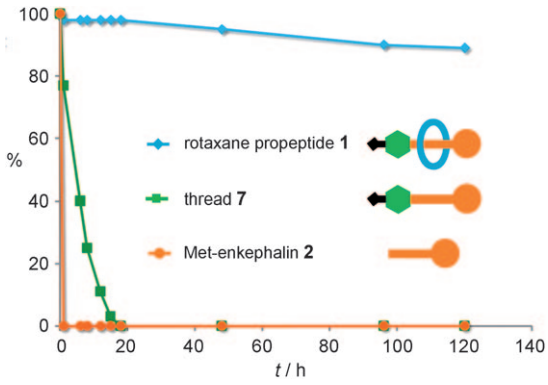

Figure 4. Stability of rotaxane propeptide **1** (blue diamonds), thread **7** (green squares), and Met-enkephalin **2** (orange circles) in human plasma reconstituted from lyophilized powder with 0.01 M Tris (tris(hydroxymethyl)aminomethane) buffer at pH 7.4, at 37 °C.

remarkable, if the parent peptide cannot ultimately be liberated from the molecular sheath then the structure can have no utility as a propeptide system. HPLC showed that the incubation of **1** with *E. coli* β-galactosidase in phosphate buffer (0.02 M, pH 7.0) at 37 °C resulted in the disappearance of **1** over 2–3 minutes (traces 2 and 3 in Figure 5b) and the emergence of a new peak with a retention time of 28 minutes and *m*/*z* 1318, which corresponds to the degalactosylated rotaxane **9**.[18] This peak also quickly disappeared (traces 3 and 4 in Figure 5b) concomitantly with the appearance of benzylic alcohol **6** (the product formed by spontaneous reaction with water of the quinone methide intermediate released by self-immolation of the nitrohydroxybenzyl unit (Scheme 1)), the dethreaded macrocycle (*m*/*z* 532), and free Met-enkephalin **2**. Despite the presence of the macrocycle in **1**, and its efficacy in protecting the peptide portion of the rotaxane axle from enzymes, the remote siting of the β-galactose trigger results in no significant difference between

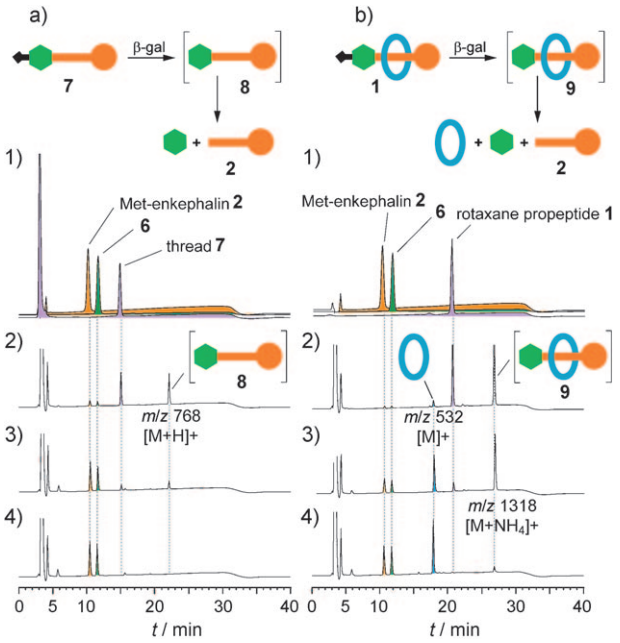

Figure 5. 1) Reference HPLC trace of individual components: a) **7**, **2** and **6**; b) **1**, **2** and **6**. 2–4) HPLC traces of the enzymatic hydrolysis of a) thread **7** and b) rotaxane propeptide **1** with *E. coli* β-galactosidase (β-gal) in 97.5% phosphate buffer (0.02 M, pH 7.0), 2.5% DMSO, at 37 °C using 10 U μmol^{-1} of substrate: 2) after 1 min; 3) after 2 min; 4) after 10 min.

the rate of formation of free Met-enkephalin from rotaxane propeptide **1** and thread **7** (Figure 5).

In conclusion, we have demonstrated a rotaxane-based molecular device in which an oligopeptide can be protected from a broad range of peptidases for several days and then released in bioactive form in a matter of minutes through a specific glycosidase-mediated controlled-release mechanism. The concept may prove useful for the development of practical propeptide delivery methods, derivatizing the macrocycle to further improve the properties and characteristics of the system.

Received: June 14, 2009
Published online: July 27, 2009

Keywords: delivery systems · peptides · prodrugs · rotaxanes · supramolecular chemistry

[1] a) T. D. Nguyen, H.-R. Tseng, P. C. Celestre, A. H. Flood, Y. Liu, J. F. Stoddart, J. I. Zink, *Proc. Natl. Acad. Sci. USA* **2005**, *102*, 10029–10034; b) K. C.-F. Leung, T. D. Nguyen, J. F. Stoddart, J. I. Zink, *Chem. Mater.* **2006**, *18*, 5919–5928; c) T. D. Nguyen, K. C.-F. Leung, M. Liong, C. D. Pentecost, J. F. Stoddart, J. I. Zink, *Org. Lett.* **2006**, *8*, 3363–3366; d) T. D. Nguyen, Y. Liu, S. Saha, K. C.-F. Leung, J. F. Stoddart, J. I. Zink, *J. Am. Chem. Soc.* **2007**, *129*, 626–634; e) T. D. Nguyen, K. C.-F. Leung, M. Liong, Y. Liu, J. F. Stoddart, J. I. Zink, *Adv. Funct. Mater.* **2007**, *17*, 2101–2110; f) S. Angelos, Y.-W. Yang, K. Patel, J. F. Stoddart, J. I. Zink, *Angew. Chem.* **2008**, *120*, 2254–2258; *Angew. Chem. Int. Ed.* **2008**, *47*, 2222–2226; g) K. Patel, S. Angelos, W. R. Ditchel, A. Coskun, Y.-W. Yang, J. I. Zink, J. F. Stoddart, *J. Am. Chem. Soc.* **2008**, *130*, 2382–2383; h) D. P. Ferris, Y.-L. Zhao, N. M. Khashab, H. A. Khatib, J. F. Stoddart, J. I. Zink, *J. Am. Chem. Soc.* **2009**, *131*, 1686–1688.

[2] a) E. Arunkumar, C. C. Forbes, B. C. Noll, B. D. Smith, *J. Am. Chem. Soc.* **2005**, *127*, 3288–3289; b) E. Arunkumar, N. Fu, B. D. Smith, *Chem. Eur. J.* **2006**, *12*, 4684–4690; c) J. R. Johnson, N. Fu, E. Arunkumar, W. M. Leevy, S. T. Gammon, D. Piwnica-Worms, B. D. Smith, *Angew. Chem.* **2007**, *119*, 5624–5627; *Angew. Chem. Int. Ed.* **2007**, *46*, 5528–5531; d) J. J. Gassensmith, E. Arunkumar, L. Barr, J. M. Baumes, K. M. DiVittorio, J. R. Johnson, B. C. Noll, B. D. Smith, *J. Am. Chem. Soc.* **2007**, *129*, 15054–15059.

[3] A. G. Cheetham, M. G. Hutchings, T. D. W. Claridge, H. L. Anderson, *Angew. Chem.* **2006**, *118*, 1626–1629; *Angew. Chem. Int. Ed.* **2006**, *45*, 1596–1599.

[4] a) V. Dvornikovs, B. E. House, M. Kaetzel, J. R. Dedman, D. B. Smithrud, *J. Am. Chem. Soc.* **2003**, *125*, 8290–8301; b) X. Bao, I. Isaacsohn, A. F. Drew, D. B. Smithrud, *J. Am. Chem. Soc.* **2006**, *128*, 12229–12238; c) J. Zhu, B. E. House, E. Fleck, I. Isaacsohn, A. F. Drew, D. B. Smithrud, *Bioorg. Med. Chem. Lett.* **2007**, *17*, 5058–5062; d) X. Wang, X. Bao, M. McFarland-Mancini, I. Isaacsohn, A. F. Drew, D. B. Smithrud, *J. Am. Chem. Soc.* **2007**, *129*, 7284–7293; e) J. Zhu, M. McFarland-Mancini, A. F. Drew, D. B. Smithrud, *Bioorg. Med. Chem. Lett.* **2009**, *19*, 520–523.

[5] a) T. Ooya, N. Yui, *Crit. Rev. Ther. Drug Carrier Syst.* **1999**, *16*, 289–330; b) T. Ooya, N. Yui, *J. Controlled Release* **1999**, *58*, 251–269; c) T. Ooya, K. Arizono, N. Yui, *Polym. Adv. Technol.* **2000**, *11*, 642–651; d) M. Eguchi, T. Ooya, N. Yui, *J. Controlled Release* **2004**, *96*, 301–307.

[6] a) D. A. Leigh, A. Murphy, J. P. Smart, A. M. Z. Slawin, *Angew. Chem.* **1997**, *109*, 752–756; *Angew. Chem. Int. Ed. Engl.* **1997**, *36*, 728–732; b) G. W. H. Wurpel, A. M. Brouwer, I. H. M. van Stokkum, A. Farran, D. A. Leigh, *J. Am. Chem. Soc.* **2001**, *123*, 11327–11328; c) G. Brancato, F. Coutrot, D. A. Leigh, A. Murphy, J. K. Y. Wong, F. Zerbetto, *Proc. Natl. Acad. Sci. USA* **2002**, *99*, 4967–4971; d) M. Asakawa, G. Brancato, M. Fanti, D. A. Leigh, T. Shimizu, A. M. Z. Slawin, J. K. Y. Wong, F. Zerbetto, S. Zhang, *J. Am. Chem. Soc.* **2002**, *124*, 2939–2950; e) T. Da Ros, D. M. Guldi, A. Farran Morales, D. A. Leigh, M. Prato, R. Turco, *Org. Lett.* **2003**, *5*, 689–691; f) G. Bottari, D. A. Leigh, E. M. Pérez, *J. Am. Chem. Soc.* **2003**, *125*, 13360–13361; g) J. S. Hannam, S. M. Lacy, D. A. Leigh, C. G. Saiz, A. M. Z. Slawin, S. G. Stitchell, *Angew. Chem.* **2004**, *116*, 3322–3326; *Angew. Chem. Int. Ed.* **2004**, *43*, 3260–3264; h) D. A. Leigh, M. Á. F. Morales, E. M. Pérez, J. K. Y. Wong, C. G. Saiz, A. M. Z. Slawin, A. J. Carmichael, D. M. Haddleton, A. M. Brouwer, W. J. Buma, G. W. H. Wurpel, S. León, F. Zerbetto, *Angew. Chem.* **2005**, *117*, 3122–3127; *Angew. Chem. Int. Ed.* **2005**, *44*, 3062–3067.

[7] *Peptide-Based Drug Design Methods in Molecular Biology, Vol. 494* (Ed.: L. Otvos), Humana Press, New York, **2008**.

[8] This is likely a result of the folding of the thread through strong intramolecular hydrogen bonding in the nonpolar solvents used to promote hydrogen bond-template rotaxane formation. Yields of rotaxanes from related pentapeptide threads attempted in our laboratory were typically less than 1%.

[9] P. Garner, J. U. Yoo, *Tetrahedron Lett.* **1993**, *34*, 1275–1278.

[10] a) S. J. Rowan, J. F. Stoddart, *J. Am. Chem. Soc.* **2000**, *122*, 164–165; b) D. W. Zehnder, D. B. Smithrud, *Org. Lett.* **2001**, *3*, 2485–2487; c) S.-H. Chiu, S. J. Rowan, S. J. Cantrill, J. F. Stoddart, A. J. P. White, D. J. Williams, *Chem. Eur. J.* **2002**, *8*, 5170–5183; d) T. J. Kidd, T. J. A. Loontjens, D. A. Leigh, J. K. Y. Wong, *Angew. Chem.* **2003**, *115*, 3501–3505; *Angew. Chem. Int. Ed.* **2003**, *42*, 3379–3383; e) O. Š. Miljanić, W. R. Dichtel, I. Aprahamian, R. D. Rohde, H. D. Agnew, J. R. Heath, J. F. Stoddart, *QSAR Comb. Sci.* **2007**, *26*, 1165–1174; f) J. M. Spruell, W. R.

Dichtel, J. R. Heath, J. F. Stoddart, *Chem. Eur. J.* **2008**, *14*, 4168 – 4177.

[11] a) I. S. Zagon, P. J. McLaughlin, *Neuropeptides* **2003**, *37*, 79 – 88; b) J. Fichna, A. Janecka, *Cancer Metastasis Rev.* **2004**, *23*, 351 – 366; c) I. S. Zagon, P. J. McLaughlin, *Neuropeptides* **2005**, *39*, 495 – 505; d) I. S. Zagon, K. A. Rahn, P. J. McLaughlin, *Neuropeptides* **2007**, *41*, 441 – 452; e) F. Cheng, I. S. Zagon, M. F. Verderame, P. J. McLaughlin, *Cancer Res.* **2007**, *67*, 10511 – 10518; f) F. Cheng, P. J. McLaughlin, M. F. Verderame, I. S. Zagon, *Mol. Biol. Cell* **2009**, *20*, 319 – 327.

[12] a) H. Cheng, X. Cao, M. Xian, L. Fang, T. B. Cai, J. J. Ji, J. B. Tunac, D. Sun, P. G. Wang, *J. Med. Chem.* **2005**, *48*, 645 – 652; b) L. F. Tietze, F. Major, I. Schuberth, *Angew. Chem.* **2006**, *118*, 6724 – 6727; *Angew. Chem. Int. Ed.* **2006**, *45*, 6574 – 6577; c) A. Kamal, V. Tekumalla, A. Krishnan, M. Pal-Bhadra, U. Bhadra, *ChemMedChem* **2008**, *3*, 794 – 802.

[13] a) P. D. Senter, C. J. Springer, *Adv. Drug Delivery Rev.* **2001**, *53*, 247 – 264; b) K. D. Bagshawe, *Expert Rev. Anticancer Ther.* **2006**, *6*, 1421 – 1431.

[14] a) S. Papot, I. Tranoy, F. Tillequin, J.-C. Florent, J.-P. Gesson, *Curr. Med. Chem. Anti-Cancer Agents* **2002**, *2*, 155 – 185; b) I. Tranoy-Opalinski, A. Fernandes, M. Thomas, J.-P. Gesson, S. Papot, *Anti-Cancer Agents Med. Chem.* **2008**, *8*, 618 – 637.

[15] a) F. Coutrot, E. Busseron, J.-L. Montero, *Org. Lett.* **2008**, *10*, 753 – 756; b) F. Coutrot, C. Romuald, E. Busseron, *Org. Lett.* **2008**, *10*, 3741 – 3744; c) F. Coutrot, E. Busseron, *Chem. Eur. J.* **2008**, *14*, 4784 – 4787; d) F. Coutrot, E. Busseron, *Chem. Eur. J.* **2009**, *15*, 5186 – 5190.

[16] a) C. Gros, B. Giros, J. C. Schwartz, *Biochemistry* **1985**, *24*, 2179 – 2185; b) H. Terashima, N. Bunnett, *J. Gastroenterol.* **1995**, *30*, 696 – 704.

[17] J. Lanzillo, J. Stevens, Y. Dasarathy, H. Yotsumoto, B. Fanburg, *J. Biol. Chem.* **1985**, *260*, 14938 – 14944.

[18] Intermediates **8** and **9** are only stable for a few minutes at pH 7 at 37 °C. However, they survive for hours at pH 2 at room temperature (the equilibrium between the phenol and phenolate forms is shifted toward the phenol and elimination occurs only slowly). In the β-gal-catalyzed reactions, aliquots were withdrawn from the reaction medium and diluted with a solution of trifluoroacetic acid (to pH 2) before being injected into the HPLC apparatus with the mobile phase buffered at pH 2 (see the Supporting Information).

